PROCEEDINGS OF THE 2nd JOINT SYMPOSIUM ON THE NATURAL HISTORY AND GEOLOGY OF THE BAHAMAS

June 2017

Edited by
Tina M. Niemi and Kathleen Sullivan Sealey

Gerace Research Centre
San Salvador, The Bahamas
2020

Cover image - "The cliff at Clifton Heritage Park, New Providence Island"
(Photograph by Tina M. Niemi)

PROCEEDINGS

OF THE

SECOND JOINT SYMPOSIUM

ON THE

NATURAL HISTORY AND GEOLOGY OF THE BAHAMAS

Edited by
Tina M. Niemi
and
Kathleen Sullivan Sealey

ORGANIZER:

Troy A. Dexter

Executive Director
Gerace Research Centre
University of The Bahamas
San Salvador, The Bahamas

2020

ISBN: 978-0-935909-67-8

TABLE OF CONTENTS

FOREWARD

The 2nd Joint Symposium on the Natural History and Geology of The Bahamas was held at the Gerace Research Centre on the island of San Salvador during June 8-12, 2017. Whereas this is only the second conference combining both geology and natural history, it follows a long tradition of over thirty years of scientific symposia hosted on the island. Executive Director, Troy Dexter, organized the conference with the able assistance of the staff of the Gerace Research Centre. The program co-chairpersons were Tina M. Niemi from the University of Missouri-Kansas City and Kathleen Sullivan Sealey from the University of Miami. In all, there were 38 abstracts submitted to the conference with 18 talks and 20 poster presentations. The more than 40 participants were welcomed the first evening of the symposium by the opening remarks of Troy Dexter and kind words from Bahamian administrator, Gilbert Kemp. Participants received a tote bag made from fabric depicting the islands from the Bahama Hand Print shop in Nassau and voted on entries in the 9th annual photography contest. In lieu of a pre-meeting field trip, participants had the option to attend an all-day High Cay Field Trip which included boat ride, snorkeling, hiking, and a lobster lunch with refillable beverages serviced in a conch shell. It was quite the adventure!

On the first evening of the conference, our keynote speaker, Dr. Kam-biu Liu, gave his address entitled "Paleotempestology of the Caribbean and Gulf Coast Region: Emerging research questions and methods." Dr. Liu is the George William Barineau III Professor in the Department of Oceanography and Coastal Sciences, College of the Coast and Environment, at Louisiana State University and is recognized as a pioneer and leader in *paleotempestology*—a scientific field that uses the geological record to study past hurricane activity. As a paleoclimatologist and paleoecologist, Professor Liu's broader research interests include the use of fossil pollen, lake sediments, and ice cores to reconstruct the global and regional patterns of climate and environmental changes on timescales of centuries to millennia. During the past three decades, he has been using coastal sedimentary records to reconstruct past hurricane activities in the U.S. Atlantic and Gulf of Mexico coasts, the Caribbean region, and the Pacific coast of Mexico. He has published more than 130 research papers and is an editor and author of the book, *Hurricanes and Typhoons: Past, Present, and Future*, published by Columbia University Press. In addition, his research has been featured in numerous newspapers, magazines, documentary films, and TV programs in the U.S. and internationally. Dr. Liu is a Fellow of the American Association for the Advancement of Science and had served as a member of the U.S. National Committee for the International Union for Quaternary Research.

On Saturday evening of the symposium, Mrs. Kathy Gerace gave a moving memorial in honor of her late husband, Dr. Donald T. Gerace. As the University of The Bahamas Facebook post states: "Dr. Donald T Gerace, 83, of Port Charlotte, Florida, passed away peacefully on March 6th, 2016 after a brief and sudden illness. Dr. Gerace was an educator whose passion for the marine sciences, archaeology, geology, and biology of the Caribbean inspired the scholarship of many students and researchers. A selfless person, Don Gerace dedicated his life to the work of the Gerace Centre and over the past 40 years, ensured that Bahamian students had access to countless scholarship opportunities in the United States." He will be sorely missed.

The keynote address and eight papers found in this proceedings volume represents some of the research presented at the 2nd Joint Symposium on the Natural Hisotry and Geology of The Bahamas. We thank all of the authors and reviewers for their contribution.

Tina M. Niemi (UMKC) and Kathleen Sullivan Sealey (University of Miami)

Keynote Address

PALEOTEMPESTOLOGY OF THE CARIBBEAN AND GULF COAST REGION: EMERGING RESEARCH QUESTIONS AND METHODS

Kam-biu Liu

Department of Oceanography and Coastal Sciences
Louisiana State University
Baton Rouge, LA 70803 USA

ABSTRACT

The application of novel methods in paleotempestology has permitted the development of new insights into some key research questions fundamental to understanding the processes of storm sedimentation and the spatio-temporal dynamics of paleohurricane activities in the Caribbean and Gulf Coast region. This paper uses several examples from the Gulf Coast, the Dominican Republic, and Belize to illustrate this point. The application of X-ray florescence (XRF) analysis on sediment cores taken from coastal backbarrier lakes can reveal the chemical elemental composition of storm versus non-storm deposits, which can also provide a means to assess the relative contribution between freshwater and saltwater inputs to storm sedimentation. Coupled with palynological data, the results of XRF analysis from the sedimentary records of Bay Champagne, Louisiana, suggest that fluvial processes may have played a significant role in storm deposition from Hurricane Ike relative to that from Hurricane Gustav. Another example, based on oxygen isotopic analysis of coastal sediment cores from the Dominican Republic, suggests that freshwater input from fluvial processes may have played an even bigger role in the storm deposition in a hypersaline lake, which occurs commonly in the semi-arid areas of subtropical coasts. The application of stable isotopic techniques on a Belizean stalagmite has yielded a high-resolution, 450-year reconstruction of Caribbean hurricane activity. A remarkable change in hurricane activity after AD 1870 has been interpreted in terms of a shift in hurricane tracks caused by changes in the ITCZ, the Bermuda High, and the Hadley cell driven by global climate changes. The development of novel multi-proxy techniques, and their application to a variety of paleoenvironmental archives including coastal sediments and speleothems, have advanced the frontiers of paleotempestology by shedding new light on some key concepts such as the processes of storm deposition and the spatio-temporal patterns of Caribbean paleohurricane activity.

INTRODUCTION

The basic principle of paleotempestology involves the detection of hurricane events in the sedimentary record retrieved from coastal lakes and marshes. While the identification of overwash sand layers in sediment cores collected from backbarrier lakes and marshes remains the most widely used method in paleotempestology, new proxies and new archives have been added to the "tool box" at the disposal of paleotempestology researchers for the reconstruction of paleo-storm events in a variety of environmental settings. The application of these relatively new tools, in turn, have resulted in novel discoveries and findings that have led to the formulation of new research questions and hypotheses. In this review paper I will use a few examples from my work to illustrate these points.

THE ROLE OF FRESHWATER IN STORM DEPOSITION

The classical model of storm deposition in a backbarrier lake assumes that a clastic (usually sand) layer—taken as a proxy for a hurricane

strike—is the product of seawater intrusion associated with overwash or storm surge processes (Liu, 2004, 2007). This assumption is undoubtedly true in many situations where storm surge is high (as in the case of a coastal site located close to the path of a landfalling intense hurricane) or where fluvial input to the site is low. However, there are increasing evidences to show that in many instances freshwater from fluvial flooding may play an important, yet under-appreciated, role in storm deposition. A case in point is Hurricane Harvey, a Category 4 hurricane that made landfall in coastal Texas in late-August 2017. While Harvey caused 0.3 to 3.0 m of storm surge to coastal Texas, extensive areas of southeastern Texas were flooded due to the 500-1539 mm precipitation that it brought, resulting in many rivers overflowing their banks (Blake and Zelinsky, 2017). Hurricane-generated fluvial flooding can have significant geological impacts on coastal landforms. An example comes from the Mosquitia (Mosquito Coast) of eastern Honduras (Cochran et al., 2009). During the extraordinarily active 2005 hurricane season, three late-season (October-November) tropical cyclones (Hurricanes Wilma and Beta, Tropical Storm Gamma) brought a combined total of 549 mm (21.6 inches) to this coastal region, causing major overbank flooding of the rivers. Freshwater outbursts from the overflowing rivers in turn led to the breaching of the barrier beaches along the Caribbean coast (Cochran et al., 2009) (Figure 1). It is therefore reasonable to expect that storm-generated fluvial flooding and freshwater outbursts must have changed the hydrology, chemistry, and sedimentary patterns in the backbarrier lagoons which the rivers emptied into.

Figure 1. Satellite images showing the breaching of coastal sand barriers due to the outburst of fluvially-fed freshwater from Laguna Bacalar (square) and an adjacent meander bend of the Rio Tinto (circle) in the Mosquito Coast, eastern Honduras. This breaching and freshwater outburst event occurred as a result of the heavy precipitation and fluvial flooding caused by Tropical Storm Gamma in November 2005. See Cochran et al. (2009) for details.

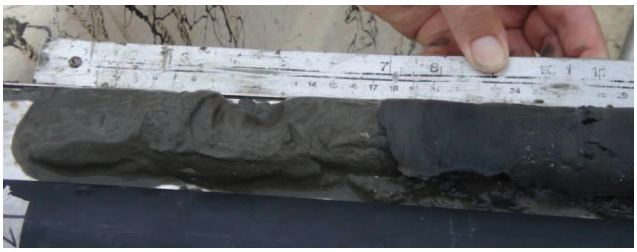

Figure 2. Core 21 from Bay Champagne, taken after Hurricanes Gustav and Ike, contains a 17 cm-thick layer of unconsolidated sandy clay at the top that represents a storm deposit caused by these hurricanes (From Liu et al., 2011).

FRESHWATER VERSUS SALTWATER INPUTS: A CASE STUDY FROM COASTAL LOUSIANA

Here I use a case study from coastal Louisiana to illustrate the importance of freshwater input in storm deposition, as well as its detection by means of X-ray fluorescence (XRF) techniques in the sedimentary record. Bay Champagne is a brackish water backbarrier lake near Port Fourchon, situated in a rapidly retreating part of the Louisiana coastal region that has experienced the highest rate of shoreline recession in the whole Gulf of Mexico (Dietz et al., 2018). In September 2008, coastal Louisiana was affected by two hurricanes consecutively within a two-week period. Hurricane Gustav made landfall in southern Louisiana as a high Category 2 hurricane, followed by Hurricane Ike which made landfall in southeastern Texas but its high storm surge caused significant coastal flooding in southern Louisiana. Cores taken after these two hurricane events from Bay Champagne contain a fresh sand layer at the top directly overlying finer sediments that are more consolidated and more clearly laminated (Liu et al., 2011). This sand layer has been interpreted to be the combined storm deposition attributed to Hurricanes Gustav and Ike (Liu et al., 2011). Accordingly, the lower part of this storm deposit was presumed to be caused by Hurricane Gustav, and the upper part by Hurricane Ike. In core 21, this storm deposit is 17 cm thick and contains a sloppy, unconsolidated section in the middle (8-13 cm) (Figure 2). We interpret this sloppy section to be the top of the Gustav deposit that was subsequently reworked by Ike. Loss-on-ignition (LOI) analysis of core 21 suggests that the Gustav-Ike sand layer at the top of each core contained low percentages of water and organic matter. In addition, it also reveals the presence of three thinner sand layers marked by low water and organic percentages in the lower part of the core, which were probably formed by older hurricanes prior to Gustav and Ike (Figure 3). X-ray fluorescence (XRF) analysis indicates that the storm deposits and the normal (non-storm) deposits have different elemental chemical characteristics. The storm deposits tend to have higher Cl/Br and Ca/Fe ratios than the finer-grained normal deposits, and typically contain lower Ti, Fe, and Mn concentrations (Liu et al., 2017). It is notable that Cl and Ca are typically enriched in seawater and the Cl/Br and Ca/Fe ratios have been used as indicators of marine incursions in coastal paleoenvironmental research, whereas Ti, Fe, and Mn are widely used as indicators of terrestrial sediment sources (Liu et al., 2014; Bianchette et al., 2016, 2017; Yao and Liu, 2018; McCloskey et al., 2015, 2018a, 2018b). Therefore, these elemental chemical characteristics suggest that the sandy storm deposits were formed by the incursion of seawater during storm surges, while the more organic, finer-grained sediments were deposited under less marine-dominated conditions.

Remarkably, within the thick sandy storm deposit at the top of the core, the upper half—attributed to Hurricane Ike—is characterized by a lower Cl/Br ratio and higher concentrations of Ti, Fe, and Mn than the Gustav-deposited lower layer (Liu et al., 2017) (Figure 3). This implies that while the coastal impacts by Hurricane Gustav were dominated by storm surge-generated marine incursion processes, the Hurricane Ike impacts were characterized by a greater contribution from freshwater influx. In addition to direct atmospheric input from heavy precipitation during Hurricane Ike, a likely source of freshwater input was from the bayou at the back of the lake, which drains the extensive wetlands in the Port Fourchon area. Hydrological data from the Bay Champagne water-

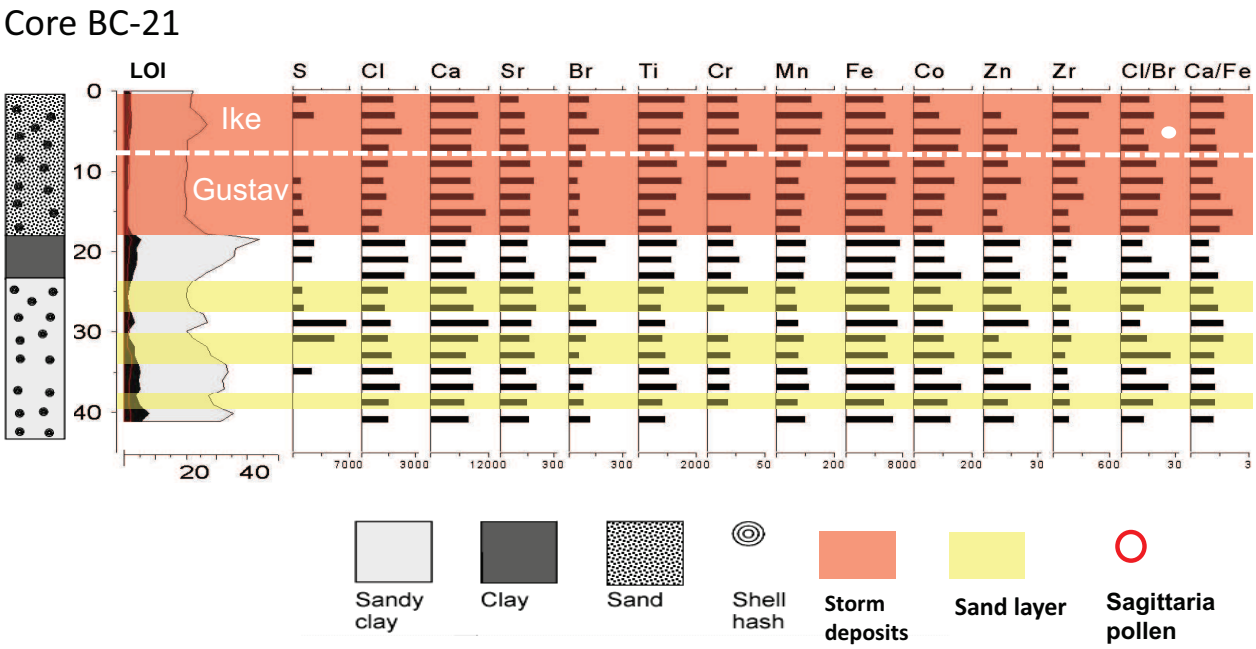

Figure 3. Loss-on-ignition (LOI) and X-ray flouresence curves of 12 chemical elements and the Cl/Br and Ca/Fe ratios from core 21 in Bay Champagne.

shed support the notion that Hurricane Ike was a wetter storm and delivered more freshwater runoff to the wetlands surrounding the lake (Dietz et al., 2016). Additional support for the higher freshwater input to Bay Champagne comes from palynological data in core 21. The pollen of *Sagittaria* (duck potato or bulltongue arrowhead), a common plant of fresh marshes, was found in the Hurricane Ike sediment layer but not in the underlying Gustav layer (Liu et al., 2011). The convergence of the geochemical, palynological, and environmental data therefore suggests that freshwater input from fluvial processes can play a significant role in hurricane-generated storm sedimentation in coastal lakes and marshes.

FRESHWATER INPUT TO COASTAL HYPERSALINE LAKES: AN EXAMPLE FROM THE DOMINICAN REPUBLIC

Coastal hypersaline lakes are common in certain arid, semi-arid, or seasonally dry environments. In these lakes hurricane rainfall may be a major source of freshwater input to an otherwise hypersaline aquatic environment. Thus, freshwater input from fluvial processes can play a significant role in storm deposition. Stable isotopic techniques have been used to detect the occurrence of hurricane-generated freshwater input events in the sedimentary record of hypersaline lakes. An example from Laguna Alejandro, a hypersaline lake on the southern coast of the Dominican Republic, illustrates this application (LeBlanc et al., 2017; Lane et al., 2017). A core (ALEJ08-5) taken from the lake contains three coarse-grained layers with allochthonous leaf litter in the lower part that were interpreted to be deposited under hurricane-generated high-energy conditions based on the sedimentary evidence. All three storm deposits were marked by significant negative excursions consistent with freshwater input derived from strongly isotopically depleted hurricane rainfall (Lane et al., 2017; Lawrence and Gedzelman, 1996). The isotopic signature of these sedimentologically-defined storm deposits allowed the detection of two more storm layers above them, even though the latter

lacked any diagnostic sedimentary evidence to support their identification (Figure 4). This case study provides another example to show that freshwater input—either from direct atmospheric precipitation or from fluvial processes, or both—can play an important role in paleotempestology.

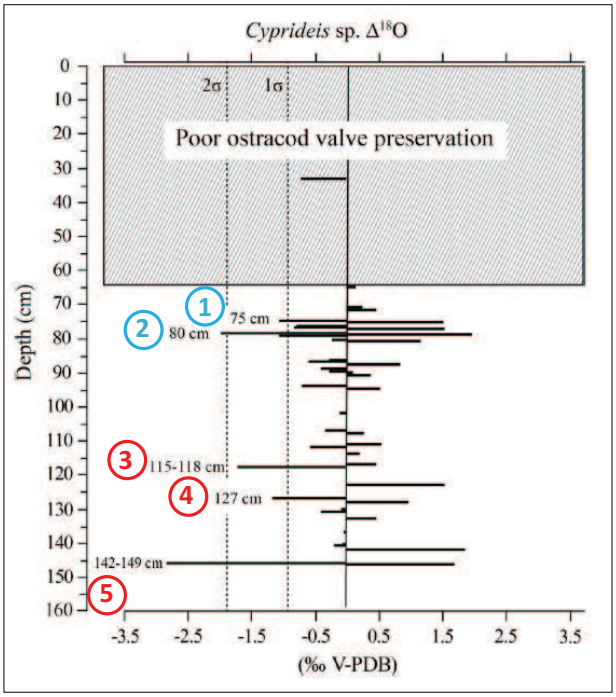

Figure 4. Results of oxygen isotopic analysis of ostracod valves from a sediment core from hypersaline Laguna Alejandro, Dominican Republic. Ostracods at 5 stratigraphic levels contained strongly negative $\delta^{18}O$ values that are typically associated with hurricane rainfall. Three of these levels (labelled as 3 – 5) in the lower part of the core correspond with hurricane events identified by sedimentary proxies. Despite the lack of sedimentary evidence, two higher levels (labelled as 1 and 2) were inferred to be hurricane deposits based on their isotopic signatures. This study shows that the detection of freshwater input into hypersaline lakes by means of oxygen isotopic analysis can provide a more complete reconstruction of paleohurricane events. (From: Lane et al., 2017).

ISOTOPIC RECORD FROM BELEZEAN SPELEOTHEM SHED NEW LIGHTS ON CARIBBEAN PALEOHURRICANE ACTIVITY

In addition to their application to paleo-hurricane detection in coastal sedimentary records as illustrated above, stable isotopic techniques have been successfully used to develop high-resolution paleo-hurricane reconstructions from speleothem records (e.g., Frappier et al., 2007), which has shed new light on the spatial and temporal patterns of Holocene hurricane activities in the Caribbean region. A recent study, based on a new index of coupled carbon and oxygen isotope ratio derived from an annually-resolved stalagmite proxy record from Belize, yields a 450-year reconstruction of tropical cyclone activity for the western Caribbean region (Baldini et al., 2016). The results suggest that during the past five centuries Atlantic tropical cyclone (TC) tracks responded sensitively to latitudinal shifts in the positons of the Intertropical Convergence Zone (ITCZ) and NH Hadley Cell driven by anthropogenic greenhouse gas and sulphate aerosol emissions. Specifically, the study postulates that since AD 1870 more TCs have followed recurving tracks in response to a southward shift of the ITCZ and an expanded Hadley Cell and Bermuda High, therefore resulting in reduced TC risks for the western Caribbean but increased risks for the Northeast Atlantic coast (Baldini et al., 2016) (Figure 5). This new model is consistent with the premises of the Bermuda High Hypothesis, which suggests that proxy-based reconstructions of hurricane activity patterns from the Caribbean to the Northeast Atlantic coast should show an out-of-phase or anti-phase relationship between the south and north as a function of long-term shifts in the predominant storm tracks in response to latitudinal migrations of the ITCZ and the Bermuda High (Liu and Fearn, 2000; Liu, 2004).

CONCLUSIONS

The application of relatively new research techniques such as XRF analysis and stable iso-

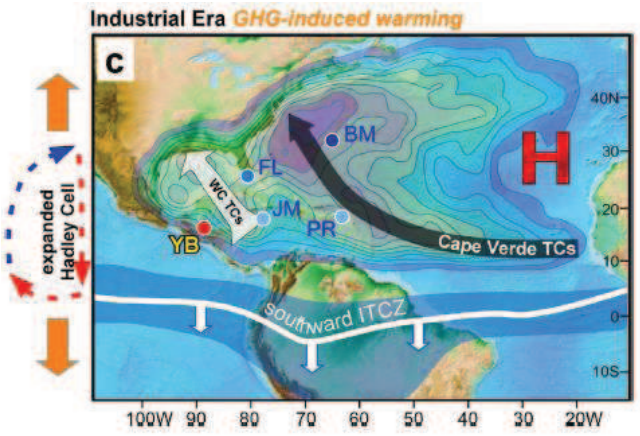

Figure 5. Inferred predominant hurricane tracks after AD 1870 based on a stable isotopic record derived from a Belizean stalagmite. Anthropogenic warming resulted in an expanded Hadley Cell and Bermuda High, while increased aerosols caused a southward shift of the ITCZ. These mechanisms combined has led to the prevalence of more recurving storm tracks, bringing higher risks to the northeastern U.S. coasts (From Baldini et al., 2016).

topic analysis to speleothems and sedimentary archives has advanced the frontiers of paleotempestology. Although XRF techniques have been applied to coastal paleoenvironmental research in the northern Gulf of Mexico (e.g., van Soelen et al., 2012; Yao et al., 2015), its application to paleotempestology—especially to distinguishing between the freshwater and saltwater inputs to storm deposition—has been limited (Liu et al., 2014). This paper shows the potential of using the XRF-derived chemical elemental signatures of different storm deposits to assess the relative contributions between saltwater intrusion and freshwater flooding associated with different hurricane events. These results help to shed new light on the potentially important role of freshwater input and fluvial processes in storm deposition in coastal environments. The role of freshwater input derived from hurricane precipitation is even more significant in hypersaline lakes in semi-arid tropical coastal environments, as the oxygen isotopic record from Laguna Alejandro in the Dominican Republic demonstrates (Lane et al., 2017). In another example of novel methodological development, the application of stable isotopic techniques on a Belizean stalagmite has resulted in an annually-resolved reconstruction of Caribbean hurricane activity that has offered new insights into the dynamic interactions between the ITCZ, Bermuda High, and hurricane tracks over the last 450 years (Baldini et al., 2016). In a nutshell, the development of novel multi-proxy techniques and their application to new environmental archives have opened new doors to enhance our understanding of past hurricane activities in the Caribbean and Gulf Coast region, and advanced the frontiers of paleotempestology.

ACKNOWLEDGMENTS

The work presented here was supported by grants from the National Science Foundation, the Inter-American Institute of Global Change Research, and the Louisiana Sea Grant/NOAA. I thank Tom Bianchette, Terry McCloskey, Marianne Dietz, and Qiang Yao for their assistance in field work and data analysis. Special thanks to Tina Niemi and Kathleen Sullivan Sealey for the opportunity to present this work as a keynote address in the 2nd Joint Symposium on the Natural History and Geology of The Bahamas, and to Troy Dexter of the Gerace Research Center for hosting the conference.

REFERENCES

Baldini, L.M., Baldini, J.U.L., McElwaine, J., Frappier, A.B., Asmerom, Y., Liu, K.B., Prufer, K., Ridley, H.E., Polyak, V., Kennett, D.J., Macpherson, C.G., Aquino, V.V., Awe, J., and Breitenbach, S.F.M. 2016. Persistent northward North Atlantic tropical cyclone track migration over the past five centuries. *Scientific Reports* 6: 37522, doi: 10:1038/srep37522

Bianchette, T.A., McCloskey, T.A., and Liu, K.B. 2016. Re-evaluating the geological evidence for Late Holocene marine incursion events along the Guerrero Seismic Gap on the Pacific Coast

of Mexico. *PLOS ONE* 11(8), e0161568. DOI: 10.1371/ journal.pone.0161568.

Bianchette, T.A., McCloskey, T.A., and Liu, K.B. 2017. A 7000-year history of coastal environmental changes from Mexico's Pacific coast: A multi-proxy record from Laguna Mitla, Guerrero. *The Holocene*, DOI: 10.1177/0959683616687379

Blake, E. S. and Zelinsky, D. A. 2017. National Hurricane Center Tropical Cyclone Report-Hurricane Harvey, website: https://www.nhc.noaa.gov/data/tcr/AL092017_Harvey.pdf

Cochran, D.M., Reese, C.A., and Liu, K.B. 2009. Tropical Storm Gamma and the Mosquitia of eastern Honduras: A little-known story from the 2005 hurricane season. *Area* 41: 425-434.

Dietz, M., Liu, K.B., Bianchette, T.A., Yao, Q., and McCloskey, T.A. 2016. Using geochemistry to differentiate storm event deposits in a back-barrier lake in coastal Louisiana. Paper presented at the fall meeting of the American Geophysical Union (AGU), San Francisco, December 12-16, 2016.

Dietz, M.E., Liu, K.B., and Bianchette, T.A. 2018. Hurricanes as a Major Driver of Coastal Erosion in the Mississippi River Delta: A Multi-Decadal Analysis of Shoreline Retreat Rates at Bay Champagne, Louisiana (USA). *Water* 10: 1480; doi:10.3390/w10101480.

Frappier, A.B., Sahagian, D., Carpenter, S.J., Gonzalez, L.A, and Frappier, B.R. 2007. Stalagmite stable isotope record of recent tropical cyclone events. *Geology* 35: 111–114.

Lane, C.S., Hildebrandt, B., Kennedy, L.M., LeBlanc, A.R., Liu, K.B., Wagner, A.J., and Hawkes, A.D. 2017. Verification of tropical storm deposits with oxygen isotope analyses of coeval ostracod valves. *Journal of Paleolimnology* 57: 245-255.

Lawrence, J.R. and Gedzelman, S.D. 1996. Low stable isotope ratios of tropical cyclone rains. *Geophysical Research Letters* 23: 527–530.

LeBlanc, A.R., Kennedy, L.M., Liu, K.B., and Lane, C.S. 2017. Linking hurricane landfalls, precipitation variability, fires, and vegetation response over the past millennium from analysis of coastal lagoon sediments, southwestern Dominican Republic. *Journal of Paleolimnology*; doi:10.1007/s10933-017-9965-z

Liu, K.B. 2004. Paleotempestology: Principles, methods, and examples from Gulf coast lake-sediments. Pp. 13-57. In R. Murnane and K.B. Liu, (Eds.). *Hurricanes and Typhoons: Past, Present, and Future*. Columbia University Press, New York.

Liu, K.B. 2007. Uncovering prehistoric hurricane activity. *American Scientist* 95: 126-133.

Liu, K.B. and Fearn, M.L. 2000. Reconstruction of prehistoric landfall frequencies of catastrophic hurricanes in northwestern Florida from lake sediment records. *Quaternary Research* 54: 238-245.

Liu, K.B., Li, C.Y., Bianchette, T.A., McCloskey, T.A., Yao, Q., and Weeks, E. 2011. Storm deposition in a coastal backbarrier lake in Louisiana caused by Hurricanes Gustav and Ike. *Journal of Coastal Research* SI 64: 1866-1870.

Liu, K.B., McCloskey, T.A., Ortego, S., and Maiti, K. 2014. Sedimentary signature of Hurricane Isaac in a *Taxodium* swamp on the western margin of Lake Pontchartrain, Louisiana, USA. Pp. 421-428. In *Sediment Dynamics from the Summit to the Sea*. IAHS Publication 367.

Liu, K.B., Bianchette, T.A., and McCloskey, T.A. 2017. Marine or terrestrial? Using geochemical data derived from XRF analysis in paleotempestology and coastal paleoenvironmental studies. Paper presented at the annual meeting of the

Association of American Geographers, Boston, April 5-9, 2017.

McCloskey, T.A., Bianchette, T.A., and Liu, K.B. 2015. Geological and sedimentological evidence of a large tsunami occurring ~1100 year BP from a small coastal lake along the Bay of La Paz in Baja California Sur, Mexico. *Journal of Marine Science and Engineering* 3: 1544-1567.

McCloskey, T.A., Smith, C.G., Liu, K.B., Marot, M., and Haller, C. 2018a. How could a freshwater swamp produce a XRF chemical signature characteristic of a saltmarsh? *ACS Earth and Space Chemistry* 2: 9-20. DOI: 10.1021/acsearthspacechem.7b00098

McCloskey, T.A., Smith, C.G., Liu, K.B., and Nelson, P.R. 2018b. The effects of tropical cyclone-generated deposition on the sustainability of the Pearl River Marsh, Louisiana: The importance of the geologic framework. *Frontiers in Ecology and Evolution* 6: 179, doi:10.3389/fevo. 2018.00179.

van Soelen, E.E., Brooks, G.R., Larson, R.A., Damsté, J.S.S., Reichart, G.J. 2012. Mid- to late-Holocene coastal environmental changes in southwest Florida, USA. *The Holocene* 22: 929-938.

Yao, Q. and Liu, K.B. 2018. Changes in modern pollen assemblages and soil geochemistry along coastal environmental gradients in the Everglades of south Florida. *Frontiers in Ecology and Evolution* 5: 178, doi:10.3389/fevo.2017. 00178.

Yao, Q., Liu, K.B., Platt, W.J., and River-Monroy, V.H. 2015. Palynological reconstruction of environmental changes in coastal wetlands of the Florida Everglades since the mid-Holocene. *Quaternary Research* 83: 449-458.

PALEOSOL AND CAVE MINERALOGY FROM ELEUTHERA, THE BAHAMAS

Jonathan B. Sumrall[1], Kaitlyn L. Gauvey[1], Jeanne L. Sumrall[1], Kristin E. Sides[2], and Erik B. Larson[3]

[1]Department of Geosciences, Fort Hays State University
600 Park Street, Hays, KS 67601

[2]Department of Geography and Geology, Sam Houston State University
1905 University Avenue, Huntsville, TX 77340

[3]Department of Natural Sciences, Shawnee State University
940 2nd Street, Portsmouth, OH 45662

ABSTRACT

Paleosols on Eleuthera were sampled to determine the clay mineralogy from outcrops and inside Hatchet Bay Cave. In addition, cave mineral samples were collected from other flank margin and littoral sea caves. K-saturation, Mg-saturation, heating, and gylcolnation were used to determine the specific clay mineralogy of each sample. Petrographic thin sections were prepared to determine characteristics of each type of paleosol. Cave samples were powdered and analyzed using powdered X-ray diffraction (XRD).

The dominant clay mineral present in the paleosols on Eleuthera was Fe-rich chlorite ($(Fe^{+2},Mg,Al,Fe^{+3})_6(Si,Al)_4O_{10}(OH,O)_8$) and Illite ($K_{0.6}(H_3O)_{0.4}Al_{1.3}Mg_{0.3}Fe^{+2}_{0.1}Si_{3.5}O_{10}(OH)_2 \cdot (H_2O)$) based on the 14Å and 10Å peaks of samples. The larger [002] 7Å peak compared to the [001] 14Å peak indicates a Fe-rich chlorite. In addition, a peak shift from 14Å to 6.1Å in several samples, possibly suggests the presence of Boehmite (AlO(OH)). Non-clay materials include low-Mg calcite and quartz.

Cave minerals included carbonates (calcite and aragonite), sulfates (gypsum), phosphates (hydroxyapatite, fluorapatite, chlorapatite, and woodhouseite), and Mn-oxides. All minerals except woodhouseite have previously been reported from Bahamian caves. Woodhouseite ($CaAl_3(SO_4)(PO_4)(OH)_6$) is part of the Alunite supergroup, previously reported as the product of bat guano in cave environments. Woodhouseite samples came from Hatchet Bay Cave, specifically from small crusts found on the exposed paleosol within the cave. The presence of woodhouseite was confirmed in three samples spatially distributed in the cave. Woodhouseite formation in this instance likely represents phosphate-rich leachate derived from seawater and guano interacting with the various aluminum-rich phases found in the clay fraction of the paleosol. Previous studies of Bahamian cave minerals did not have access to exposed paleosols within caves, making this an interesting addition to the diverse inventory of cave minerals of The Bahamas.

GEOGRAPHIC AND GEOLOGIC SETTING

The Bahamas in the Atlantic Ocean stretches over 1000 km from the coast of Florida to Great Inagua just off the coast of Cuba (Figure 1). Eleuthera is located on the western edge of the Great Bahama Bank is less than 15 km across at its widest point, and is approximately 125 km long (Figure 1). Unlike some islands in The Bahamas (e.g. San Salvador), Eleuthera occupies the northeastern margin of the Great Bahama Bank. This means that the island of Eleuthera becomes part of a much larger island when sea level drops and exposes the Great Bahama Bank.

The large Bahama Banks represent a Mesozoic to present tectonically stable platform with more than 5 km of shallow water carbonates (Melim and Masaferro, 1997). Today, surficial geology is almost entirely Quaternary limestone that has been modified by karst processes (Carew and

Mylroie, 1995; Mylroie and Carew, 1995; Mylroie and Mylroie, 2007).

The Bahama Banks are steep-sided platforms with an average water depth of ~10 m. Glacioeustatic sea level controls the geology of The Bahamas. For example, Eleuthera is a relatively small island on a larger platform that is exposed during glacioeustatic lowstands to form a much larger island. However, during highstands, the platforms are mostly submerged by marine water, initiating carbonate production. These carbonate sediments are carried by waves and currents and deposited as beach sediments, where eolian processes deposit these sediments as calcareous sand dunes (eolianites). During the initial transgressive phase of platform flooding, eolianites are produced as wave action constantly keeps lagoon and beach sediment mobilized, forming transgressive-phase eolianites. Transgressive-phase eolianites are often characterized by lacking trace fossils of colonizing vegetation referred to as vegemorphs (Birmingham et al., 2008; Mylroie et al., 2017).

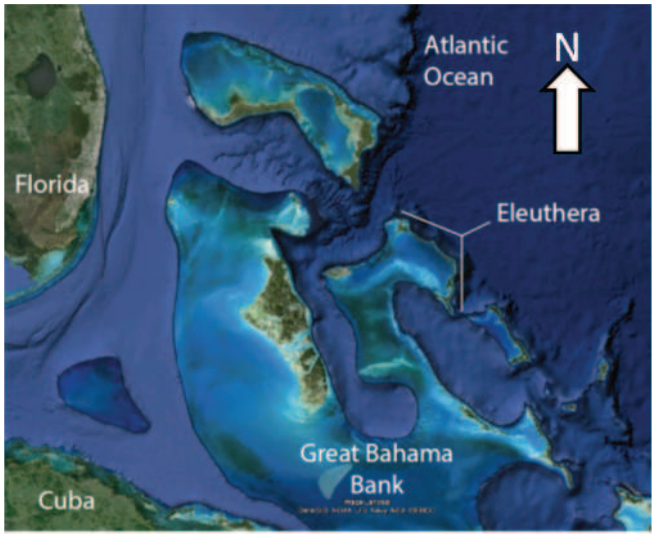

Figure 1. Location of Eleuthera, The Bahamas (Source: Google Earth ©).

Coral reefs grow to wave-base, producing quiescent lagoons during highstands. This causes a reduction in eolian production, causing strand plains to prograde into lagoons (Infante, 2012). During sea level regression, the declining wave base mobilizes lagoonal sediments. This produces regressive-phase eolianites. These regressive-phase eolianites often overstep reefs and subtidal deposits (Carew and Mylroie, 1995). Regressive-phase eolianites are also colonized by vegetation and contain abundant vegemorphs (Birmingham et al., 2008; Mylroie et al., 2018).

Platform exposure causes epikarst development and pedogenic processes to initiate. Collection of insoluble material from African dust produces fossilized soil horizons called terra rossa paleosols (Muhs et al., 1990). Carbonate paleosols have been studied to determine the main source of Bahamian soils and paleosols to be consistent with an airborne source. The Quaternary stratigraphy of The Bahamas consists of depositional packages separated by *terra rossa* paleosols formed during sea level lowstands. The stratigraphy of Eleuthera consists of the Middle Pleistocene Owl's Hole Formation, which contains several *terra rossa* paleosols; the Late Pleistocene Grotto Beach Formation, which consists of the French Bay Member, the Cockburn Town Member, and is topped by a *terra rossa* paleosol; the Late Pleistocene Whale Pont Formation, bounded by *terra rossa* paleosols and only reported on Eleuthera; and the Holocene Rice Bay Formation, which consists of the North Point Member and the Hanna Bay Member (Figure 2). The Holocene units are too young to have developed a terra rossa paleosol.

Bahamian karst

The young rocks of The Bahamas represent carbonate sequences that have only undergone eogenetic diagenesis. All of the karst features present in The Bahamas must be explained within this constraint. There are specific types of karst features found on islands that are specific to carbonate coastlines, that include surface karst, such as karren and kamenitza; pit caves; blue holes (many of these are the result of the collapse of large conduit caves at depth produced by sea-level lowstands (Larson and Mylroie, 2014)); and flank margin caves. This study specifically focuses on cave minerals, so flank margin caves will be the main type of karst discussed. Another type of cave exists in The Bahamas; however, these caves are erosional, pseudokarst features called littoral caves or sea

caves produced by wave action, and tafoni produced by wind action.

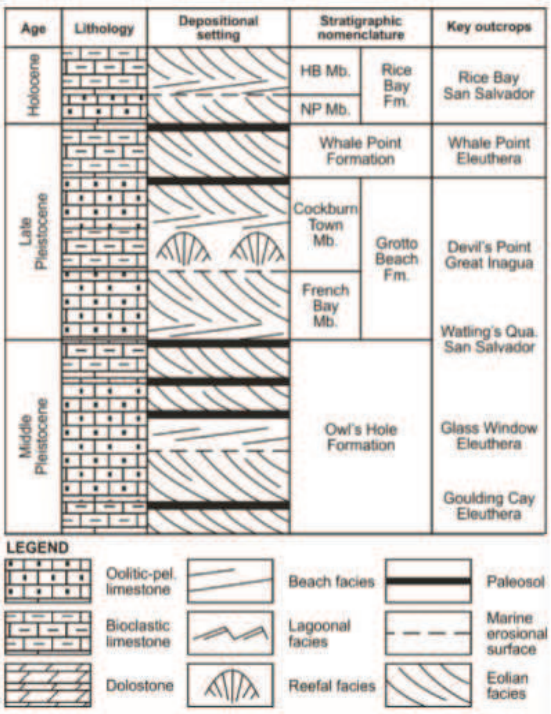

Figure 2. Complete stratigraphy of The Bahamas with key outcrops included (from Kindler et al., 2010).

Flank margin caves are the largest karst features on Eleuthera. These caves develop in the distal margin of the freshwater lens at the flank of the enclosing landmass (Mylroie and Carew, 1995). Three factors at this location result in increased solubility of carbonates: 1) mixing dissolution at the vadose-phreatic mixing zone at the top of the lens superimposed with mixing dissolution at the marine-fresh water mixing zone located at the bottom of the lens, 2) decomposition of organic material that collects at density interfaces (e.g. top and bottom of the lens), and 3) increase in flow velocity as lens cross section decreases at the lens margin. Another type of cave, called Banana Holes, found in The Bahamas forms by a similar mechanism as flank margin caves, in prograding strand plains during highstands as syndepositional voids (Infante, 2012; Mylroie et al., 2015).

Caves and types of speleothems and cave minerals

Fifteen caves were investigated in January 2016 on Eleuthera. Seven of these caves were flank margin caves, four were littoral caves, two were blue holes, one was a pit cave, and the final cave was a overprinted cave (likely flank margin with littoral overprinting). In the present study, the majority of speleothems investigated were collected from caves assigned to the flank margin category.

Previous investigations of cave minerals on San Salvador Island in The Bahamas revealed the presence of approximately twenty minerals despite the limited carbonate lithology (Onac et al., 2001, 2009). The presence of bat guano and marine ions provide the necessary chemistry for formation. In addition, the two previous studies expanded sample collection to crusts and earthy aggregates collected within fresh and desiccated guano piles instead of focusing on traditional speleothems. The main goal of this study is to investigate the mineral diversity on Eleuthera and compare to previous studies on San Salvador Island.

METHODS

Paleosol sample

One sample was collected from a paleosol within Hatchet Bay Cave. The sample was air-dried, powdered using a low-speed dental drill, sieved through 45 μm mesh, and analyzed for bulk mineralogy. Bulk mineralogy was analyzed by a Rigaku Miniflex 600 diffractometer. XRD patterns were obtained as follows: continuous mode, 0.002° per step, 4° 2θ per minute, 3° -70° 2θ CuKα radiation. Relative mineral percentages were estimated from relative intensities of peak heights of XRD lines. In addition to bulk mineralogy, the paleosol sample was processed to remove carbonates and organics before fractionating by size. Treatments (K-saturation, Mg-saturation, heating, and gylcolnation) were used to determine the specific clay mineralogy.

Table 1. Cave mineral occurrence by cave type

	Calcite	Mg-Calcite	Aragonite	Gypsum	Fluorapatite	Hydroxylapatite	Chlorapatite	Carbonate-hydroxylapatite	Whitlockite	Brushite	Woodhouseite	Halite
Flank Margin Caves												
Hatchet Bay Cave	X	X	X	X	X	X	X	X	X	X	X	
Preacher's Cave	X	X		X	X		X			X		
Garden Cave	X		X									
Fleeing Lizard Cave	X			X								
Ten Bay Cave	X	X		X	X	X	X		X	X		
Knip Cave	X			X						X		
Littoral Caves												
Blow Hole Cave	X											X
Boiling Hole Cave	X											X

Cave mineral samples

A total of 36 samples were collected from flank margin caves on Eleuthera plus another 12 samples from littoral caves, pit caves, and blue holes. All 48 samples were analyzed for mineral identification. The location of mineral samples varied from cave to cave due to several factors including: number of entrances, humidity, presence of guano (fresh and degraded), presence of excavation pits within guano, and accumulations of crusts on walls and ledges. Most samples collected from Eleuthera caves were weathered crusts, earthy nodules, residual rinds beneath mined guano layers, and precipitates beneath active drips.

The identification of minerals was primarily done by means of XRD and inspection using a binocular microscope. Samples were air-dried, pulverized, sieved through a 45 micron mesh, and analyzed on a Rigaku Miniflex 600 at Sam Houston State University. XRD patterns were obtained as follows: continuous mode, 0.02° 2θ per step, 2° 2θ per minute, 3°–70° 2θ, CuKa radiation. An internal quartz standard was used. The overall results of the XRD analyses are tabulated in Table 1, and the representative XRD patterns are shown in figures 3 and 9.

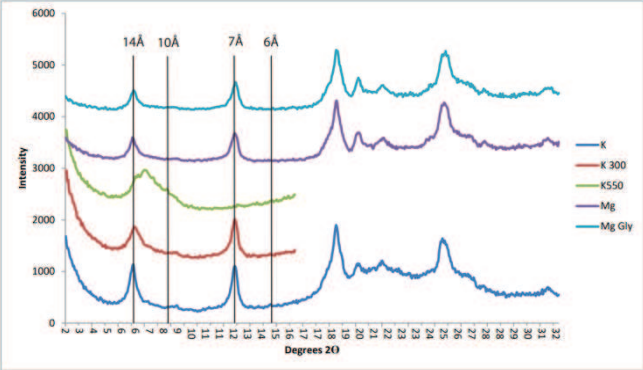

Figure 3. XRD analysis showing the various treatments of clay fractions of the paleosol sample from Hatchet Bay Cave.

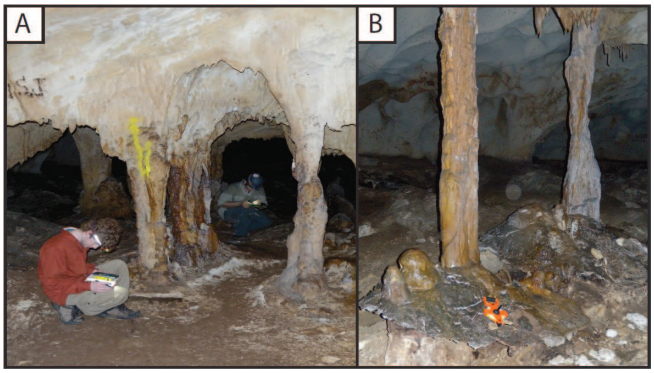

Figure 4. Both inactive (A) and active (B) carbonate speleothems in Hatchet Bay Cave.

RESULTS AND DISCUSSION

Paleosols

XRD analysis indicated the paleosol sample consists of a Fe-rich Chlorite, Illite, and Boehmite (Figure 3). Clay minerals observed were Fe-rich Chlorite ($(Fe^{+2},Mg,Al,Fe^{+3})_6(Si,Al)_4O_{10}(OH,O)_8$) and Illite ($K_{0.6}(H_3O)_{0.4}Al_{1.3}Mg_{0.3}Fe^{+2}_{0.1}Si_{3.5}O_{10}(OH)_2\cdot(H_2O)$) based on the 14 Å and 10 Å reflections. Boehmite (AlO(OH)) was identified by a reflection peak shift from 14 Å to 6.1 Å (Figure 3). Non-clay minerals included low Mg-calcite and quartz. Illite and chlorite were identified from the presence of 10Å and 14Å reflections which did not shift after treatment with ethylene glycol or collapse after heating to 550° C. The slightly larger [002] 7Å compared to the [001] 14Å peak indicates a Fe-rich chlorite. The origin of chlorite is most likely of a detrital nature from African dust.

Cave minerals

In the fifteen caves investigated, twelve cave minerals were identified. Hatchet Bay Cave contained eleven of the twelve minerals. Overall, flank margin caves contained more diverse accumulations of cave minerals compared to their littoral counterparts. The cave mineral results are summarized in Table 1. Only calcite was identified from pockets in the walls of pit caves and blue holes on Eleuthera, so those results were omitted from Table 1.

Specific mineral groups: Carbonates

Calcite is found in every cave investigated, making up the bulk of most of the speleothems (Figure 4). Aragonite is plentiful in drier portions of flank margin caves, such as Hatchet Bay Cave and Garden Cave, but it is mainly restricted to erratic speleothems, such as small helictites and eccentrics. No further details are given for calcite and aragonite due to their common appearance in the cave environment.

Specific mineral groups: Sulfates

Gypsum ($CaSO_4\bullet 2H_2O$) was the only documented sulfate mineral found during this reconnaissance. These gypsum deposits form mostly as crusts and blisters in several caves on Eleuthera (Figure 5). There are two mechanisms for Bahamian gypsum crusts: 1) evaporative processes acting on sea spray or saline water bodies in caves and 2) oxidation of biogenic pyrite producing sulfuric acid that reacts with eolianites (Bottrell et al., 1993; Onac et al., 2001, 2009).

Specific mineral groups: Phosphates

The second most abundant (by number) mineral group in Bahamian cave environments is the phosphate group due to the interaction of guano and leachates with carbonate rocks (Figure 6). Four varieties of apatite were documented (with only Hatchet Bay Cave hosting all four varieties). Brushite, whitlockite, and woodhouseite were other phosphates identified in Eleuthera caves. There were no ammonium phosphates identified, possibly because samples were not collected beneath active bat locations.

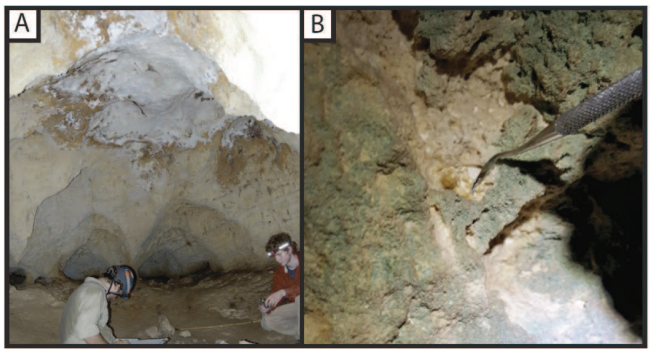

Figure 5. A) Gypsum crust on ceiling pocket of Knip Cave. B) Small gypsum blisters in Preacher's Cave.

Figure 6. Excavated guano pit with earthy phosphatic crusts at the guano-limestone interface and nitrate minerals located in the guano residue within the pit.

The apatite group (hydroxylapaite, $Ca_5(PO_4)_3(OH)$; chlorapatite, $Ca_5(PO_4)_3$ (Cl); carbonate-hydroxylapatite, $Ca_5(PO_4,CO_3)_3$ (OH); and fluorapatite, $Ca_5(PO_4)_3(F)$ was the most common phosphate mineral group identified in Eleuthera caves. The presence of fluorapatite and chlorapatite require marine waters to form and exist stably. These minerals are found in Hatchet Bay Cave, Ten Bay Cave, and Preacher's Cave, which all experience marine water spray. Dryer caves or caves with freshwater pools did not contain these two types of apatite.

The next most abundant phosphate was brushite ($CaHPO_4 \bullet 2H_20$). It formed small light brown crusts near the bottom of walls and on guano covered breakdown blocks. Brushite was almost always found in association with apatite mineral crusts. Similar relationships have been documented between apatite and brushite, which were interpreted to represent brushite replacement of hydroxylapatite (Onac et al., 2009).

Whitlockite ($Ca_9Mg(PO_3OH)(PO_4)_6$) was identified in Hatchet Bay Cave and Ten Bay Cave on wall crusts at the base of cave wall deposits. The whitlockite likely formed by the Mg-enriched solutions derived from sea-spray descending through guano deposits.

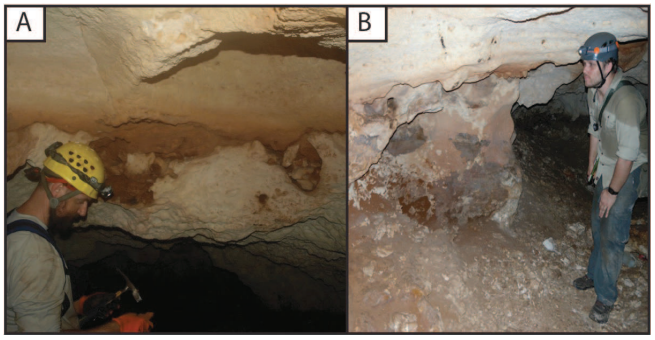

Figure 7. A) Paleosol surface within Hatchet Bay Cave collecting guano in small pockets. B) Sampling location showing bat guano (brownish red) accumulating on paleosol within Hatchet Bay Cave. Dark Brown crust on paleosol was identified as woodhouseite. Whitlockite was also found on the wallrock at the base of the wall, well below the woodhouseite crust.

Woodhouseite ($CaAl_3(SO_4)(PO_4)(OH)_6$) is part of the alunite supergroup and has been previously been reported as the product of bat guano in cave environments (Hill and Forti, 1997). This mineral has not been previously reported from caves in The Bahamas. Woodhouseite samples came from Hatchet Bay Cave, specifically from small crusts found on the exposed paleosol within the cave (Figures 7 and 8). The presence of

woodhouseite was confirmed in three samples from various locations within the cave using XRD analysis (Figures 8 and 9). Woodhouseite formation in this instance likely represents phosphate-rich leachate derived from the combination of seawater and guano interacting with the various aluminum-rich phases found within the clay fraction of the paleosol.

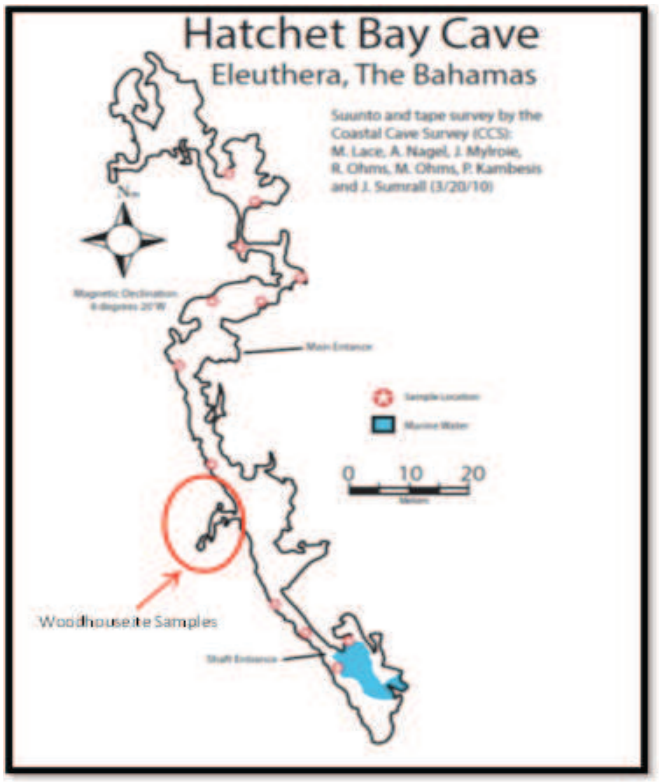

Figure 8. Simplified cave map of Hatchet Bay Cave showing sampling locations, noting the key locations of woodhouseite.

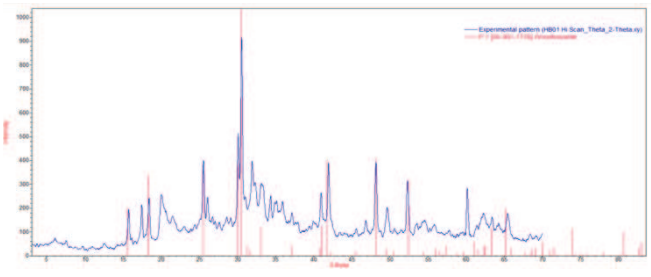

Figure 9. Representative XRD spectrum of woodhouseite from Hatchet Bay Cave.

Specific mineral groups: Halides

Halite (NaCl) was identified by XRD analysis at two locations on Eleuthera, Blow Hole Cave and Boiling Hole Cave. Both locations are littoral caves that fall well within the wave action zone. The origin of halite was interpreted as precipitation from aerosols and wave-splashed seawater inside the cave. The samples were found in ceiling and wall pockets during low tide as white crusts.

Specific mineral groups: Silicates

Clay minerals and quartz were documented in the paleosol found in Hatchet Bay Cave. While these were not considered cave minerals as being the product of a cave environment, their presence inside of the cave is worth documenting. Quartz specifically has an origin as an aerosol dust from Africa.

Relationship between paleosols and cave minerals

Bahamian caves, especially flank margin caves, have shown a relatively high diversity of cave minerals (Onac et al., 2001, 2009). Eleutheran caves show no exception to this trend. One difference that has been documented in Eleutheran caves was sampling from a cave that has a paleosol within it (Hatchet Bay Cave). Paleosol mineralogy was explored after woodhouseite was positively identified in three samples from Hatchet Bay Cave. The mechanism of woodhouseite's origin was dependent upon the identification of an aluminum bearing phase in an environment where both sulfate and phosphate ions were readily accessible. Clay mineral analysis of paleosols from Hatchet Bay Cave revealed that aluminum phases (boehmite, illite, and chlorite) were present. The interaction with phosphatic solutions leached from bat guano coupled with either sea spray or marine groundwater would account for the anion complexes found in woodhouseite. It is hypothesized that the interaction of this leachate specifically with the minerals found in the paleosol in the cave would account for woodhouseite formation, as well as other non-silicate mineral phases. This study suggests that other flank margin caves with exposed paleosols should also contain the appropriate environment for woodhouseite formation. Cave microclimate

may have also play a role, especially in determining the humidity, temperature, and other geochemical parameters required for woodhouseite formation in The Bahamas. It is also uncertain the role that previous highstands of sea level (i.e. MIS 5e) would play in older guano deposits. These questions are beyond the scope of this study, but they warrant future study.

CONCLUSIONS

Eleuthera caves contain a wide variety of minerals associated with marine water and bat guano. The presence of paleosols in a flank margin cave environment allowed for the documentation of one particularly rare phosphate mineral, woodhouseite ($CaAl_3(SO_4)(PO_4)(OH)_6$) that has not been previously documented in Bahamian caves. Paleosol analyses revealed the presence of mineral phases capable of forming complex phosphate minerals when exposed to guano in a cave environment. Mineralogic evidence from Hatchet Bay Cave was interpreted to represent the interaction of aluminum phases from an exposed paleosol with leachate from bat guano. In addition to woodhouseite, several mineral groups are well represented in the caves of Eleuthera. However, more samples are needed from additional locations within caves and additional caves to achieve a better cave mineral inventory.

ACKNOWLEDGMENTS

The authors would like to thank Dr. John Mylroie for logistical assistance in planning this research, Mike Lace for assistance with cave data, and the BEST Commission in The Bahamas for permission to do this work.

REFERENCES

Birmingham, A.N., Carew, J.L. and Mylroie, J.E. 2008. The use of plant tracefossils to differentiate transgressive-phase from regressive-phase Quaternary eoliancalcarenites, San Salvador Island, Bahamas. In *2008 Joint Meeting of The Geological Society of America, Soil Science Society of America, American Society of Agronomy, Crop Science Society of America, Gulf Coast Association of Geological Societies with the Gulf Coast Section of SEPM.*

Bottrell, S.H., Carew, J.L., and Mylroie, J.E. 1993. September. Inorganic and bacteriogenic origins for sulfate crusts in flank margin caves, San Salvador Island, Bahamas. Pp. 17-21. In B. White and D.R. Gerace (Eds.). *Proceedings of the Sixth Symposium on the Geology of the Bahamas*. Port Charlotte, Florida, Bahamian Field Station.

Carew, J.L., and Mylroie, J.E. 1995. Geology of the Bahamas. *Bahamas Journal of Science 2*(3): 2-16.

Hill, C.A., and Forti, P. (Eds.). 1997. *Cave Minerals of the World* (Vol. 2). National Speleological Society, 463 p.

Infante, L.R. 2012. The origin of banana holes on San Salvador Island, The Bahamas. Mississippi State University.

Kindler, P., Mylroie, J.E., Curran, H.A., Carew, J.L., Gamble, D.W., Rothfus, T.A., Savarese, M. and Sealey, N.E. 2010. *Geology of Central Eleuthera, Bahamas: A Field Trip Guide*. Gerace Research Centre, San Salvador.

Larson, E.B., and Mylroie, J.E. 2014. A review of whiting formation in the Bahamas and new models. *Carbonates and Evaporates* 29(4): 337-347.

Melim, L.A. and Masaferro, J.L. 1997. Geology of the Bahamas: subsurface geology of the Bahamas banks. Pp. 161-182. In H.L. Vacher and T. Quinn (Eds.). *Geology and Hydrogeology of Carbonate Islands*, Developments in Sedimentology 54, Elsevier, Amsterdam.

Muhs, D.R., Bush, C.A., Stewart, K.C., Rowland, T.R. and Crittenden, R.C. 1990.

Geochemical evidence of Saharan dust parent material for soils developed on Quaternary limestones of Caribbean and western Atlantic islands. *Quaternary Research* 33: 157-177.

Mylroie, J.E. and Carew, J.L. 1995. Geology and karst geomorphology of San Salvador Island, Bahamas. *Carbonates and Evaporites* 10: 193-206.

Mylroie, J.R., and Mylroie, J.E. 2007. Development of the carbonate island karst model. *Journal of Cave and Karst Studies* 69: 59-75.

Mylroie, J. E., Ho, H.C., Infante, L.R., Kambesis, P.K., and Leist, J.W. 2015. Banana holes as syndepositional flank margin caves within an advancing strandplain and their prediction using fuzzy-based modeling. Pp. 222-236. In B. Glumac and M. Savarese (Eds.). *Proceedings of the 16th Symposium on the Geology of the Bahamas and other Carbonate Regions*. Gerace Research Centre, San Savador, The Bahamas.

Mylroie, J.E., Birmingham, A.N., and Mylroie, J.R. 2017. Vegemorphs as a means to differentiate transgressive-phase from regressive-phase Quaternary eolian calcarenites, San Salvador Island, Bahamas. *The 2nd Joint Symposium on the Natural History and Geology of The Bahamas* [abstract].

Onac, B.P., Mylroie, J.E., and White, W.B. 2001. Mineralogy of cave deposits on San Salvador island, Bahamas. *Carbonates and Evaporites* 16: 8-16.

Onac, B.P., Sumrall, J., Mylroie, J.E. and Kearns, J.B. 2009. *Cave Minerals of San Salvador Island, Bahamas*. University of South Florida Tampa Library, 70 p.

HURRICANE JOAQUIN IMPACTS ON OYSTER POND, SAN SALVADOR, THE BAHAMAS

Dawn M. Ford, Jalana Abernathy, Luke Black,
Ann Holmes, Ashton Mitchell, Sabrina Novak, and Alex Schwartz

The University of Tennessee at Chattanooga
615 McCallie Avenue, Chattanooga, TN 37403

ABSTRACT

In 2015, Hurricane Joaquin directly impacted San Salvador and disturbed the mangrove vegetation, pond biota, and sediment of many interior ponds, including Oyster Pond. Oyster Pond is a fully marine pond lined by red mangroves (*Rhizophora mangle*) and has several conduits connecting the pond to the ocean and perhaps to other ponds. The post-hurricane recovery of pond biota, specifically those species living on biotic outcroppings and mangrove prop roots, was investigated with a focus on macroalgae and macroinvertebrates. Comparisons with pre-hurricane data reveal that while there was not a reduction in macroinvertebrate species richness, there has been a loss of three red macroalgal species and one green algae since the hurricane. Further, in comparing the western side of the pond to the less impacted eastern side of the pond, the data suggest that more damaged mangroves can support fewer algal and macroinvertebrate species and in less abundances than healthier mangroves. The detrital nature of mangrove systems may explain this finding. An interesting discovery was a small crab documented for the first time in Oyster Pond and the identification of this species is still being investigated.

INTRODUCTION

Impacts of hurricanes on natural systems

Hurricanes occur commonly in The Bahamas, and on average, a tropical storm or hurricane has impacted San Salvador every 2.42 years since 1851 (Hurricanecity.com, 2017). Hurricanes cause large-scale disturbance to coastal ecosystems. For example, a meta-analysis of data from over 280 coral reef sites revealed that coral cover declines an average of 17% in the year following a hurricane impact (Gardner et al., 2005). The loss of coral increases with hurricane intensity and with time passed since impact; reefs seem to take at least eight years to recover to the pre-hurricane state (Gardner et al., 2005).

Hurricane impacts on seagrass beds have been studied extensively (Anton et al., 2009; Carlson et al., 2010). Seagrass beds are relatively resistant to storms as seagrasses have a deeply rooted rhizome system. In Florida and the Caribbean, seagrass beds are dominated by *Thalassia testudinum* (turtle grass) and are mixed with two other seagrass species and many macroalgal species. Studies have shown that seagrass coverage declines by only a few percent after a hurricane while the green calcareous macroalgae show much greater losses (24%-70%) (Cruz-Palacious and Van Tussenbrock, 2005; Fourqurean and Rutten, 2004).

In mangrove forests, hurricanes can cause mangrove trees to be broken, defoliated, and killed by high winds, storm surge, and lightning strikes (Zhang et al., 2016). Some species of mangroves are more susceptible to disturbances than others. For example, rhizophoraceae mangrove species, like the red mangrove, have higher mortality rates from hurricanes as compared to non-rhizophoraceae groups (Wang et al., 2014). Hurricane damage to red mangroves takes 4-7 months to reach full extent and trees take 2-6 years to recover (Feller et al., 2015).

While much research has been done on the hurricane impacts of coral reefs, seagrass beds, and mangroves, few studies have focused on inland ponds and lakes. San Salvador's landscape has high ridges and a high density of inland lakes and ponds. Often these ponds and lakes offer unique archives of storm records in the form of tempestites

(Park et al., 2009; Mattheus and Fowler, 2015). Tempestites are sedimentary layers composed of grains, including ooids, rounded shell fragments, etc., that originated in a beach environment and have been transported by storms into low-energy environments such as marshes and ponds. Tempestites have been reported from many coastal San Salvador ponds (Button et al., 2007; McCabe and Niemi, 2008; Park et al., 2009; Sipahioglu et al., 2010; Park, 2012; Dalman and Park, 2012; Mattheus and Fowler, 2015; Billingsley and Niemi, 2016).

Previous studies of inland ponds and lakes have been focused on specific groups of organisms. Park et al. (2009) found that ostracods in a hypersaline lake increase in abundance and diversity after storm events. Yannarell et al. (2007, p. 576) reported that microbial mats in a hypersaline pond experienced a "significant shift" in the cyanobacteria and diazotrophs post-hurricane, with a dominance of organisms that were rare before the hurricane. Cole et al. (2007) compared a modestly hypersaline pond lacking outlets to the sea with a marine pond served by numerous conduits and found that the scaly pearl oyster responded differently depending on how quickly marine salinity was restored following heavy rainfall. The current study adds to the work of hurricane impacts on interior ponds, but focuses on the broad biotic response of macroinvertebrates and macroalgae in an interior marine pond. Specifically, we compared the macroalgal and macroinvertebrate species richness and species composition before and after the hurricane in Oyster Pond.

Hurricane Joaquin

Hurricane Joaquin was a Category 4 storm (Saffir-Simpson Hurricane Wind Scale) when it affected the central and southeastern Bahamas (Figure 1; Berg, 2016). It was the strongest October hurricane impacting The Bahamas since 1866 and made landfall as a major hurricane on San Salvador on October 2, 2015. The eyewall passed directly over the island. Hurricane Joaquin had estimated maximum sustained winds of 138 mph when the eye of the storm passed between Crooked Island and Long Island. Joaquin produced storm surges of 4-5 m (12-15 ft), and while there were no official rainfall measurements, the Bahamas Department of Meteorology estimated 130-260 mm (5-10 inches) (Berg, 2016). The impact of this storm to San Salvador has been mostly described in terms of infrastructure. The National Hurricane Center reported that San Salvador's roads were impassable, the airport was destroyed, homes were damaged, and power lines were downed (Berg, 2016). Since the storm, the airport has been rebuilt, power lines repaired, and most roads are passable again.

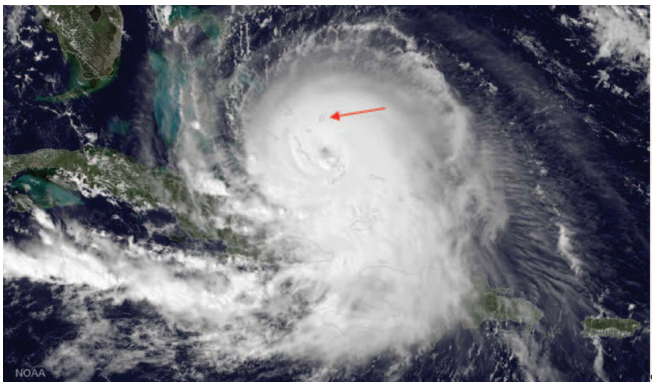

Figure 1. NOAA satellite image, October 1 2015, near central and southeastern Bahamas. Arrow points to San Salvador.

For this study, our research question was: How did Hurricane Joaquin impact Oyster Pond? To address this question, we analyzed the macroinvertebrate and macroalgal species composition, sediment (for tempestites), and water chemistry of the pond.

FIELD SITE DESCRIPTION

Oyster Pond is a marine pond on the north end of the island of San Salvador (Figure 2). This pond is a dissolution and collapse feature that formed from the dissolution of diagenetically immature eogenetic limestones (Park Boush et al., 2014). The pond has conduits that connect it with the ocean and therefore, has a marine salinity and diurnal tidal fluctuations of 20-30 cm. Oyster Pond, like many interior ponds, contains several microhabitats (Figure 3). Red mangroves and their

prop roots ring the pond's margin, protecting the pond from strong winds and erosion. Many epibiota make their home on the prop roots. Away from shore, an organic flocculent layer rests along the hard carbonate bottom of the pond and is made up of decomposing organisms and mangrove leaves. Outcroppings emerge from the carbonate bottom as an accumulation of biotic growths consisting of a variety of algae and invertebrate species. Conduit mouths, which connect Oyster Pond to the ocean, are also home to a few species.

Figure 2. Oyster Pond (marked by red triangle) is approximately one mile south of the Gerace Research Centre (marked by yellow star), along the GRC trail (shown as a white line).

METHODS

The epibiota of mangrove prop roots, the biota of outcroppings, water chemistry, and sediment content were evaluated post-hurricane in March 2016, March 2017, and June 2017. The biota and water chemistry data were compared to pre-existing pre-hurricane data from March 2015. Pre-hurricane data were from a visual survey and not separated by microhabitat type, so comparisons to 2015 are limited to overall species presence/absence and species richness.

In March 2016 and 2017, 20 m transects were established along the shoreline of the pond. Four were sampled in 2016 (east and west of pond entrance) and four were sampled in 2017 (east, west, north, and south sides of the pond). At 5 m intervals, a 1-m^2 quadrat was used (0.25 m^2 quadrant used in 2016). Within each quadrat, percent coverage of species was estimated and all visible macroinvertebrate and macroalgae species were documented. The quadrats formed a vertical window against the prop roots.

In March 2016 and 2017, outcroppings were surveyed *in situ* using the line intercept method with transects starting from the north edge of the pond toward the middle of the pond until the outcroppings disappeared (approximately 25 m). Three transects were sampled in 2016 and four transects in 2017. Within 1 m quadrats, species were identified, and percent coverage was estimated.

Additional data collection: In March 2017, conduit mouths and the flocculent layer were studied through a brief visual survey (no transects or quadrats). In June 2017, a brief visual survey of mangrove prop roots and outcroppings was conducted, and these additional documented species are included in the results. All of these post-hurricane data were compared to March 2015 data reported by Ford and Abernathy (2017).

During every data collection period, biotic samples and photographs of the outcroppings and mangrove roots were taken for further identification and analysis using webpages, a digital microscope (Plugable USB 2.0), and identification books and field guides including *Marine Plants of the Caribbean* (Littler et al., 1989), *Caribbean Reef Plants* (Littler and Littler, 2000), and *Natural History of Northeastern San Salvador Island* (Godfrey et al., 1994). Also during every data collection period, two water samples were collected within 1 m of the water surface of the pond for testing. The pH and salinity of the water samples were measured using a standard calibrated pH meter and refractometer (salinity).

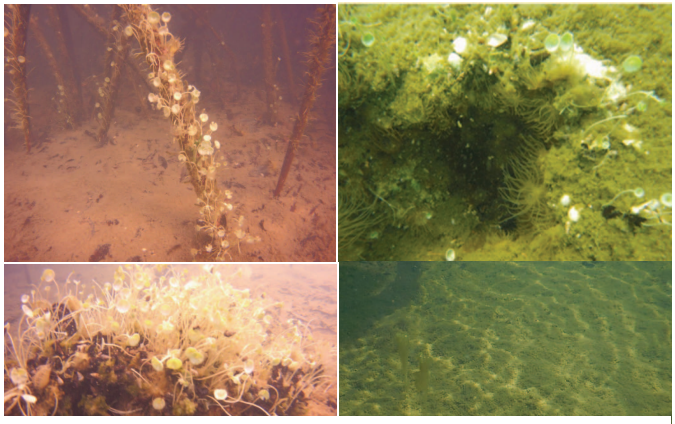

Figure 3. Microhabitats found in Oyster Pond: a) Red mangrove prop roots, b) Conduit mouth, c) Biotic outcropping, d) Flocculent layer.

For the sediment core in March 2016, a clear 3 inch diameter, 30-cm-long polycarbonate tube was used. The tube was pushed into the pond's bottom layers. A plastic cap was applied to the top of the tube creating suction, and the core was slowly extracted. Another plastic cap was placed on the bottom of the core before removing from the pond to better contain the unconsolidated core constituents.

RESULTS

Pre-Hurricane Biota

In March 2015, we documented a total of 24 macroinvertebrate and macroalgal species on mangrove roots, biotic outcroppings, and the flocculent layer. These organisms included 3 species of red algae and an uncommon type of green algae, *Pedobesi*a (Table 1) which were all found on the mangrove roots. General observations and photographs indicate that the water was very clear and the flocculent layer had some lugworm egg sacs.

Post-Hurricane Biota

Overall Oyster Pond species presence & richness

Post-hurricane, a total of 19 macroinvertebrate and macroalgal species were identified in 2016 and 23 species in 2017 (Table 1). The macroinvertebrate species richness stayed consistent in 2016 (no decrease after hurricane). However, a higher number of invertebrate species were documented in 2017, which is probably due to the researchers spending more time in Oyster Pond. For macroalgae, the number of species documented in 2016 (5) was half of pre-hurricane numbers and in 2017, that number increased to 6. All red algae species identified in 2015 have not been seen since the hurricane.

Mangrove prop roots

In 2016 and 2017, red mangroves were visibly impacted (defoliation and broken branches) compared to pre-hurricane conditions (Figure 4). The impact was more severe on the western and northern sides (pond entrance is on the north end), as compared to the eastern and southern sides of the pond. This trend is also reflected in the biotic coverage of the prop roots sampled in 2017 (Table 2).

The dominant macroalgae and invertebrate species on mangrove prop roots post-hurricane varied across areas of the pond, but there were some species in common (Table 1). Two species of *Acetabularia*, a common green alga, were very abundant in all sampled areas along with *Isognomon alatus* (black mangrove oyster).

Biotic outcroppings

The species that dominated biotic outcroppings post-hurricane were like those that dominated the mangrove prop roots. *Pinctada longisquamosa*, *Isognomon alatus,* species of *Acetabularia,* and species of sea anemone (*Bartholomea annulate*, *Aiptasia pallida*) (Table 2). A new species found on outcroppings not documented before in Oyster Pond was an undetermined crab in summer 2017. This crab was very small with a carapace approximately 0.75 cm in diameter.

Water chemistry and sediment

Water chemistry in Oyster Pond has slightly varied over time (Table 3). It seems that the pond recovered quickly after the hurricane in October 2015 as the post-hurricane data are very similar to the pre-hurricane data. The pH is slightly basic, and salinity is marine.

Scientific Name	2015 Pre-Hurricane	2016 Post-Hurricane	2017 Post-Hurricane	Microhabitat*
MACROINVERTEBRATES				
Annelids				
Trypanosyllis spp., Claparède, 1864	x	x	x	OC
Arenicola cristata, Simpson 1856	x	x	x	CM, FL
Harmothoe spp., Kinberg, 1856			x	OC
Arthropods				
Gammarus spp., Fabricius ,1775	x	x	x	OC
Undetermined crab species			x	OC
Cnidarians				
Aiptasia pallida, Agassiz in Verrill 1864	x	x	x	CM, MR, OC
Bartholomea annulate, Le Sueur 1817	x	x	x	MR, OC
Bougainvillia spp., Lesson 1830	x	x	x	MR
Echinoderms				
Synaptula hydriformis, Lesueur, 1824	x	x	x	OC
Ophiuroidea spp., Gray 1840	x	x	x	OC
Mollusks				
Batillaria spp., Benson 1842	x	x	x	MR, OC
Bulla umbilicate, Montagu, 1803			x	OC
Cerithium lutosum, Menke 1828	x	x	x	CM, MR, OC
Isognomon alatus, Gmelin, 1791	x	x	x	CM, MR, OC
Pinctada longisquamosa, Dunker 1852	x	x	x	CM, MR, OC
Sponges				
Chondrilla nucula, Schmidt, 1862	x	x	x	MR, OC
Unknown sponge species	x	x	x	OC
Macroinvertebrate Species Richness	**14**	**14**	**17**	
MACROALGAE				
Green Algae				
Acetabularia crenulate, J.V. Lamouroux, 1816	x	x	x	CM, MR, OC
Acetabularia calyculus, J.V. Lamouroux 1824	x	x	x	CM, MR, OC
Anadyomene stellate, (Wulfen) C. Agardh 1823	x		x	CM, MR
Batophora oerstedii, J. Agardh 1854	x	x	x	MR, OC
Cladophoropsis macromeres, W.R. Taylor 1928	x	x	x	OC
Dictyosphaeria ocellata, (M. Howe) Olsen-Stojkovich 1985	x	x	x	MR, OC
Pedobesia spp., MacRaild & Womersley, 1974	x			MR
Red Algae				
Dasya crouaniana, Agardh, 1890	x			MR
Polysiphonia spp., Greville 1823	x			MR
Spyridia spp., Harvey 1833	x			MR
Macroalgae Species Richness	**10**	**5**	**6**	
TOTAL SPECIES RICHNESS	**24**	**19**	**23**	

*Table 1. Oyster Pond species richness data. Microhabitat codes: CM (conduit mouth), FL (flocculent layer), OC (outcropping), MR (mangrove root). * The three color morphs of the naked sea cucumber (clear, brown, and tiger-striped) were documented*

	North	West	South	East
Total Biotic Coverage of Prop Roots	50%	40%	80%	70%
Dominant Species by Percent Coverage (in order)	*Acetabularia spp.* *Isognomon alatus* *Pinctada longisquamosa* *Batophora oerstedii*	*Bougainvillia spp.* *Acetabularia spp.* *Isognomon alatus*	*Isognomon alatus* *Bougainvillia spp.* *Acetabularia spp*	*Acetabularia spp.* *Pinctada longisquamosa* *Isognomon alatus* *Batophora oerstedii*

Table 2. Mangrove prop root biotic coverage and dominant species in areas of the pond (March 2017).

The Oyster Pond sediment core contained 3.5 cm shell-hash layer resting directly on bedrock, capped by ~10 cm of reddish-brown clay, which was overlain by ~2 cm of a second shell hash layer, topped by ~2 cm of flocculent layer (Figure 5). There was no evidence of tempestites in this core.

	2012* (pre-hurricane)	2015 (pre-hurricane)	2016 (post-hurricane)	2017 (post-hurricane)
pH		7.74	7.45	7.49
Salinity (ppt)	37.1	34.5	35.0	37.0

Table 3. Water chemistry results, 2012-2017 Rothfus (2012).

Oyster Pond has an interesting and unique set of organisms that inhabit the mangrove prop roots, biotic outcroppings, the conduit mouths, and flocculent layer. While there were obvious biological impacts from the hurricane, it is important to note that the biota of the pond seem to naturally change from year to year without disturbance. For example, the first year we explored the pond in 2014, there was an extensive sponge garden on the north end that we have not seen since. The water quality data showed little variation over time which demonstrates that despite heavy rainfall in a short period of time, the conduits provide enough connection to the ocean to recover a marine salinity and pH quickly.

Overall, the impact of Hurricane Joaquin caused a decline in macroalgae, especially species of red algae. After the hurricane, the red mangrove prop roots were more populated by epibiota on the south and east sides of the pond as compared to the north and west areas of the pond. This could be explained by the direction of the winds as the Category 4 hurricane moved over the island. The mangrove prop roots had robust populations of scaly pearl oysters and black mangrove oysters; but few burnt mussels. Cole et al. (2007) found that the scaly pearl oyster population was "relatively intact" after Hurricane Frances and found that burnt mussels dominated prop root communities (by counts, not percent coverage), which contradicts findings of this study. It seems there has been a shift in the dominant oyster species in the pond since the Cole et al. (2007) study.

Acetabularia is a very hardy green macroalgal species and is consistently the most abundant macroalgae in Oyster Pond, pre- and post-hurricane. Its thallus is calcified, and it attaches firmly by its rhizoids to substrates such as mangrove prop roots, bivalve shells, and biotic outcroppings which may contribute to its ability to withstand stressors. On the other hand, some fleshy red macroalgae (*Dasya spp.*, *Polysiphonia spp.*, *Spyridia spp.*) were seemingly wiped out by the hurricane and have not re-established as of summer 2017. These fleshy macroalgae are easily removed from substratum (Precht et al., 2009). There may be factors other than mechanical stress, such as nutrient levels, that influence the presence of these red algal species after a disturbance (Bertocci et al., 2017).

Figure 5. Oyster Pond southern conduit core taken in 2016. Shell-hash layer on bottom not visible due to lower core cap. Upper shell hash is likely hurricane deposit.

The presence of shell-hash layers along the bottom of Oyster Pond is attributed to storm events, which create high energy in a normally low-energy environment subjected only to tidal fluctuations. However, no tempestites were found in Oyster Pond. We believe this is due to the position of the pond behind high ridges and being farther inland than other coastal ponds where tempestites have been found.

A discovery of a species that has not, to our knowledge, been documented in Oyster Pond

before is a very small marine crab. While we were not able to identify the crab due to its small size and condition, there are a couple of possibilities to investigate further. More than 20 years ago, Godfrey et al. (1994) documented *Armases miersii* in the Crab Hole (tidal pool) along the same interior trail. In addition, there is a pea crab species (*Pinnixa cylindrica*) known to have a commensal relationship with lugworms that may live in the worm burrow for protection (Ruppert and Fox, 1988).

An interesting finding was the change in quantity of lug worms egg sacs over time. Lugworms are organisms that burrow into the flocculent layer of the pond. In the spring, lugworms release a gelatinous egg mass that is connected at one end to the burrow opening (Ruppert and Fox, 1988). In March 2015 – before the hurricane - there were lug worm eggs sacs present, but not in abundance. Six months after the hurricane, in March 2016, there was a high density of lug worm eggs sacs. Did the disturbance cause the lugworms to reproduce more than normal? This could be the focus of future research.

A limitation of this study is that because this study used visual and transect sampling methods, there are likely species there were not documented. Another limitation is that our sampling methods varied over time.

ACKNOWLEDGMENTS

We would like to thank the Gerace Research Centre for graciously hosting our UTC groups each year and providing much needed assistance in completing this work. This research was performed by permission of the The Bahamas Environment, Science, and Technology (BEST) Commission, Nassau, the Bahamas.

REFERENCES

Anton, A., Cebrian, J., Duarte, C.M., Heck, J., Kenneth, L., and Goff, J. 2009. Low impact of Hurricane Katrina on seagrass community structure and functioning in the northern Gulf of Mexico. *Bulletin of Marine Science 85*(1): 45-59.

Berg, R. 2016. National Hurricane Center Tropical Cyclone Report: Hurricane Joaquin. National Hurricane Center, January 12, 2016. Available: https://www.nhc.noaa.gov/data/tcr/AL112015_Joaquin.pdf.

Bertocci, I., Domínguez Godino, J. A., Freitas, C., Incera, M., Bio, A., and Domínguez, R. 2017. Compounded perturbations in coastal areas: contrasting responses to nutrient enrichment and the regime of storm-related disturbance depend on life-history traits. *Functional Ecology* 31(5): 1122-1134.

Billingsley, A.L. and Niemi, T.M. 2016. Paleoenvironmental reconstruction of Triangle Pond (San Salvador Island, Bahamas) through stratigraphic and elemental analysis of a sediment core. Pp. 84-94. In B. Glumac and M. Savarese, (Eds.). *Proceedings of the 16th Symposium on the Geology of the Bahamas and other Carbonate Regions*. Gerace Research Centre, San Salvador, The Bahamas.

Button, J.A., Lanterman, L.L., and Erdman, R.B. 2007. Physical and geological characteristics of Mermaid Pond, an anchialine lake on San Salvador Island, Bahamas. Pp. 14-20. In B.J. Rathcke and W.K. Hayes (Eds.). *Proceedings of the 11th Symposium on the Geology of the Bahamas and other Carbonate Regions*. Gerace Research Centre, San Salvador, The Bahamas.

Carlson, P.R., Yarbro, L.A., Kaufman, K.A., and Mattson, R.A. 2010. Vulnerability and resilience of seagrasses to hurricane and runoff impacts along Florida's west coast. *Hydrobiologia* 649(1): 39-53.

Cole, E., Hoft, N., Campion, J., and Cole, B. 2007. The effect of hurricane activity on scaly pearl oysters, *Pinctada longisquamosa*, in two dissimilar inland marine ponds on San Salvador

Island, Bahamas. Pp. 78-89. In B.J. Rathcke and W.K. Hayes (Eds.). *Proceedings of the 11th Symposium on the Natural History of the Bahamas.* Gerace Research Centre, San Salvador, The Bahamas.

Cruz-Palacios,V., and Van Tussenbroek, B.I. 2005. Simulation of hurricane-like disturbances on a Caribbean seagrass bed. *Journal of Experimental Marine Biology and Ecology* 324(1): 44-60.

Dalman, M.R., and Park, L.E. 2012. Tracking hurricane and climate change records in a Bahamian coastal lake: Clear Pond, San Salvador Island, Bahamas. Pp. 15-32. In D.W. Gamble and P. Kindler (Eds.). *Proceedings of the 15th Symposium on the Geology of the Bahamas and other Carbonate Regions.* Gerace Research Centre, San Salvador, The Bahamas.

Feller, I.C., Dangremond, E.M., Devlin, D.J., Lovelock, C.E., Proffitt, C.E., and Rodriguez, W. 2015. Nutrient enrichment intensifies impact in scrub mangrove ecosystems in Indian River Lagoon, Florida, USA. *Ecology* 96(11): 2960-2972. doi: 10.1890/14-1853.1.

Ford, D., and Abernathy, J. 2017. Algae, fish, and invertebrate survey of Reckley Hill, Crescent, and Oyster Ponds. Pp. 188. In C.L. Landry, L.J. Floreas, and D.S. Kjar (Eds.) *Proceedings of the 1st Joint Natural History and Geology of the Bahamas Conference* [abstract].

Fourqurean, J.W., and Rutten, L.M. 2004. The impact of Hurricane Georges on soft-bottom, backreef communities: site- and species-specific effects in south Florida seagrass beds. *Bulletin of Marine Science* 75(2): 239-257.

Gardner, T.A., Cote, I.M., Gill, J.A., Grant, A., and Watkinson, A.R. 2005. Hurricanes and Caribbean coral reefs: impacts, recovery patterns, and role in long-term decline. *Ecology* 86(1): 174-184.

Godfrey, P.J., Edwards, D.C., Smith. R.R., and David, R. Laurence. 1994. *Natural History of Northeastern San Salvador Island: A "New World" Where the New World began.* Bahamas Field Station, San Salvador, Bahamas.

HurricaneCity.com. (2017). San Salvador Island Bahamas history with tropical systems. Available at http://www.hurricanecity.com/city/sansalvador.htm.

Littler, D.S., and Littler, M.M. 2000. *Caribbean Reef Plants*. Offshore Graphics.

Littler, D.S., Littler, M.M., Bucher, K.E., and Norris, J.N. 1989. *Marine Plants of the Caribbean; a Field Guide from Florida to Brazil*. Smithsonian Institution Press.

Mattheus, C.R., and Fowler, J.K. 2015. Paleotempestite distribution across an isolated carbonate platform, San Salvador Island, Bahamas. *Journal of Coastal Research* 31: 872-858. doi 10.2112/JCOASTRES-D-14-00077.1

McCabe, J.M., and Niemi, T.M. 2008. The 2004 Hurricane Frances overwash deposition in Salt Pond, San Salvador, Bahamas. Pp. 25-41, In L.E. Park and D. Freile (Eds.). *Proceedings of the 13th Symposium on the Geology of the Bahamas and other Carbonate Regions*. Gerace Research Centre, San Salvador, The Bahamas.

Park, L.E., Siewers, F.D., Metzger, T., and Sipahioglu, S. 2009. After the hurricane hits: recovery and response to large storm events in a saline lake, San Salvador Islands, Bahamas. *Quaternary International* 195: 98-105. doi: 10.1016/j.quaint.2008.06.010

Park, L.E. 2012. Comparing two long-term hurricane frequency and intensity records from San Salvador Island, Bahamas. *Journal of Coastal Research* 28: 891-902. doi:10.2112/jcoastres-d-11-00065.1

Park Boush, L.E., Myrbo, A., and Michelson, A. 2014. A qualitative and quantitative model for climate-driven lake formation on carbonate platforms based on examples from the Bahamian archipelago. *Carbonates Evaporites* 29: 409-418.

Precht, W., Aronson, R., and Deslarzes, K. 2009. Post-hurricane assessment of sensitive habitats of the Flower Garden Banks Vicinity. NOAA Report 39574 (MO6PC00003).

Rothfus, E. 2012. Water quality monitoring of San Salvadorian inland lakes. Pp. 129-138. In D.W. Gamble and P. Kindler (Eds.). *Proceedings of the 15th Symposium on the Geology of the Bahamas and other Carbonate Regions*. Gerace Research Centre, San Salvador, Bahamas.

Ruppert, E.E., and Fox, R.S. 1988. *Seashore Animals of the Southeast: A Guide to Common Shallow-water Invertebrates of the Southeastern Atlantic Coast*. University of South Carolina Press.

Sipahioglu, S.M., Park, L.E., and Siewers, F.D. 2010. Tracking storms through time: Event deposition and biologic response in Storr's Lake, San Salvador Island, Bahamas. Pp. 220-236. In F.D. Siewers and J.B. Martin (Eds.). *Proceedings of the 14th Symposium on the Geology of the Bahamas and other Carbonate Regions.* Gerace Research Centre, San Salvador, The Bahamas.

Wang, X., Wang, W., and Tong, C. 2016. A review on impact of typhoons and hurricanes on coastal wetland ecosystems. *Acta Ecologica Sinica* 36(1): 23-29. doi: 10.1016/j.chnaes. 2015.12.006.

Yannarell, A.C., Steppe, T.F., and Paerl, H.W., 2007. Disturbance and recovery of micro- bial community structure and function fol- lowing Hurricane Frances: *Environmental Microbiology* 9(3): 576-583.

Zhang, K., Thapa, B., Ross, M., and Gann, D. 2016. Remoting sensing of seasonal changes and disturbances in mangrove forest: A case study from South Florida. *Ecosphere* 7(6): e01366. doi: 10.1002/ecs2.1366.

GEOMORPHOLOGY OF THE LATE HOLOCENE SANDY HOOK STRANDPLAIN, SAN SALVADOR ISLAND, THE BAHAMAS: A RECORD OF CHANGING HYDRODYNAMICS

Christopher R. Mattheus[1], Salam A. Farhan[2], and Joshua K. Fowler[2]

[1]Delaware Geological Survey, University of Delaware
Newark, DE

[2] Department of Geological and Environmental Sciences, Youngstown State University
Youngstown, OH 44555

ABSTRACT

The geomorphology of Sandy Hook, a late Holocene strandplain on the isolated Bahamian carbonate platform of San Salvador, is evaluated using subsurface geophysics and a GIS-based characterization of ridge orientation and spacing. The integrative dataset establishes an evolutionary framework model for the 1.5 km² strandplain, which is situated along the island's southeast coast. Four sets of *en echelon* beach ridges are distinguished at Sandy Hook. Bound by erosional surfaces that truncate paleoshorelines obliquely, they vary in ridge spacing and vegetation cover. Ground-penetrating radar data, collected perpendicular to shore, image prograding clinoform geometries within the upper 4 m of the subsurface. Seaward-inclined reflection surfaces delineate shapes of former foreshore profiles, chronicling the progression of shoreline advance. The architecture of Sandy Hook is characterized by sedimentary sequences bound by discontinuities, which are recognized by truncation of landward, older units and onlap of seaward, younger ones. This attests to a pattern of net growth punctuated by episodic erosion. Studies of siliciclastic analogs have attributed similar architectures to variances in storm climate and/or sediment supply. At Sandy Hook, it is likely that the progressive reduction in shallow-water shelf area fronting the shoreline affected strandplain development by modifying nearshore hydrology and sediment availability. This is suggested by a decrease in ridge spacing over time, which may also reflect changes in hydrodynamic forcing associated with the transition from the Hurricane Hyperactivity Period (1000-3400^{14}C yr B.P.; Liu and Fearn 2000).

INTRODUCTION

The morphology of beach ridges provides information on a variety of paleoenvironmental variables, including sea level, storm climate, and nearshore hydrology (Scheffers et al., 2011). Strandplains, which are comprised of many beach ridges (often grouped into beach ridge sets based on shared characteristics), are studied for insight into changes in environmental forcing over time (Goy et al., 2003; Dougherty et al., 2004; Nott et al., 2009; Forsyth et al., 2010; Tamura, 2012). Strandplain development requires conditions of high sediment supply and hydrodynamic variances in promotion of punctuated shoreline advance (e.g., changes in storm climate); they are most commonly affiliated with wave-dominated river mouths (Matin and Suguio, 1992; Stanley and Warne, 1993; Anthony, 1995; Bondesan et al., 1995; Vella et al., 2005) and regressive portions of barrier islands and compound spits (Timmons et al., 2010; Hein et al., 2013; Mattheus, 2016). Strandplains also occur in more confined coastal settings, such as embayments of the Laurentian Great Lakes, where they provide information on Holocene glacio-isostatic adjustments and lake-level changes (Thompson, 1992; Larsen, 1994; Lichter, 1995; Thompson and Baedke, 1995, 1997; Baedke and Thompson, 2000; Johnston et al., 2007). While many studies document beach morphodynamics and strandplain development along

siliciclastic coastal margins, carbonate platform analogs are under-represented in the literature.

Hearty et al. (1998) and Hearty and Neumann (2001) interpreted former sea-level positions from late Pleistocene Bahamian beach ridges, attesting to their usefulness as archives of paleoenvironmental information. Shinn et al. (1969) evaluated Holocene carbonate strandplains within stratigraphic context of the greater tidal flat environment of Andros Island, The Bahamas, providing architectural blueprints. Sediment textures of Pleistocene-Holocene carbonate strandplains and their implications for hydrocarbon and/or groundwater reservoir potentials were studied by Ward and Brady (1979) and Wallis et al. (1991). While these studies and others have improved our understanding of carbonate strandplain sedimentology and stratigraphic architecture, more work distinctly addressing process geomorphology is needed to facilitate paleoclimate reconstructions.

This study investigates landscape evolution at Sandy Hook, a Holocene carbonate strandplain on the Bahamian island of San Salvador, where past investigations have elucidated paleoclimate information from lacustrine and lagoonal sedimentary archives (Niemi et al., 2008; Dalman, 2009, Park et al. 2009; Dalman and Park, 2012; Park, 2012). A geomorphic model of the strandplain is presented and discussed in relation to late Holocene sea-level rise and storm climate. It builds upon prior work, including that of Boardman and Carney (1992) and Carney et al. (1993), who evaluated Sandy Hook's depositional history in context of San Salvador's framework geology and Quaternary sea levels. Addressing potential linkages between hydrodynamic variables (e.g. storm intensity and frequency), sea-level rise, and strandplain geomorphology complements ongoing late Holocene coastal reconstructive efforts on the island.

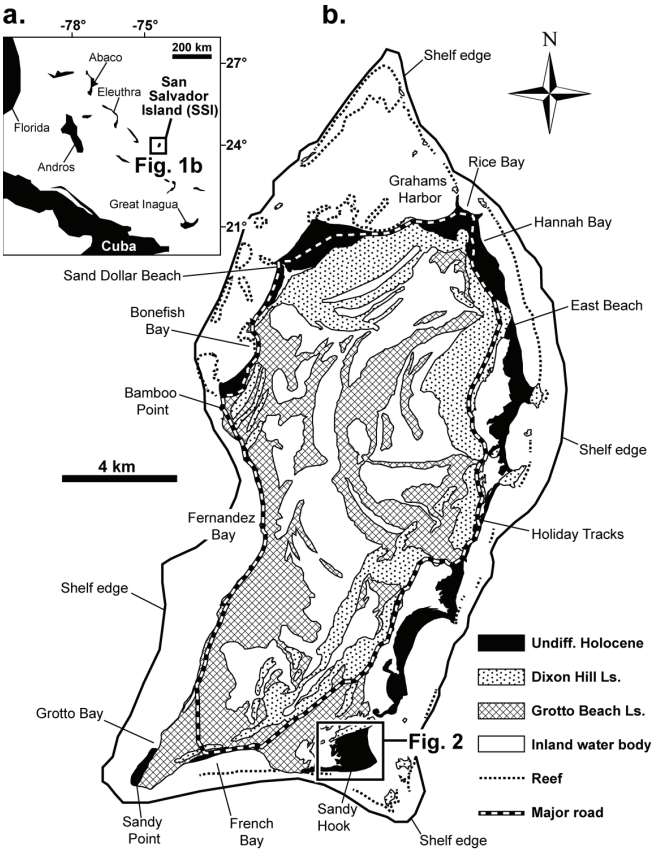

Figure 1. Maps showing the location of San Salvador Island (a) and its geology (b). The Sandy Hook study area (shown in greater detail in Figure 2) is highlighted. Prominent landform features (e.g. shelf-edge reefs) are marked and labeled. Part b is modified from maps by Robinson and Davis (1999) and Titus (1987).

FIELD SITE DESCRIPTION

San Salvador sits atop an isolated carbonate platform along the eastern edge of the Bahamian Archipelago, where shallow coastal waters (of <10 m in depth) abruptly transition to 4 km-deep Atlantic Ocean waters over a distance of around 10 km. The island is vulnerable to strong storms and hurricanes that frequent this particular region (Klotzbach, 2011). The N-S oriented San Salvador measures around 23 km in length and is up to 11 km wide. About a third of the island is covered by water as numerous shallow ponds, lakes, and lagoons occupy swale portions of a Pleistocene dune-bedrock topography (Titus, 1987; Figure 1). Holocene sediments on San Salvador are thin and discontinuous; unconsolidated sands here exist only along select stretches of coastline (Figure 1b). The Sandy Hook strandplain, which started forming around 3-5 ka (Hearty and Kindler, 1993), is the largest sandy lithosome of Holocene age. It is located in the

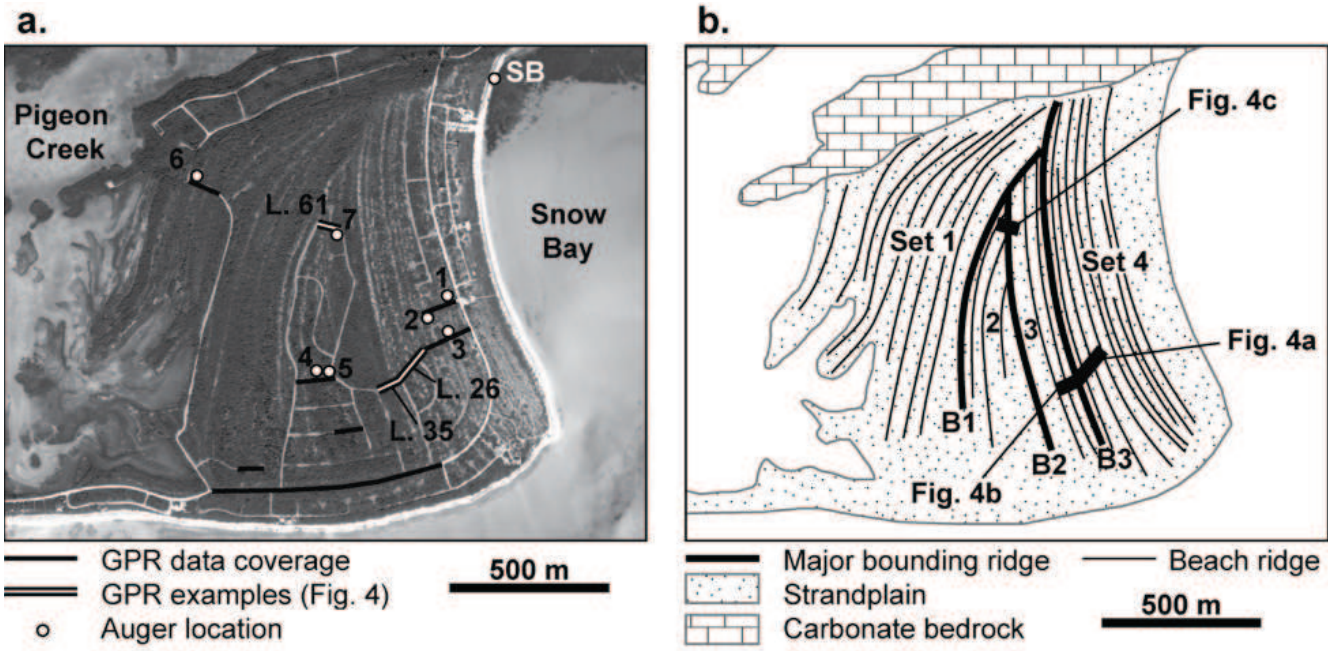

Figure 2. Annotated aerial photograph of Sandy Hook (a) and corresponding geologic map (b), plotting data distribution, axes of beach ridges, and locations of GPR examples shown in this paper (in Figure 4).

southeast corner of the island, bound on its landward side by the western arm of the Pigeon Creek tidal estuary (Figure 2). The total aerial extent of the strandplain is approximately 1.5 km^2 and it houses over 30 beach ridges (Carney et al., 1993). Sandy Hook is separated from the open Atlantic by a shelf lagoon, the 1.5 km-wide Snow Bay. It has an aerial extent of around 5 km^2 and is partly rimmed by limestone cays and shelf-edge reefs (Robinson and Davis, 1999; Figures 1b and 2). A network of unpaved roads provides access to the more landward parts of the densely shrub-vegetated strandplain, which is defined by a subtle ridge-and-swale topography averaging 3 m in elevation (Bahamian Land and Surveys Department, 1972). Sandy Hook is bound to the north by a Pleistocene carbonate-bedrock ridge, which exceeds 6 m in elevation (Titus, 1987; Carew and Mylroie, 1995; Figure 2).

METHODS

The project relied on a GIS-based study of landforms (using remotely-sensed data) and subsurface geophysics. Ground-penetrating radar (GPR) data were collected on San Salvador in March of 2015. Subsequent analysis was undertaken at Youngstown State University and Lake Superior State University facilities in Ohio and Michigan, respectively.

GIS-based mapping

Ridge orientations and spacing were determined from historic aerial photographs (dating to 1942 and 1968), obtained from the Bahamian Lands and Surveys Department, and Google Earth-derived satellite images (collected between 2012 and 2016). Mapping was performed using the ArcGIS 10.3 software package and its auxiliary toolsets. Image files were georeferenced to existing base layers using fixed and easily distinguished landmarks (e.g. road intersections). Landforms were studied from the imagery across a seasonal spectrum to help minimize biased interpretations resulting from shadow effects or obscuration by cloud cover. Differences in vegetation between ridges and swales (in terms of type and density) facilitated their delineation and classification. Interpreted/digitized ridges were grouped into sets

Table 1. Spatial metrics by ridge set.

Ridge set	# of ridges	Ridge spacing (m)	Strandplain area (km²)	Foreset angle (°)
1	10	50	0.56	N/A
2	5	40	0.21	15-27
3	4	40	0.17	13-20
4	11	30	0.61	13-20

based on common measures of spacing, orientation, and spatial association. Field notes on vegetation cover (taken during geophysical mapping) supplemented insights from remotely-sensed information.

Subsurface geophysics

A total of 1.6 km of high-resolution GPR data were collected along 10 shore-perpendicular transects using a pulse Ekko Pro system by Sensors and Software, Inc., equipped with 200 MHz antennae and a calibrated odometer trigger (Figure 2). Basic data processing was performed using the EkkoView Deluxe software package. Digital radar files required no topographic correction as non-vertical beam orientations were avoided by imaging through flat and horizontal road segments. Radar velocities were established by hyperbola fitting (during post-processing) and used to convert two-way travel time to depth. The average radar velocity used, 0.1 m/ns, is in agreement with values published for other carbonate environments (Annan, 1992; Grasmueck and Weger, 2002; Xia et al., 2004). An AGC gain function was applied to the radar files to disproportionately amplify weakened subsurface reflections at depth. Radar sequences were mapped based on fundamental stratigraphic principles (e.g. superposition and cross-cutting relationships), relying on the recognition of different stratal termination patterns.

RESULTS

This study relies on two types of information: 1) A surficial assessment of strandplain morphology, as captured by metrics of ridge spacing, orientation, and grouping; and 2) Stratigraphic interpretations based on high-resolution reflection geophysics.

Ridge orientation and spacing

Beach ridges at Sandy Hook are generally N-S trending and decrease in age eastward (i.e. in the offshore direction). They are slightly arcuate and grouped into four distinct sets, which are separated by erosional surfaces that truncate paleoshorelines obliquely (Figure 2b; Table 1). Ridge sets, which vary in aerial extent and are numbered from oldest to youngest (i.e. landward to seaward), are characterized by different ridge characteristics (Figure 2b; Table 1). Ridge Set 1, the oldest and most landward, covers an area of 0.56 km^2. It is comprised of 10 ridges at an average spacing of approximately 50 m. Ridge Set 4, the youngest, is the most extensive (at 0.61 km^2) and includes the modern beach at Sandy Hook. It contains 11 ridges, spaced an average of 30 m apart (Table 1; Figure 2). Sets 2 and 3 are less extensive (at 0.21 km^2 and 0.17 km^2, respectively) and contain fewer ridges (5 and 4). Both have a ridge spacing of around 40 m. Ridge Sets 1-3 are covered in dense *Coccothrinax* shrub (Smith, 1992; Robinson and Davis, 1999; Figure 3a). Vegetation cover across Ridge Set 4 is noticeably less dense, as shrubs are largely absent and patches of dune grass dominate the flora (Figures 3b and c).

Stratigraphic architecture

Two distinct radar facies are mapped within the upper 4 m of Sandy Hook's subsurface. These represent major sedimentary environments geologic processes of deposition of the beach system—foreshore and aeolian dune. The foreshore facies is characterized by parallel and shoreward-inclined radar-reflection surfaces, representing foreset beds of an advancing shoreline intertidal environment (Figure 4). Slopes of these inclined strata range

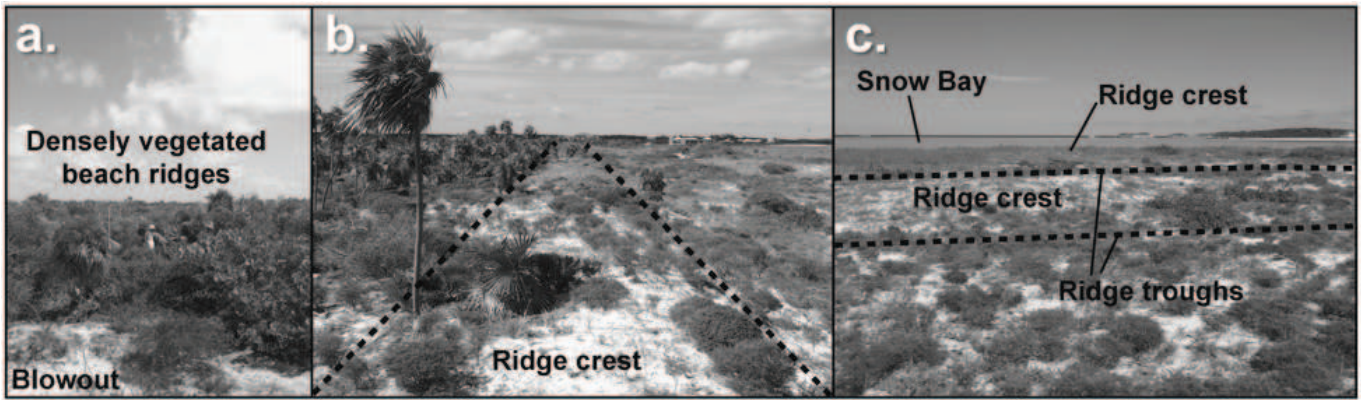

Figure 3. Field photographs taken in March of 2015, showing examples of the densely vegetated, shore-distal portion of the strandplain (a), and the sparsely-vegetated shore-proximal portion in coastal strike (b) and dip (c) orientations. The dense vegetation depicted (a) exemplifies Coccothrinax shrub (Robinson and Davis, 1999).

from 13° to 27° and there are no strong distinctions between ridge sets. While foreset slopes of Ridge Set 2 range from 15° to 27°, those for Sets 3 and 4 are between 13° and 20° (Table 1). GPR failed to image the internal architecture of Ridge Set 1 due to strong signal attenuation just below the surface. It is likely that the proximity to Pigeon Creek and diagenetic effects of sediment-groundwater interactions may be the cause.

The bottomsets of prograding clinoform profiles were not imaged in our dataset. Carney et al. (1993) report depth-to-bedrock ranges between 6.5 m and 10.5 m. Topset beds, which generally reflect accretion in backshore (e.g. berm) environments, were mostly found to be absent. Foreshore sediments are unconformably overlain by aeolian sands and/or road fill, recognized in radar imagery as parallel-horizontal reflections within the uppermost 1-1.5 m of the subsurface (Figure 4).

Disconformities mapped using GPR do not correlate distinctly with ridge-set boundaries delineated from aerial photographs. Line 26, for example, was collected across the shore-distal portion of Ridge Set 4 (Figure 2b) and is shown to contain around 10 distinct sedimentary packages, each bound by erosional surfaces (Figure 4a). However, only 3-4 ridges are recognized in aerial photographs (Figure 2b). GPR Lines 35 and 61, collected across Ridge Sets 2 and 3 (Figures 4b and 4c), are characterized by a similar degree of subsurface complexity. Again, many more signs of erosion are imaged using GPR than are inferred by aerial photography. This makes linking architectural elements of the subsurface to surficial ridge morphologies difficult. It seems that even major set-bounding ridgelines are not distinguished in the subsurface. Although aerial photographs show Line 61 crossing the boundary between Ridge Sets 2 and 3 (Figure 2), no stratigraphic manifestation of what is interpreted as a major event is distinguished among the handful of erosional surfaces recognized in the reflection imagery (Figure 4c).

DISCUSSION

A model of landform succession is presented for the Sandy Hook strandplain. No absolute geochronology exists for this framework; it is based on key stratigraphic and geomorphologic principles alone. The evolution of Sandy Hook is likely to have taken place over the last 3-5 ka, based on sea-level reconstructions, constraint of bedrock topography, and the proposed timing of initial platform inundation (Boardman et al., 1988; Boardman and Carney, 1992). A reduction in the rate of sea-level rise from 1.7 m/kyr (from 3-6 ka) to 0.3 m/kyr (from 0-3 ka) likely facilitated the growth of the strandplain.

Sediment accommodation and strandplain development

Variances in beach-ridge height, spacing, and/or orientation are commonly attributed to changing

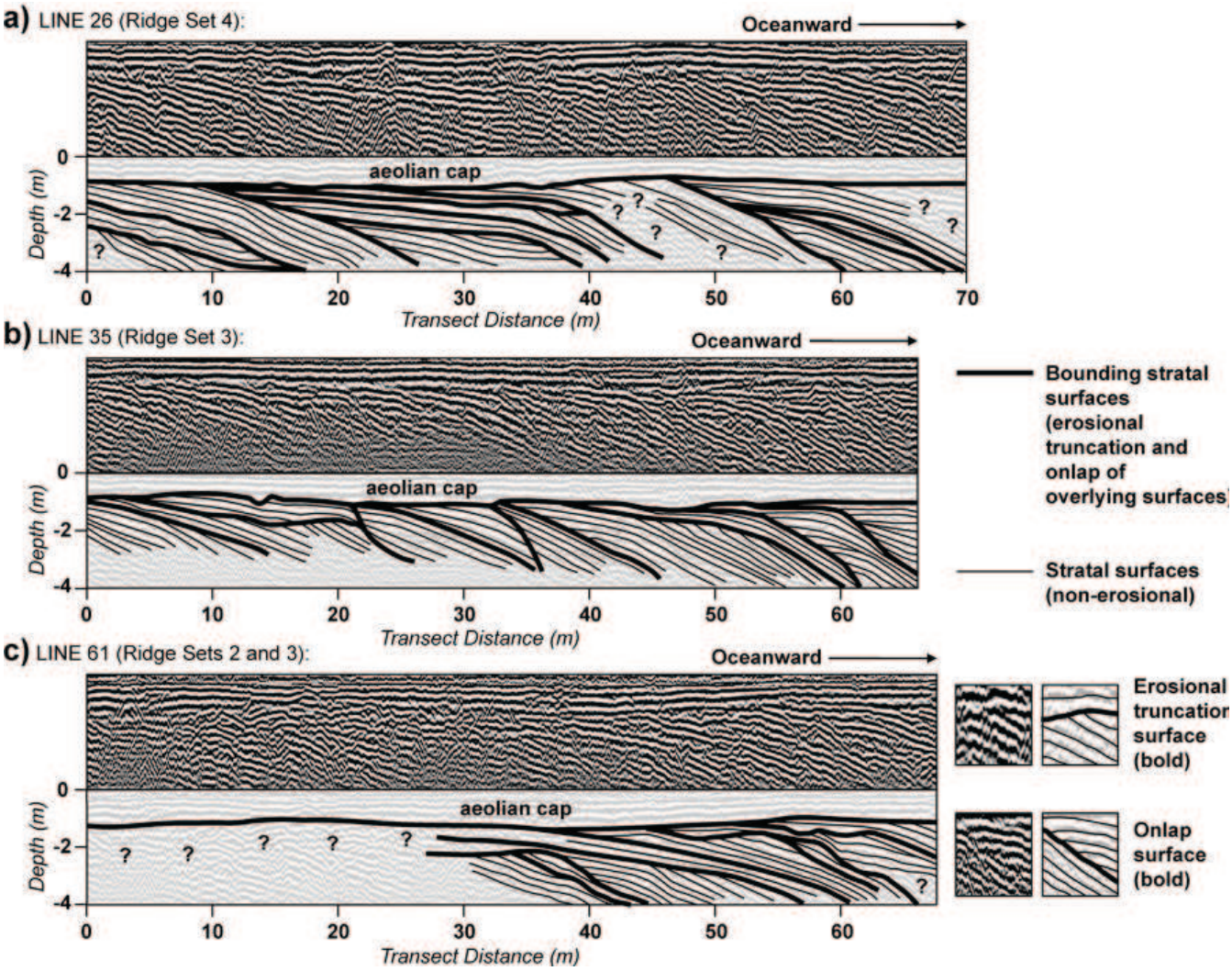

Figure 4. Raw and interpreted GPR reflection images of portions of Line 26 (a), Line 35 (b), and Line 61 (c). Locations are shown in Figure 2. Interpreted surfaces are traced in two distinct thicknesses, emphasizing cross-cutting relationships. Parallel-horizontal reflection configurations are not traced, but labeled 'aeolian cap'. Shoreward-inclined radar surfaces represent prograding foreshore deposits. Depths are based on an averaged radar velocity of 0.1 m/ns, derived by hyperbola fitting during post-processing.

hydrodynamic conditions (e.g. sea-level rise and storm climate) and/or sediment supply (Tanner, 1988; Taylor and Stone, 1996; Mattheus, 2016). While this study lacks detailed topographic information, ridge spacing and orientation, well-constrained from aerial photographs, should reflect the nature of hydrodynamic forcing. Ridge Set 1, representing the oldest preserved episode of progradation, has the widest ridge spacing (at around 50 m), while Set 4, the youngest, is affiliated with the narrowest (at around 30 m; Table 1; Figure 2b). These end-members represent an environmental gradient. The reduction in the rate of sea-level rise and/or the progressive loss of shallow-water shelf area fronting the active beach (due to sedimentation; Figure 5) are likely culprits for the observed morphologic variances. Sandy Hook's present shoreline is around 1 km seaward of Ridge Set 1. An additional 4-5 km^2 of shallow-water shelf area would have therefore characterized the initial growth phase, factoring into different wave run-up and littoral

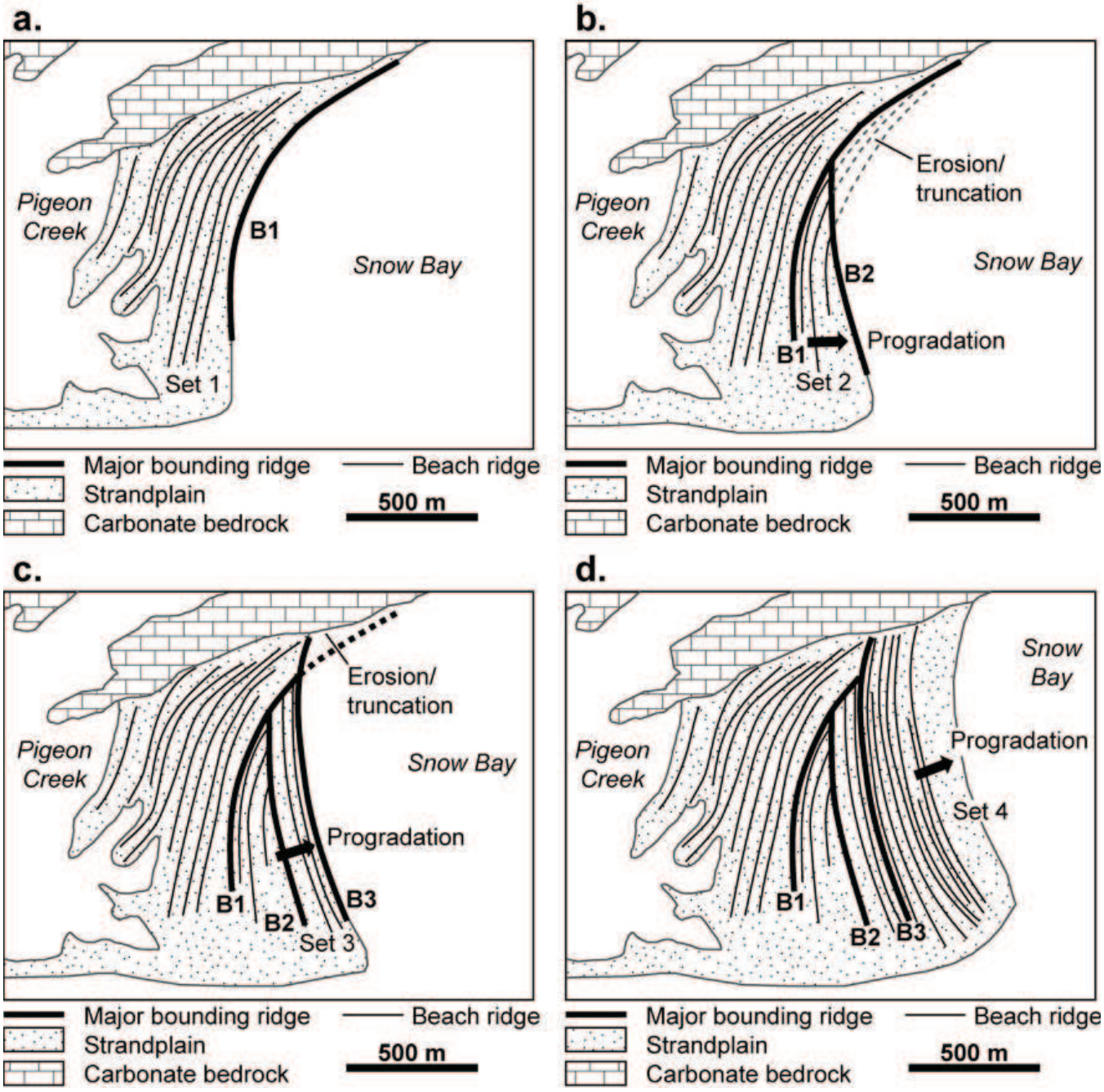

Figure 5. Model of landform succession for Sandy Hook in four stages: 1) The initial growth phase constructed Set 1, the portion of the strandplain closest to the western arm of Pigeon Creek (a); 2) Continued progradation created Set 2, which became truncated by B2 (b); 3) Following another episode of progradation (Set 3), erosional ridgeline B3 truncated the northern extent of the strandplain, including beach ridges of Set 1 (c); and 4) Steady strandplain growth (Set 4) ensued into modern times (d).

dynamics. Additional support to the idea of changing hydrodynamics is provided by the documented presence of ooids in foreshore deposits of Ridge Set 1 (Carney et al., 1993). Ooids, which are absent in today's beach sands, form under conditions of repeated grain resuspension and $CaCO_3$ coating under agitated water conditions (common to shoaling environments). Sandy Hook's early development might have favored such conditions, given the larger shelf area (i.e. of Snow Bay; Figure 5). However, a change in sediment source cannot be ruled out as their presence possibly relates to the reworking of ooid-rich Pleistocene dune deposits during early shelf inundation (Boardman and Carney, 1992).

Climate forcing

Insights by Boardman et al. (1988) and Boardman and Carney (1992) into the timing of platform inundation imply that the early growth of Sandy Hook occurred during the Hurricane Hyperactivity Period (HHP), which lasted from around 3.4 to 1.0 ka (Liu and Fearn, 2000). Lacustrine deposits along San Salvador's perimeter contain evidence of this period of heightened Caribbean storminess manifested as coastal washover layers (Park, 2012; Mattheus and Fowler, 2015; Mattheus and Yovichin, 2018). It is possible that the relatively large ridge spacing of Set 1 relates not only to the presence of a more extensive shallow-water shelf area during early strandplain development (Boardman and Carney, 1996), but also heightened storm activity and/or severity. While lack of an absolute geochronology prevents a more detailed reconstruction, the aerial extents of individual ridge sets may offer some insight into the relative timing of formation. Set 4 represents the most recent episode of progradation and is likely to be the most complete, given lack of truncation by the modern shoreline (Figure 5). It represents 39% of Sandy Hook's aerial extent and is thought to have formed during the quiescent period of the last 1,000 yrs. The uniform (and narrow) ridge spacing and sparse vegetation cover, which differentiate this portion of the strandplain from older ridge sets, support the idea of a fundamental hydrodynamic shift. That this occurred with the transition from HHP is suggested by the proportionality of the 1,000 yr timeframe, representing around a third of the evolutionary history of Sandy Hook based on insights by Boardman et al. (1988) and Boardman and Carney (1992), and the relative size of Set 4 (at ~39% of Sandy Hook's area). It must be stated that the sizes of ridge sets at their full extent (before truncation) are unknown and that older strandplain materials recycled by wave erosion have been incorporated into younger ridges, offsetting temporal linkages between morphology and implied environmental change.

Establishing more distinct causal linkages between late Holocene climate change and patterns of strandplain growth requires chronostratigraphic constraint. This is difficult to achieve in carbonate environments, where dating using Optically-Stimulated Luminescence, the preferred means of dating beach ridges and dunes in siliciclastic environments (Nott et al., 2009; Tamura, 2012), cannot be employed. Regardless of these shortcomings, the evolutionary model of Sandy Hook provides conceptual insights into carbonate strandplain morphodynamics that offer comparison to siliciclastic system analogs.

Comparison to siliciclastic analogs

Several characteristics distinguish Sandy Hook from siliciclastic margin analogs. First, the nature of sediment supply varies as a function of intrinsic production rate and delivery. While climatic and hydrodynamic factors influence sediment delivery, in a carbonate system there is no reliance on a terrigenous source. In contrast, siliciclastic strandplains, such as those associated with river deltas, rely heavily on fluvial inputs, which can vary significantly over time. Systems along regressive portions of compound barrier islands can also benefit from high littoral sediment supply. Second, Sandy Hook's partial confinement by San Salvador's Pleistocene carbonate-bedrock topography set the bounds of sediment accommodation and determined the direction of strandplain growth. Siliciclastic systems (e.g. barrier islands), on the other hand, are for the most part unconfined. There are few restrictions on lateral movement, which

often comes at the expense of older landforms as ridge preservation by means of shoreline progradation is inhibited (Mattheus, 2016). Sandy Hook more closely resembles embayed strandplains of the Laurentian Great Lakes, which are similarly perched atop shallow bedrock platforms and experience a progressive loss of accommodation space (albeit as a function of isostatic uplift in addition to sedimentation). Unlike carbonate strandplains, these systems also undergo cyclical changes in lake level (at seasonal to decadal timescales), which superimpose on the effects of isostatic uplift (Johnson et al., 2012). From a base-level perspective, Sandy Hook is more comparable to other oceanic (i.e. passive margin) systems, experiencing the effects of progessive late Holocene sea-level rise.

CONCLUSIONS

The depositional architecture of the Sandy Hook strandplain is mapped using GPR and aerial photographs. The resulting model of landform succession suggests that changing environmental conditions are responsible for variances in the spacing and orientation of beach ridges. Four distinct ridge sets, defined by an overall decrease in ridge spacing over time, are separated by erosional strandlines that truncate older landforms obliquely. The subsurface shows that there are many more discontinuities; however, no correlation is established between subsurface structures and surface topography. Older ridge sets are characterized by larger ridge spacing than more recent ones and were likely emplaced during a period of increased hurricane activity at ca 3.5 to 1 ka (Liu and Fearn, 2000). Additional work, particularly constraint of landform ages, is needed to more closely establish linkages between late Holocene climate and Sandy Hook's geomorphology.

ACKNOWLEDGMENTS

This work was made possible by a permit to conduct scientific research on San Salvador through the Bahamas Environment, Science & Technology (BEST) Commission, active from 2014 to 2016. Our sincerest gratitude is extended to the Gerace Research Centre staff for providing vehicles, lodging, sustenance, and laboratory space. Data collection was enabled by the Department of Geological and Environmental Sciences at Youngstown State University, as part of a field-based geologic research course.

REFERENCES

Annan, A.P. 1992. Ground penetrating radar workshop notes: Sensors and Software Inc., Mississauga, Ontario, Canada.

Anthony, E.J. 1995. Beach ridge development and sediment supply: Examples from West Africa. *Marine Geology* 129: 175-186.

Baedke, S.J., and Thompson, T.A. 2000. A 4,700-year record of lake level and isostasy for Lake Michigan. *Journal of Great Lakes Research* 26: 416-426.

Boardman, M.R., Neumann, A.C., and Rasmussen, K.A. 1988. Holocene sea level in the Bahamas. Pp 45-52. In J.E. Mylroie, J.E. and D.R. Gerace. (Eds.). *Proceedings of the Fourth Symposium on the Geology of the Bahamas*. Bahamian Field Station, Bahamas.

Boardman, M.R., and Carney, C. 1992. *The geology of Columbus' landfall: A field guide to the Holocene geology of San Salvador, Bahamas*. Ohio Department of Natural Resources Division of Geological Survey Miscellaneous Report No. 2, 49 p.

Boardman, M.R., and Carney, C. 1996. *Pigeon Creek and Tidal Delta – A Field Trip Guide.* Bahamian Field Station, San Salvador, Bahamas, 8 pp.

Bondesan, M., Favero, V., and Vinals, M.J. 1995. New evidence on the evolution of the Po-Delta Coastal Plain during the Holocene. *Quaternary International* 29/30: 105-110.

Carew, J.L., and Mylroie, J.E. 1995. Late Quaternary geology of San Salvador Island and the Bahamas. Pp. 16-24. In M. Boardman, M. and D.R. Suchy. (Eds.). *Proceedings of the Seventh Symposium on the Geology of the Bahamas*. Bahamian Field Station, San Salvador, Bahamas.

Carney, C., Stoyka, G.S., Boardman, M.R., and Kim, N. 1993. Depositional history and diagenesis of a Holocene strand plain, Sandy Hook, San Salvador, Bahamas. Pp. 35-45. In B. White. (Ed.). *Proceedings of the Sixth Symposium on the Geology of the Bahamas*. Bahamian Field Station, San Salvador Island, Bahamas.

Dalman, M.R. 2009. Paleotempestology and depositional history of Clear Pond, San Salvador Island, Bahamas. M.S. Thesis. University of Akron, Akron, OH, USA.

Dalman, MR., and Park, L.E. 2012. Tracking hurricane and climate change records in a Bahamian coastal lake: Clear Pond, San Salvador Island, Bahamas. Pp. 15-32. In D.W. Gamble and P. Kindler. (Eds.). *Proceedings of the 15th Symposium on the Geology of the Bahamas and other Carbonate Regions*. Gerace Research Centre, San Salvador, Bahamas.

Dougherty, A.J., Fitzgerald, D.M., and Buynevich, I.V. 2004. Evidence for storm-dominated early progradation of Castle Neck barrier, Massachusetts, USA. *Marine Geology* 210: 23-134.

Forsyth, A.J., Nott, J., and Bateman, M.D. 2010. Beach ridge plain evidence of a variable late-Holocene tropical cyclone climate, North Queensland, Australia. *Palaeogeography and Palaeoclimatology* 297: 707-716.

Goy, J.L., Zazo, C. and Dabrio, C.J. 2003. A beach ridge progradation complex reflecting periodical sea-level and climate variability during the Holocene (Gulf of Almeria, western Mediterranean). *Geomorphology* 50: 251-268.

Grasmueck, M., and Weger, R. 2002. 3D GPR reveals complex internal structure of Pleistocene oolitic sandbar. *The Leading Edge* 21: 634-639.

Hearty, P.J., and Kindler, P. 1993. New perspectives on Bahamian geology: San Salvador Island, Bahamas. *Journal of Coastal Research* 9: 577-594.

Hearty, P.J., Neumann, A.C., and Kaufman, D.S. 1998. Chevron ridges and runup deposits in the Bahamas from storms late in oxygen-isotope substage 5e. *Quaternary Research* 50:309-322.

Hearty, P.J., and Neumann, A.C. 2001. Rapid sea level and climate change at the close of the Last Interglaciation (MIS 5e): Evidence from the Bahama Islands. *Quaternary Science Reviews* 20: 1881-1895.

Hein, C.J., Fitzgerald, D.M., Cleary, W.J., Albernaz, M.B., Menezes, D., Thadeau, J. and Klein, A.H.D.F. 2013. Evidence for a transgressive barrier within a regressive beach ridge plain system: Implications for complex coastal response to environmental change. *Sedimentology* 60: 469-502.

Johnston, J.W., Thompson, T.A., and Baedke, S.J. 2007. Systematic pattern of beach ridge development and preservation: Conceptual model and evidence from ground penetrating radar. Pp. 47-58. In G.S. Baker and H.H. Jol. (Eds.). *Stratigraphic Analyses Using GPR*. Geological Society of America Special Paper 432.

Johnston, J.W., Argyilan, E.P., Thompson, T.A., Baedke, S.J., Lepper, K., Wilcox, D.A., and Forman, S.L. 2012. A Sault-outlet-referenced mid- to late-Holocene paleohydrograph for Lake Superior constructed from strandplains of beach ridges. *Canadian Journal of Earth Science* 49: 1263-1279.

Klotzbach, P.J. 2011. A simplified Atlantic basin seasonal hurricane prediction scheme from 1

August. *Geophysical Research Letters* 38: L16719.

Lands and Surveys Department, Government of the Bahamas. 1972. Topographic Map of San Salvador Island, Bahamas. Lands and Surveys Department, scale 1:25,000, 1 sheet.

Larsen, C.E. 1994. Beach ridges as monitors of isostatic uplift in the upper Great Lakes. *Journal of Great Lakes Research* 20: 108-134.

Lichter, J. 1995. Lake Michigan beach ridge and dune development, lake level, and variability in regional water balance. *Quaternary Research* 44: 181-189.

Liu, K., and Fearn, M.L. 2000. Reconstruction of Prehistoric landfall frequencies of catastrophic hurricanes in northwestern Florida from lake sediment records. Q*uaternary Research* 54: 238-245.

Martin, L., and Suguio, K. 1992. Variation of coastal dynamics during the last 7000 years recorded in beach ridge plains associated with river mouths: example from the central Brazilian coast. *Palaeogeography, Palaeoclimatology, Palaeoecology* 99: 119-140.

Mattheus, C.R., and Fowler, J.K. 2015. Paleotempestite distribution across an isolated carbonate platform, San Salvador Island, Bahamas. *Journal of Coastal Research* 31: 842-858.

Mattheus, C.R. 2016. GIS-based geomorphologic study of Presque Isle Peninsula, a compound lacustrine barrier-spit system along the south-central Lake Erie margin. *Journal of Great Lakes Research* 42: 336-347.

Mattheus, C.R., and Yovichin, R.D. 2018. Hurricane trajectory and irregular bedrock topography as drivers of washover fan geomorphology on an isolated carbonate platform. *Journal of Coastal Research* 34: 1328-1340.

Niemi, T.M., Thomason, J.C., McCabe, J.M., and. Daehne, A. 2008. Impact of the September 2, 2004 Hurricane Frances on the coastal environment of San Salvador Island, the Bahamas. Pp. 43-63. In L.E. Park and D. Freile. (Eds.). *Proceedings of the 13th Symposium on the Geology of the Bahamas and other Carbonate Regions*. Gerace Research Centre, San Salvador, Bahamas.

Nott, J., Smithers, S., Walsh, K., and Rhodes, E. 2009. Sand beach ridges record 6000-year history of extreme tropical cyclone activity in northeastern Australia. Q*uaternary Science Reviews* 28: 1511-1520.

Park, L.E. 2012. Comparing two long-term hurricane frequency and intensity records from San Salvador Island, Bahamas. *Journal of Coastal Researc*h 28: 891-902.

Park, L.E., Siewers, F.D., Metzger, T., and Sipahioglu, S. 2009. After the hurricane hits: Recovery and response to large storm events in a saline lake, San Salvador Island, Bahamas. *Quaternary International* 195: 98-105.

Robinson, M.C., and Davis, L. 1999. Preliminary geographical information system analysis and maps of physical, hydrological, archaeological, and biological resources, San Salvador Island, Bahamas. Pp. 101-109. In H.A. Curran and J.E. Mylroie. (Eds.). *Proceedings of the 9th Symposium on the Geology of the Bahamas and other Carbonate Regions*. Bahamian Field Station, San Salvador Island, Bahamas.

Scheffers, A., Engel, M., Scheffers, S., Squire, P. and Kelletat, D. 2011. Beach ridge systems – archives for Holocene coastal events. *Progress in Physical Geography* 36: 5-37.

Shinn, E.A., Lloyd, R.M., and Ginsburg, R.N. 1969. Anatomy of a modern carbonate tidal-flat, Andros Island, Bahamas. *Journal of Sedimentary Petrology* 39: 1202-1228.

Smith, R.R. 1992. *Field Guide to the Vegetation of San Salvador Island, the Bahamas*. CCFL Bahamian Field Station, San Salvador Island, Bahamas.

Stanley, D.J. and Warne, A.G. 1993. Nile Delta: Recent geological evolution and human impact. *Science* 260: 628-634.

Tamura, T. 2012. Beach ridges and prograded beach deposits as palaeoenvironment records. *Earth Science Review* 114: 279-297.

Tanner, W.F. 1988. Beach ridge data and sea level history from the Americas. *Journal of Coastal Research* 4: 81-91.

Taylor, M. and Stone, G.W. 1996. Beach ridges: a review. *Journal of Coastal Research* 12: 612-621.

Thompson, T.A. 1992. Beach ridge development and lake-level variation in southern Lake Michigan. *Sedimentary Geology* 80: 305-318.

Thompson, T.A., and Baedke, S.J. 1995. Beach ridge development in Lake Michigan: Shoreline behavior in response to quasi-periodic lake-level events. *Marine Geology* 129: 163-174.

Thompson, T.A., and Baedke, S.J. 1997. Strandplain evidence for late Holocene lake-level variations in Lake Michigan. *Geological Society of America Bulletin* 109: 666-682.

Timmons, E.A., Rodriguez, A.B., Mattheus, C.R., and DeWitt, R. 2010. Transition of a regressive to a transgressive barrier island due to back-barrier erosion, increased storminess, and low sediment supply: Bogue Banks, North Carolina, USA. *Marine Geology* 278: 100-114.

Titus, R. 1987. Geomorphology, stratigraphy, and the Quaternary history of San Salvador. Pp. 155-164. In H.A. Curran and D.T. Gerace (Eds.). *Proceedings of the Third Symposium on the Geology of the Bahamas*. CCFL Bahamian Field Station, San Salvador, Bahamas.

Vella, C., Fleury, T.J., Raccasi, G., Provansal, M., Sabatier, F., and Bourcier, M. 2005. Evolution of the Rhône delta plain in the Holocene. *Marine Geology* 222-223: 235-265.

Ward, W.C., and Brady, M.J. 1979. Strandline sedimentation of carbonate grainstones, upper Pleistocene, Yucatan Peninsula, Mexico. *AAPG Bulletin* 63: 362-369.

Xia, J., Franseen, E.K., Miller, R.D. and Weis, T.V. 2004. Application of deterministic deconvolution of ground-penetrating radar data in a study of carbonate strata. J*ournal of Applied Geophysics* 56: 213-229.

FORAMINIFERA IN BEACH DEPOSITS OF SAN SALVADOR ISLAND, THE BAHAMAS

Christopher R. Mattheus[1], Thomas P. Diggins[2], Brittany A. Stockmaster[3], and Veronica J. Klein[4]

[1]Department of Geology and Physics
Lake Superior State University
Sault Sainte Marie, MI 49783, USA

[2]Department of Biological Sciences
Youngstown State University
Youngstown, OH 44555, USA

[3]School of Coastal and Marine Systems Science
Coastal Carolina University
Conway, SC 29528, USA

[4]Department of Geology and Physics
Lake Superior State University
Sault Sainte Marie, MI 49783, USA

ABSTRACT

Beach sands were sampled for microfossil analysis along the isolated Bahamian carbonate platform of San Salvador Island in an effort to assess and explain spatial variances in foraminiferal content. This preliminary survey work, conducted at the suborder taxonomic level, was performed to aid future paleoenvironmental research efforts by addressing general distribution trends in relation to geographic variables. Shoreline deposits of San Salvador predominantly contain calcareous tests of shallow-water benthic foraminifera of the Miliolina and Rotaliina suborders. Spatial changes in suborder ratio are discussed in context of coastal geologic framework and beach-sediment texture. Sediment texture and microfossil content should reflect hydrodynamic and sediment-sourcing regimes. The Miliolina suborder dominates the island-wide beach assemblage, comprising over 75% of picked individuals. However, suborder ratios vary considerably between the 13 embayed beaches studied. Different habitat characteristics (e.g. makeup of live populations) likely contribute to these variances and should be addressed. Coastal hydrodynamics and post-mortem test alteration are also likely to influence beach-assemblage compositions. While the dynamic and coarse-grained beach environment at Sandy Point, for example, contains highly-altered specimens of *Archaias angulatus* in abundance, a large and relatively abrasion-resistant miliolid, finer-grained sands from more sheltered beach environments are more species-diverse and contain more fragile Rotaliina specimens. This general trend is captured in island-wide PCA analysis, which broadly distinguishes beaches from windward and leeward sides of the island, respectively. Coastal hydrodynamics and foraminiferal dispersal patterns require additional constraint, offering opportunity for continued work.

INTRODUCTION

The Bahamian island of San Salvador sits atop an isolated carbonate platform that faces the open Atlantic (Figure 1). Its isolation, rapid transition to deep water (with 4 km of ocean depth found just 10 km from shore), irregular carbonate bedrock

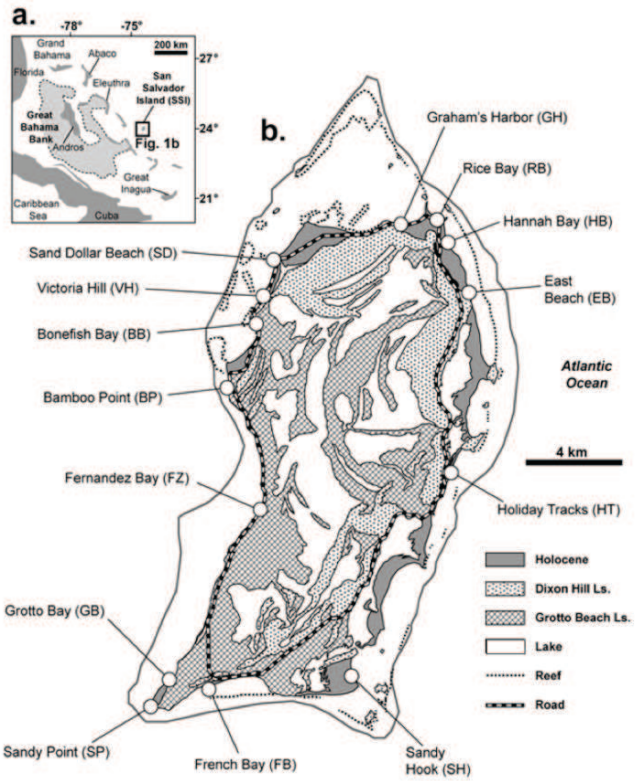

Figure 1. Geologic map of San Salvador Island and surrounding shelf (solid gray outline) showing the locations of sampled beaches and abbreviations used throughout the text for referencing. This geologic framework is based on work by Titus (1987); while updates to the Pleistocene carbonate bedrock units have since occurred, they are of little relevance to this study as the map delineates extent of Holocene sand cover equally well. Reef distribution shown here is adapted from maps by Robinson and Davis (1999); this is an incomplete picture of reef distribution as many popular patch reefs such as Snapshot Reef and Telephone Pole Reef, which are situated within Fernandez Bay (FZ) are not shown at this scale. Table 1, which lists site characteristics, is based on this map. Patch reefs and seagrass beds are common throughout the shelf system; it is beyond the scope of this paper to address the live habitats and our analysis focuses solely on island-wide trends in the ratio of miliolids to rotaliids, offering insights into potential influences thereupon (rather than establishing distinct sourcing pathways).

framework (Titus, 1982, 1984), and high susceptibility to hurricane impacts (Caviedes, 1991; Klotzbach, 2011) have made San Salvador a popular site for late Holocene climate studies (Niemi, 2008; Park et al., 2009). Microfossils (e.g. ostracods and foraminifera) found in many of the island's coastal sedimentary archives (e.g. lagoons and ponds) have proven useful indicators of past storm (overwash) activity and been widely used to aid paleoenvironmental and climatic reconstructions (Bowman and Teeter, 1982; Sanger and Teeter, 1982; Teeter et al., 1987; Sipahioglu, 2008; Dalman, 2009; Park, 2012; Michelson and Park Boush, 2016). This paper documents an effort to inventory foraminifera within beach deposits of San Salvador, the proximal source for overwash; the investigation was prompted by work on storm deposits and hydrodynamics (Mattheus and Fowler, 2015; Mattheus and Yovichin, 2017). This island-wide study was undertaken to elucidate potential spatial trends that could relate to coastal setting, offshore habitat characteristics (e.g. reef occurrence), and/or wave and current exposure.

Foraminifera, a type of marine protist, construct tests of cemented calcium carbonate or agglutinated grains. Live benthic specimens, which exist as substrate-attached, encrusting, and/or mobile varieties, are documented across San Salvador's shelf environment. They are common within seagrass beds and reefs, but are found attached to other hard substrates as well (Lewis, 2004; Buchan and Lewis, 2008; Morgan and Lewis, 2012; Darroch et al., 2016; Martin and Lewis, 2016). Sensitivity to a number of environmental variables, including nutrient availability, salinity, temperature, and water energy, make benthic foraminifera useful paleoecologic indicators (Murray, 1991; Morgan and Lewis, 2012). Upon death, their tests disperse due to wave and current activity and are incorporated into sediments often removed from the original habitat. While live and death assemblages have been documented across several of San Salvador's seagrass, reef, and nearshore communities (Lewis, 2004; Buchan and Lewis, 2009; Morgan and Lewis, 2012; Darroch et al., 2016), little is known about test accumulation along the beach

shorelines. Characterizing death assemblages here could offer insight into transport pathways (i.e. dispersal patterns) from the offshore live communities, provided population dynamics of the source area are known. Furthermore, as beaches supply sand for storm overwash, constraint of assemblage patterns here could offer information to help characterize paleostorm events from coastal pond and lagoon deposits. Areas of recurrent marine incursion are plentiful along San Salvador's coastal perimeter and the emplacement of beach-derived sands has been the subject of several investigations (Park, 2012; Mattheus and Fowler, 2014). As factors such as storm trajectory and strength influence coastal hydrodynamics (i.e. surge levels and current patterns; Parnell et al., 2004; Mattheus and Yovichin, 2018), constraint of live and fossil assemblages across the shelf and shoreline systems offers a potential blueprint for studying paleostorm characteristics from coastal deposits.

As our study focus was geared at evaluating micropaleontological data in context of coastal setting (e.g. shoreline orientation) and beach-nearshore energy (i.e. degree of wave and current exposure), discussion benefited from prior work addressing differences between live and death assemblages and the influences of test-degradation processes. Glenn-Sullivan and Evans (2001) infer that habitat preferences control live foraminiferal assemblages (in offshore habitats) while sediment (i.e. death) assemblages are highly influenced by wave energy. Sediments are therefore generally enriched with respect to larger, more robust tests as small, delicate species are more heavily impacted by predation, dissolution, and abrasion. Time and distance from source should therefore significantly alter assemblage compositions. This type of biased preservation is strongly suggested by studies of differential test abrasion and dissolution of reef-dwelling foraminifera (Peebles and Lewis, 1988, 1989; Kotler et al., 1991, 1992). How these insights, derived in part by physical experiments in laboratory settings, apply to the San Salvador coastal system requires constraint. A summary of background information on test resiliency follows, providing context for this investigation.

BACKGROUND

Taphonomic studies of benthic foraminifera in The Bahamas have provided insight into species distributions across shallow carbonate shelves (Bowman, 1982; Bowman and Teeter, 1982; Peebles and Lewis, 1988, 1991). Prior work has also addressed zonation patterns across several of San Salvador's offshore areas, focusing mainly on factors such as water depth and substrate type (Buchan, 2006; Buchan and Lewis, 2009; Morgan and Lewis, 2010; Martin and Lewis, 2016). In general, the Miliolina suborder (of which *Archaias angulatus* is dominant) appears to dominate the back-reef lagoons while the Rotaliina (e.g. *Amphistegina*) are more common in the fore-reef slope environment (Martin, 1988; Lewis, 2004). Post-mortem test preservation is impeded by several factors, including bacterial degradation, predation, dissolution, and physical abrasion (Peebles et al. 1989; Kotler et al., 1991). Test size, structure, and desirability to microboring organisms (e.g. gastropods) impact rates of dissolution and abrasion, which can result in pronounced differences between live and death assemblages, even if little transport is involved. Peebles et al. (1988), who investigated preservation potentials in reef and lagoon settings, demonstrated that differences in test microstructure can relate to the degree of infestation (by borers). The Rotaliina are generally not as heavily bored as the Miliolina, which has implications for test deterioration. Weakened tests can break apart more easily and dissolution can more effectively attack those that are heavily bored due to increased surface area. It must be noted that Peebles et al. (1989) infer opportunistic rather than selective predation. Gastropods tend to feed on the dominant taxa; counter-intuitively, miliolines (e.g. *Archaias*) were found to be more abrasion-resistant on San Salvador, despite heavier infestation by microboring organisms and being more dissolution-prone than rotaliines (given higher Mg content). This observation stands in contrast to other studies that downplay the role of preferential abrasion on assemblage compositions at the suborder level. It is subsequently suggested that abrasion alone is an unimportant agent of test destruction in natural carbonate settings, even high-energy ones (Kotler et

al., 1992). In studying the effects of abrasion on tests of common Caribbean foraminifera of Discovery Bay (Jamaica), Kotler et al. (1991) noticed that abrasion was not sufficient to destroy foraminifera in low-energy settings and played only a minor role in altering foraminiferal assemblages in high-energy settings. Dissolution is arguably a more effective agent of test destruction, particularly in low-energy settings; however, the effects of abrasion should become more noticeable as transport distance and/or beach energy increases.

It is clear from prior work that many complex processes are involved in modifying foraminiferal death assemblages in shelf settings, including predation, dispersal (by currents), abrasion, and dissolution. Tests found in beach deposits should thus serve as a point of comparison to offshore assemblages and may help address post-mortem alteration histories and transport pathways and/or distances. The following section describes the sampling locations along the San Salvador coastal perimeter.

FIELD SITES

San Salvador covers an area of around 160 km^2. The N-S trending island is close to 21 km in length and up to 8 km wide (Figure1). It is characterized by an irregular carbonate bedrock topography, sculpted by episodic inundation and exposure throughout the Quaternary (Titus, 1982, 1984, 1987; Carew et al., 1984; Boardman et al., 1988; Carew and Mylroie, 1995). The highly-embayed and topographically-varied shoreline, which totals around 60 km in length, has been shaped by the interaction of coastal hydrodynamic processes (i.e. waves) with the bedrock terrain (aeolianites, beach rock, and reef deposits). Unconsolidated Holocene sand deposits are sparse on San Salvador, comprising a thin, discontinuous veneer atop consolidated Pleistocene sediments. The thickest and most extensive sandy lithosome occurs at Sandy Hook (SH), situated on the windward E/SE part of the island (Figure 1).

Thirteen embayed beaches from all sides of the island were sampled for this study. They are distinguished by beach/shelf morphology, offshore reef and seagrass occurrence, and sediment fabric, which serves as a proxy for wave energy. A 1972 Bahamian Lands and Surveys Department map and its digital derivatives (Robinson and Davis, 1992) plot the distribution of major offshore reefs and offer insight into beach and shelf widths. Average beach widths range from around 0.02 km for Rice Bay (RB) to around 0.06 km at Sandy Point (SP, Figure 1 and Table 1). Shelf widths vary from approximately 0.3 km at SP to around 1.7 km at Bonefish Bay (BB). The spatial distribution of patch reefs and shelf-edge reefs is highly heterogeneous (Figure 1; Table 1). The compartmentalization of the island perimeter into separate coastal cells (i.e. embayments) sets the stage for a comparison of beach-sand textures and foraminiferal content to shelf morphometric variables. The geologic framework of San Salvador and prior texture studies of beach sands (Lee et al., 1986; Clark et al., 1989; Gardner, 1993) suggest minimal sediment exchange between coastal cells; however, the shelf hydrodynamics have yet to be concretely established. The following section details the field-sampling, data processing, and statistical procedures employed to gain a better understanding of what beach-sand fabric and foraminiferal content might reveal about sediment sourcing and/or coastal hydrodynamics.

Beach site	Offshore reef	Shelf width (km)	Beach aspect	Beach width (km)
RB	Yes	0.7	N/NE	0.02
HT	Yes	0.8	E/SE	0.03
SP	No	0.3	SW	0.06
HB	Yes	0.9	E/NE	0.02
EB	Yes	1.4	E	0.04
SD	Yes	1.5	W	0.03
VH	Yes	1.6	W/NW	0.04
BB	Yes	1.7	W	0.04
FZ	No	1.5	W/NW	0.02
GB	No	0.9	N/NW	0.03
FB	Yes	0.8	S	0.04
SH	Yes	1.5	E/NE	0.04
GH	Yes	5.6	N/NW	0.02

Table 1. Study area characteristics by study site, including beach and offshore shelf variables. Shelf and beach morphometrics were derived from GoogleEarth imagery while offshore reef occurrence was assessed from maps by Robinson and Davis (1999), which captured only major (e.g. shelf-edge) reef lines.

METHODS

Previously-published texture data for San Salvador beaches were not incorporated into this analysis. Grain-size and microfossil assessments were performed on the same sediment samples to ensure meaningful comparisons. Sediment grabs were retrieved in March of 2014 from foreshore, backshore, and dune systems (total n=36; Figure 1; Table 1). The sampling was performed in adherence to a schematic targeting major sedimentary beach sub-environments (Figure 2). The foreshore was recognized as the portion of the beach influenced by daily tidal inundation under non-storm conditions. It sloped seaward, lacked aeolian structures (e.g. wind ripples), and was devoid of leaf litter and/or other organic detritus. Wrack lines (i.e. storm debris) often separated this environment from the backshore, which is less frequently inundated by the sea (i.e. only during storm events) and visibly reworked by aeolian processes. The dune environment was situated landward and often separated from the backshore by an erosional scarp (Figure 2). Three surface scoops of ~100 g were homogenized per sample. Processing and analysis commenced at the Gerace Research Centre (GRC). After drying in an oven overnight (at 100° C), samples were run through a sample splitter to generate unbiased subsamples for microfossil ID and sediment-texture studies. Grain-size analysis was performed at the GRC using the standard sieve method, whereby relative weight constituencies of gravel and major Wentworth sand classes were established. Samples for microfossil analysis were transported to Youngstown State University's Clastic Sedimentology lab and Lake Superior State University facilities for analysis. Samples were repeatedly split until a manageable size for identifying foraminifera was derived (around 50 g). Foraminifera were extracted under binocular microscopes using a fine, wetted brush and glued to micro-slides for identification and cataloguing. The goal of the analysis was n=50 per sample; however, most samples yielded fewer specimens. Foraminifera were identified using guides and plates provided by literature sources (Peebles and Lewis, 1988, 1989, 1991; Kotler et al., 1992; Javaux and Scott, 2003; Lewis, 2004) and online databases (e.g. World Foraminifera Database). Statistical analyses were performed at the sub-order taxonomic level, even though many specimens could be identified to the genus level (or beyond). Key foraminiferal taxa in the shallow waters surrounding San Salvador are the miliolines, rotaliines, and textulariines. The taphonomic states (pristine to heavily altered) were described for the abundant and large miliolid *Archaias angulatus.* This approach was similar to that used by Buchan and Lewis (2009) and Morgan and Lewis (2010), who ranked samples from pristine to highly altered. In our study, the assessment of test alteration used the following classes: A rating of 'A' was applied if <33% of specimens picked from a sample displayed visible signs of modification (e.g. pitting and/or fractured edges); a rating of 'B' was assigned when 33-66% of foraminifera were visibly altered and a rating of 'C' was assigned when >66% of foraminifera were distinctly modified. This analysis was treated as a qualitative indicator of overall degree of alteration.

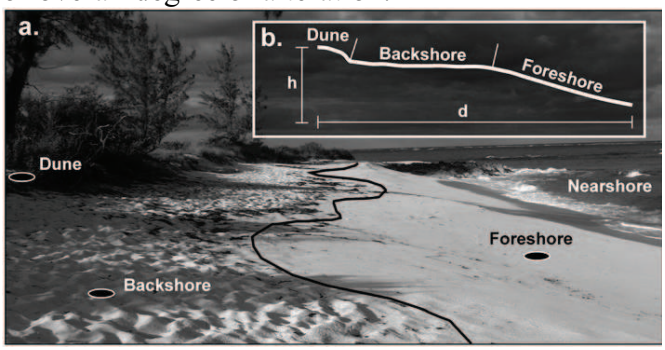

Figure 2. Field photograph of a beach on San Salvador Island showing respective sedimentary sub-environments sampled for analysis (a) and where they plot along a conceptual topographic profile across the beach (b). Dune, backshore, and foreshore environments are distinctly separated by pronounced breaks in slope, surface texture (e.g. swash-smoothed versus wind-rippled), and mean grain size.

STATISTICAL PROCEDURES

Relative Miliolina and Rotaliina abundances and weight percentages of different sediment size fractions were subjected to Principal Components

Analysis (PCA; SPSS version 20) for each spatial position (shoreface, backshore, and dune) at each of the thirteen beaches. The Textulariina (only two specimens total) and the silt/clay sediment fraction (occurring in only three dunes and at <0.5%) were not included due to their trivial contributions to the data set. The first two PCA axes (Eigen values of 3.40 and 1.69, and percent variance explained of 42.5 and 21.1, respectively) are presented as an ordination. A third PCA axis was marginally statistically useful (Eigen value of 1.11 and explaining 14.0% of variance), but was not included in the ordination for the sake of brevity and clarity. Also, this third PCA reflects predominantly the gravel fraction, which never constituted more than 3.2% of sediments in any sample, thus offering little meaningful explanatory value over the first two PCA axes that were graphed.

Environment	Suborder	RB	HT	SP	HB	EB	SD	VH	BB	FZ	GB	FB	SH	GH
Shoreface	Miliolina	17	23	25	32	31	34	36	27	9	32	41	20	46
Shoreface	Rotaliina	20	18	0	10	14	7	4	16	3	14	2	11	3
Shoreface	Textulariina	0	0	0	0	0	0	0	0	0	0	0	0	0
	Total	**37**	**41**	**25**	**42**	**45**	**41**	**40**	**43**	**12**	**46**	**43**	**31**	**49**
Backshore	Miliolina	28	36	22	24	25	40	38	2	27	4	44	22	42
Backshore	Rotaliina	19	10	1	20	20	2	8	5	12	3	2	13	3
Backshore	Textulariina	0	0	1	0	0	0	0	0	0	0	0	0	0
	Total	**47**	**46**	**24**	**44**	**45**	**42**	**46**	**7**	**39**	**7**	**46**	**35**	**45**
Dune	Miliolina	24	32	22	39	26	33	46	38	34	28	36	31	37
Dune	Rotaliina	18	5	0	8	17	8	4	9	7	17	2	4	5
Dune	Textulariina	0	0	0	0	1	0	0	0	0	0	0	0	0
	Total	**42**	**37**	**22**	**47**	**44**	**41**	**50**	**47**	**41**	**45**	**38**	**35**	**42**

Table 2. Results of foraminiferal counts, grouped by suborder and organized by beach sub-environments for all study-area locations.

RESULTS

Microscopy

The Miliolina dominate the general beach assemblage, accounting for around 78% of all individuals picked in this study (Table 2). The dominant suborder species is *Archaias angulatus*, easily recognized by its relatively large ammonoid-like test form (Figure 3). Rotaliina is the second-most common suborder (approximating 22% overall). The most common rotaliid specimen was *Homotrema rubrum*. Only two specimens belonging to the Textulariina suborder were identified (Table 2). Given a near total absence of Textulariina in beach deposits, assemblage compositions are expressed as variances of relative Miliolina and Rotaliina abundances, which show distinct spatial trends (Figure 4). The highly exposed, energetic, and coarse-grained shoreline at SP, which represents an end-member beach in terms of grain size (Figure 5), is dominated almost exclusively by Miliolina. Nearby Fernandez Bay (FZ) is also characterized by very low Rotaliina percentages (25%, 37%, and 17% of the total specimen population from foreshore, backshore, and dune environments, correspondingly; Table 2). Foreshore samples from east-facing beaches, the island's windward side, contain higher Rotaliina percentages than elsewhere, particularly SW-facing ones (Figure 4). Pristine foraminifera, occasionally found in foreshore and backshore samples, were rarely

encountered in dune deposits and *Archaias angulatus* specimens sampled from dune deposits were observed to be more highly degraded (marked by pronounced pitting and broken chambers) than those from backshore and foreshore environments. Additionally, foraminifera picked from east-facing beaches (e.g. EB, HB, and RB; Figure 1) were noticeably less altered, in general, than those from beaches on the island's west side (Table 3).

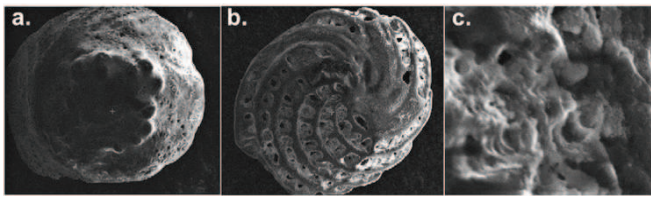

Figure 3. Scanning electron images taken with a JEOL JSM-6100 SEM (between 50 and 75 X magnification), showing Discorbis rosea, also known as Rotorbinella rosea (a) and Archaias angulatus (b), commonly encountered species of the Rotaliina and Miliolina suborders, respectively. An additional close-up image (>100 X magnification) provides a textural glimpse of the effects of post-mortem test alteration (c). Scales are approximations (given uncertainties relating to antiquated equipment and processing software); images serve merely to offer visual aid for textures and should not indicate size relationships between specimens.

Sediment texture

Results of grain-size analysis capture variances in sediment texture from beach to beach and between beach subenvironments. These stem from varying amounts of reef debris (i.e., bioclasts), peloids, and aggregate grains and reflect different coastal hydrodynamic and sediment-sourcing regimes. Foreshore samples relate more directly to ambient hydrodynamic conditions while backshore and dune samples characterize past conditions (e.g. storm lags) and modification by aeolian processes (e.g. sorting; Figure 2). The foreshore environment is coarsest along the SW and NW portions of San Salvador (Figure 5). The SP site contains the coarsest shoreface, backshore, and dune sediments, comprised of around 77%, 71%, and 83% coarse sand, respectively (Table 4). The NW beaches (VH, SD, and GH) are also dominated by coarse-grained sand. A fine-grained sand modal class, on the other hand, characterizes beaches along the NE portion of the island. Fine-grained sand percentages in foreshore deposits at HB and EB, for example, exceed 50%, while backshore and dune deposits here contain slightly less fine-grained sand, with medium-grained sand representing the dominant size class (Figure 5; Table 4). An absence of coarse-grained sand or very low percentages thereof (<10%) stand in noticeable contrast to the beaches in the SW (SP and GB) and NW (VH, SD, and GH) of San Salvador (Table 4).

PCA results

Sediment types and foraminiferal suborders segregated distinctly in PCA ordination space, indicating the potential quantitative association between them. Sand fractions were clearly distinguished along the PCA 1 axis, which explains 42.5% of data variance, with coarser sands to the left of the y axis (Figure 6). Likewise, the two dominant foraminiferal suborders diverged, with Miliolina to the left and Rotaliina to the right of the y axis. In contrast, there were no clear gradients *along* the y axis, which explains a further 21.1% of data variance. However, examination of the ordination plot in Figure 6 suggests some degree of "arch" or "horseshoe" effect, despite the general resistance of PCA to this when using environmental data such as sediment grain-size distributions. The reader should note how the gradient in sand fractions from very coarse to very fine follows not a straight line in ordination space, but a curved trajectory from the upper left quadrant to the upper right, hence precluding a clear interpretation of the PCA 2 axis. Shoreface, backshore, and dune samples at some beaches clustered closely in ordination space (e.g. at SP, SH, FB), whereas most did not (at HT, BB, VH, EB). Divergence among the different spatial position samples at individual beaches was typically greater along the PCA 2 axis than along the more definitively interpretable PCA

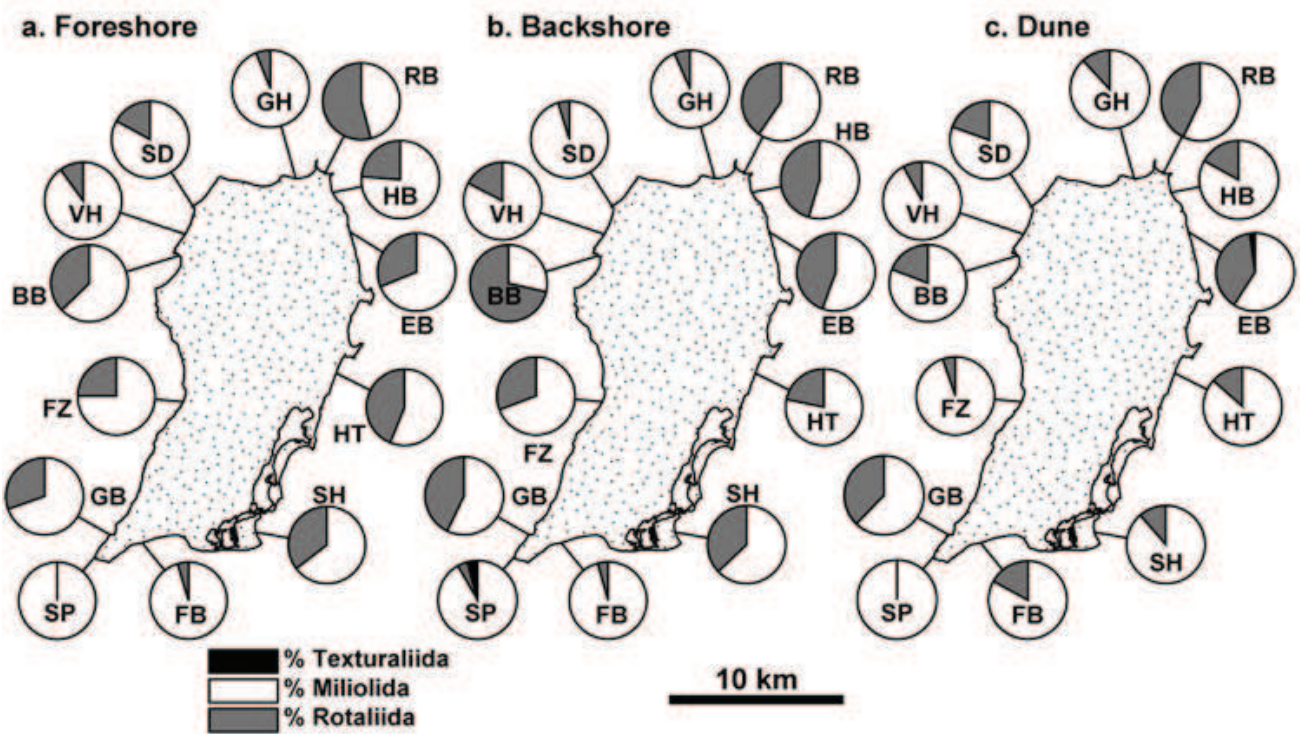

Figure 4. Distribution plots showing relative abundances of the three studied suborders of foraminifera in foreshore (a), backshore (b), and dune (c) deposits across San Salvador Island.

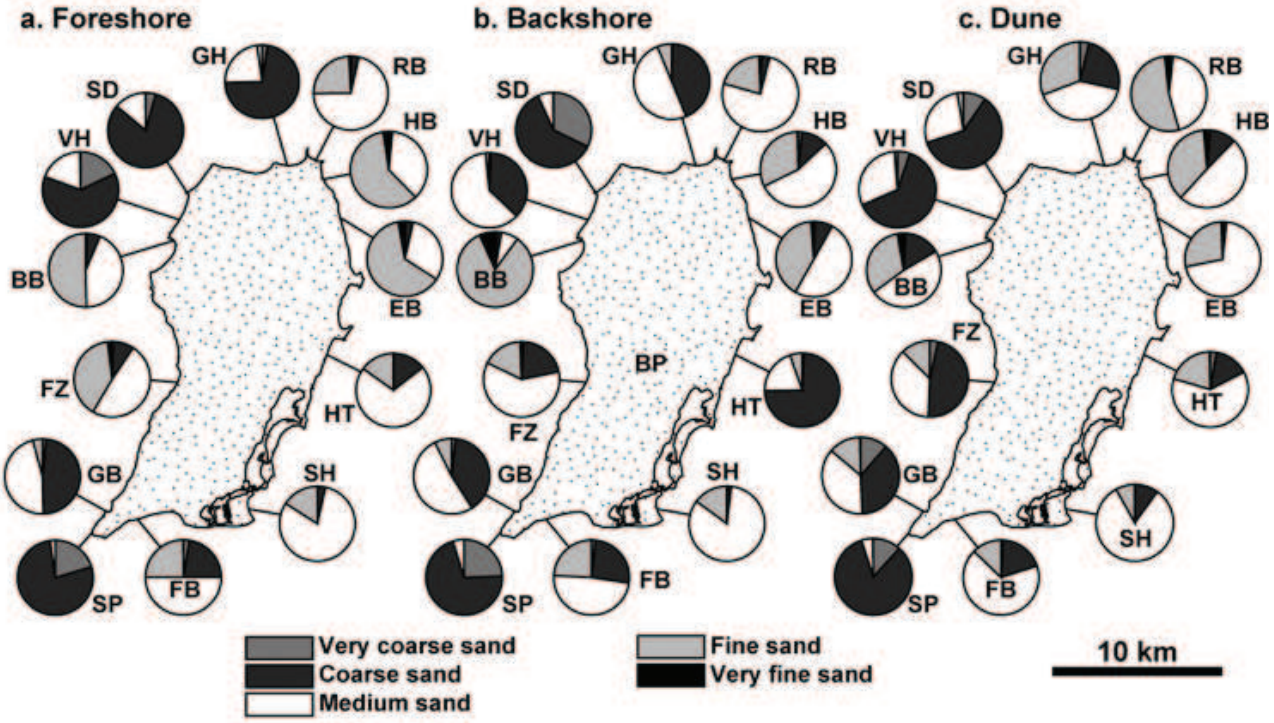

Figure 5. Distribution plots showing relative abundances of sand fractions in foreshore (a), backshore (b), and dune (c) deposits across San Salvador Island.

East-facing beaches	Foreshore	Backshore	Dune	Other beaches	Foreshore	Backshore	Dune
RB	A	A	A	SP	C	B	B
HT	A	C	C	SD	C	C	C
HB	C	A	C	VH	B	C	C
EB	B	B	C	BB	B	A	B
SH	B	B	B	GB	C	A	B
FZ	A	B	B	GH	C	C	B
				FB	C	C	C

Table 3. Results of an assessment of post-mortem test alteration performed on sampled foraminifera using the following classes: A (<33% of specimens show clear signs of modification such as pitting, fractured edges, etc.), B (33-66% of foraminifera are visibly altered), and C (>66% of foraminifera are distinctly altered). This analysis is not species-specific and was performed on all specimens collected from respective sediment samples. The results are to be used as a qualitative measure of overall degree of degradation.

Environment	Suborder	RB	HT	SP	HB	EB	SD	VH	BB	FZ	GB	FB	SH	GH
Shoreface	Miliolina	46	56	100	76	69	83	90	63	75	70	95	65	94
Backshore	Miliolina	60	78	92	55	56	95	83	29	69	57	96	63	93
Dune	Miliolina	57	86	100	83	59	80	92	81	83	62	95	89	88
Environment	**Grain size**													
Shoreface	Diameter at 50 %	227	527	924	501	217	877	845	241	197	798	568	500	681
Backshore	Diameter at 50 %	438	478	1,011	432	448	964	615	167	524	608	531	485	585
Dune	Diameter at 50 %	261	515	969	273	241	786	816	-	-	634	311	537	250
	Reef Association	Yes	Yes	No	Yes	Yes	Yes	Yes	Yes	No	No	Yes	Yes	Yes
	Beach aspect	N/NE	E/SE	SW	E/NE	E	W	W/NW	W	W/NW	N/NW	S	E/NE	N/NW
	Shelf width (km)	0.02	0.03	0.06	0.02	0.04	0.03	0.04	0.04	0.02	0.03	0.04	0.04	0.02

Table 4. Synthesis of patterns in the distribution of foraminiferal suborders, mean sediment size, and environmental aspects of studied beach sites

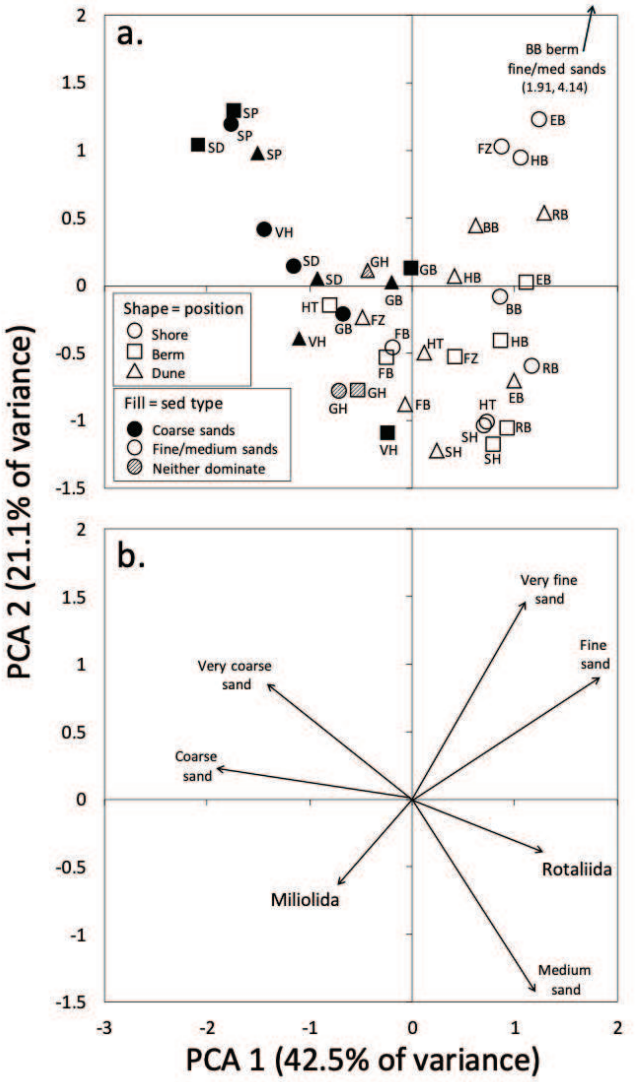

Figure 6. Principle Components Analysis (PCA) ordination of foraminifera orders and sediment grain sizes at San Salvador beaches, identified in panel (a) by site (abbreviations as used in other Figures and Tables), beach position (marker shapes), and dominant sediment fraction (marker fill). Vector arrows in panel (b) denote loadings (i.e. coefficients) for variables in the analysis. These loadings, which can range from -1 to +1, are multiplied by two in order to enhance readability on this plot.

1. There did not appear to be any island-wide pattern in ordination space differentiating among shore, backshore, and dune samples overall (Figure 6).

DISCUSSION

A broad survey of San Salvador beach sands offers data on foraminiferal suborder ratios, spatial variances therein, and associated sediment textures. This preliminary assessment provides insights to help guide future research endeavors to better constrain distribution dynamics, which should relate to foraminiferal habitat preference (and thus geologic framework), dispersal patterns (i.e. coastal hydrodynamics), and differential test resiliency. Prior studies that compare live and death assemblages across offshore habitats (e.g. seagrass and reef environments) have related compositional variances to differential test deterioration (Peebles and Lewis, 1988, 1989; Kotler et al., 1991, 1992). Some species undergo more rapid deterioration following death given poor resiliency to chemical and physical breakdown. The result of this is that live and death assemblages may differ significantly, even within the primary habitat. Increased travel distance should amplify such variances. Studies addressing assemblage dynamics offer some discussion points for contextualizing foraminiferal content in beach sands of San Salvador. Prior work in seagrass sites at Cut Cay, situated in the NE portion of the island (Buchan and Lewis 2006, 2009; Morgan and Lewis, 2012), and reef habitats along the western coast (Lewis, 2004), resolved offshore-trending assemblage gradients relating to environmental factors such as water depth and substrate type. At Cut Cay, where 54 species of foraminifera were described, very few specimens of the Miliolina suborder were found in seagrass beds, which were dominated by the Rotaliina (Morgan and Lewis, 2012). The latter, typified by smaller and more fragile tests, showed a strong substrate preference; while larger miliolines such as *Archaias angulatus* were not as common on the seagrass vegetation (as the rotaliines), they accumulated in sediments more easily due to their relative resistance to abrasion (Martin, 1986). The miliolines are the dominant constituent in our beach samples and *Archaias angulatus* was the most abundant species found, a stark contrast to offshore observations. Greater transport distance (or increased time since death) is more likely to alter tests (by abrasion and dissolution), which leads

to a relative enrichment of beach deposits in more robust species.

Variances in preservation potential have previously been entertained as possible mechanisms for generating diverse foraminiferal assemblages in sedimentary records (Peebles and Lewis, 1989; Kotler et al., 1992). Factors such as test size, composition (high versus low-Mg calcite), and architecture (e.g. coiled agglutinated) represent intrinsic variables influencing these dynamics.

Suggestively, trends in dominant suborder ratios in San Salvador beach sands reveal a spatial correlation with mean grain size, which reflects the energy levels of respective depositional settings (Figures 4 and 5). This is resolved from an island-wide PCA analysis associating coarser-grained deposits (which largely dominate the island's westward-facing shores) with Miliolina assemblage-dominance. The SP site, in particular, is characterized by the coarsest beach sediments on San Salvador (Figure 5) and exclusively contains miliolines (Figure 4). Almost all foraminifera sampled from this beach are heavily altered *Archaias angulatus*, known for its large size and abrasion-resistant test comprised of high-Mg calcite (Martin, 1988; McIntyre-Wressnig, 2011). While its dominance likely relates, in part, to its size (i.e. depositional dynamics as a function of particle diameter), resiliency characteristics may contribute to its relative enrichment. SP, which is located in close proximity to the SW platform edge (Figure 1), is not only an exceptionally dynamic beach (in terms of wave and current exposure; Loizeaux et al., 1993; Beavers et al., 1995; Voegeli et al., 2006), it is also more distal to reef and seagrass habitats, where foraminiferal abundances and diversity are high. Greater transport distances and longer/more intense abrasion histories, as evidenced by the high degree of test alteration (Figure 3), likely factor into the lack of foraminiferal diversity at SP.

Past work has downplayed the role of abrasion as an important agent of test destruction (Kotler et al., 1991, 1992); however, much of the research focus was on lower-E shelf settings, where dissolution and infestation (by microborers) take on major roles in the process of test degradation. Littoral and beach dynamics, as influenced by wave and current activity, should influence assemblage compositions by promoting abrasion and the loss of less robust species with time. Separation of foraminifera by size is another likely process factoring into changes in death-assemblage composition in shoreline sediments, given the range of different textures observed (Figure 5). The geologic and ecologic complexities of San Salvador, which include high along-strike variances in shelf morphology, offshore reef and seagrass bed occurrence (Table 1; Figure 1), offer many opportunities to study the dynamics of sediment (and foraminiferal) sourcing and routing. Although more information from the offshore realm is needed to address this (e.g. hydrodynamic and ecologic data), our assessment of beach sands offers some preliminary insights. The qualitative observation that foraminiferal tests recovered from dune sands were generally more highly abraded than those from respective foreshore samples reflects both distance traveled (across/along the interface of terrestrial and aquatic environments) and age. Grains here are also subjected to heavier dissolution given increased freshwater influence (i.e. rainfall). It should be mentioned that the loss of fine surface textures by pitting, a clear result of dissolution, is more likely to obscure the recognition of some types of foraminifera, particularly smaller ones. Some 'fresh' foraminifera can be transported landward quickly by surge waters (i.e. without undergoing a long history of abrasion in the nearshore/beach environment). With exception of such outliers, which may offer useful information on storm occurrence, weathering and assemblage composition gradients likely exist from offshore habitat to beach. These should generally relate to time of alteration by physical and chemical processes. Grains in the subaerial realm have generally traveled far and are highly degraded. A more detailed assessment foraminifera at the species level in each of the subenvironments along this spatial gradient (and their test conditions) would likely offer additional insights.

The role of *Homotrema rubrum* (a rotaliine) as a transport indicator is particularly important to consider in future work, given its distinct appearance (red color) and documented abundance in outer reef settings (MacKenzie et al., 1965; Pilarczyk and Reinhardt, 2012; Pilarczyk et al., 2014).

Tichenor and Lewis (2018) have documented its abundance in nearshore areas of San Salvador. Improving our understanding of sediment sourcing and linkages between offshore habitats and foraminiferal distributions across beach environments would require detailed documentation of what is living in the vicinity of each particular beach and assessing hydrodynamics (e.g. tidal currents). The role of storms is an additional point to address as varying storm paths and wave characteristics may have varying impacts on dispersal patterns, which could be elucidated from foraminiferal taphonomy of the subaerial realm (e.g. storm washover deposits).

CONCLUSIONS

Beach sands from the small isolated carbonate platform of San Salvador Island, Bahamas, offer a glimpse into spatial variances in the ratio of dominant foraminiferal suborders. This survey of the island's beaches offers a jumping-off point for studying foraminiferal dispersal patterns from offshore habitats (e.g. seagrass beds and reefs). Different preservation potentials of tests, related largely to composition, size, and architecture, cause assemblages to change with increasing dispersal distance and time spent undergoing reworking in nearshore and shoreline sediments. High-E shoreline sites on the island are depleted with respect to smaller and weaker tests and are dominated by highly abraded *Archaias angulatus,* a large and relatively robust species of the Miliolina suborder. Distance traveled and the continuous reworking within high-E beach environments appear to influence foraminiferal death assemblages, whereby smaller, less resilient tests (which are less impacted by boring) are more quickly destroyed and larger, robust ones enriched in sediments over time. Physical and chemical alteration processes within nearshore and shoreline environments may trump biological effects on test degradation, which are probably more pronounced in lower energy settings (or closer to the source region). The roles of biologic effects on test degradation are complex as factors involving predator habitat preferences and other ecologic variables are difficult to pinpoint and are beyond the scope of this initial assessment. Observed spatial trends in foraminiferal suborder ratio probably also relate to habitat type as certain foraminifera prefer certain settings (e.g. *Homotrema rubrum* abundance in outer reefs). A PCA analysis comparing relative contributions of the Miliolina (with respect the overall assemblage) to mean grain size of corresponding beach deposits (viewed as a proxy for energy of respective coastal cells) distinguishes east- from west-facing (i.e. windward from leeward) beaches. This should relate to a combination of different habitat preferences, abrasion histories, and test resilience. Continued study of how death assemblages vary across offshore and nearshore environments of San Salvador may provide useful information for studying foraminifera in coastal hurricane deposits (e.g. paleostorm trajectory). Particular emphasis on evaluating potential transport indicator species (e.g. *Homotrema rubrum*) would be particularly helpful in this regard.

ACKNOWLEDGMENTS

We would like to extend our gratitude to Youngstown State University's Department of Geological and Environmental Sciences, the Lake Superior State University Department of Geology and Physics, and the Gerace Research Centre for facilitating this research. A class excursion to San Salvador in March of 2014 offered the opportunity to sample and analyze sediments. We thank Joshua Fowler for his assistance in the field and in the lab and also wish to acknowledge Ben Southwell for his assistance with LSSU's Scanning Electron Microscope.

REFERENCES

Beavers, R.L., Curran, H.A., and Fox, W.T. 1995. Long-term, storm-dominated sediment dynamics on East Beach and Sandy Point, San Salvador Island, Bahamas. Pp. 1-15. In M. Boardman and D.R. Suchy (Eds.). *Proceedings of the 7th Symposium on the Geology of the Bahamas*. Bahamian Field Station, San Salvador, Bahamas.

Boardman, M.R., Neumann, A.C., and Rasmussen, K.A. 1988. Holocene sea level in the Bahamas. Pp. 45-52. In J.E. Mylroie and D.T. Gerace (Eds.). *Proceedings of the 4th Symposium on the Geology of the Bahamas*. Bahamian Field Station, San Salvador, Bahamas.

Buchan, O.C. 2006. Relationships between large benthic foraminifera and their seagrass habitats, San Salvador Island, Bahamas. MS Thesis. Auburn University, Auburn, AL, USA.

Buchan, O.C., and R.D., Lewis. 2009. Recent benthic foraminifera as indicators of seagrass-bed characteristics, San Salvador, Bahamas: The Addition of Taphonomy. SEPM Special Publication No. 93, 83-92.

Carew, J.L., Mylroie, J., Wehmiller, J.F., and Lively, R.S. 1984. Estimates of Late Pleistocene sea level high sStands from San Salvador, Bahamas. Pp. 153-175. In J.W. Teeter (Ed.). *Proceedings of the 2nd Symposium on the Geology of the Bahamas*. CCFL Bahamian Field Station, San Salvador, Bahamas.

Carew, J.L., and Mylroie, J.E. 1995. Late Quaternary geology of San Salvador Island, and the Bahamas. Pp. 16-24. In M. Boardman and D.R. Suchy (Eds.). *Proceedings of the 7th Symposium on the Geology of the Bahamas*. Bahamian Field Station, San Salvador, Bahamas.

Caviedes, C. 1991. Five hundred years of hurricanes in the Caribbean: Their relationship with global climatic variabilities. *GeoJournal* 23: 301–310.

Clark, D.D., Mylroie, J.E., and Carew, J.L. 1989. Texture and composition of Holocene beach sediment, San Salvador Island, Bahamas. Pp. 83-93. In J.E. Mylroie and D.T. Gerace (Eds.). *Proceedings of the 4th Symposium on the Geology of the Bahamas*, Bahamian Field Station, San Salvador, Bahamas.

Dalman, M.R. 2009. Paleotempestology and depositional history of Clear Pond, San Salvador Island, Bahamas. M.S. Thesis. University of Akron, Akron, OH, USA.

Gardner, R.B. 1993. *A statistical analysis of sand grain size in San Salvador, Bahamas*. Bahamian Field Station Occasional Paper No. 1, San Salvador Island, Bahamas.

Glenn-Sullivan, E.C., and Evans, I. 2001. The effects of time-averaging and taphonomy on the identification of reefal sub-environments using larger foraminifera: Apo Reef, Mindoro, Phillippines. *Palaios* 16(3): 39-408.

Javaux, E.J. and Scott, D.B. 2003. Illustration of modern benthic foraminifera from Bermuda and remarks on distribution in other subtropical/tropical areas. *Palaeontologia Electronica* 6: 1-9.

Klotzbach, P.J. 2011. A simplified Atlantic basin seasonal hurricane prediction scheme from 1 August. *Geophysical Research Letters* 38:doi: 10.1029/2011GL048603

Kotler, E., Martin, R.E., and Liddell, W.D. 1991. Abrasion-resistance of modern reef-dwelling foraminifera from Discovery Bay, Jamaica – implications for tests preservation. Pp. 125-138. In R. Bain (Ed.). *Proceedings of the 5th Symposium on the Geology of the Bahamas*, Bahamian Field Station, San Salvador, Bahamas.

Kotler, E., Martin, R.E., and Liddell, W.D. 1992. Experimental analysis of abrasion and dissolution resistance of modern reef-dwelling foraminifera: Implications for the preservation of biogenic carbonate. P*ALAIOS* 7: 244-276.

Lands and Surveys Department, Government of the Bahamas, 1972. San Salvador Island, Bahamas, 1:25,000 topographic map.

Lee, Y.I., Lindsey, B., May, T., and Mann, C.J. 1986. *Grain size distribution of calcareous beach sand, San Salvador Island, Bahamas*. Occasional Paper No. 1, CCFL Bahamian Field Station, San Salvador, Bahamas.

Lewis, R.D. 2004. Foraminiferal assemblages and reef-sediment petrographic criteria as evidence for relative distance from shore for Pleistocene reefs, San Salvador, Bahamas: Preliminary Results. Pp. 83-94. In R.D. Lewis and B.C. Panuska (Eds.). *Proceedings of the 11th Symposium on the Geology of the Bahamas and other Carbonate Regions*. Gerace Research Centre, San Salvador, Bahamas.

Loizeaux, N.T., Curran, H.A., and Fox, W.T. 1993. Seasonal sediment migration and dediment dynamics on Sandy Point Beach, San Salvador Island, Bahamas. Pp. 83-93. In B. White and D.R. Gerace (Eds.). *Proceedings of the 6th Symposium on the Geology of the Bahamas*. Bahamian Field Station, San Salvador, Bahamas.

MacKenzie, F., Kulm, L.D., Cooley, R. L., and Barnhart, J.T. 1965. *Homotrema rubrum* (Lamarck), a sediment transport indicator. *Journal of Sedimentary Petrology* 35: 265-272.

Mattheus, C.R. and Fowler, J.K. 2015. Paleotempestite distribution across an isolated carbonate platform, San Salvador Island, Bahamas. *Journal of Coastal Research* 31: 842-858.

Mattheus, C.R., and Yovichin, R.D. III. 2018. Hurricane trajectory and irregular bedrock topography as drivers of washover fan geomorphology on an isolated carbonate platform. *Journal of Coastal Research* 34: 1328-1340.

Martin, R.E. 1986. Habitat and distribution of the foraminifer *Archaias angulatus* (Fichtel and Moll; Miliolina, Sortidae). *Journal of Foraminiferal Research* 16: 01-206.

Martin, L.D., and Lewis, R.D. 2016. Growth of attached (encrusting) benthic foraminifera along an onshore-offshore transect, Fernandez Bay, San Salvador, Bahamas: Preliminary results. Pp. 111-123. In B. Glumac and M. Savarese (Eds.). *Proceedings of the 16th Symposium on the Geology of the Bahamas and Other Carbonate Regions*. Gerace Research Centre, San Salvador, Bahamas.

McIntyre-Wressnig, A., Bernhard, J.M., McCorkle, D.C., and Hallock, P. 2011. Non-lethal effects of ocean acidification on two symbiont-bearing benthic foraminiferal species. *Biogeosciences Discussions* 8: 9165-9200.

Michelson, A.V., and Park Boush, L.E. 2016. Paleosalinity records from three lakes on San Salvador Island, Bahamas, inferred from preserved ostracod assemblages. Pp. 124-140. In B. Glumac and M. Savarese (Eds.). *Proceedings of the 16th Symposium on the Geology of the Bahamas and Other Carbonate Regions*. Gerace Research Centre, San Salvador, Bahamas.

Morgan, J.L. and Lewis, R.D. 2012. Benthic foraminiferal assemblages at Cut Cay: A microcosm study of the effects of water energy and substrate preference, San Salvador Island, Bahamas. Pp. 150-162. In F.D. Siewers and J.B. Martin (Eds.). *Proceedings of the14th Symposium on the Geology of the Bahamas and other Carbonate Regions.* Gerace Research Centre, San Salvador, Bahamas.

Murray, J.W. 1991. *Ecology and Palaeoecology of Benthic Foraminifera*. University of Southhampton Press, Southhampton, UK, 397 p.

Niemi, T.M., J.C. Thomason, J.M. McCabe, and Daehne, A. 2008. Impact of the September 2, 2004 Hurricane Frances on the coastal environment of San Salvador Island, the Bahamas. Pp. 43-63. In L.E. Park and D. Freile. (Eds.). *Proceedings of the 13th Symposium on the Geology of the Bahamas and other Carbonate Regions*. Gerace Research Centre, San Salvador, Bahamas.

Park, L.E., Siewers, F.D., Metzger, T., and Sipahioglu, S. 2009. After the hurricane hits: Recovery and response to large storm events in a saline lake, San Salvador Island, Bahamas. *Quaternary International* 195: 98-105.

Park, L.E. 2012. Comparing two long-term hurricane frequency and intensity records from San Salvador Island, Bahamas. *Journal of Coastal Researc*h 28(8): 91-902.

Parnell, D.B., Brommer, D., Dixon, P.G., Brown, M.E., and Gamble, D.W. 2004. A survey of Hurricane Frances damage on San Salvador. *Bahamas Journal of Science* 12: 2-6.

Peebles, M.W. and Lewis, R.D. 1988. Differential infestation of shallow-water benthic foraminifera by microboring organisms: Possible biases in preservation potential. *Palaios* 3: 345-351.

Peebles, M.W. and Lewis, R.D. 1989. Notes on the taphonomy of common shallow-water benthic foraminifera from San Salvador, Bahamas. Pp. 267-273. In J.E. Mylroie and D.T. Gerace (Eds.). *Proceedings of the 4th Symposium on the Geology of the Bahamas.* Bahamian Field Station, San Salvador, Bahamas.

Peebles, M.W. and Lewis, R.D. 1991. Surface textures of benthic foraminifera from San Salvador Island, Bahamas. *Journal of Foraminiferal Research* 21(2): 85-292.

Pilarczyk, J. E. and E.G. Reinhardt. 2012. *Homotrema rubrum* (Lamarck) taphonomy as an overwash indicator in marine ponds on Anegada, British Virgin Islands. N*atural Hazards* 63: 85-100.

Pilarczyk, J. E., Goff, J., Mountjoy, J., Lamarche, G., Pelletier, B., and Horton, B.P. 2014. Sediment transport trends from a tropical Pacific lagoon as indicated by *Homotrema* rubra taphonomy: Wallis Island, Polynesia. *Marine Micropaleontology* 109: 21-29.

Robinson, M.C. and Davis, L. 1999. Preliminary geographical information system analysis and maps of physical, hydrological, archaeological, and biological resources, San Salvador Island, Bahamas. Pp. 101-109. In H.A. Curran and J.E. Mylroie (Eds.). *Proceedings of the 9th Symposium on the Geology of the Bahamas and other Carbonate Regions*,. Bahamian Field Station, San Salvador Island, Bahamas.

Sanger, J.W. and Teeter., J.W. 1982. The distribution of living and fossil ostracoda and their use in the Iinterpretation of the post Pleistocene of Little Lake, San Salvador Island, Bahamas. Pp. 27-31. In *Proceedings of the 1st Symposium on the Geology of the Bahamas.* CCFL Bahamian Field Station, San Salvador, Bahamas.

Sipahioglu, S.M. 2010. Tracking storms through time: event deposition and biologic response in Storr's Lake, San Salvador Island, Bahamas. M.S. Thesis. University of Akron, Akron, OH, USA.

Teeter, J.W., Beyke, R.J., Bray, T.F. Jr., Brocculeri, T.F., Bruno, P.W., Dremann, J.J., and Kendall, R.L. 1987. Holocene depositional history of Salt Pond, San Salvador, Bahamas. Pp. 145-150. In H.A. Curran (Ed.). *Proceedings of the 3rd Symposium on the Geology of the Bahamas.* CCFL Bahamian Field Station, San Salvador, Bahamas.

Tichenor, H.R. and Lewis, R.D. 2018. Distribution of Encrusting Foraminifera at San Salvador, Bahamas: A Comparison by Reef Types and Onshore-Offshore Zonation. *Journal of Foraminiferal Research* 48:373-387.

Titus, R. 1982. Quaternary stratigraphy of San Salvador, Bahamas. Pp.1-5. *Proceedings of the 1st Symposium on the Geology of the Bahamas.* CCFL Bahamian Field Station, San Salvador, Bahamas.

Titus, R. 1984. Physical stratigraphy of San Salvador Island, Bahamas. Pp. 209-228. In J.W. Teeter (Ed.). *Proceedings of the 2nd Symposium on the Geology of the Bahamas*. CCFL Bahamian Field Station, San Salvador, Bahamas.

Titus, R. 1987. Geomorphology, stratigraphy, and the Quaternary history of San Salvador. Pp. 155-164. In H.A. Curran (Ed.). *Proceedings of the 3rd Symposium of the Geology of the Bahamas*.

CCFL Bahamian Field Station, San Salvador, Bahamas.

Voegeli, V.J., Simonti, A.L., and Curran, H.A. 2006. Seasonal sediment transport and unusually large spit development at Sandy Point, San Salvador, Bahamas. Pp. 233-240. In R.L. Davis and D.W. Gamble (Eds.). *Proceedings of the 12th Symposium on the Geology of the Bahamas and other Carbonate Regions*. Gerace Research Centre, San Salvador, Bahamas.

FLANK MARGIN CAVE COLLAPSE IN THE BAHAMAS: PREDICTIVE METHODS

Orry P. Lawrence and John E. Mylroie

Department of Geosciences, Mississippi State University,
Mississippi State, MS 39762

ABSTRACT

The risk of sinkhole collapse in The Bahamas is almost entirely caused by failure of cave roofs. Cover-collapse sinkholes, common elsewhere (e.g. Florida) and caused by catastrophic sediment flow into underground voids, are almost non-existent in The Bahamas because soil cover is thin. On the large carbonate banks of The Bahamas, conduit flow at depth leads to large collapse features that under current sea-level conditions become blue holes. Predicting this collapse is difficult. On large and small banks, flank margin caves, formed in the distal margin of the fresh-water lens at a past sea-level highstand, are common, as is a subset of that cave type, the banana hole. Flank margin caves have three entrance types: dissolution pit, side breach, or ceiling collapse. The latter two are the result of mass erosional forces; pits form by focused vadose dissolution (and can be confused with breached bell holes). Banana holes typically result in roof collapse due to their location in Pleistocene strand plains which cause them to form with thin roofs predisposed to failure.

The use of surface slope as a proxy for controlling factors in Bahamian flank margin cave collapse was initiated. This study demonstrated that 7.5 minute topographic maps cannot resolve slopes in enough detail to predict potential collapse locations. Field surveys with 1 m contours allowed for a more concise slope range in which each entrance type preferentially occurred; collapse breaches and pits were common on gentle slopes and side breaches on steep slopes. The location of flank margin caves and banana holes can be simply found in a general sense, but the specific position of these voids within those localities cannot be determined. Further investigation into the location of subsurface voids and the collapse risk associated with such voids can be performed using various geophysical methods including GPR and gravity surveys, although these methods are labor intensive and time consuming.

INTRODUCTION

Sinkhole formation by sudden subsidence or collapse in soluble rocks results from failure of material overlying dissolutional voids (White, 1988). If the failure is in the bedrock roof of the void, it is called *cave collapse*. If the failure is in a soil arch formed by overlying sediment trickling through a hole in the bedrock into a void through time, it is called a *cover collapse*. Most catastrophic sinkhole collapse seen in news reports from areas like Florida are cover collapse events, as the unconsolidated sediment overlying the limestone there is commonly 10 to 30 m thick (Polk and Brinkman, 2013). In this setting, sediment loss down even small openings into a cave below can, given enough time, form large soil arches in the unconsolidated material, leading to eventual catastrophic failure. Such collapses can be triggered by large rainfall events (increasing soil weight and flushing sediment downward), drought (loss of soil cohesion and drop in the water table with buoyancy loss), or artificial actions (e.g. groundwater withdrawal, focusing of drainage, loading by building construction). In comparison, cave collapse is relatively rare. However, if the limestone surface has little or no sediment cover, then cover collapse events cannot occur, and sudden collapse events will be caused solely by failure of the bedrock roof of the cave.

Figure 1. Images of Bahamian flank margin caves showing characteristic entrances. A) Collapse entrance to Babylon Cave, Acklins Island, with collapse blocks visible in the background. B) Large collapse entrance in 1702 Cave, Crooked Island; Figure 13 shows a map of this cave, the collapse shown is the one on cross section line (c), the image was taken looking northeast into the collapse. C) Fenestral Cave, Crooked Island, showing a side breach entrance caused by storm wave erosion; note also the thin roof making roof collapse likely in the future. D) Duncan Pond Cliff Cave, Acklins Island, a large side breach entrance, with portions of the collapsed hillside visible in the background. The cave ceiling shows small pit entrances which are most likely breached bell holes.

Cave roof collapse is a land-use hazard that has long been of concern in the carbonate island setting, such as The Bahamas, but field reconnaissance costs and the logistical difficulties of field work have left much unanswered about cave roof collapse risk. Caves and karst landscapes are recognized as a geologic hazard (White, 1988), including the special issue of islands (Wilson et al., 1995). Flank margin caves (Figure 1), which form by dissolution at the margin of the freshwater lens, are a major type of cave in carbonate islands (Mylroie and Mylroie, 2007; Mylroie, 2013). Flank margin caves commonly have portions that have collapsed (Figure 1A and 1B), as well as areas where the roof is thin and prone to collapse (roof in Figure 1C). Side breaches caused by cliff or slope retreat can also occur (Figures 1C and 1D). Banana holes (Figure 2), typically found in late Pleistocene progradational strand plains throughout The Bahamas, are small, immature flank margin caves with thin roofs (Ho et al., 2013). Banana holes are thought to pose the greatest potential collapse hazard (in terms of frequency) due to their thin roofs. The roofs are thin because most banana holes are

Figure 2. Banana holes, San Salvador Island, The Bahamas. A) Banana hole showing the common circular shape and vertical walls caused by collapse. B) Another banana hole, showing a portion with an intact roof.

located just beneath the surface of low elevation (3-8 m), relatively level, late Pleistocene strand plain terraces (e.g. 49% of San Salvador Island is below 6 m elevation, Wilson et al., 1995). Because flank margin caves form near the flank of the enclosing landmass at the sea-water contact, and banana holes form in late Pleistocene progradational strand plains, their *general* locations are relatively easy to predict. However, *specific* location predictions remain elusive. Flank margin caves, as well as banana holes, form as entranceless caves that cannot be observed from the surface until they are breached by hill retreat, roof collapse, or a pit intersection (Figure 1D). Remote sensing and GIS technology provide venues by which spatial research on cave roof collapse can be conducted (e.g. Ho et al., 2013). The slope of the overlying topography is the only parameter that can be viewed remotely in efforts to infer what is happening beneath the surface. The slope would have an effect on roof thickness; steep slopes being more stable and gentle slopes leading to greater risk of collapse. The problem is that inexpensive highly accurate satellite data are not readily available for The Bahamas. The resolution of the topographic data will affect the ability to calculate roof thickness and in turn define the potential to predict flank margin cave collapse.

The Carbonate Island Karst Model (CIKM) was developed and validated via extensive fieldwork on numerous islands in The Bahamas and elsewhere. That fieldwork included surveying and mapping cave location and extended profile (Jenson et al., 2006; Mylroie and Mylroie, 2007; Mylroie, 2013). The CIKM describes island karst as being controlled by sea water and fresh water mixing, sea-level position (eustatic and/or tectonic), rock age (usually youthful, termed *eogenetic*), and island geology (from simple to complex). The Bahamas are classified in the Simple Carbonate Island category under the conditions of the CIKM (Mylroie and Mylroie, 2007), meaning only carbonate rocks form the land surface and the aquifer holding the fresh-water lens. The Bahamas provide a useful study area to develop a test model for cave roof collapse due to the islands' young age, relatively simple geology, and lack of tectonics (except for Mayaguana Island, see Kindler et al., 2010).

Cave maps with detailed surveys were created for caves on many islands throughout The Bahamas over the past four decades (Mylroie and Mylroie, 2013). Though the rationale behind the search for caves has not been to predict cave roof collapse, years of data from the development of the CIKM, funded primarily by petroleum companies as a paleokarst reservoir project (Labourdette et al., 2007), can now be used to assist in dealing with a

potentially dangerous land-use hazard. The CIKM explains that the caves on many of these islands are not conduits, but rather mixing chambers, lacking evidence of turbulent flow (Mylroie and Mylroie, 2007). Vacher and Mylroie (2002, p. 183) differentiated "island karst" from "karst on islands" by explaining that "island karst" are those features which formed under the influence of the CIKM rather than the typical continental interior stream-cave model. The category "karst on islands" represents karst behavior similar to that seen on continents, commonly in large island interiors. The CIKM led to much advancement in karst related research that was previously difficult due to the lack of understanding of "island karst".

Another collapse feature found in The Bahamas and other carbonate platforms around the world is the blue hole. Blue holes are deep water-filled voids that form by a number of different mechanisms (Mylroie et al., 1995): 1) flooding of pit caves and deep sinkholes due to the rise of sea level during an interglacial; 2) failure of the bank margin, leading to development of deep fissures on platform perimeters; and 3) collapse of large, deep conduit caves well below current sea level in the carbonate platform. The last feature is a true cave collapse, but predicting them requires knowing were the conduits are, a difficult task given the rigors of cave diving, and the low number of such caves available to cave divers for exploration and survey. Because open blue holes are usually found only on islands or in nearby protected lagoons, the true number of blue holes is not known. Blue holes that have developed out on the open platform are currently filled with Holocene carbonate sediment. Extrapolation from island blue hole inventory counts suggests that in-filled, open platform blue holes exist in the thousands in The Bahamas (Larson and Mylroie, 2014). The conduits that collapse and form the blue holes result from lower sea-levels, when the carbonate platforms are exposed and the large catchment area drives traditional conduit flow development to discharge meteoric water from the fresh-water lens. The work reported here does not consider the blue hole collapse risk as surface topography has mimimal impact on blue hole expression.

Can cave location along with the slope of the overlying topography address cave roof collapse potential? The goal of this research is to establish a set of protocols to assess cave roof collapse risk for flank margin caves in The Bahamas. More specifically, the objective is to determine whether the Bahamas Lands and Surveys 7.5-minute topographic quadrangle map sheets from the early 1970s have the resolution necessary to predict flank margin cave collapse. Can the distal slope of the overlying dune be used to predict where bedrock is suspected to be the thinnest? Roof thickness and maximum chamber width are the two factors that cause collapse in caves (White, 1988). Neither of the two factors that lead to collapse are viewable from the surface. Since the slope of the topography can be remotely sensed and/or calculated, this project will test whether the slope can be used as a proxy for roof thickness. This research is important because up to this point, there is no way to predict flank margin cave roof collapse. Finding a way to predict flank margin cave collapse would be a significant step in land development practices in The Bahamas (as well as other carbonate islands and coastlines).

METHODOLOGY

Data collection

There were three types of data needed to conduct this research: 1) cave location data (GPS points, 15 m accuracy); 2) cave maps; and 3) topographic maps for the entire study area. The SRTM (Shuttle Radar Topography Mission) digital elevation maps (DEMs) available from the US government have 90 m accuracy. The STRM DEMs provide less accuracy than the Bahamas Lands and Surveys 7.5-minute topographic quadrangle maps, which have 20 ft (6 m) contours. For this reason, topographic maps from the Lands and Surveys Department of The Bahamas were used to obtain the slope overlying each cave. These topographic maps have 20-ft (6-m) contour lines and allow the location of the cave to be plotted on the surface, as well as calculation of the slope for that area. Some maps have a 10-ft (3-m) contour line placed

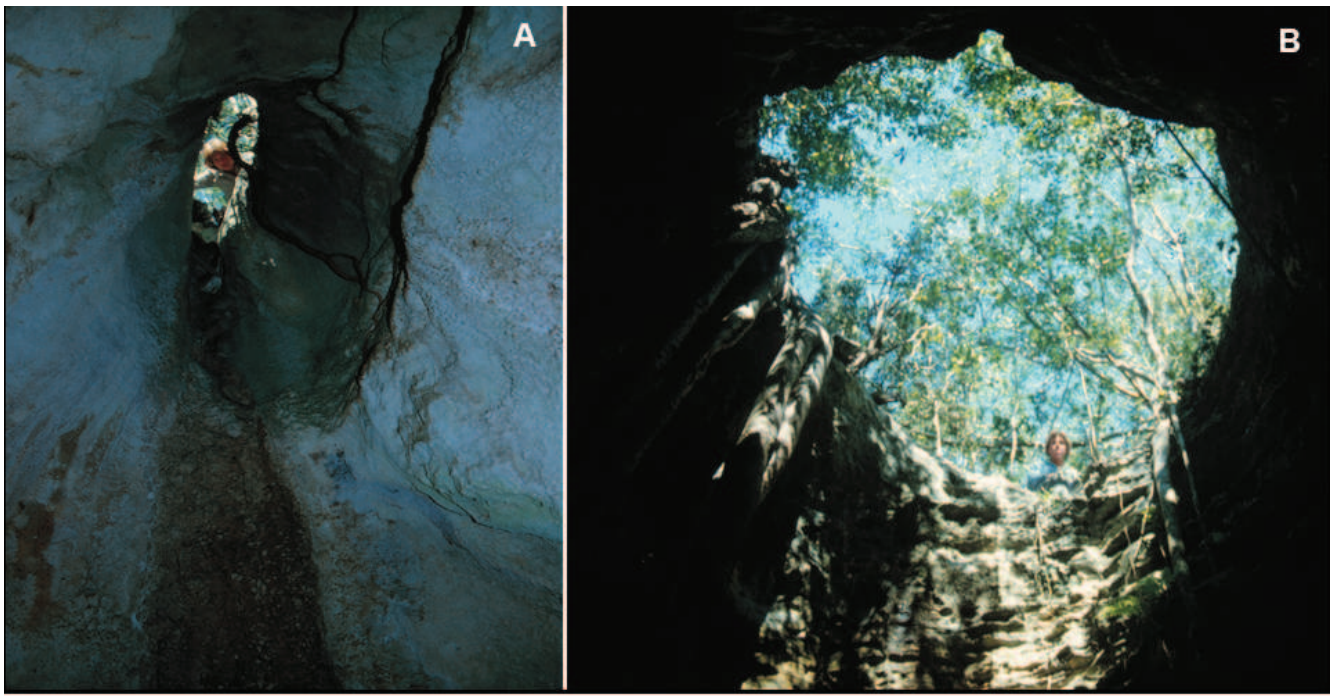

Figure 3. Pit caves, San Salvador Island, Bahamas. A) Pit cave with a small cross section but still deep. Note the elongated shape of the shaft. B) A large cross section pit cave. Both pits lead into the same cave, the aptly named Deep Hole Cave.

between the 20 ft (6 m) elevation and sea level in coastal areas, for better resolution of coasts and tidal position.

Slope analysis

First, the caves were plotted on the associated 7.5-minute topographic map using GPS location data acquired from Coastal Cave Survey, directed by Michael Lace. This survey is a repository for island cave maps for islands from around the world (Lace and Mylroie, 2013). The location of each cave, given by x-y coordinates, was input into Google Earth and then manually plotted onto each island's topographic map. The topographic map set for each island consisted of 2 to 28 sheets to cover the entire island and various cays surrounding each island. Cave maps and/or topographic maps were not available for every cave that had a GPS point; only the caves with GPS location, a detailed cave map, and the corresponding topographic map sheet were used in the study. Each cave was located on the topographic map, and the slope inputs (rise/run) were manually measured using calipers and the map scale. The slope inputs were then recorded in Microsoft Excel to populate rise and run columns. Next, using functions offered in Excel, the slope was derived by using the following formula: Slope=DEGREES (ATAN (rise/run). By analyzing the slope of the flank of the dune, properly placing the cave and its vertical profile in relation to that slope, which sections demonstrate collapse and how thick the roof (overburden) is in those areas could be estimated.

Cave entrances

These analyses should aid in the prediction of potential cave collapse risk in regions with unknown caves using a slope/collapse relationship. Some caves have many entrances and areas with collapse, while others may have a single entry point with little to no evidence of collapse. When analyzing each cave map, each cave entrance was recorded in Excel and categorized by the following

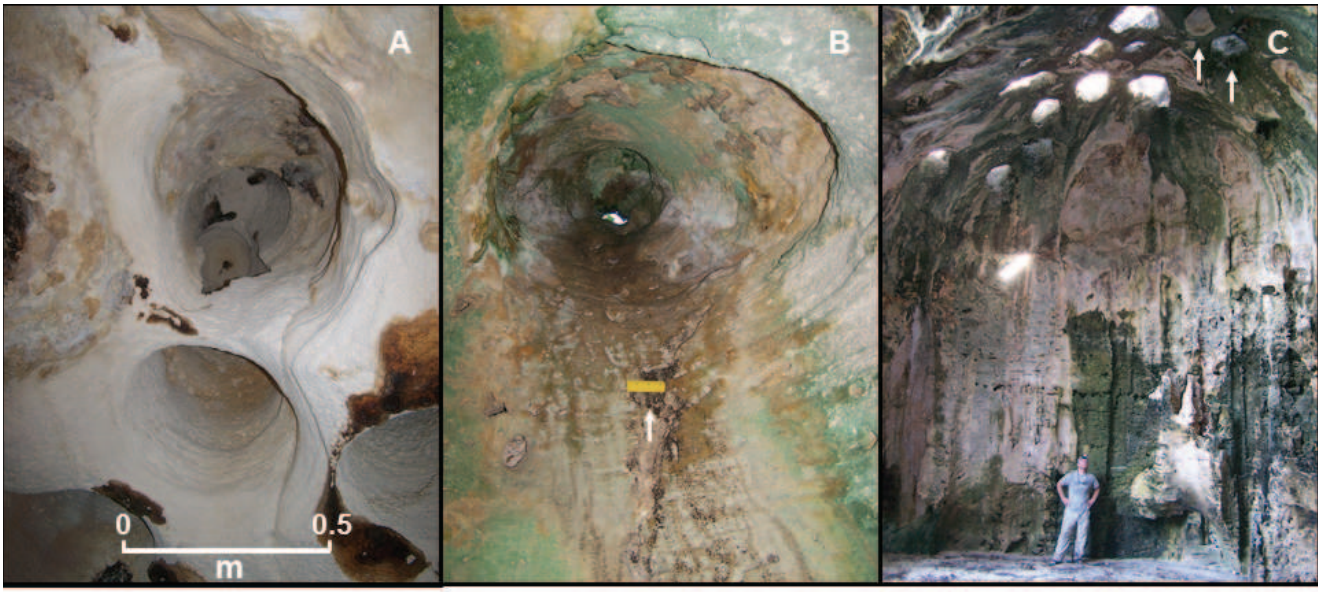

Figure 4. Bell holes from Bahamian Caves. A) Typical bell hole, showing the cylindrical shape, bell hole in upper center is 40 cm across and 2 m high (from the ceiling lip), Jumby Hole, Acklins Island. B) Bell hole from Osprey cave, Crooked Island, showing a small hole where surface denudation has just breached the bell hole to admit daylight. Scale bar (arrow) 8 cm long for scale. C) Breached bell holes from Fenestral Cave (see Figure 1C), Crooked Island; surface denudation has taken off the top of the domes in these bell holes, but others can be seen that are as yet un-breached (arrows).

entrance types: side breach from slope retreat (Figure 1C and 1D); roof collapse (Figure 1A and 1B); or pit intersection (Figure 3). The differentiation between collapse and pit intersection was subject to interpretation; if the hole in the roof was small and no collapse breccia was noted on the floor of the cave, the entrance classification was interpreted as pit intersection. The total number of entrances was also recorded. The slope of the overlying topography was plotted against each of the three categories of entrances, plus number of entrances, in an effort to determine if a relationship between slope and entrance type exists. Subsequently, during analysis, side and collapse entrances were treated as a single entrance type (mass wasting), to differentiate them from the simple downward dissolution formation mechanism of pit entrances.

After the entrance analyses work was completed, it was realized that entrances that had been classified as pit caves were actually two entrance types. The initial pit cave interpretation, and now what are understood to be the intersection of bell holes by the land surface. Bell holes are vertical, cylindrical tubes in the ceiling of many Bahamian caves (Figure 4A). Their origin has been highly controversial (Birmingham et al., 2010) with three separate speleogenetic mechanisms having been proposed. The mechanism supported by Birmingham et al. (2010), that the bell holes are dissolutional features formed by slow vertical convection when the cave initially developed, is the one used here. After cave development, the overlying land surface is slowly lowered by dissolutional surface erosion (i.e. denudation), by meteoric processes, such that the tops of the bell holes become opened, at first gradually (Figure 4B), and then entirely (Figure 4C). To casual observation, the difference between a breached bell hole and a vertical pit produced by downward vadose flow may not be obvious. It is critical to recognize that proper identification of breached bell holes indicates a significant amount of surface denudation. Such denudation thins the cave roof and makes subsequent cave roof collapse more likely. The results reported in this paper for pit cave entrances conflate two different processes. This issue will be dealt with further in the Results and Discussion sections.

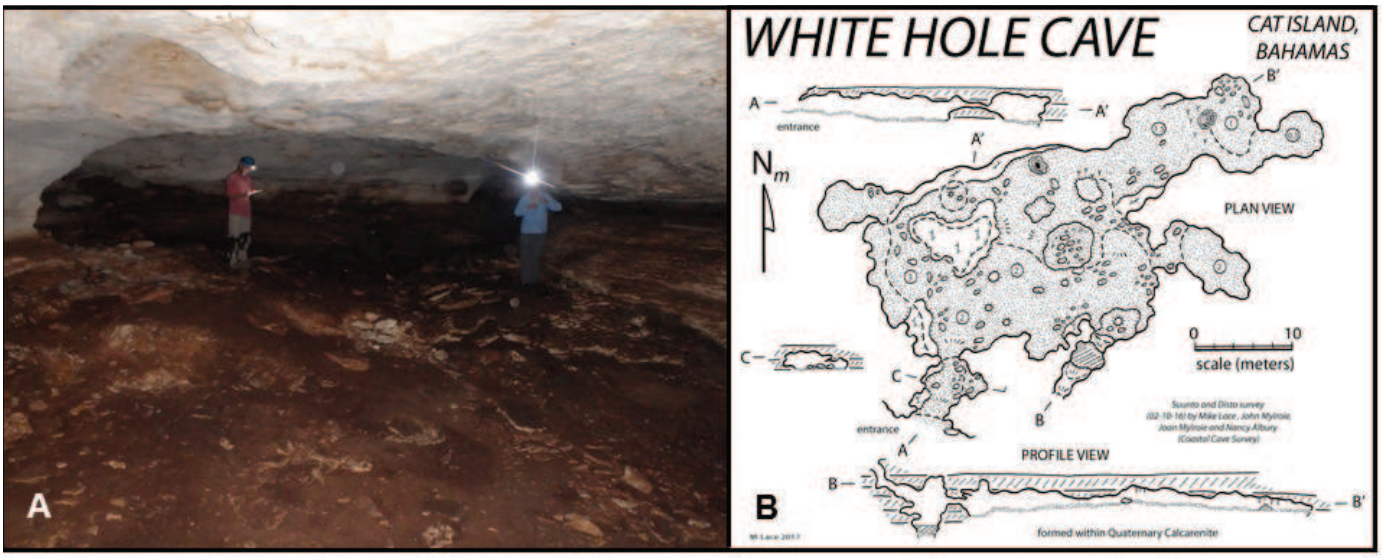

Figure 5. White Hole Cave, Cat Island, Bahamas. A) Central chamber of the cave, showing a wide, unsupported span. B) Map of the cave, which was used to determine span dimensions. The image in (A) was taken looking north through the largest room in the cave. The dark brown on the cave floor is bat guano, the host rock is white.

Unsupported span (maximum chamber width)

The maximum chamber width was recorded to help determine the relationship between roof span and roof collapse (Figure 5). By documenting the maximum unsupported span, along with the overlying slope, it could be further demonstrated what effect slope has on roof thickness, that in turn controls aspects of collapse. For example, a cave with maximum chamber size (x) and an overlying slope (z) does not demonstrate collapse, but another cave with equal chamber size (x) and a lesser overlying slope (y) does demonstrate collapse. This approach demonstrates how chamber size affects collapse potential when coupled with roof thickness. It is not believed that cave chamber size alone is the cause for collapse, as there are caves with very large chambers with very little to zero collapse. It has been proposed that slope has an effect on beam thickness; the cause for collapse is beam thickness coupled with the maximum unsupported span, neither of the two causes collapse by itself (White, 1988).

Data analysis

The data collected are not distributed normally. The data will be presented by histograms as a nonparametic display to determine if there is a relationship between the cave entrances and cave chambers, and the slopes that surround them.

RESULTS

A total of 107 caves across eight islands (consisting of over 70 topographic map sheets) were analyzed to determine if slopes calculated from topographic maps were predictive of the degree of flank margin cave collapse. Figure 6A shows the islands utilized in the research. Figure 6B shows Abaco Island cave locations, as a representative island, with the cave locations plotted into Google Earth using GPS data points. The full table of results for slope, entrance type/quantity, and maximum chamber width for each cave, as well as cave location maps for all islands displayed in Figure 6A, are shown in Lawrence (2014).

A summary of those results is as follows: There were a total of 408 cave entrances. Of the 408 total, there were 123 side breach entrances, 185 pit entrances, and 100 collapse entrances recorded. Signs of roof collapse were absent in 61 of the 107 caves analyzed. As previously stated, if the hole in the roof was small and no collapse breccia was noted on the floor of the cave, the entrance classification was defaulted to pit intersection (it is now recognized that many of these pit entrances were bell holes intersected by surface denudation). Histograms of slope vs entrance type are shown in Figures 7. Rare slopes greater than 14 degrees are not included (all having side entrances). These steeper slopes range from 17 to 90 degrees, accounting for 12 slopes and 15 side entrances. The full data are in Lawrence (2014). The histograms of slope vs entrance type (total, side, collapse, and pit) do not indicate a relationship detectable between slope and any single type of entrance category (Figure 7B) from topographic data of 20 ft (6 m) resolution. The large number of pit cave entrances for slopes of 3 degrees or less may represent bell hole intersections by surface denudation. Each cave in the study had one slope measurement (Figure 8A). The total number of slope measurements of each slope value was plotted to determine the slope abundance for each slope (14 degrees or below) used in the study (Figure 7). Both side and collapse breaches are a result of large-scale surface erosion, unlike pit entrances which form by focused dissolution or bell hole intersection. For this reason the number of surface erosion cave entrances (side and collapse) per cave were plotted along with slope abundance (Figure 8B); the number of cave entrances exceeds slope abundance. Therefore, most caves have more than one macroscopic entrance. Pit caves' distribution differed

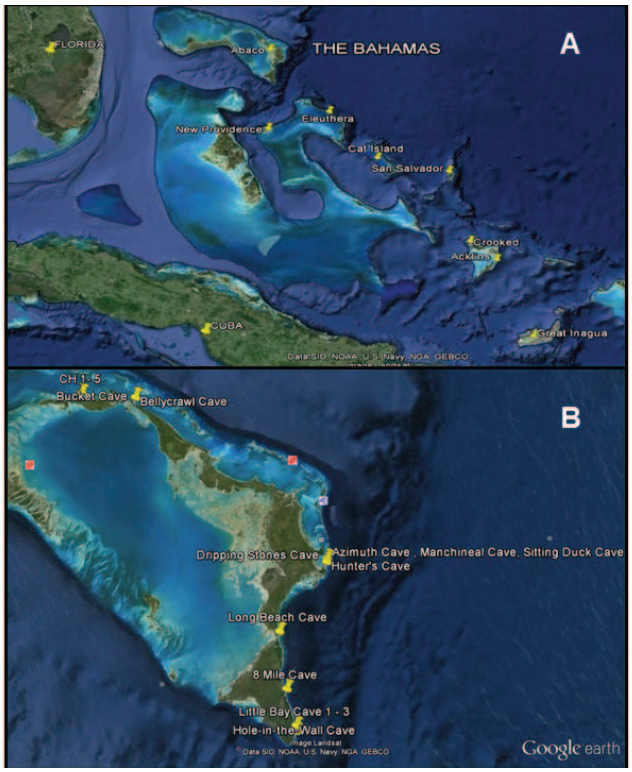

Figure 6. Location maps of caves in The Bahamas, from Google Earth. A) Map of The Bahamas, showing islands used (not including Florida and Cuba). B) Map of Abaco Island, showing cave locations; all islands included in the study had a similar map (see Lawrence 2014 for all maps).

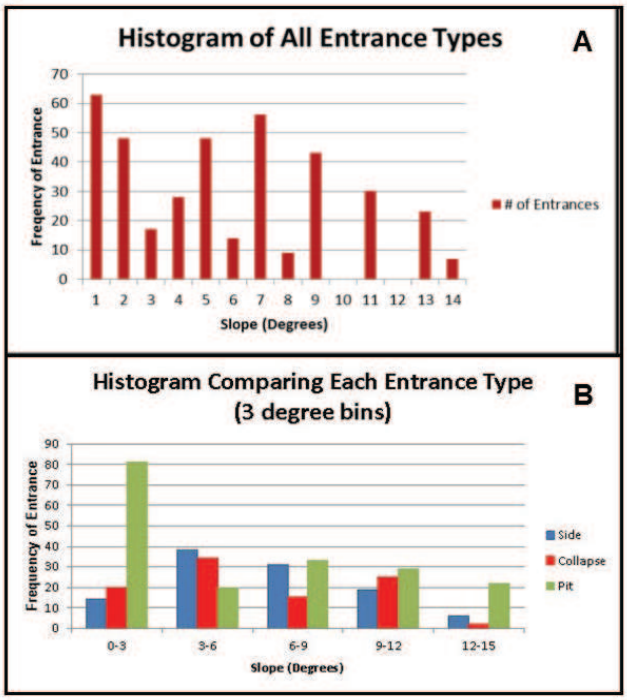

Figure 7. Histograms of overall slope and cave entrance data. A) Number of entrances for each slope measured from 7.5-minute topographic maps. B) Frequency of entrance type based on combining the slopes into 3 degree bins.

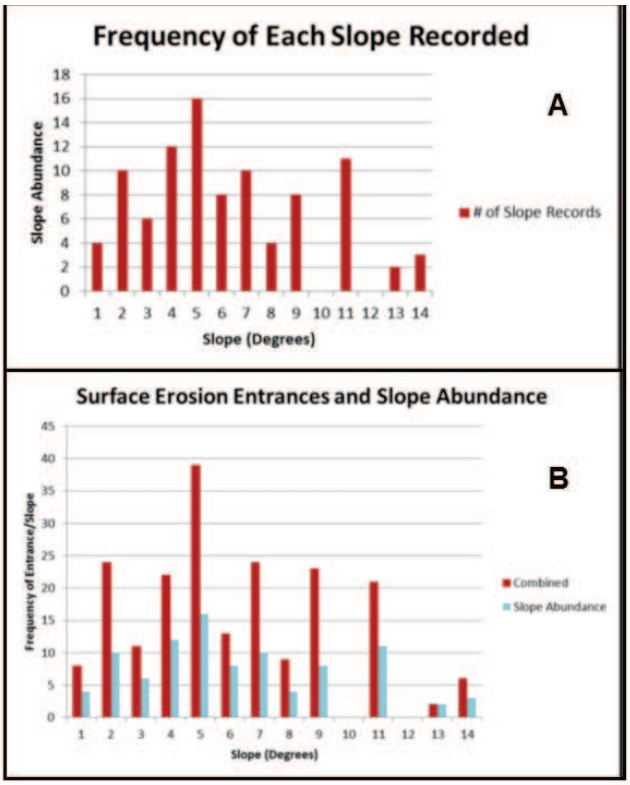

Figure 8. Histograms of slope frequency and surface erosion abundance. A) Frequency of each slope recorded in the database from 7.5-minute topographic maps. B) Combination of side breach and collapse entrance abundances with slope abundance (by degree of slope); the data show most caves have approximately two entrances of this type.

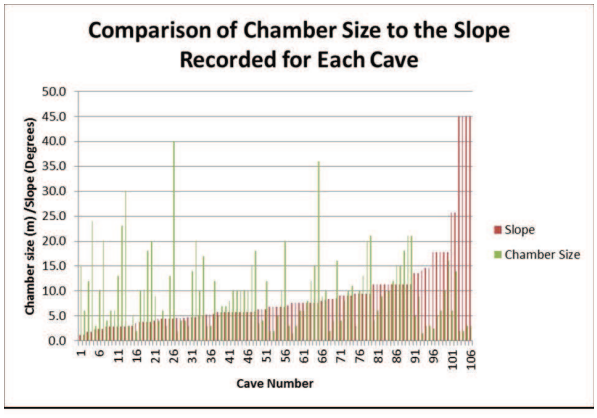

Figure 9. Comparison of chamber size to the degree of slope. There is no recognizable pattern.

from that of side and collapse breach (Figure 7B).

Chamber size (maximum chamber width) was analyzed to see what effect it may play in collapse risk. The slope or each cave, along with the chamber size was plotted on a histogram for each of the caves in the study (Figure 9). This plot allows the variance in chamber size to be observed, and helps the user realize how unpredictable chamber size is. Since chamber size and roof thickness are coupled as the causes for collapse, this unpredictability of chamber size further complicates using slope as a predictor of collapse.

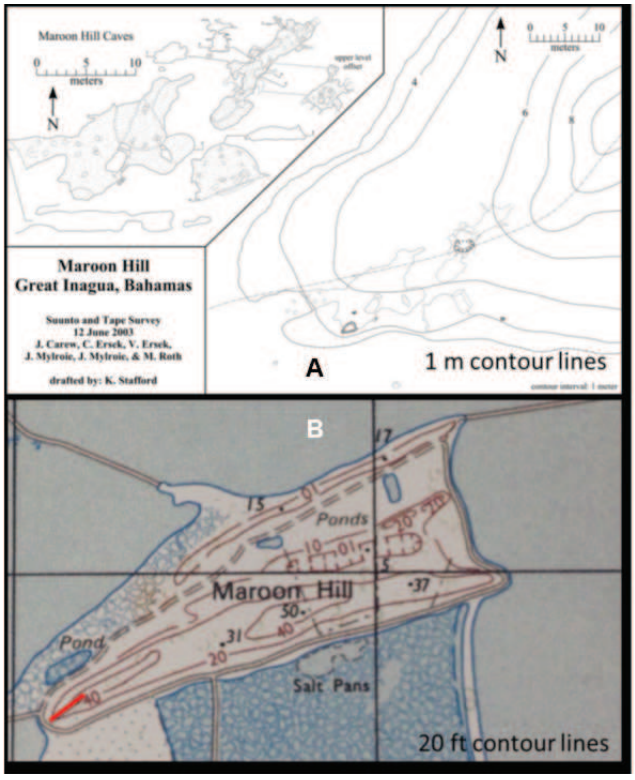

Figure 10. Maroon Hill Cave, Bahamas. A) One meter contour map surveyed over the caves of Maroon Hill. B) Compare with A, 7.5-minute topographic map segment showing Maroon Hill. The caves and survey of (A) shown by the short line at the southeast tip of the hill. Maroon Hill Cave was one of six caves for which high resolution contours were surveyed, see Lawrence (2014) for all cave maps and overlying contour surveys.

The low resolution of the topographic maps made much of the results inconclusive. Some caves had been mapped with surface topography included. Data were extracted from cave maps with the field surveyed (1 or 2 meter) contours overlaid for six caves (e.g. Figure 10). The higher resolution of spatial data leads to a more detailed analysis; these data allowed the slope to be calculated over the entire cave as well as the slope over the sections that showed collapse. A visual comparison of the two data types helps to clarify the limitations of this study. Figure 11 does show some trends. Side entrances fall towards the high slope angle end of the plot, collapse entrances towards the low slope angle end of the plot. Pit caves are strongly biased to the lower slope angles.

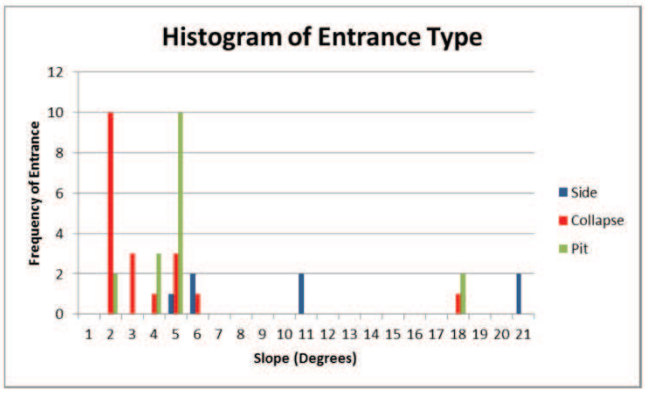

Figure 11. Histogram for the six caves with high resolution contour surveys

At this point, a realization was made that the accuracy of the calculated slope was not good enough to estimate roof thickness from the cave map data. The original methodology included a few steps that incorporated the estimation of roof thickness for areas of collapse using the calculated slope from the topographic maps, but due to the limitations of the data accuracy, these methods were not performed.

DISCUSSION

Topographic map analysis

This project focused on whether or not 7.5-minute topographic map sheets could be used to predict cave roof collapse; the resolution of the topographic maps does not allow such predictions to be produced. Using the calculated slope of 107 caves from data extracted from the topographic map sheets is based on the idea that slope can be used as a proxy for roof thickness (roof thickness being one of the critical components that initiates collapse). The resolution of the currently available topographic data allows the roof overhead to be crudely estimated using the slope derived from the topographic maps, but this slope is not accurate enough to determine roof thickness as the spatial data limitations are simply transferred. The variations in the hillslope, which are not noticeable from the topographic maps, can lead to an inaccurate roof thickness reading. With many areas having terraced slopes (Figure 12), the roof thickness can vary much over what appears to be a steady slope on the topographic maps but is not so in the real world. The map of 1702 Cave on Crooked Island (Figure 13, (c) and (d) cross-section lines) is an excellent example of how the flat areas (wider contour spacing) allows for collapse.

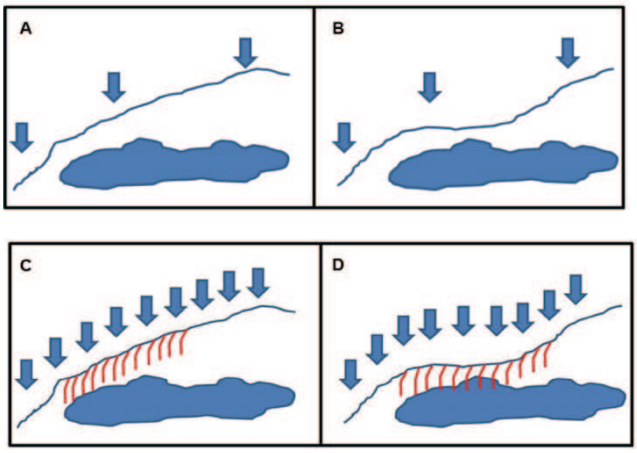

Figure 12. Consequences of slope contour resolution. A) Hypothetical slope based on extrapolation of a 20m ft (6 m) contour interval, with a cave underneath. B) A lessoning of slope with a concurrent of rock thinning over a cave roof would also fit the 20 ft (6 m) data. C) Same as in (A) showing how pit caves (vertical kinked lines) of a uniform shallow depth hit the cave only a few times. D) Same as in (B), showing how a lessoning of slope produces far more pit cave intersections with the underlying cave.

Figure 12 demonstrates the problem with this approach because of the resolution of topographic map sheets. If a prediction model was made, it would be misleading. In turn, the model could overlook a collapse risk (e.g. say that it is safe to build) by assuming a steady slope when in reality the landscape may have a varying slope (introducing flat areas with potentially thin roofs), as Figure 13 demonstrates. If this model was constructed using inadequate spatial resolution, it could result in someone building in a location that is actually prone to collapse (an accident). The worst-case scenario of this development would be a collapse event resulting in loss of life, time, and/or investment capital.

Flank margin cave entrances are interesting due to the fact that flank margin caves form as entranceless voids beneath the surface. The caves remain entranceless until the cave is breached by cliff retreat (side entrance), roof collapse (overhead entrance due to roof thickness and unsupported span), or pit intersection (overhead entrance occurs by localized active dissolution) and bell hole breaching. The 408 cave entrances consisted mostly of pit entrances (185); pits are typically the smallest type of entrance. Side breach entrances were the next most common entrance type (123) and are the largest entrance type, typically allowing one to walk/crawl into the cave from the side. Collapse breaches (100) are the most dangerous entrance type and often have a large area of collapse over gentle slopes. Side breach entrances are common near the coastline or where cliff retreat has occurred, commonly a steeper slope (e.g. Figure 13, the two smaller caves to the northwest on the map). Pit entrances are non-selective to their location of formation; pit entrances occur by the downward dissolution of rock as explained by epigenic karst processes (meteoric water). Side breach and collapse entrances are the result of processes that occurred after the hypogenic (decoupled from surface hydrology) speleogenesis of the cave was complete; pit entrances form by active epigenic (coupled to surface hydrology) speleogenesis. Bell hole entrances are the result of the chemical lowering of the landscape, which intersects these features. In that way they are the result of unfocused surface dissolution, whereas true pit caves are focused surface dissolution.

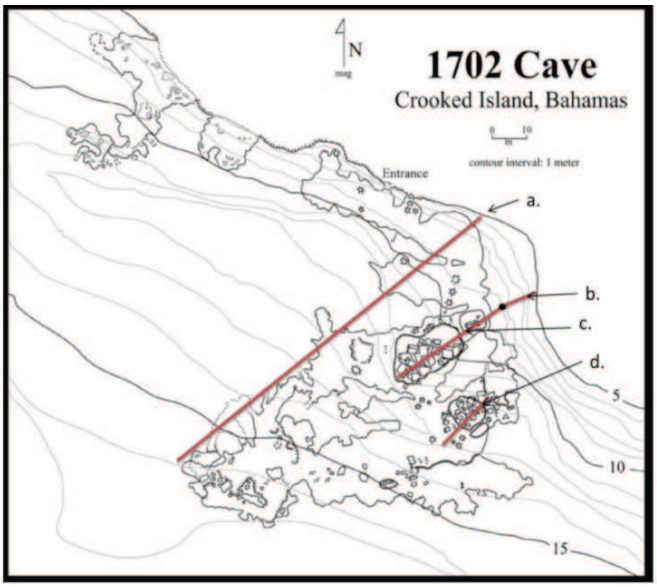

Figure 13. 1702 Cave, Crooked Island, The Bahamas, showing the value of high-resolution contour plots. Cross section (a), using only its endpoints, produces the same data as from a 7.5- minute topographic map with 20 ft (6 m) contours. Cross sections (b), (c), and (d) show how the slope actually varies in steepness. Note that the two large collapse entrances to the cave (circular structures outlined in bold on cross sections (c) and (d)) occur where the slope is both gentle and low elevation, creating a thin bedrock roof condition. Collapse at (c) shown in Figure 1B.

Many caves with the same overlying slope had a different entrance type, supporting the idea that it is more than just roof thickness that effect collapse; chamber width coupled with roof thickness controls the initiation of collapse. Chamber size and the slope for each cave were plotted together in a histogram, and as expected, there is no relationship between these two variables (Figure 9). Flank margin caves are de-coupled from surface processes, and their formation is controlled by the geochemistry and flow dynamics of the fresh-water lens margin. Therefore, as Figure 9 demonstrates, chamber size has no relationship to slope.

On the data plots for the 7.5 minute topographic maps, pit entrances show a relationship with low angle or gentle slopes (Figure 7B). That relationship persists when the slope is calculated from a 1-m-contour survey (Figure 11). Side and collapse entrances seem to show a relationship to gentle to moderate slopes (Figure 7B), but that apparent relationship is an artifact of slope abundance. Figure 8B demonstrates when side and collapse entrances are combined as a single mass wasting entrance type, the ratio of those entrances to slope abundance stays around 2. When the more detailed slope analysis using 1 m contours is displayed (Figure 11), collapse and pit entrances clustered near the low slope end of the plot and side entrances at the middle or high end of the plot.

The distribution of entrances as to slope angle is based on entrance origin. Pit entrances result from localized vadose flow dissolving its way downward. These pits are commonly only a few meters deep, but they can be as much as 10 m deep on rare occasions (Figure 2). When the slope is low, the amount of rock over the cave is less than when the slope is steep (Figure 12). As a result, a dissolution pit only a few meters deep is more likely to enter a cave when the slope is low and the roof is thin, regardless of the chamber size below and the amount of unsupported room span. Pits can have a variety of depths, but small depths are more common. While pit entrances are found on all slopes, they predominate at low slopes where the cave roof *must* be thin (under a steep slope, the cave roof can be thick or thin, depending on chamber size). Bell holes are phreatic dissolutional features formed in the roofs of caves (Figure 3). As surface lowering occurs over time, these will be the first cave features intersected. Their presence actually decreases the total mass of the roof, allowing roofs to stay stable when denudation has made the roofs thin, as in Figures 1C and 3C.

Collapse entrances result from roof failure. The thinner the roof (low beam thickness), or the wider the chamber (high unsupported span value), or both, the more likely is roof collapse. However, chamber width has no relation to slope (Figure 9), so collapse can occur at any slope but does seem to occur mostly at lower slopes which would create a thinner bedrock roof (Figure 12). This slope preference is hinted at in Figure 7B, but is better displayed in Figure 11 when higher slope resolution data are available.

Side entrances result from mass wasting and erosion of hillslopes. Because flank margin caves form under the flank of the land, at the distal margin of the fresh-water lens, to become exposed by surface erosion (as opposed to collapse or pit development) requires that the hillslopes retreat laterally so that the cave is intersected. The key is lateral retreat. The margin of a fresh-water lens during the last interglacial was at about 6 m elevation. A gentle slope starts out at an elevation below 6 m, and to reach that elevation must retreat significantly. A steep slope will reach the 6 m point after less slope retreat; a gentle slope must retreat farther to intersect a cave than a steep slope (Figure 14). While the data in Figure 7A are ambiguous regarding slope, the data in Figure 11 are much more convincing, with side entrances preferentially found at higher slope angles. Figure 11 again demonstrates the necessity of high-resolution slope analysis.

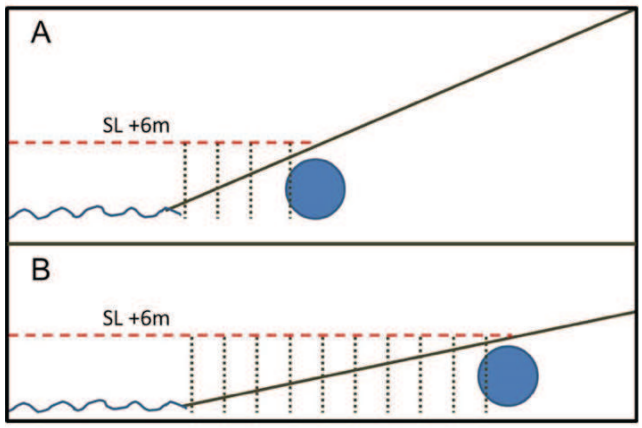

Figure 14. Cartoon showing how slope retreat intersects flank margin caves formed by a +6m sea-level highstand. A) On a steep slope, minor slope retreat is required to breach the cave wall. B) A gentle slope requires a greater degree of slope retreat to achieve cave wall intersection. Note that cave roof thickness is greater upslope for (A) as opposed to (B), providing more roof stability. This cartoon may explain the cave entrance distribution pattern in Figure 11.

Geophysical methods

Gravity surveys have been a successful tool used to locate flank margin caves and banana holes in The Bahamas (Kunze and Mylroie, 1991). GPR (ground penetrating radar) was used to locate voids when the San Salvador airport runway was extended from 4000 to 8000 feet in length. Over 25 voids were located and infilled during this project (most likely banana holes) (William Wilson, personal communication). Gravity, while successful, was labor intensive and not amenable to broad reconnaissance (Kunze and Mylroie 1991). The GPR was very successful, but the work was carried out on level, cleared land. In the vegetated, irregular areas, GPR would likely be less successful. Kunze and Mylroie (1991) state that the dense brush of The Bahamas make GPR impractical. Both GPR and gravity are promising methods for determining the location and size of voids, and void depth, but the use of such tools must be site specific and preferably the site be cleared of the native bush. When an area is predicted to be at risk for collapse due to the slope of the landscape and the assumption of a large span at depth, it is then that geophysical methods could be used to check for voids beneath the surface.

Future work

Slope varies depending on where the transect is drawn. Using Lidar or advanced satellite data (both capable of sub-meter accuracy) in this type of study would open up other opportunities to address the cave collapse problem on carbonate islands. The cost for Lidar or advanced satellite data far exceeded the budget of this research project. The satellite data that were available had worse resolution than the topographic maps (90 m vs 6 m, respectively). Using GIS, the slope could be calculated for an entire study area using the slope tool in spatial analyst. Instead of the slope being calculated over chosen transects, each cell within the raster would have a slope value. The slope calculation in spatial analyst assigns each cell a slope value by taking the maximum change in elevation and dividing it by the distance between the cell and its eight neighbors. The consistency of the GIS slope calculation process removes human error and human bias from the process of slope calculation. With a full sample size of caves, cave maps, and high accuracy elevation data (e.g. Lidar), along with the computing potential of GIS, it is possible that a correlation between slope and collapse risk may be found.

CONCLUSION

The purpose of this study was to test the hypothesis that topographic maps produced by the Bahamas Lands and Surveys Department are insufficient in resolution to be used as a predictor of flank margin cave collapse risk in The Bahamas.

Analysis of 107 caves using over 70 topographic map sheets on eight islands shows no clear relationship between derived slopes and cave collapse. The topographic maps were not of sufficient resolution to create a cave collapse prediction model. Even use of slopes derived from six caves with 1-m contour survey produced only a moderate predictive pattern. There is a visually recognizable pattern using the higher accuracy data, especially for pit entrances, but an accurate prediction of collapse cannot be guaranteed. Cave collapse is not only dependent on slope as a proxy for roof thickness but on the configuration of the underlying cave. Flank margin caves are a series of globular chambers with widely varying chamber sizes and roof heights. This cave configuration makes it difficult to determine when any given slope has created a thin roof condition, which would be prone to collapse. Only banana holes, found in low-lying late Pleistocene stand plains, are guaranteed thin roofs; however specific prediction of the location of the next collapse event is not possible. Geophysical techniques have promise but are labor intensive, especially in remote island settings. Flank margin cave collapse is a very complicated problem. It was illustrated in previous literature that flank margin cave collapse was a fairly straightforward issue, but the use of slope as an indicator for roof collapse is not effective. Slope does demonstrate a relationship with entrance types that are the result of large-scale surface erosion (side breach and collapse breach). However, the prediction of those entrances is not possible due to the

complexities of the initiation of an entrance. Many things must be taken into account to predict collapse (roof thickness, chamber size, and chamber configuration). Flank margin caves and banana holes are easy to localize; flank margin caves are under the edges of dune ridges, and banana holes are in late Pleistocene strandplains. However, the specific location of these voids within those localities eludes easy analysis. This study should be used as a guide to evaluate the landscape and consider if geophysical methods are needed for a particular area before development.

ACKNOWLEDGMENTS

This project would not have been possible if it was not for Mr. Mike Lace and The Coastal Cave Survey; Mike supplied many gps locations and cave maps from various projects throughout The Bahamas. Dr. John Rodgers and Dr. Bill Cooke provided valuable insight in the data analysis. The Erwin-Russell Geology Endowment Fund, Department of Geosciences, Mississippi State University, provided funding to purchase the needed topographic map sheets. We are indebted to The Gerace Research Centre and its staff on San Salvador Island, The Bahamas for logistical and financial support for this research. The research permit was issued by the Bahamian government's Bahamas Environment, Science and Technology (BEST) Commission through the Gerace Research Centre.

REFERENCES

Birmingham, A.N., Lace, M.J., Mylroie, J.R., and Mylroie, J.E. 2010. Bell hole origin: Constraints on developmental mechanisms, Crooked Island, Bahamas. Pp. 18-30. In J.B. Martin and F.D. Siewers (Eds.). *Proceedings of the 14th Symposium on the Geology of the Bahamas and Other Carbonate Regions.* Gerace Research Centre, San Salvador Bahamas.

Ho, C.H., Mylroie, J.E., Infante, L R., and Rodgers, J.R. III. 2013. Fuzzy-based spatial modeling approach to predict island karst distribution: a conceptual model. *Environmental Earth Science* 71: 1369-1377. DOI 10.1007/s12665-013-2543-4.

Jenson, J.W., Keel, T.M., Mylroie, J.R., Mylroie, J.E., Stafford, K.W., Taborosi, D., and Wexel, C. 2006. Karst of the Mariana Islands: The interaction of tectonics, glacioeustasy and freshwater/sea-water mixing in island carbonates. *Geological Society of America Special Paper* 404: 129-138.

Kindler, P., Mylroie J.E., Curran, H.A., Carew, J.L., Gamble, D.W., Rothfus, T.A., Savarese, M., and Sealey, N.E. 2010. *Geology of Central Eleuthera, Bahamas: A Field Trip Guide*. Gerace Research Centre, San Salvador Bahamas, 74 p.

Kunze, A.W.G. and Mylroie, J.E. 1991. Use of gravity techniques to detect shallow caves on San Salvador Island, Bahamas. Pp 139-149. In R.J. Bain, (Ed.). *Proceedings of the 5th Symposium on the Geology of the Bahamas*. Bahamian Field Station, Port Charlotte, FL.

Labourdette, R., Lascu, I., Mylroie, J., and Roth, M. 2007. Process-like modeling of flank margin caves: From genesis to burial evolution. *Journal of Sedimentary Research* 77: 965-979.

Lace, M.J., and Mylroie, J.E. (Eds.). 2013. *Coastal Karst Landforms*. Coastal Research Library 5, Springer, Dordrecht, 429 p.

Larson, E.B., and Mylroie, J.E. 2014. A review of whiting formation in the Bahamas and new models. *Carbonates and Evaporites* 29: 337-347. DOI 10.1007/s13146-014-0212-7.

Lawrence, O.P. 2014. Predicting flank margin cave collapse in The Bahamas. MSc. Thesis. Mississippi State University, Mississippi State, MS, USA. 83 p. http://sun.library.msstate.edu/ETD-db/theses/available/etd-04042014-132659/

Mylroie, J.E., Carew, J.L., and Moore, A.I. 1995. Blue holes: Definition and genesis. *Carbonates and Evaporites* 10: 225-233.

Mylroie, J. E. and Mylroie J.R. 2007. Development of the carbonate island karst model: *Journal of Cave and Karst Studies* 69(5): 9-75.

Mylroie, J.E. 2013. Coastal karst development in carbonate rocks. Pp. 77-109. In M.J. Lace and J.E. Mylroie. (Eds.). *Coastal Karst Landforms.* Coastal Research Library 5, Springer, Dordrecht.

Mylroie, J.E., and Mylroie, J.R. 2013. Caves and karst of the Bahama Islands. Pp. 147-176. In M.J. Lace and J.E. Mylroie. (Eds.). *Coastal Karst Landforms.* Coastal Research Library 5, Springer, Dordrecht.

Polk, J.S., and Brinkman, R. 2013. Climatic influences on coastal cave and karst development in Florida. Pp. 317-345. In M.J. Lace and J.E. Mylroie. (Eds.). *Coastal Karst Landforms*. Coastal Research Library 5, Springer, Dordrecht.

Vacher, H.L., and Mylroie, J.E. 2002. Eogenetic karst from the perspective of an equivalent porous medium. *Carbonates and Evaporites* 17: 182-196.

White, W.B., 1988. *Geomorphology and hydrology of karst terrains*. Oxford University Press, New York, 464 p.

Wilson, W.L., Mylroie, J.E., and Carew, J.L. 1995. Quantitative analysis of caves as a geologic hazard on San Salvador Island, Bahamas. Pp. 103–121. In M. Boardman (Ed.). *Proceedings of the 7th Symposium on the Geology of the Bahamas.* San Salvador Island, Bahamian Field Station.

THE EFFECTS OF HURRICANE JOAQUIN ON THE ONSHORE-OFFSHORE ZONATION OF ENCRUSTING FORAMINIFERA AT SAN SALVADOR, THE BAHAMAS

Ronald Lewis, Sarah Asher, Sara Speetjens Gilley, and Sally Sundbeck

Department of Geosciences
Auburn University, Auburn, AL 36849, U.S.A.

ABSTRACT

Benthic foraminifera that are firmly attached to hard substrates (encrusting foraminifera) have been studied as part of the reef ecosystem and in actualistic studies to aid in paleoenvironmental reconstructions of shallow-water carbonates. A common research technique is to investigate their distribution by collecting cobble-sized pieces of reef rubble and other clasts from a range of environments. One benefit of focusing on encrusting foraminifera is that they are less likely to be transported out of their habitats than are free foraminifera. However, even large clasts can be transported great distances during high-energy storm events, an issue that has caused some concern for researchers.

The small Bahamian island of San Salvador provides a good test case to see if major storms alter the distributional patterns seen previously because its encrusting foraminifera are well known, and the island was impacted directly by Hurricane Joaquin, a Category 4 hurricane with sustained winds of 130 mph, which hit the island in early October 2015. We visited the island March 13-18, 2016 (5.5 months after the event). Cobbles were examined *in situ* and collected from 7 previously studied sites. Prior studies on San Salvador have shown that near-shore assemblages are dominated by well-preserved *Homotrema rubrum*; lagoonal patch reefs are varied but typically have prominent *Planorbulina*; bank barrier reefs are dominated by *Homotrema* but have some *Gypsina plana*; and shelf-margin assemblages are dominated by large *Gypsina plana*. Assemblages were compared before and after the storm based on 2008 and 2015 data, and individual cobbles were plotted on ternary diagrams showing the three principal taxa. Offshore sites, those from the middle of the lagoon to the shelf edge, showed no change. Nearshore sites displayed a small amount of possible shoreward transport and in-place disturbance (only one cobble was clearly upside down). Even cobbles with encrusting foraminifera found on land at French Bay did not seem to have been moved large distances based on the foraminiferal assemblages. Overall, the pattern of distribution observed previously was still intact.

INTRODUCTION

Benthic foraminifera that are cemented by calcium carbonate or are otherwise firmly fixed to hard surfaces are known as attached or encrusting foraminifera. Relatively few actualistic studies focus on the use of encrusting foraminifera as paleoenvironmental indicators compared to the vast literature on free-living foraminifera. However, because of their sensitivity to certain environmental variables that correlate with water depth and distance from shore on shallow-water carbonate platforms, these encrusting species are potentially useful in paleoecologic research.

Encrusting foraminifera have been studied *in situ* on the walls of underwater caves (e.g., Logan, 1981; Logan et al., 1984) and directly attached to coral heads in open water (e.g., Jackson and Winston, 1982; Martindale, 1992). In addition, settlement studies, in which artificial substrates are left on the seafloor for known periods of time, provide an important source of information on growth histories as well as distribution (e.g., White, 2002; Richardson-White and Walker, 2011; Walker et

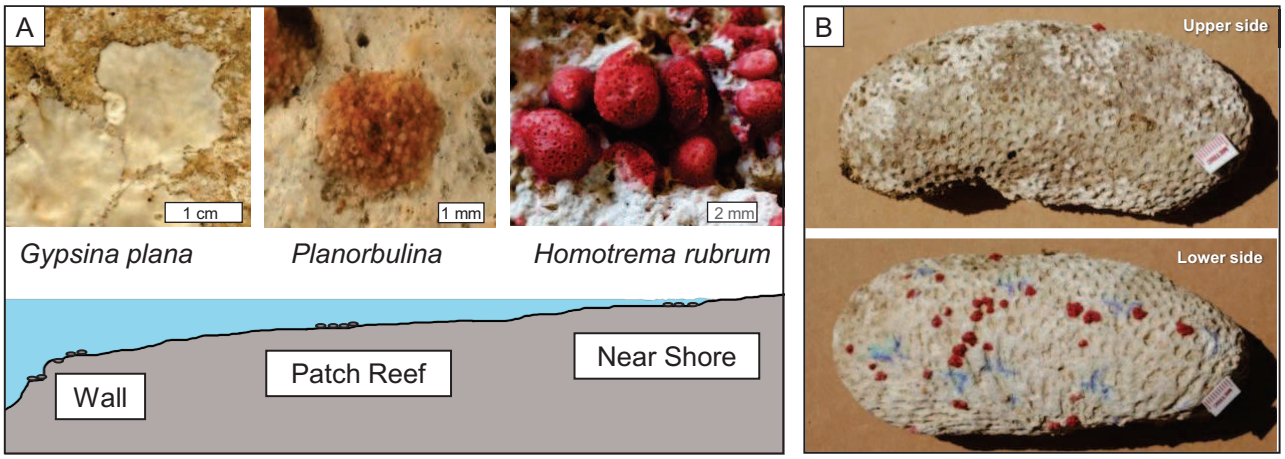

Figure 1. Distributional patterns of encrusting foraminifera. A) The "Tichenor-Lewis model" showing the typical distribution of encrusting foraminifera from shoreline to the wall at the platform margin, first seen at Fernandez Bay, San Salvador (after Tichenor and Lewis, 2009). B) The contrast between the top side of a cobble, bearing attached algae and Planorbulina, versus the underside, which is largely devoid of photosynthesizing organisms but includes the majority of encrusting foraminifera such as Homotrema rubrum, show here; cobble from Site 1, Telephone Pole Reef.

Site no.	Type	Location	Coordinates	Distance from shore	Water depth
1	Shoreline	Station 1 of Telephone-Pole Reef transect (rocky coastline: beachrock)	24° 02' 6.23" N 74° 31' 31.22" W	20 m	1 m
2	Mid-shelf patch reef	Snapshot Reef	24° 02' 14.7" N 74° 31' 55.3" W	275 m	5.2 m
3	Platform margin, ledge on wall	Narrow ledge on wall	24° 02' 13.2" N 74° 31' 55.3" W	582 m	27.1 m
4	Nearshore patch reef	Dump Reef	24° 07' 15.8" N 74° 28' 25.6" W	32–68 m	1–2 m
5	Bank Barrier Reef	Gaulins Reef	24° 08' 53.01" N 74° 28' 32.50" W	2,910 m N of island	3 m
6	Nearshore Reef	Near Salt Pond	24° 01' 24.2" N 74° 26' 59.35" W	20 m	1–1.5 m
7	Lagoonal Patch Reef	Near Salt Pond	24° 01' 20.1" N 74° 26' 56.1" W	135 m	4.5–6.0 m
8	French Bay	French Bay	23° 56' 54.5" N 74° 31' 16.7" W	N/A	N/A

Table 1: Sites studied. Location and water depth of localities visited in this study and in previous years; see Fig. 2.

al., 2011; Martin and Lewis, 2015). In the present study, we follow a method dating from the early 1980s, in which cobbles are recovered from the seafloor and taken back to the laboratory for study (Choi and Ginsburg, 1983; Meesters et al., 1991; Gischler and Ginsburg, 1996; Gischler, 1997).

These clasts have the advantage of making the foraminifera available for microscopic examination in the laboratory rather than trying to make identifications from underwater photographs or by direct observation in the field, and they are natural materials as opposed to artificial panels of some

kind. Cobbles are available at reefs as part of the coral rubble at the base of coral heads and near shore as fragments of beachrock or lithified beach or dune facies. They can be taken from the island (with Bahamian government permission) with minimal damage to reefal ecosystems. The foraminiferal species are few in number and are distinctive (most are even "color coded"), allowing for easy data collection by student assistants.

Over the last decade, the senior author and students at Auburn University have studied the encrusting foraminifera at San Salvador (Tichenor and Lewis, 2009; 2011; 2018; Martin and Lewis, 2015) and other Bahamian outer islands (Smith, 2015; Smith and Lewis, 2016; Eubanks and Lewis, 2017; Eubanks, 2018) and have established the distributional pattern shown in Figure 1A: *Homotrema rubrum* dominates nearshore assemblages; lagoonal assemblages are diverse, but are characterized primarily by *Planorbulina* spp*;* and platform margin reefs have sparse, small foraminifera except for the very large tests of *Gypsina plana.* We refer to this as the Tichenor-Lewis model. Cobbles from bank barrier reefs, not shown in Figure 1A, are typically densely covered by *Homotrema* with some *Gypsina plana* and *Carpenteria.* In addition, *Nubecularia* can be common nearshore, *Carpenteria* is not, and *Haddonia* is restricted to the platform margin.

We have been asked, "Couldn't your cobbles have been transported from somewhere else?" We point out that cobbles are less likely to be transported out of their habitats than are free foraminifera, but of course transport is possible -- even boulders can be transported during high-energy events (e.g., Niemi, 2017). Storms are known to have an impact on subtidal encrusting communities in coastal settings by overturning clasts (Osman, 1977; Sousa, 1979; Wilson, 1987). A number of studies have assessed the impact of storms on coral reefs including sediment movement (e.g., Woodley et al., 1981; Hubbard et al., 1991; Hubbard, 1992), and Pleistocene coral rubble accumulations have been studied in order to recognize storm events based on encrusting organisms (e.g., Martindale, 1992; Perry, 2001).

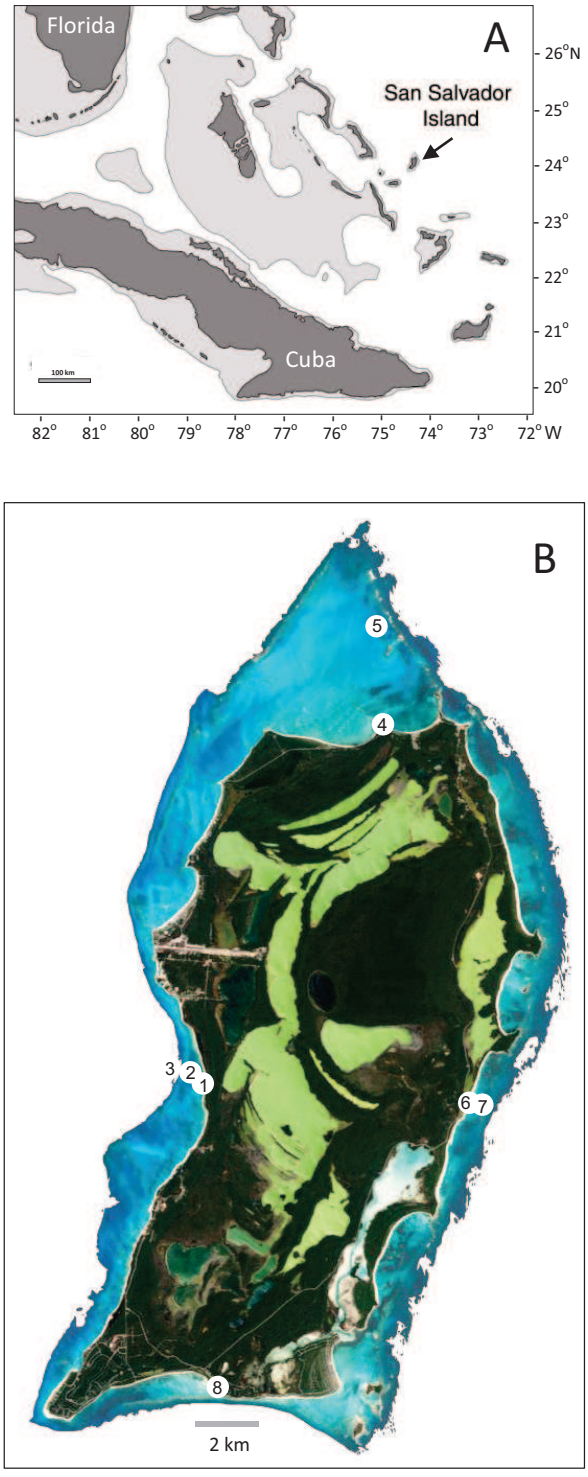

Figure 2. San Salvador island, showing the sites visited: A) Location of San Salvador. B) The sites visited in 2016: 1) Telephone Pole Reef nearshore, 2) Snapshot Reef, 3) Vicki's Reef, 4) Dump Reef, 5) Gaulins Reef, 6) Salt Pond nearshore, 7) Salt Pond patch reef, and 8) French Bay. See Table 1 for site data.

With regard to transport, individual foraminiferal tests have been shown to have moved back and forth between lagoons and forereef slopes (Chun et al., 1997). Specifically, pieces of the red-colored *Homotrema rubrum* have been used as an easily recognizable transport indicator in washover deposits (Pilarczyk and Reinhardt, 2012; Pilarczyk et al., 2014) and fully marine foraminifera, such as *Archaias,* found in lake cores on San Salvador are interpreted as indicators of hurricanes (e.g., Park, 2012).

San Salvador provides a particularly good test case for the question of whether the distribution of encrusting foraminifera found on cobbles can be taken at face value or whether storms move cobbles out of the habitat to such an extent that patterns are disturbed. The same sites have been sampled repeatedly over many years (with consistent results) prior to the direct impact of a major hurricane. In early October 2015, Hurricane Joaquin, a Category 4 hurricane with sustained winds of 130 mph, moved very slowly (5-6 mph) into the Bahamas from the northeast passing east of San Salvador, then turned north and hit Rum Cay before crossing San Salvador from southwest to northeast on October 2. With storm surge as high as 15 feet in some areas, it eroded cays and deposited sediment on the island itself. We visited the island in March 2016, ~ 5.5 months after the event.

RATIONALE

Attached organisms provide important clues to cobbles being overturned or transported out of the habitat. Photosynthetic organisms such as non-calcareous algae grow on the exposed, upper surface of cobbles and produce a green to brown color on the tops of cobbles, whereas the undersides are often lighter (Figure 1B). Most encrusting foraminifera are found on the underside, where competition for space is reduced. A notable exception is *Planorbulina*, which grows on the upper as well as the lower sides. Thus, overturned cobbles can be recognized as such.

Applying the Tichenor-Lewis model, encrusting foraminifera can be used to see if cobbles have been transported out of habitat. For example, cobbles transported from the platform margin (wall) shoreward will carry the large tests of *Gypsina plana* and *Haddonia* into shallower water where these tests are rarely found. Reef rubble transported oceanward from nearshore environments will have abundant *Homotrema rubrum* relative to *Planorbulina.*

Foraminifera grow quickly; some settle and grow to full size in a few months. Such is the case for *Planorbulina,* as has been shown by in-habitat experiments (e.g., Parsons, 1993; Martin and Lewis, 2015). However, the best-known species, *Homotrema rubrum,* does not appear until sometime between 6 months and one year, and *Gypsina plana* only shows up after one year on the wall site, and is less than 5 mm wide even then (Martin and Lewis, 2015). At approximately 5.5 months after the storm event, *Planorbulina* and *Nubecularia* may have grown on newly imported cobbles, but other taxa were most likely transported from their prior habitat.

METHODS

During a Spring Break field course on San Salvador, March 13-18, 2016, three undergraduate students participated in this post-storm study. Cobbles were examined *in situ*, and clasts were collected from the following, previously studied sites: Telephone Pole Reef, Dump Reef, and Salt Pond 1 (near-shore); Snapshot Reef and Salt Pond 2 (patch reefs); Gaulins Reef (bank barrier reef); and Vicki's Reef (platform margin). In addition to the six sites previously studied, one site showing obvious storm impact was examined (Figure 2; Table 1). Three of these sites, Snapshot Reef and Salt Pond nearshore and patch reef, had been sampled very recently (June 2015) and thus provide good "before" data. Other sites were sampled in 2008 and 2010. The condition of reefs was observed and photographed at each site, and cobbles were examined in situ prior to collection. In the laboratory at Auburn University, cobbles were washed and brushed to remove debris, encrusting foraminifera were identified using binocular microscopes, and their taphonomic states were assessed as was done previously (Buchan and Lewis, 2009; Lewis and Tichenor,

2018). The overall taphonomic state of each assemblage was described by the quality of preservation index (QPI), defined as the percent of all pristine and good specimens. Bar graphs were constructed to show the total assemblage for each site before and after the storm; ternary diagrams show the relative proportions of the three key taxa on a cobble-by-cobble basis.

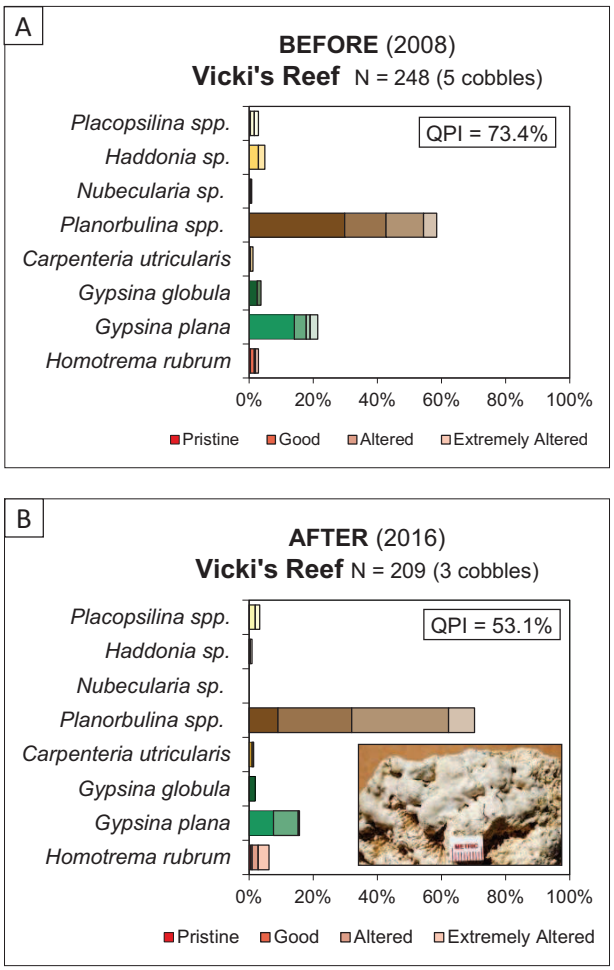

Figure 3: Foraminiferal assemblages before (A) and after (B) the storm at the "wall" off Fernandez Bay. Relative proportions are based on counts of individual tests; QPI stands for Quality of Preservation Index, the sum of all pristine and good individuals.

RESULTS

Offshore sites

Vicki's Reef (Site 3). This wall site, visited many times through the years by the senior author, showed no effects of storm damage. Samples were recovered from the platform-margin reef at a depth of 89 ft. (27.1 m). Cobbles were very eroded and heavily encrusted. The foraminiferal assemblages before and after the storm (Figure 3) were very similar: *Planorbulina* was most abundant based on counts of individuals, but *Gypsina plana* was second and, because of its large size, it accounts for most of the area covered by encrusters. *Haddonia*, an indicator of the wall habitat, was found on all three cobbles (and not on any of the other samples). The ternary diagram (Figure 4) shows a fairly tight grouping of all cobbles both before and after the storm.

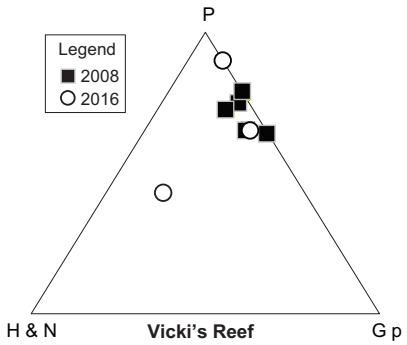

Figure 4: Figure 4. Ternary diagram for Vicki's reef showing the relative proportions of Homotrema rubrum plus Nubecularia sp. (H & N), Planorbulina (P), and Gypsina plana (G p) based on counts of individual tests. Individual cobbles before the storm are shown by black squares; cobbles recovered after the storm (this study) are shown by white circles.

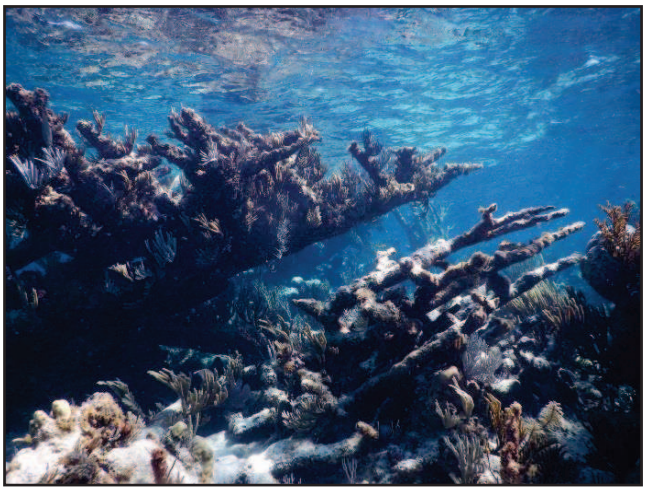

Figure 5. Erect Acropora palmata at Gaulins Reef, March 14, 2016.

Gaulins Reef (Site 5). Large, erect colonies of *Acropora palmata* near the spire known as "the seahorse" showed no signs of damage (Figure 5). Reef rubble was abundant, but no more than usual; in some places sand may have been deposited on the rubble. The cobbles were recognizable as flat pieces of *A. palmata* and other corals, densely encrusted by foraminifera. Assemblages before and after the storm (Figure 6) were dominated by *Homotrema rubrum* (including the globular morphotype) with *Carpenteria* second in abundance. *Planorbulina* was noticeably rare. The cobble-by-cobble analysis showed no outliers (Figure 7).

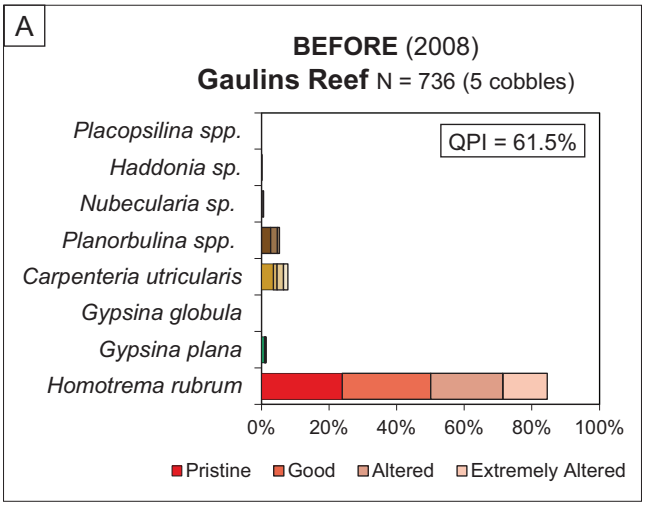

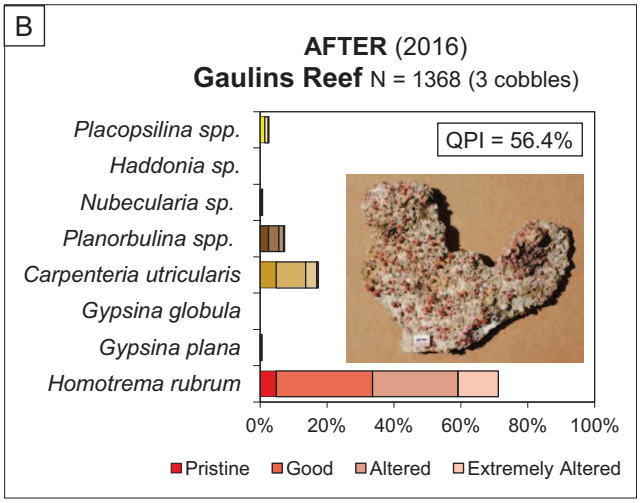

Figure 6. Foraminiferal assemblages before (A) and after (B) the storm at Gaulins Reef. Relative proportions are based on counts of individual tests; QPI stands for Quality of Preservation Index, the sum of all pristine and good individuals.

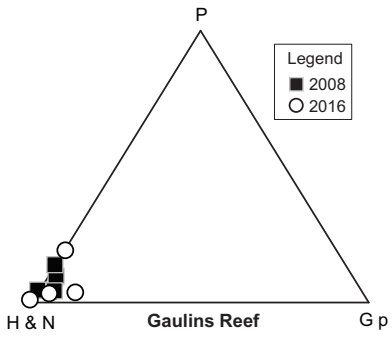

Figure 7. Ternary diagram showing the relative proportions of Homotrema rubrum plus Nubecularia sp. (H & N), Planorbulina (P), and Gypsina plana (G p) based on counts of individual tests. Individual cobbles before the storm are shown by black squares; cobbles recovered after the storm (this study) are shown by white circles.

Snapshot Reef (Site 2). This was one of the sites sampled in 2015 allowing for three collection times, and the assemblages are virtually identical over the eight-year time span (Figure 8). Numerous small tests of *Planorbulina* are dotted over otherwise relatively sparsely covered and somewhat abraded coral fragments. One cobble collected after the storm (Figure 9) plots at a distance from the others, but examination of this specimen shows it to be like all the others except for an unusually high number of *Homotrema rubrum.* Other elements of the assemblage, including minor amounts of small *G. plana,* and the rounded and abraded aspect of the cobble lead us to conclude that it was not transported from another habitat. A second patch reef (site 7), discussed below, was also much the same before and after the storm.

Nearshore sites

Telephone Pole Reef (Site 1). Nine cobbles were collected from ~1m water depth near the shoreline. Many of the cobbles showed evidence of overturning. This included the presence on all sides of yellow and brownish-gray staining, attached filamentous algae, and an abundance of *Planorbulina*, all of which indicate exposure to sunlight. In addition, even the largest cobbles had at least some *H. rubrum* on both upper and lower sides. We selected three cobbles for analysis which had a

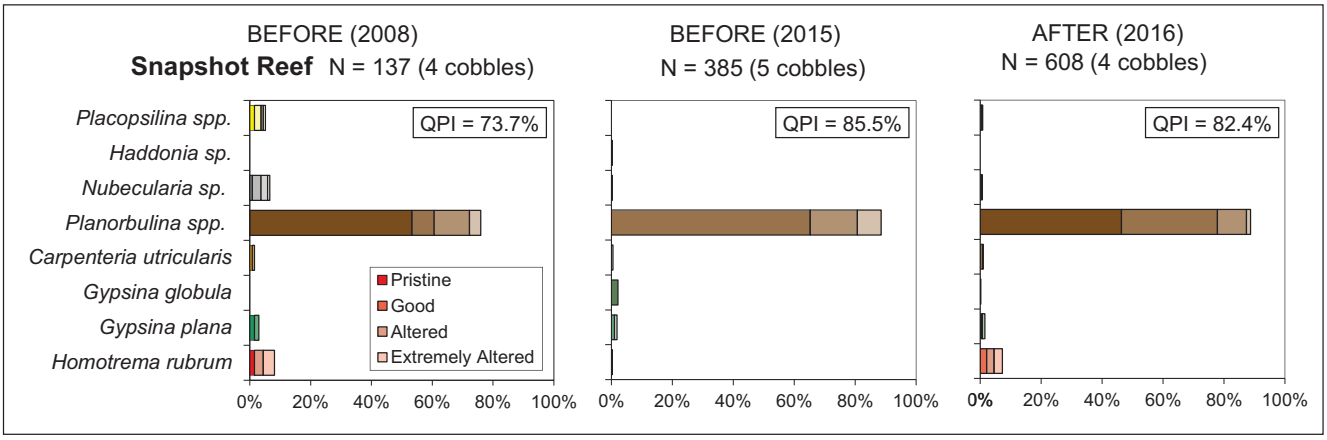

Figure 8. Foraminiferal assemblages from Snapshot Reef based on two recoveries before the storm, one in 2008 and another in June 2015, as well as the one after the storm. Note the consistency in assemblages throughout this time interval.

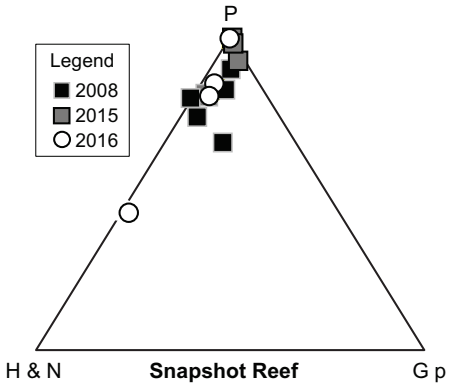

Figure 9. Ternary diagram showing the relative proportions of Homotrema rubrum plus Nubecularia sp. (H & N), Planorbulina (P), and Gypsina plana (G p) at Snapshot reef. Cobbles collected before the storm are shown by black and gray squares; cobbles recovered after the storm (this study) are shown by white circles. Note one outlier; see text for discussion.

relatively distinct lower side, which is in keeping with our standard protocol. Foraminiferal assemblages before and after the storm (Figure 10) were similar in that *H. rubrum* was first in abundance, however the post-storm data had proportionately more *Planorbulina*. Figure 11 shows the cobble that contributed most to this graph: the outlier plotting far from the other cobbles. Re-examination of

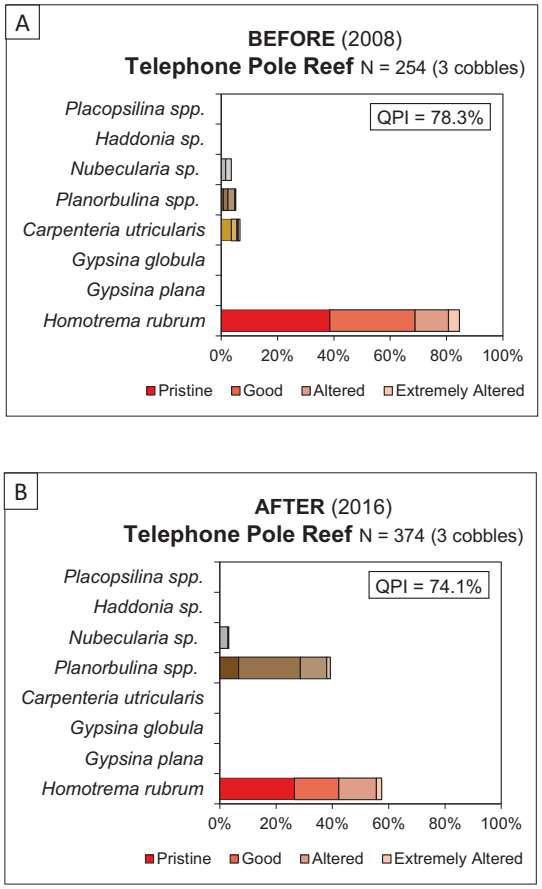

Figure 10. The foraminiferal assemblages before (A) and after (B) the storm near the shoreline at Telephone Pole Reef, Fernandez Bay. See text for a discussion of the increase in the relative amount of Planorbulina.

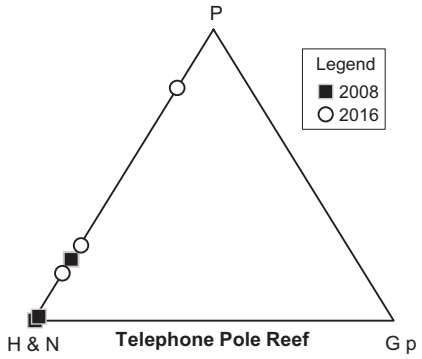

Figure 11. Ternary diagram for the Telephone Pole Reef site showing the relative proportions of Homotrema rubrum plus Nubecularia sp. (H & N), Planorbulina (P), and Gypsina plana (G p). Note one cobble with an unusually large proportion of Planorbulina suggesting possible transport from offshore.

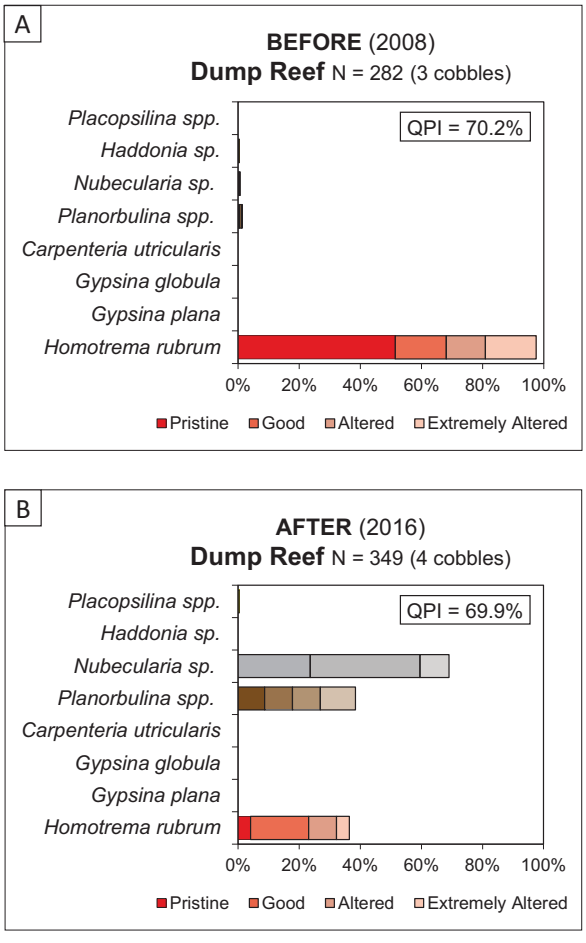

Figure 12. The foraminiferal assemblages before (A) and after (B) the storm at Dump Reef. Note the increase in Nubecularia in the 2016 dataset.

this cobble shows that the high number of *Planorbulina* cannot be explained by repeated overturning because it is the cobble we had chosen early on as an example of top versus bottom (Figure 1)! It could have been washed in from the lagoon, although the absence of minor taxa (e.g., *Carpenteria*) and the presence of *Nubecularia* do not support this interpretation.

Dump Reef (Site 4). This nearshore reef was sampled at its proximal (~32 m from shore) and distal (~68 m from shore) edges. Cobbles found in 2016 were more varied than those assessed in 2008 (Figure 12) with some having nothing but *H. rubrum*, and others with a significant amount of *Nubecularia* as well as *Planorbulina*. The relatively large proportion of *Planorbulina* found on cobbles at the distal edge (Figure 13) and the debris associated with them may indicate their having been washed ashore and piled up at the edge of the reef. On the proximal side of the reef a cobble was found in an upside-down orientation, as determined by the encrusting foraminifera on the top and algae on the bottom.

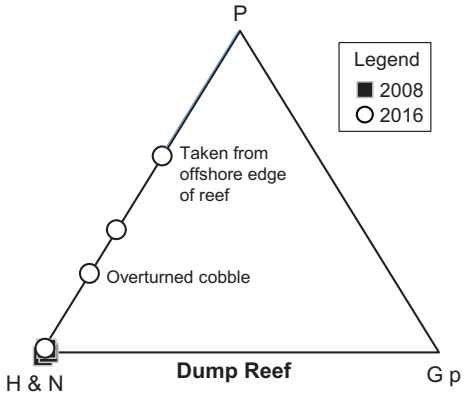

Figure 13. Ternary diagram showing the relative proportions of Homotrema rubrum plus Nubecularia sp. (H & N), Planorbulina (P), and Gypsina plana (G p) at Dump Reef. The three cobbles collected in 2008 had nearly 100% Homotrema, but those recovered in this study showed more variability, and one cobble was overturned.

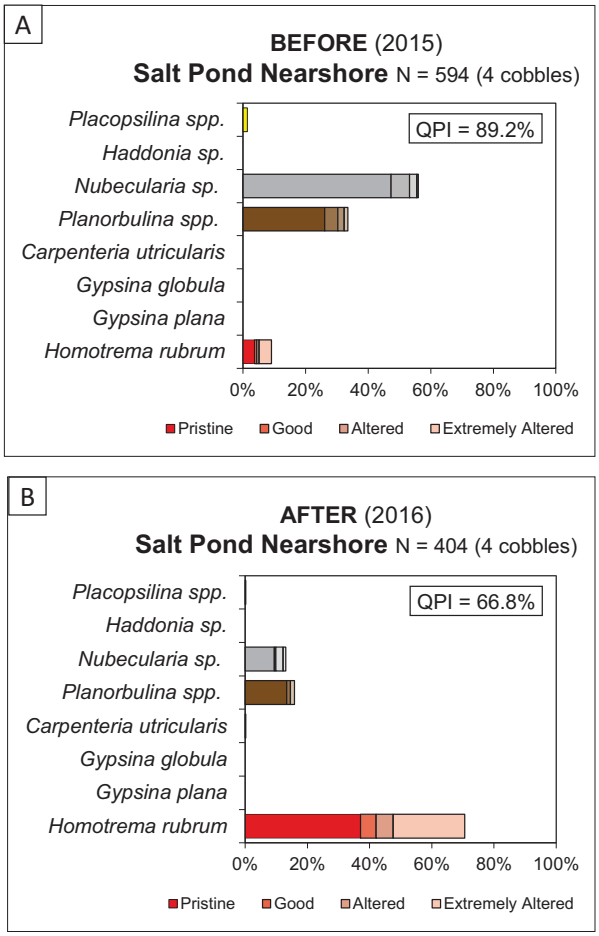

Figure 14. The foraminiferal assemblages before (A) and after (B) the storm near the shore at Salt Pond. See text for discussion.

Salt Pond (Site 6 and 7). Across the road from Salt Pond are two sites on the high-energy east side of the island. Both of these sites were found to be rich in *Nubecularia* sp. when first sampled in 2015; this was explained by the observation that this fast-growing species sometimes takes the place of *Homotrema rubrum* in nearshore settings, a phenomenon seen on Cat Island as well as San Salvador (Smith, 2015; Lewis and Tichenor, 2018). The 2016 re-sampling of the nearshore site (Figures 14 and 15) shows an assemblage more typical of nearshore environments: that is, *Homotrema rubrum* is much more abundant than any other taxon. One of these cobbles has a nodular surface resembling the patch reef cobbles sampled in 2015 suggesting shoreward transport.

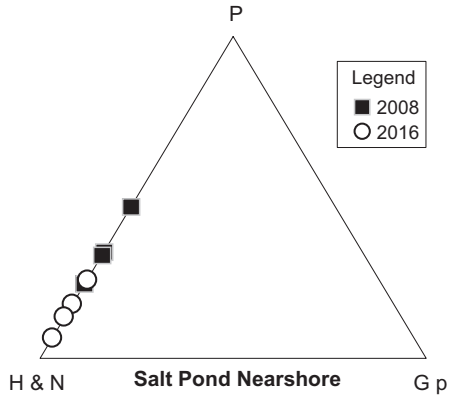

Figure 15. Ternary diagram for the Salt Pond nearshore site showing the relative proportions of Homotrema rubrum plus Nubecularia sp. (H & N), Planorbulina (P), and Gypsina plana (G p) based on counts of individual tests. Individual cobbles before the storm are shown by black squares; cobbles recovered after the storm (this study) are shown by white circles.

The patch reef (Site 7) sampled approximately 100 m offshore from Site 6 has nearly equal numbers of *H. rubrum*, *Nubecularia,* and *Planorbulina* both before and after the storm. The slight increase in *H. rubrum* between the two graphs (Figure 16) is consistent with the growth of this taxon shown at the nearshore site. As noted in 2015, *H. rubrum* tests were smaller at the patch reef than those at the nearshore site. Individual cobbles show a fairly wide variation in assemblage composition (Figure 17), which may be explained, in part, by differences in cobble size: the smaller cobbles may have been transported.

French Bay (Site 8). Samples were taken at the shoreline and in a nearby rubble field south of the road at the east end of French Bay (Figure 18). Both sets of cobbles were very well rounded, especially those taken at the water's edge, where foraminifera were only observable in protected pockets that had escaped abrasion. Both the assemblage from shore samples and the rubble-field assemblage were dominated by *Homotrema*, with significant amounts of *Planorbulina* as well (Figure 19).

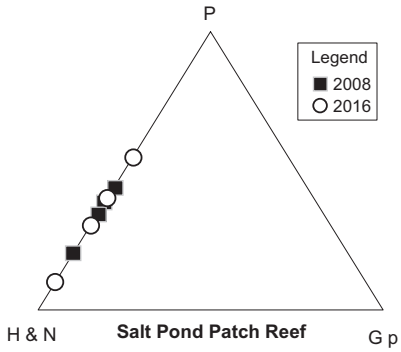

Figure 16. The foraminiferal assemblages before (A) and after (B) the storm at the patch reef off Salt Pond. Note the similarity in graphs; see text for discussion.

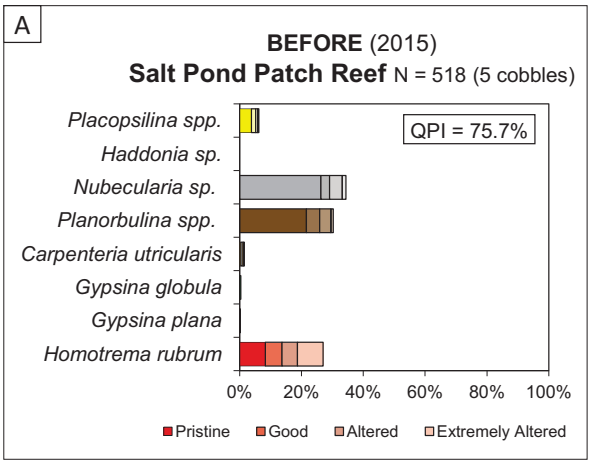

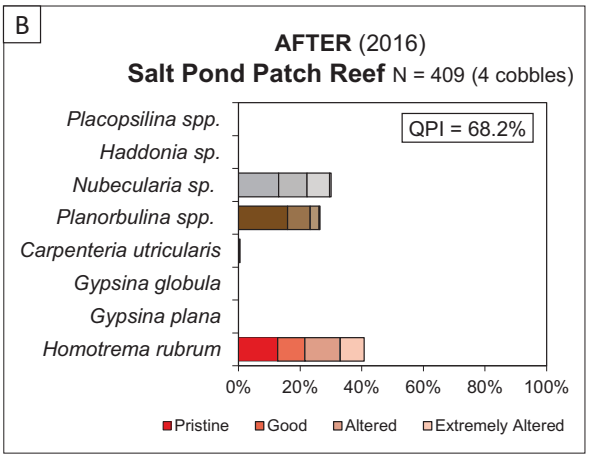

Figure 17. Ternary diagram for the Salt Pond patch reef showing the relative proportions of Homotrema rubrum plus Nubecularia sp. (H & N), Planorbulina (P), and Gypsina plana (G p) based on counts of individual tests. Individual cobbles before the storm are shown by black squares; cobbles recovered after the storm (this study) are shown by white circles.

French Bay was not included in earlier studies by the Auburn team, so no data is available from before the storm event. However, the large, low-profile morphotype of *Homotrema*, which is usually found near shore rather than in mid-shelf and outer reef environments, was common; and the *Homotrema*-dominated assemblage suggests a nearshore origin for these cobbles.

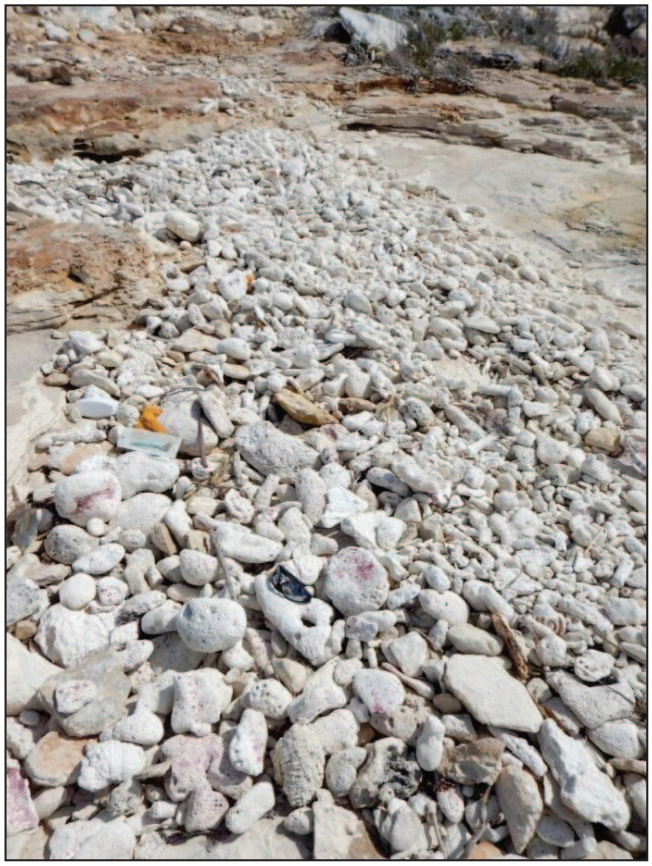

Figure 18. The rubble field south of the road at French Bay. Note sunglasses, lower middle, for scale. Samples were taken here and at the shoreline nearby.

DISCUSSION

Each of the offshore sites examined in this study have distinct assemblages of encrusting foraminifera. Vicki's Reef, like the other wall sites we have studied on Cat Island (Smith, 2015) and Mayaguana (Eubanks, 2017), is strikingly different from all other sites because of the abundance of large *Gypsina plana* tests in contrast to the small size of other taxa. None of these unique cobbles

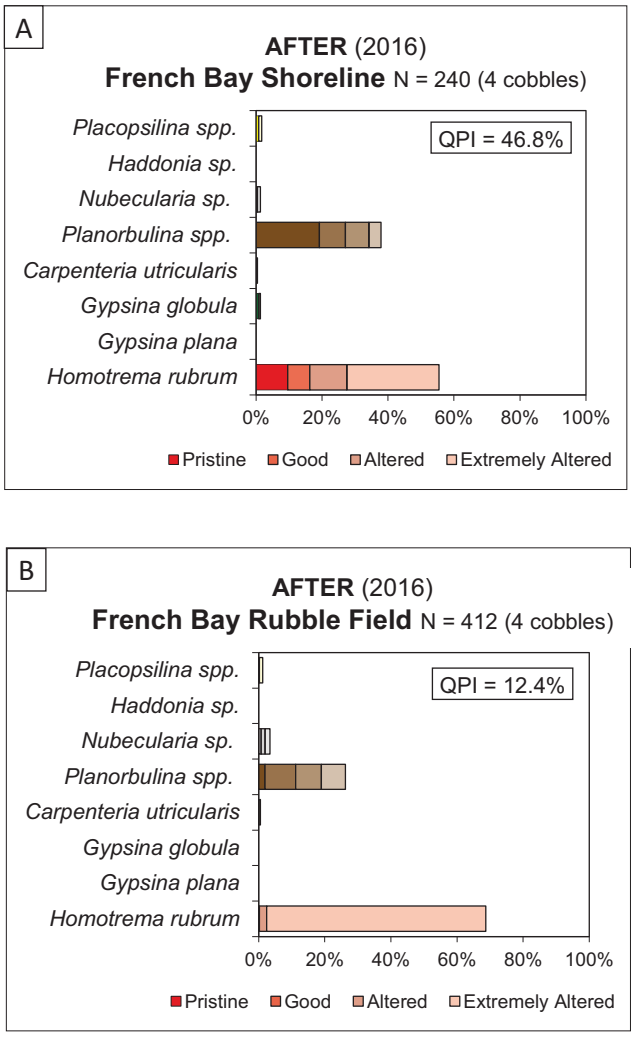

Figure 19. Foraminiferal assemblages found on cobbles recovered from the shoreline (A) and the rubble field (B). See text for discussion.

were found at other localities. The corals at Gaulins Reef seemed to have been undisturbed by Hurricane Joaquin, and the foraminiferal assemblages on coral rubble were very similar before and after the storm, with the same ranking of the top three taxa: *Homotrema* >> *Carpenteria* > *Planorbulina*. Even the relatively low QPI value, 61.5% vs 56.4%, was nearly the same after eight years. Consistency through the years was also shown at Snapshot Reef, a mid-shelf patch reef. The assemblages were overwhelmingly dominated by well-preserved *Planorbulina*. Even at the level of individual cobbles (Figure 9), three of the four cobbles plotted exactly as expected. The hurricane did not alter the pattern seem previously in these three offshore sites.

Nearshore and inner-lagoon samples are varied even in prolonged fair-weather intervals (Tichenor and Lewis, 2018), perhaps because of the effects of past storms. This is not surprising since *Planorbulina* grows on the tops of cobbles, and the relative amount of *Planorbulina* on the underside of cobbles increases with distance from shore. Therefore, either overturning or shoreward transport, or both, can increase the amount of *Planorbulina* relative to *Homotrema*. Even so, the observed effects of Hurricane Joaquin were minimal. As discussed above, one cobble at the Telephone Pole Reef site had an unusually high abundance of *Planorbulina*, suggesting that it may have been transported shoreward. On the north end of the island, the Dump Reef site showed possible evidence of the storm including the wide variation in *Homotrema-Planorbulina* ratios, with the highest amount of *Planorbulina* on the distalmost cobble, and one overturned cobble near shore.

The growth of *Nubecularia* at this site and at the Salt Pond sites complicates interpretation. This genus is not reported by other authors, but from our prior research (Martin and Lewis, 2015) we know it to grow within 3 months in nearshore settings; it seems to be a boom-and-bust opportunist, commonly found instead of/in addition to *Homotrema* in nearshore sites (e.g, Smith, 2015). *Nubecularia* was abundant in 2015 at the Salt Pond nearshore site but was replaced by *Homotrema* after the storm (Figure 14). Although more research needs to be done on the growth trajectories of these taxa, both graphs show assemblages indicative of a nearshore setting -- before and after the storm.

The extensive rubble field between the shore and the highway at French Bay on the south end of the island is clear evidence of the power of the hurricane. Sand also covered part of the road in this area. However, the encrusting foraminifera we examined do not indicate cobble transport for long distances. It is not clear if the cobbles in the rubble field came the shoreline area or further out in the bay, but the abundance and the morphology of the *Homotrema* indicate that the clasts were not moved very far.

CONCLUSIONS

Was the distribution of encrusting foraminifera shown in the Tichenor-Lewis model disturbed by the impact of a Category 4 hurricane? The answer is no. It may be that none of our sites suffered a direct hit; none of the reefs examined in this study showed effects of recent storm damage to the corals themselves. However, this may reflect the spotty nature of hurricane damage. The fact is that our sites were distributed around the circumference of the island and from the shore to the wall at the shelf edge. Bar graphs of foraminiferal assemblages from the three deeper water, offshore sites showed no effects of the storm. None of the distinctive cobbles from these sites were found in shallow-water, nearshore localities. Although nearshore sites showed possible transport of cobbles shoreward, none of them appeared to have originated further than the inner parts of the lagoon. The onshore-offshore zonation observed previously and even the site-to-site faunal compositions were not altered significantly by the direct impact of a Category 4 hurricane.

ACKNOWLEDGMENTS

The authors would like to thank Debbie Weeks, Troy Dexter and the staff of the Gerace Research Centre at San Salvador for their assistance with logistics. Funding was provided in part by the Auburn University Department of Geosciences Advisory Board through the Spencer Waters and Dan Folse Memorial Award, which was granted to Sarah Asher, Sarah Speetjens Gilley, and Sally Sundbeck. Travis Barefield assisted with the laboratory work and data collection.

REFERENCES

Buchan, O.C., and Lewis, R.D. 2009. Recent large benthic foraminifera as indicators of grassbed characteristics, San Salvador, Bahamas: The addition of taphonomy. Pp. 83–92. In T.D. Demchuk and A.C. Gary (Eds.). *Geologic Problem Solving with Microfossils: A Volume in Honor of Garry D. Jones*, SEPM Special Publication 93.

Choi, D.R., and Ginsburg., R.N. 1983. Distribution of coelobites (cavity-dwellers) in coral rubble across the Florida Reef Tract. *Coral Reefs* 2: 165−172.

Chun, L., Jones, B., and Blanchon, P. 1997. Lagoon-shelf sediment exchange by storms: Evidence from foraminiferal assemblages, east coast of Grand Cayman, British West Indies. *Journal of Sedimentary Research* 67: 17−25.

Eubanks, E. 2018. Distribution of encrusting foraminifera at Mayaguana, Bahamas: Determining assemblage composition and relationship of test size and density to food availability. M.S. thesis, Auburn University, Auburn, Alabama.

Eubanks, E., and Lewis, R.D. 2017. Distribution of encrusting foraminifera at Mayaguana, Bahamas: Determining assemblage composition and relationship to food availability. *Geological Society of America Abstracts with Programs* 49, No. 6, ISSN 0016-7592 doi: 10.1130/abs/2017AM-306599.

Gischler, E. 1997. Cavity dwellers (coelobites) beneath coral rubble in the Florida reef tract. *Bulletin of Marine Science* 61: 467–484.

Gischler, E., and Ginsburg, R.N. 1996. Cavity dwellers (coelobites) under coral rubble in southern Belize barrier and atoll reefs. *Bulletin of Marine Science* 58: 570–589.

Hubbard, D.K. 1992. Hurricane-induced sediment transport in open-shelf tropical systems; an example from St. Croix, US Virgin Islands. *Journal of Sedimentary Research* 62: 946–960.

Hubbard, D.K., Parsons, K.M., Bythell, J.C., and Walker, N.D. 1991. The effects of Hurricane Hugo on the reefs and associated environments of St. Croix, U.S. Virgin Islands: A preliminary

assessment. *Journal of Coastal Research* 8: 33–48.

Jackson, J.B.C., and Winston, J.E. 1982. Ecology of cryptic coral reef communities. I. Distribution and abundance of major groups of encrusting organisms. *Journal of Experimental Marine Biology and Ecology* 51: 135–147.

Logan, A. 1981. Sessile invertebrate coelobite communities from shallow reef tunnels, Grand Cayman, B.W.I. Pp. 735-744. In *Proceedings of the 4th International Coral Reef Symposium*, Manila, Phillipines.

Logan, A., Mathers, S.M., and Thomas, L.H. 1984. Sessile invertebrate communities from reefs of Bermuda: Species composition and distribution. *Coral Reefs* 2: 205–213.

Martin, L.D., and Lewis, R.D. 2015. Growth of attached (encrusting) benthic foraminifera along an offshore-onshore transect, Fernandez Bay, San Salvador, Bahamas: Preliminary results. Pp. 111–123. In B. Glumac and M. Savarese (Eds.). *Proceedings of the 16th Symposium on the Geology of the Bahamas and other Carbonate Regions*. Gerace Research Centre, San Salvador, Bahamas.

Martindale, W. 1992. Calcified epibionts as palaeoecological tools: Examples from Recent and Pleistocene reefs of Barbados. *Coral Reefs* 11:167–177.

Meesters, E., Knijn, R., Willemsen, P., Pennartz, R., Roebers, G., and van Soest, R.W.M. 1991. Sub-rubble communities of Curaçao and Bonaire coral reefs. *Coral Reefs* 10: 189–197.

Niemi, T.M. 2017. Large boulders on Green Cay, San Salvador Island, The Bahamas. Pp. 121–129. In C.L. Landry, L.J. Florea, and D.S. Kjar (Eds.). *Proceedings from the 1st Joint Symposium on the Natural History and Geology of the Bahamas*. Gerace Research Centre, San Salvador, Bahamas.

Osman, R.W. 1977. The establishment and development of a marine epifaunal community. *Ecological Monographs* 47: 37–63.

Park, L.E. 2012. Comparing two long-term hurricane frequency and intensity records from San Salvador Island, Bahamas. *Journal of Coastal Research* 28: 891–902.

Parsons, K.M., 1993, Taphonomic Attributes of Mollusks as Predictors of Environment of Deposition in Modern Carbonate Systems: Northeastern Caribbean: Unpublished Ph.D. dissertation, The University of Rochester, Rochester, N.Y., 418 p.

Perry, C. 2001. Storm-induced coral rubble deposition: Pleistocene records of natural reef disturbance and community response. *Coral Reefs* 20: 171–183.

Pilarczyk, J.E., Goff, J., Mountjoy, J., Lamarche, G., Pelletier, B., and Horton, B.P. 2014. Sediment transport trends from a tropical Pacific lagoon as indicated by *Homotrema rubra* taphonomy, Wallis Island, Polynesia. *Marine Micropaleontology* 109: 21–29.

Pilarczyk, J.E., and Reinhardt, E.G. 2012. *Homotrema rubrum* (Lamarck) taphonomy as an overwash indicator in marine ponds on Anegada, British Virgin Islands. *Natural Hazards* 63: 85–100.

Richardson-White, S., and Walker, S.E. 2011. Diversity, taphonomy, and behavior of encrusting foraminifera on experimental shells deployed along a shelf-to-slope bathymetric gradient, Lee Stocking Island, Bahamas. *Palaeogeography, Palaeoclimatology, Palaeoecology* 312: 305–324.

Smith, C. 2015. Distribution of encrusting foraminifera at Cat Island, Bahamas: Implications for foraminiferal assemblages in the geologic record. M.S. thesis, Auburn University, Auburn, Alabama.

Smith, C. and Lewis, R. 2016. The characteristics and distribution of encrusting foraminifera at Cat Island, Bahamas. *Geological Society of America, Abstracts with Programs* 48:7, doi: 10.1130/abs/2016AM-286285.

Sousa, W.P. 1979. Disturbance in marine intertidal boulder fields: The nonequilibrium maintenance of species diversity. *Ecology* 60: 1225–1239.

Tichenor, H.R., and Lewis, R.D. 2009. Assemblages of attached (encrusting) foraminifera across a small, carbonate platform, San Salvador, Bahamas. *Geological Society of America Abstracts with Programs* 41:105.

Tichenor, H.R., and Lewis, R.D. 2011. Zonation of attached (encrusting) foraminifera across a small carbonate platform, based on species assemblages and area covered, San Salvador, Bahamas. *Geological Society of America Abstracts with Programs* 43: 71.

Tichenor, H.R., and Lewis, R.D. 2018. Distribution of encrusting foraminifer at San Salvador, Bahamas: A comparison by reef types and onshore-offshore zonation. *Journal of Foraminiferal Research* 48, in press.

Walker, S.E., Parsons-Hubbard, K., Richardson, S., White, B., Brett, C., and Powell, E., 2011. Alpha and beta diversity of encrusting foraminifera that recruit to long-term experiments along a carbonate platform-to-slope gradient: Paleoecological and paleoenvironmental implications. *Palaeogeography, Palaeoclimatology, Palaeoecology* 312: 325–349.

White, S. 2002. Encrusting foraminifera from Lee Stocking Island, Bahamas: Taphonomy, shelf-to-slope distribution, and behavior. M.S. Thesis, The University of Georgia, Athens, Georgia.

Wilson, M.A. 1987. Ecological dynamics on pebbles, cobbles, and boulders: *Palaios* 2: 594–599.

Woodley, J.D., Chornesky, E.A., Clifford, P.A., Jackson, J.B.C., Kaufman, L.S., Knowlton, N., Lang, J.C., Pearson, M.P., Porter, J.W., Rooney, M.C., Rylaarsdam, K.W., Tunnicliffe, V.J., Wahle, C.M., Wulff, J.L., Curtis, A.S.G., Dallmeyer, M.D., Jupp, B.P., Koehl, M.A.R., Neigel, J., and Sides, E.M. 1981. Hurricane Allen's impact on Jamaican coral reefs. *Science* 214: 749–755.

AERIAL PHOTOGRAPHY OF COASTAL EROSION AND LARGE BOULDER TRANSPORT FROM HURRICANE MATTHEW (2016) ALONG CLIFTON BEACH, NEW PROVIDENCE ISLAND, THE BAHAMAS

John D. Rucker, Tina M. Niemi, Joseph A. Nolan, and
Tori Rose

Department of Earth and Environmental Sciences
University of Missouri-Kansas City
Kansas City, MO 64110, U.S.A.

ABSTRACT

In October 2016, Hurricane Matthew passed as a Category 4 storm across western New Providence island in The Bahamas. A comparison of satellite and high-resolution aerial imagery along with field observations and boulder measurements allowed for damage analysis of Clifton Heritage Park and surrounding areas. At Flipper Beach in the Park, storm surge deposited significant amounts of large debris well inland in an area previously cleared of vegetation. Nearby locations not cleared of vegetation arrested inland inundation of storm surge debris. Loyalist period drystone walls also were unexpectedly resistant to storm surge damage. At the nearby Pirate Stairs, evidence of storm surge overwash included moved boulders and sea wrack deposited atop an approximately 6-m-high cliff. This is in stark contrast to the reported storm surge of 2.5 m. The measurements and locations of transported boulders, including a 6 m^3 boulder and the large block which had formerly formed the lintel over the Pirate Stairs, suggest that the method of movement was sliding and/or hydroplaning. Local focusing of wave energy is likely the mechanism for high storm surge and boulder movement.

INTRODUCTION

In the Caribbean and The Bahamas, hurricanes have been a threat with occasional devastating results during the past five centuries (e.g. Neuman et al., 1987; Shaklee, 1997). Hurricanes have also been an important factor in shaping the environment, geography, and even the physical shape of the islands (Shaklee, 1997; Sealey, 2006). As the islands do not have large amounts of topographic relief, they are particularly vulnerable to storm surge. Furthermore, due to their generally thin soils, the islands are vulnerable to wind damage to vegetation, as evidenced by our own observations of uprooted trees.

In March 2017, we had the opportunity to conduct field research on New Providence Island. The damage to the island from Hurricane Matthew was quite evident. We examined two areas along the western coast of New Providence Island–Flipper Beach at Clifton Heritage Park, and the famous Pirate Stairs near Clifton Pier (Figure 1). Clifton Pier is a small port built on the west side of New Providence island. Deep oceanic water close to the island margin allows tankers to offload fuel for the nearby Clifton Pier oil power plant. In this study we collected high-resolution aerial images with a photographic drone to document the damage caused by Hurricane Matthew along this section of the coastline. We photographed and measured boulders that had moved as a result of the hurricane; in most cases their original position was discernable. This study of the movement of boulders by hurricane storm surge is important because identifying these shoreline boulder deposits and characterizing them is critical to modeling the potential energy of storms, as well as understanding the processes forming coastal topography in The Bahamas. Drone aerial imagery provides high-resolution imaging of hurricane damage fields and

Figure 1: Location of the study area on the west side of New Providence Island in The Bahamas.

potentially provides a baseline for future monitoring of the coastal environment and identification of sites of inundation vulnerability.

HURRICANE MATTHEW

Hurricane Matthew began as a tropical storm that formed about 28 km north-northwest of Barbados on September 28, 2016 (Figure 2). The storm intensified and developed into a tropical cyclone, reaching a peak intensity of Saffir-Simpson Category 5 on October 1. This occurred when the storm was located less than 150 km north of Punta Gallinas, Colombia. This makes Matthew the southernmost Category 5 hurricane recorded in the Atlantic Basin (Stewart, 2017). Hurricane Matthew began to weaken as it tracked slightly west of north. It crossed the western end of Haiti as a Category 4 hurricane and weakened to Category 3 as it crossed the eastern end of Cuba. Matthews's track continued through the middle of the Bahamian archipelago, re-strengthening to Category 4 as it moved along the deep water of the Tongue of the Ocean between the islands of Andros and New Providence causing severe flooding on New

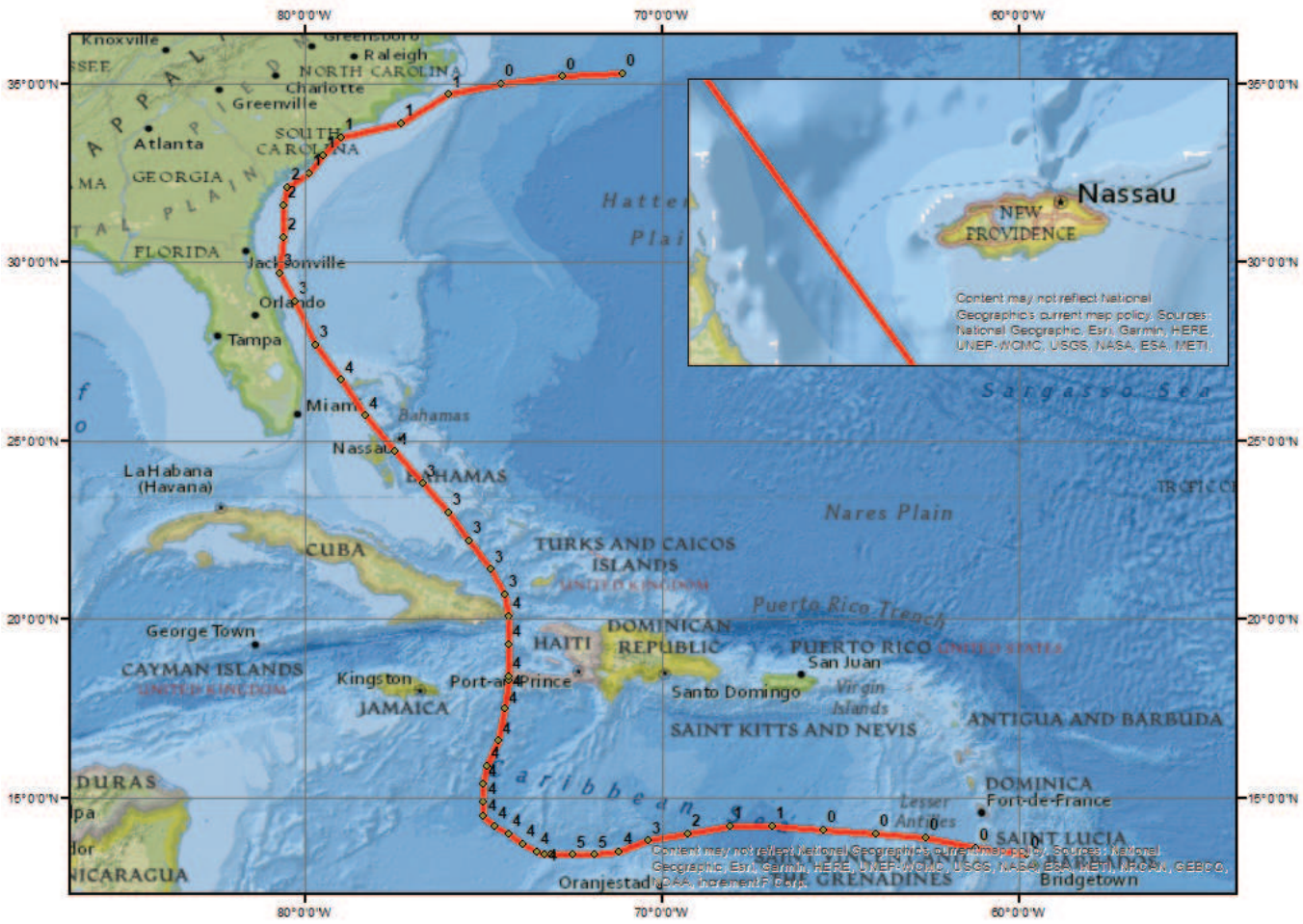

Figure 2: Hurricane Matthew storm track between September 29, 2016 to October 9, 2016. Numbers indicate the intensity of the storm on the Saffir-Simpson scale.

Providence Island (Stewart, 2017). It then weakened again as it moved north, passing over Grand Bahama Island as a Category 3 hurricane on October 7. It then followed the east coast of the United States, as for north as South Carolina, before turning east and gradually dissipating on October 9.

On October 6, 2016, Matthews's eyewall passed directly over the far western end of New Providence Island, the location of Clifton Heritage Park. At that time, Matthew was a Category 4 hurricane with wind speeds measured at ca. 230 kph. According to the US National Oceanic and Atmospheric Administration (NOAA) Hurricane Matthew report (Stewart, 2017), Matthew had a recorded storm surge of 2.5 m along the southern coast of New Providence. The rainfall from this hurricane varied sharply from as little as 75 mm to as much as 500 mm, eastern to western archipelago, respectively (Stewart, 2017).

CULTURAL HISTORY

The Bahamas has a long cultural history. From the Lucayans who arrived between 500 and 800 CE (Craton and Saunders, 1999), serving as a haven for pirates through the 17th century, to the settlement of American Loyalists in the late 18th century (Caviedes, 1991), and today's citizens, all have had to and continue to contend with hurricanes.

Today's Bahamians also seek to record and display the long history of settlement and the unique culture created here. In terms of public policy, this included a number of different legislative

acts, beginning with the National Trust Act of 1959, and including the Abandoned Wreck Act of 1965, the Public Records Act of 1971 (which led to the Department of Archives being designated as the agency responsible for cultural resources) and the Antiquities, Monuments and Museums Act of 1998 (Siegel and Righter, 2011). Archaeologically, first steps in this direction were of the classificatory-descriptive paradigm of archaeology, and in general, Bahamian archaeology has followed the succession of theoretical models common to North American archaeology (Berman, 2015). Today, however, a trend towards not only scientific exploration but also explication to the public at large is becoming more prominent (Siegel and Righter, 2011). A centerpiece of this historic preservation and education effort is the Clifton Heritage Park on New Providence Island. The park, which opened in 2009 after a lengthy and controversial battle between real estate developers and historic preservationists (Siegel and Righter, 2011), serves as an important monument both in itself, and as a symbol for success of cultural resource management in The Bahamas (Siegel and Righter, 2011).

The Park today occupies the area of the former Whylly and Johnston plantations, located on the western point of New Providence Island, and features the ruins of the plantations, as well as reconstructions of the slave quarters (Siegel and Righter, 2011).

Not as obtrusive, but more important to our study, are the many drystone field walls in the area. These walls, built both as markers of the edges of agricultural fields and of property boundaries, are ubiquitous throughout those Islands of the Bahamas settled by British Loyalists that fled the new United States after the American War of Independence. In addition to their obvious functional role, they are also the almost inevitable result of the need to clear rocks from the fields for agriculture.

Approximately 400 m southeast of Flipper Beach and just north of the Clifton Pier lie the Pirate Stairs. This is a relatively well-known tourist attraction on New Providence and is a stop in the New Providence Island field trip guide (Mylroie et al., 2012). It consists of a narrow (<1 m in places) stairway cut into the Pleistocene bedrock of the island, leading from the top of an approximately 6.5 m cliff to a wave-cut platform at sea level. Prior to Hurricane Matthew, a large boulder cut into a rough rectangle formed a lintel over the stairs. While known as the Pirate Stairs, and with local legend having nefarious buccaneers carrying chests laden with doubloons up and down this hidden stairway, it is much more likely it is associated with the Loyalist period, and served as a landing point for passengers or small cargo (the stairway is narrow) for the nearby plantations. It is possible that it does predate the loyalist plantations, but due to the low population of the island during the 17th century, it is unlikely that pirates would have found it necessary to create such an architectural feature so far from the main settlement of the island. After all, when Woodes Rogers sailed into Nassau in 1718 as the first Royal Governor of the Bahamas, and proclaimed a general amnesty for pirates who would reform, he only encountered 500-600 inhabitants on the island (not counting 'about 4 score who made their escape') (Cash et al., 1991). On the other hand, the earliest map available of New Providence Island (Figure 3), *An exact draught of the island of New Providence one of the Bahama Islands in the West Indies,* (dated around 1750) contains the somewhat mysterious notation "Rogers" not far from the location of the Pirate Stairs, which does suggest some human activity of some kind there.

DATA ACQUISITION

This study required two separate methods. First, pedestrian survey and direct observation and measurement of dislodged and moved boulders. Second, collection and analysis of aerial and satellite imagery of the two locations using a DJI Phantom 3 Quadcopter mounted with 12 Megapixel, 4K video camera with geo-referencing to produce orthophoto mosiacs. For this project, a programmed flight path obtained photos at 50 m of elevation with 60% overlapping. Agisoft Photoscan Professional produced orthophoto mosaics for this project; software versions 1.2.4 build 2399. Using Google Earth historic

Figure 3: An Exact Draught of the Island of New Providence One of the Bahama Islands. Variously dated between 1700-1750. Note inverted orientation (North is down).

Figure 4: Google Earth images of the Flipper beach area, and the cleared area inland, bounded by Loyalist drystone walls. Dates: A) 11/5/2000, B) 10/31/2014, C) 12/16/2014, D) 2/13/2015, E) 1/16/2016 F) 10/7/2016. It is possible to see the clearance, regrowth, and, in image F standing water, as the image was taken the day after Hurricane Matthew passed.

vegetation to post-Matthew vegetation loss, pre-existing boulders and inundation related transport, and changes in coastal morphology.

OBSERVED HURRICANE DAMAGE

Flipper Beach, a popular snorkeling location for tourists, is located within Clifton Heritage Park on the western end of New Providence. In addition to a small beach with an approximately 25-m-long sandy shoreline, there was a small cabana or shelter just above the crest of the beach dune before Hurricane Matthew. The topography of Flipper Beach is very flat, with only a few meters rise in elevation from the beach to the northern end of the cleared square north of shore. Our analysis of the Google Earth archived images for this area from 2014 to 2016 showed (Figure 4) that an area to the north of the beach approximately 55 m^2 cleared of vegetation between December 2014 and February 2015. The fresh soil visible in the 2015 image suggests that it was a recent clearing at that time. A fortuitous satellite image taken October 7, 2016, a day after the hurricane, reveals this area succumbed to storm surge inundation and ocean water remained standing in this area.

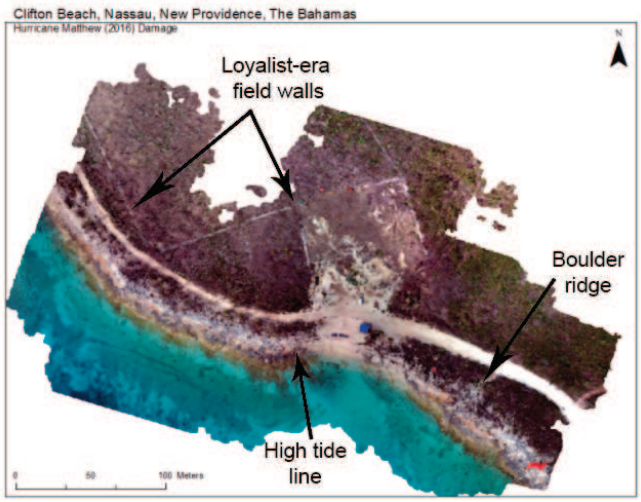

Figure 5: Drone image of Flipper Beach showing the area inundated by storm surge in Hurricane Matthew and Loyalist-era field walls. Beachrock present along the coast has broken into boulders that have been transported above the high tide line.

From field acquired orthophoto mosaics (Figure 5), field walls are visible. These walls, normally covered with vegetation such that only faint hints can be seen on aerial imagery now lay exposed clearly in imagery. Debris is piled against these field walls and surrounding trees (Figure 6). The cabana/beach shelter was deposited in the northwestern corner in a pile of debris. In many places the soil washed away, leaving large patches of bare bedrock. Interestingly, along the shoreline, to either side of the sand beach (which had also suffered severe erosion), imbricated boulders lined the edges of the vegetated edge of the beach dune. Aerial imagery (Figure 5) shows the boulder ridge extends along the coast.

At the nearby Pirate Stairs location (Figure 7), the topography has changed to a steep cliff exposure. Hand cut from bedrock, The Pirate Stairs create a path from a wave-cut platform at sea level about 6 m from the low tide level up to the top of the cliff (Figure 8). This cliff exposes the late Pleistocene rocks of the Cockburn Town Member of the Grotto Beach Formation topped by a *terra rossa* paleosol (Mylroie et al., 2012). The bedrock is a calcarenite with herringbone cross stratification and tabular and planar cross-beds which deposited in a subtidal to intertidal environment. Iron-rich red caliche line the vertical and horizontal fractures in the bedrock (Figure 8). These fractures form weaknesses in the bedrock that facilitate collapse and cliff retreat in storms.

When we visited this site, it was immediately clear that storm surge had affected this area along the cliff front and at the top of the cliff. Based on the exposed white unweathered color of the cliff face, one section of the cliff had clearly collapsed to the shallow water below. The erosional retreat of the cliff left smaller boulders dislodged at the top of the section. Analysis of the high-resolution drone imagery also shows numerous very large blocks submerged near the cliff edge (Figure 7).

Along the top of the cliff, Australian pine trees (*Casuarinas* sp.*)* lay uprooted and large boulders (up to 6 m^3) moved inland. Sea wrack, mostly brown seaweed (*Sargassum* sp.) became trapped in a fence toppled by boulders that subsequently rest on top of it (Figure 9 and 10). Boulders transported

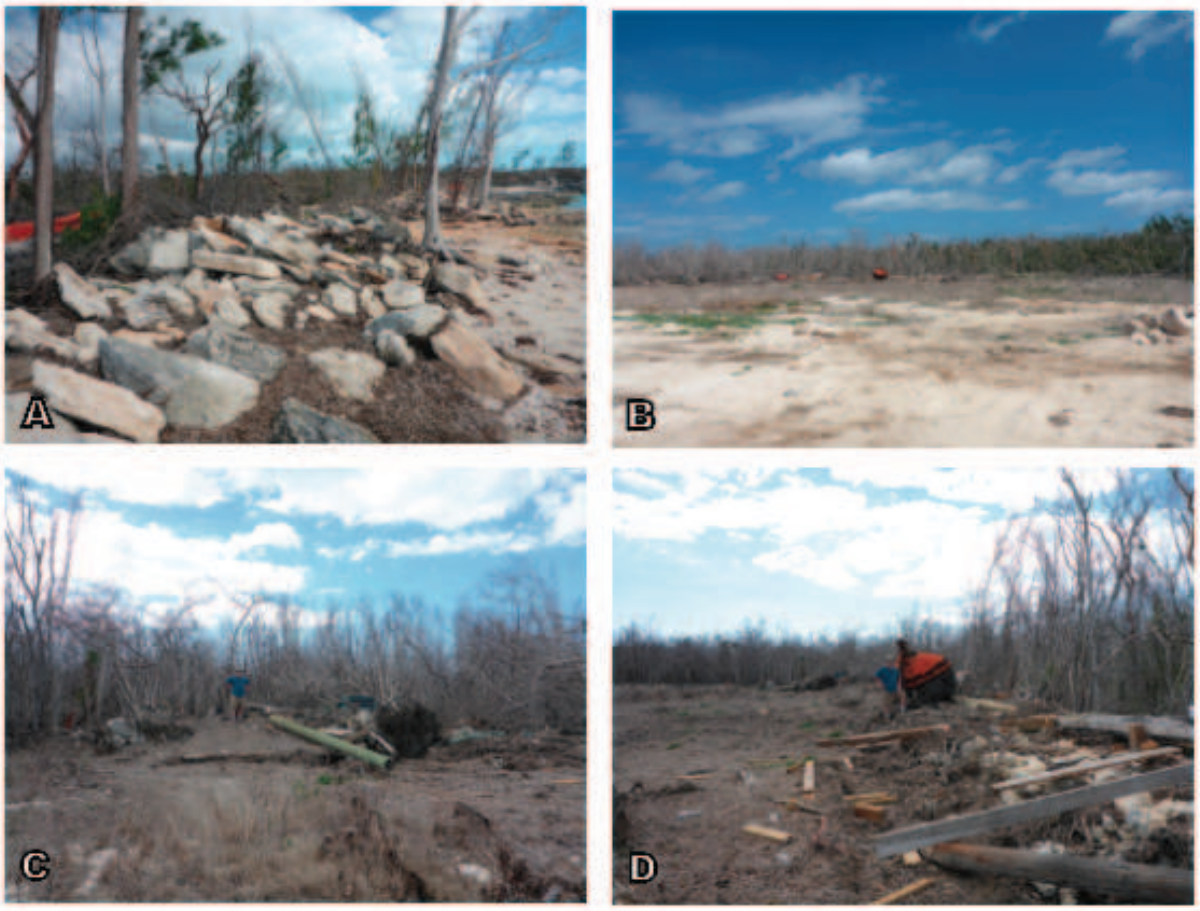

Figure 6: A) Imbricated boulders just east of Flipper Beach. B) Cleared area inland of the beach, post hurricane Matthew, showing bare bedrock patches. C) Remains of beach house/cabana in western corner of the cleared quadrangle (author for scale). D) Large navigation buoy against drystone wall on northern edge of cleared quadrangle (author for scale) (buoy also visible in Figures 6 and 7 B).

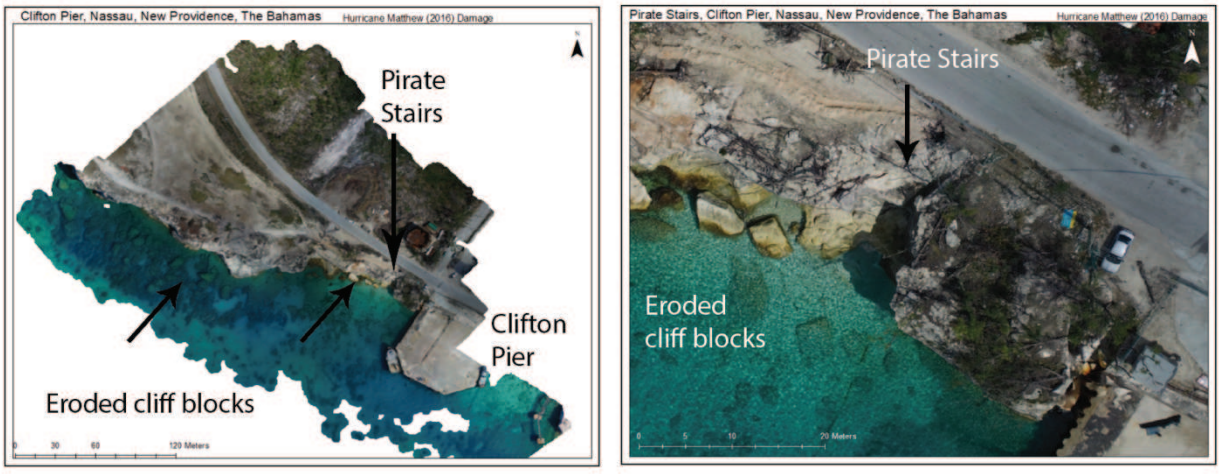

Figure 7: Drone imagery of the area around Clifton Pier and the Pirate Stairs showing large blocks of bedrock that have been eroded from the cliff. Hurricane Matthew storm surge transported debris to the top of the 6.5-m-high cliff.

Figure 8: The Pirate Stairs near Clifton Pier showing damage from Hurricane Matthew. A) Photograph from June 2012, and B) Photograph from March 2017. Note the fence that once stood at the edge of the cliff and around the stairs in the 2012 image and the broken and transported lintel block.

by storm surge is evidenced by *Sargassum* found under boulders themselves. This is a strong argument against its arrival by some other means than storm surge. At this site, we recorded dimensions and orientation of several large boulders that showed clear evidence of recent movement. Table 1 provides measurements of some of the largest boulders. While there are many large boulders that moved inland by water at this site, there are two that stand out. First, the boulder that previously served as a lintel over the narrow stairway has broken off and shifted over on top of the broken base of the steel post that previously held the fence along the edge of the cliff. Other boulders are now sitting on other parts of this fence as well. Second is a large slab of concrete. We hypothesize that it was excess concrete out of a cement truck, possibly during construction of the fence. In any case this concrete formed a rough lens shape about 2 m by 3 m, but only about 20-30 cm thick (~1.8 m^3). It originally formed in a slight depression in the bare bedrock. Based on marks in the bedrock, this slab slid about 2 m inland requiring very high wave energy.

Boulder	Long axis	Short axis	Thickness	Notes
A	190	110	65	
B	120	85	35	
C	120	105	30	on top of fence
D	105	90	25	
E	310	230	85	upside down
F	320	130	60	
G	130	110	60	
H	185	165	55	
I	190	130	30	

Table 1: Boulders transported by storm surge

Figure 9: A) Cliff showing bedrock exposure immediately to the west of the Pirate Stairs. B) Very large boulder dislodged form top edge of approximately 6-m-high cliff, west of the Pirate Stairs (researcher for scale). Note the red caliche that lines the vertical and horizontal fracture surfaces. The unweathered surface of the cliff and boulders indicates recent collapse and movement. C) Boulder deposited on top of flattened fence. Also note uprooted Casuarinas Sp. D) Boulder moved inland and uprooted Casuarinas sp. E) Boulder deposited on top of remains of fence with uprooted tree and sea wrack. F) Waste concrete slab apparently lifted and slide inland. It's original location in approximately where the "F" is located on the image.

Figure 10: A) Small boulder apparently moved by rolling. B) Sea wrack entangled in the fallen fence. One of the boulders now resting atop the fence is visible at top of image. C) This is the very large slab of rock that previously formed the lintel over the Pirate Stairs. It has been shifted up, inland, and slightly to the west, and now rests directly atop the sheared off base of one of the metal fence posts (visible in the crevice). This slab is visible in Figure 8 A, as it originally rested, and the corner of it is visible on the right edge of Figure 8 B, in its post Hurricane Matthew location.

DISCUSSION AND CONCLUSIONS

Our observations of the damage from Hurricane Matthew at these two sites located along the western shore of New Providence island provide evidence for three conclusions. First, it is not possible to overstate the power of vegetation in resisting storm surge inundation. Even when that vegetation is later killed by the saltwater contamination, it holds soil, and resists even the battering of large boulders, shown by the difference in the effects on the cleared area at Flipper Beach and the surrounding vegetated areas. It is likely that the very common high peaked ridge of imbricated boulders has its origin in boulders coming to rest against even a relatively small area of vegetation. It is also curious that the drystone field walls resisted the inundation so well. It may well be the presence of the overgrowing vegetation, and its ingrowing roots that supports the field walls against the water's erosion. However, we hypothesize that in both cases–the shoreline vegetation and the field walls, it is only necessary that they stop the first few boulders or bits of flotsam and jetsam. As boulders imbricate, and debris accumulates, they are effectively armoring themselves against further erosion.

Second, at the Pirate Stairs, the boulders did not roll. In general, they are flattish slabs of bedrock, similar to an airfoil, that have been plucked loose and slid along. We hypothesize that the mechanism for this is that water is \forced under them and lifts them on a cushion of water as they slide. This is particularly evident for the concrete described above. Also, the NOAA report on Hurricane Matthew records a 2.5 m storm surge on New Providence (Stewart, 2017). At the Pirate Stairs, we have clear evidence of boulder movement and flotsam and jetsam at the top of an approximately 6-m-high cliff. The reason for this discrepancy is likely an offshore storm surge focusing mechanism, probably the deep water immediately offshore.

Third, even lacking prior data, it was possible to determine direction, and distance of movement of the boulders at the Pirate Stairs through observation (and application of the law of superposition). This direct observation and measurement has proven very effective, even lacking clear pre- and post-event images. However, the combination of historic satellite images with our high resolution aerial photomosaic has also provided a powerful tool for quantifying the effects of events such as hurricanes.

ACKNOWLEDGMENTS

This project would have been impossible without the collaboration of Kathleen Sullivan

Sealey and especially Nikita Shiel-Rolle, Director of the Young Marine Explorers, research funding from the University of Missouri-Kansas City, and support from the Gerace Research Centre.

REFERENCES

Berman, M.J. 2014. New Perspectives on Bahamian Archaeology; the Lucayans and their World. *Journal of Caribbean Archaeology* 15: 2-22.

Cash, P., Gordon, S.C., and Saunders, G. 1991. *Sources of Bahamian History*. Macmillan Caribbean, London, 374 p.

Caviedes, C.N. 1991. Five Hundred Years of Hurricanes in the Caribbean: Their Relationship with Global Climatic Variabilities. *GeoJournal* 23(4): 301-310.

Craton, M., and Saunders, G. 1999. *Islanders in the Stream: A History of the Bahamian People. Volume One: From Aboriginal Times to the End of Slavery*. University of Georgia Press, Athens, Georgia, 496 p.

Mylroie, J.E., Carew, J.L., Curran, H.A., Godefroid, F., Kindler, P., and Sealey, N.E. 2012. *Geology of New Providence Island, Bahamas: A Field Trip Guide*. Gerace Research Centre, San Salvador, Bahamas, 30 p.

Neumann, C.J., Jarvinen, B.R., Pike, A.C., and Elms, J.D. 1987. *Tropical Cyclones of The North Atlantic Ocean, 1871-1986*. North Carolina National Climate Data Center, Asheville, North Carolina, 186 p.

Sealey, N.E. 2006. *Bahamian Landscapes: An introduction to the Geology and Physical Geography of The Bahamas* (3rd Edition), MacMillan Caribbean, Oxford, 174 p.

Shaklee, R.V. 1997. Historical Hurricane Impacts on The Bahamas: 1500-1749. Part 1. *Bahamas Journal of Science.* 5(1): 7-9.

Siegel, P.E., and Righter, E. 2011. *Protecting Heritage in the Caribbean*. University of Alabama Press, Tuscaloosa, Alabama, 216 p.

Stewart, S.R. 2017. *Hurricane Matthew* (AL142016): National Hurricane Center Tropical Cyclone Report. NOAA National Hurricane Center, 96 p.

DETECTION OF BOULDER TRANSPORT VIA STORM SURGE USING DRONE IMAGERY ON GREEN CAY, SAN SALVADOR, THE BAHAMAS

Joseph A. Nolan and Tina M. Niemi

Department of Earth and Environmental Sciences
University of Missouri-Kansas City
Kansas City, MO 64110, U.S.A.

ABSTRACT

Green Cay is a 6-m-high island located along the northwest reef barrier of San Salvador island in The Bahamas that separates deep Atlantic Ocean from the shallow water of Graham's Harbour. Given its low elevation, Green Cay is often overtopped by waters of hurricanes with sufficient storm surge height. In order to understand the boulder transport processes and change in the coastal environment, we conducted field and underwater snorkel surveys of the southeast shore of Green Cay. We also collected high-resolution, drone aerial imagery in June of 2016 and March of 2017 that was processed into orthophoto mosaics. These data were collected before and after Hurricane Matthew that passed 170 km southwest of San Salvador as a Category 3 storm on October 5, 2016. The Hurricane Matthew storm surge was high enough to overtop Green Cay and move several small boulders which we document in this study.

INTRODUCTION

The Bahamian archipelago is a series of NW-SE-trending, carbonate islands between about 23-20°N latitude in the Atlantic Ocean, located to the east of the Straits of Florida and to the north of the islands of Cuba and Hispaniola. The dynamics of the coastal environment of Bahamian islands is dependent on the configuration of lithified bedrock along the shoreline and whether the beach is sandy or rocky (Sealey, 2006). Sediment delivered to the coastal environment is predominantly dependent on carbonate sources produced in the nearshore environment, or weathering and erosion of carbonate bedrock. Soils are poorly developed on remote islands like The Bahamas (Sealey, 2006) and are augmented by long-term input of airborne dust accumulation (Muhs et al., 2007). Thus, the dynamics and morphology of the coastal or beach environment is controlled by the redistribution of available carbonate sediment.

Due to the location of The Bahamas, the islands experience a frequent number of storms during the Atlantic Ocean hurricane season between June and November. Storm surge is the most dominant factor in rapid change of the coastal morphology. As a storm surge moves on land, large amounts of debris carried from the ocean including human and natural flotsam and jetsam, sand, gravel, and sometimes boulders, are deposited inland. According to calculations by Nott (2003), boulders as large as 2.5 – 3 m^3 and weighing hundreds of tonnes depending on density and porosity are transported in hurricanes. The maximum height of a storm surge is controlled by a number of factors including sustained wind speed, storm forward speed and direction, gradient of the barometric pressure of the storm to atmospheric pressure, beach and coastline topography, and bathymetry (e.g. Weisberg and Zheng, 2006). Riparian vegetation can help reduce damage to coastline. Once damaged, the vegetation needs to recover or the coastline will be vulnerable to additional wave damage in subsequent storms (Bush et al., 1996). When inundated, inland vegetation struggles due predominantly to increased salinity and often dies out until such time that soil conditions can once again become favorable to the native species (Rodgers et al., 2009). Removal of inland vegeta-

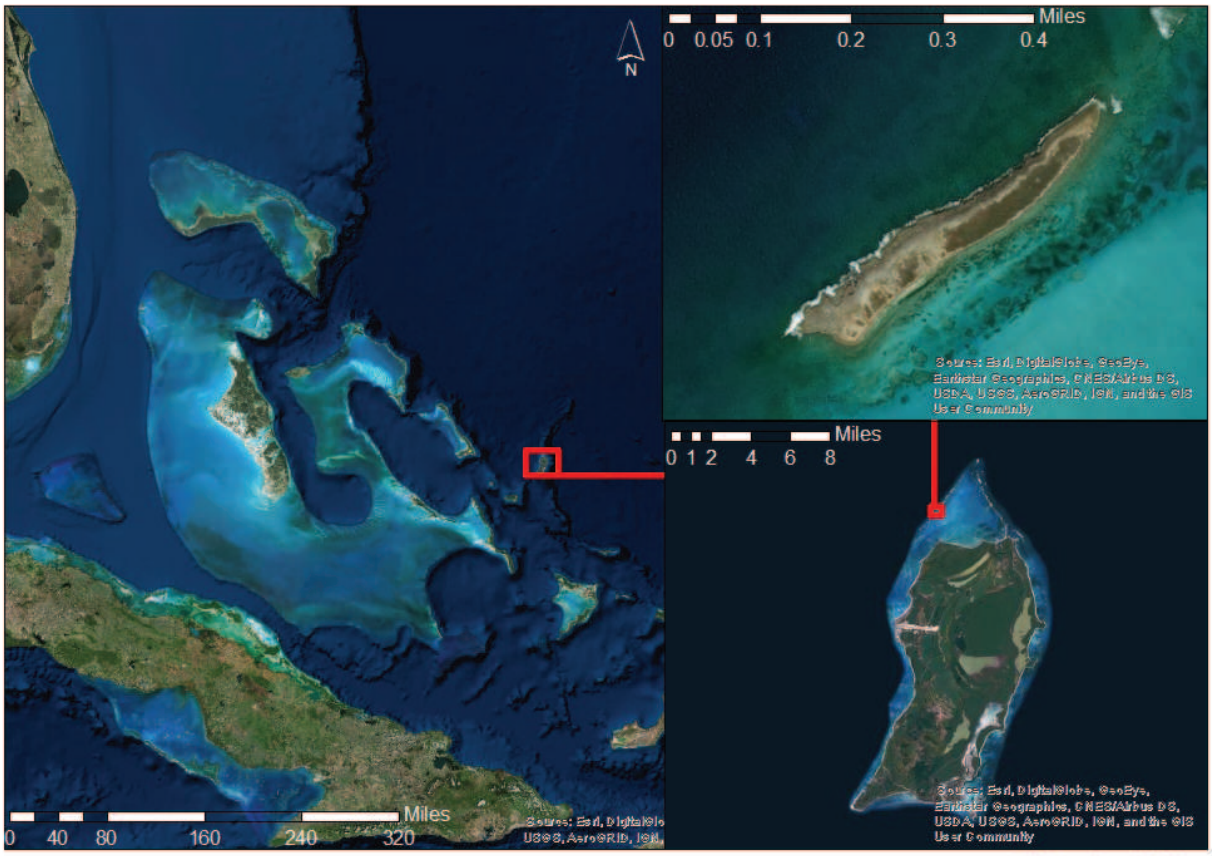

Figure 1: Satellite image of showing the location of San Salvador along the eastern edge of the of the Bahamian platform. Green Cay is a small island along the northwest side of San Salvador helping to enclose the shallow water lagoon of Graham's Harbour.

tion can lead to an increase in maximum inundation distance.

Hurricane Matthew developed as a tropical storm on September 28, 2016 in the Lesser Antilles and rapidly developed into a Category 5 hurricane—the first since 2007 in the Caribbean Sea (Stewart, 2017). The hurricane then moved north between Haiti and Cuba before curving to the northwest in The Bahamas. Hurricane Matthew traveled through The Bahamas as a Category 3 storm with the eyewall passing between Andros and New Providence on October 5, 2016 before moving to the coast of Florida and up the southeast coastal U.S. (Figures 1 and 2). San Salvador island was less impacted by this hurricane compared to direct landfalls of Hurricane Hurricane Floyd in 1999 (Curran et al., 2001; Walker et al., 2001), Frances in 2004 (Parnell et al., 2004; Niemi et al., 2008; Niemi, 2017), and Joaquin in 2015 (Preisberga et al., 2016). With the high frequency of hurricanes on such a small island (Shaklee, 1996), San Salvador Island is an excellent location for studying geomorphological processes caused by storms. In this study, we utilize aerial imagery and field observations from before (June, 2016) and after (March, 2017) Hurricane Matthew to determine the movement of boulders and the change in the morphology on Green Cay—a tiny island at the northwest reef barrier margin of San Salvador.

STUDY AREA

San Salvador Island is located along the northeast edge of the Bahamian archipelago and is an isolated island surrounded by deep Atlantic Ocean water. As a carbonate island, San Salvador

Figure 2: Storm track of Hurricane Matthew from September 28, to October 9, 2016 (NOAA, 2017). https://www.weather.gov/ilm/Matthew

grows through marine sediment being deposited on the margins (Carew and Mylorie, 1985; Hearty and Kindler, 1993). Featuring a relatively low-lying topography, San Salvador is also home to a number of inland lakes, which occur as blue holes, interdunal troughs, or cutoff lagoons, many of which are hypersaline (Teeter, 1995). The sedimentology of the island is comprised of calcarenites, which are grain-supported, fine-to-coarse grained ooids, peliods, and bioclasts sands or calcrudites and boundstones built from Pleistocene coral, and calcretes (Carew and Mylorie, 1985; 1995; Hearty and Kindler, 1993). The calcarenites that form topographic ridges are fossilized sand dunes, often called aeolinites.

Green Cay is a small island located 2.5 km northwest of Barker's Point on San Salvador island. Measuring only 600 m from end to end and 85 m at maximum width, Green Cay is located among a line of islands and shoals forming a separation from deep Atlantic waters from Graham's Harbour, a large, shallow lagoon. The island has a gentle slope toward the southeast and a northeast-trending ridge that marks the crest of the Pleistocene aeoliniate (Carew and Mylroie, 1985). The northwestern margin of Green Cay is steeper and marked by active cliff retreat erosion. Areas of extensive mass wasting are evident where arcuate-shaped, headwall scarps punctuate the ocean-facing island margin. The highly weathered, pitted, and jagged surface of the bedrock is a product of karst weathering.

The bedrock stratigraphy of Green Cay is exposed along the cliffs that face toward the northwest and can be divided into two units. The lower rock section is comprised of a cross-bedded, carbonate sandstone (calcarenite). The upper section is a heavily bioturbated calcarenite with plant trace fossils, including root casts and tree trunk molds (e.g. Mylroie and Carew, 2008). Capping the bioturbated unit is either a calcrete crust or remnants of a terra rossa paleosol. Geologically, the rocks are interpreted as fossilized Pleistocene sand dunes (aeolianites) that were heavily vegetated and rapidly lithified. The morphology of Green Cay preserves some of the original Pleistocene sand dune topography.

DATA COLLECTION

During three separate visits to San Salvador Island in June of 2016 and March and June of 2017, we made field observations of the boulders on the Green Cay island and in the shallow water southeast of the island. We photographed the boulders within the erosional cove and within the washover zone along the southwestern portion of the island. We also conducted a snorkel survey south of Green Cay and within the Graham's Harbour near the island to determine if there is a large subtidal boulder field adjacent to the island.

These field observations were compared to aerial photos obtained using a DJI Phantom 3 Quadcopter mounted with 12 Megapixel, 4K video camera with geo-referencing. Flight plans were laid out utilizing Pix4D Capture, version 3.0.1 in June 2016 and version 3.7.1 in March 2017. Pix4D Capture is a GPS-enabled Android application for quadcopters that allows the user to create projects with multiple missions allowing the same path to be flown multiple times. Flight height, coverage

pattern, photograph overlap percentage, and camera angle can all be controlled, as well as offline maps allowing usage in remote areas and still providing a base map for accuracy. For this project, a programmed flight path obtained photos at 50 m of elevation with 70% overlap with 100% vertical camera angle, collecting 420 and 474 images, respectively, of the Green Cay study area. Extra photos were taken in March of 2017 due to extremely high winds stalling the quadcopter resulting in gaps in coverage, these areas had to be flown again.

Orthophoto mosaic photos and Digital Elevation Models (DEM) were created with Agisoft Photoscan Professional; software versions 1.2.4 build 2399 and 1.3.0 build 3772, respectively. To produce these images, photo alignment was performed at high accuracy with a key point limit of 40,000, and a 10,000 tie point limit utilizing the adaptive camera model fitting feature. A dense cloud was then constructed under the highest quality setting with aggressive depth filtering. Next, a height field-type mesh was produced from the dense cloud with high face count and interpolation enabled. Finally, the texture was assembled from the orthophoto, with mosaic blending, and texture size/count set to 8192 x 1 with both color correction and hole filling enabled.

Using ARCGIS, the two orthophoto mosaic images (Figure 3 and 4) were made into base maps. Visual comparisons were made between 2016 and 2017 of potential boulder movement. Orthophotos and DEMs created and exported from Agisoft should be in a projected coordinate system for measurement of area. Shapefiles were obtained from GADM and used for georeferencing. Boulders were measured in ArcMap using changes in elevation. Using a point vector feature class, 6-8 locations around the boulders and three on the top of each boulder were selected using DEM and Z-values were gathered using Extract Values to Points tool. The Z-values around the boulders were used to generate an average ground elevation and the three points on the boulders were averaged to determine a change in height with respect to the ground, generating the height of each boulder. Using the ArcMap measuring tool, the 2-dimensional area of the top face of each boulder was measured, allowing for the approximate volume of each boulder.

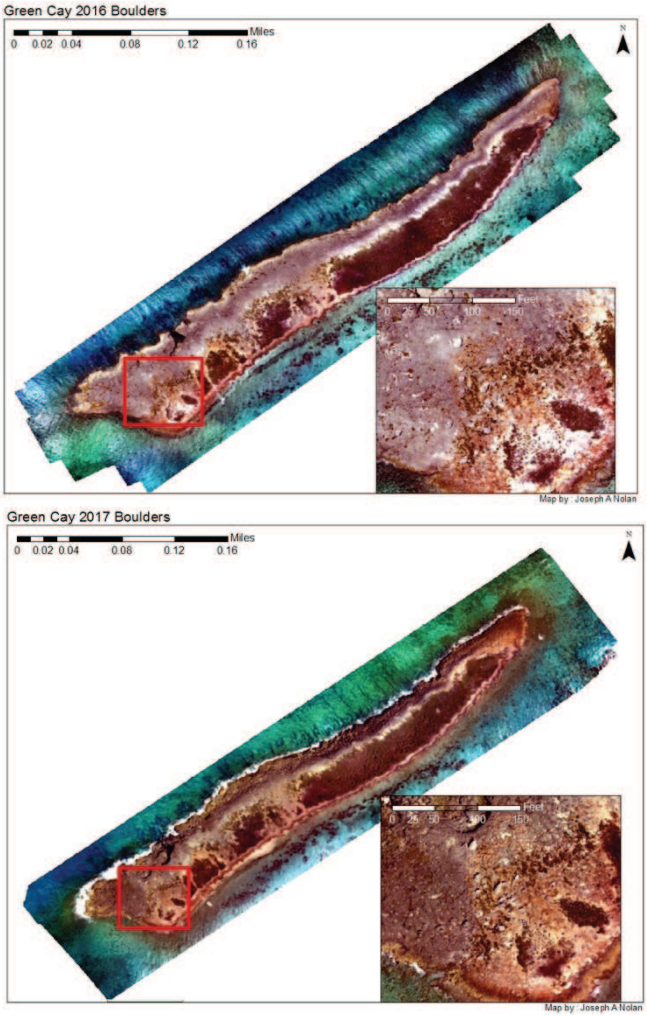

Figure 3: Orthophoto mosaics of Green Cay that were created by processing drone imagery acquired in June 2016 (upper image) and in March 2017 (bottom image). Details of the southwest area is shown in Figure 4.

RESULTS

Two orthophoto mosaic images were made into base maps (Figure 3 and 4) and a visual comparison was made between the 2016 and 2017 images to identify potential boulder movement. The southern end of Green Cay has a large overwash zone that is largely devoid of brush vegetation as storm surge has repeatedly overtopped the island at this

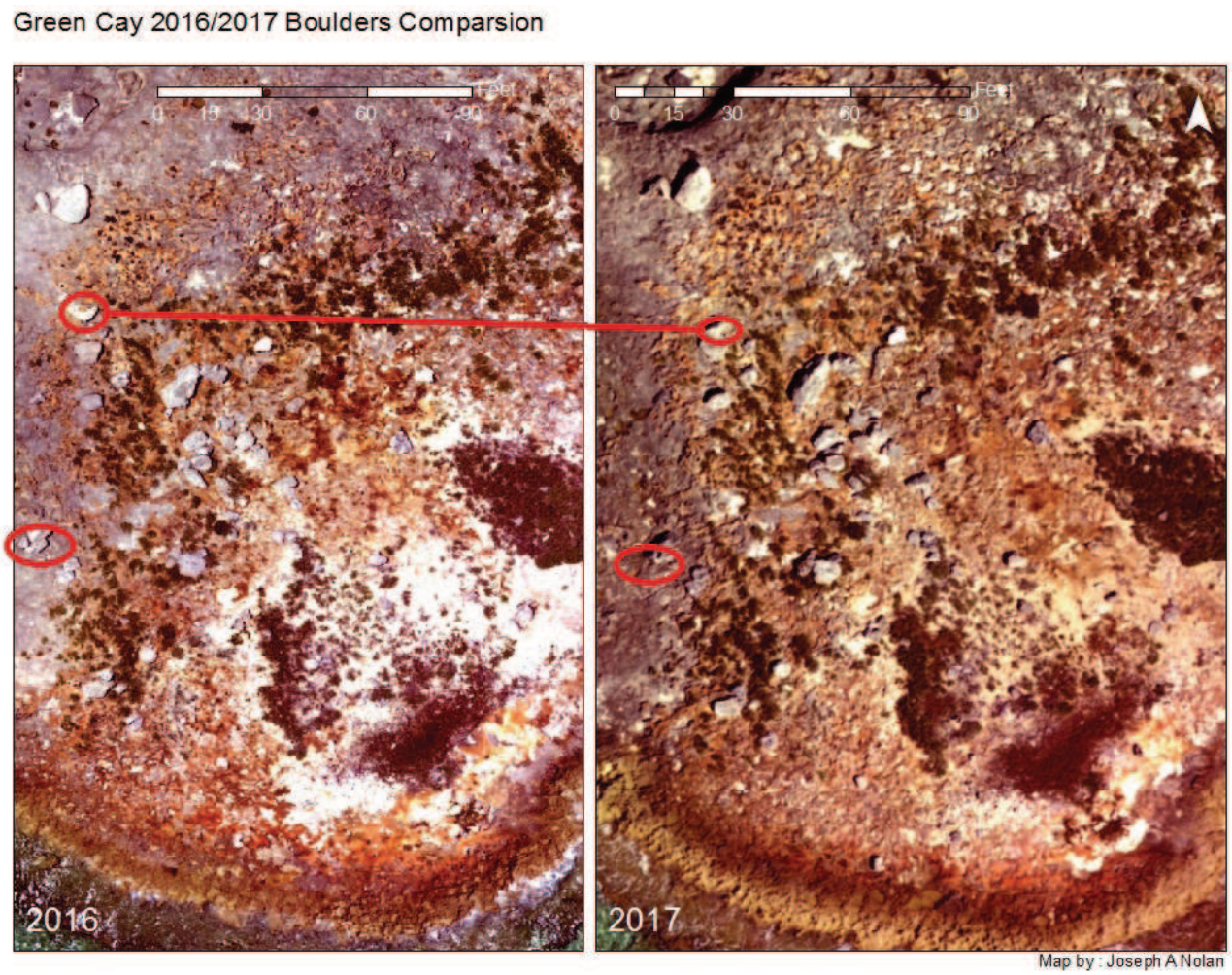

Figure 4: Detailed images of the scattered boulder field on the south side of Green Cay. Circles note the areas where boulder movement was documented.

location. In the overwash zone, there is a boulder field that is characterized by large isolated boulders and small clusters of boulders (Figure 5). Boulders in the field are widely spaced. We identified four boulders on Green Cay that moved between 2016 and 2017 (Figure 4). These boulders measure approximately <0.5 m in width and length. Very large boulders clearly were neither translated or rotated and can be directly matched in the two aerial images. It is likely that many smaller boulders and cobbles were transported, but this movement is beyond the resolution of this method. The biggest storm to have passed through The Bahamas in this time period was Hurricane Matthew.

Our field observations indicate that boulders are currently forming a boulder ridge along the crest of Green Cay. The boulder ridge is only seen at several locations and is not continuous (Figure 6). The imbricated boulders have a fresh, unweathered appearance on at least one of their faces. This indicates transportation in recent storms.

Our underwater snorkel survey identified a subtidal boulder field located south and southeast of Green Cay in ca. 3m of water. The clast size in this location is cobbles to small boulders. In very shallow water, a boulder field with boulders >1m in the long dimension was found (Figure 7). These boulders are likely to have been transported off of Green Cay in previous hurricanes and accumulated in the underwater boulder field close to the island. They are unlikely to move farther.

Together these data support an earlier study by Niemi (2017) that showed that the boulder field was produced by storm surge transport of cliff-

derived boulders. Cliff retreat that is accelerated within coves found along the northwest cliff provide the boulders that are transported. Very large boulders >1m in long dimension can be transported in a Category 4 hurricanes such as Hurricane Frances in 2004 (Niemi, 2017). Because Hurricane Matthew was only a Category 3 storm and the eye of the storm tracked over 170 km southwest of San Salvador, our study documented that only a few small boulders were transported by the Matthew storm surge.

Figure 5: Photograph of the crest of Green Cay looking toward the southwest across the along washover zone. The black arrow points to very large boulders in the distance along the downslope (SE) side of the island. The deep water of the Atlantic Ocean is on the right (west) and the shallow protected water of Graham's Harbour is on left (east). Transported boulder in the foreground next to 2 m stick. Measuring stick for scale with 2 cm increments. View toward the southwest.

DISCUSSION AND CONCLUSIONS

A correlation between storm intensity and wind speed predicts storm surge height based on the Saffir-Simpson scale (Irish et al., 2008). Although wind speed is a factor in the magnitude of the storm surge, it is not the only factor. Lowering the normal atmospheric pressure causes the water itself to swell upward in the eyewall. Weisberg and Zheng (2006) state that "wind stress acting on the sea surface, when confronted by a rigid boundary, causes water to accumulate along that boundary such that the pressure gradient force associated with the surface slope, times the water depth, tends to balance the difference between the wind and bottom stresses." The forward speed and direction of the storm, atmospheric pressure fields, angle of approach, and geographic locations are just as important in maintaining the storm surge accumulation (Weisberg and Zheng, 2006). Higher forward speed add to the maximum surge accumulation. The difference in forward speed of the hurricane can make a difference of up to 37% more surge peak (Rego and Li, 2009). Conversely, a slower speed hurricane can be more damaging; while the peak surge amplitude may be smaller, the storm has more time to bring a larger volume of water onshore (Rego and Li, 2009). Topography, bathymetry, sand grain size, vegetation, and beach profile all play roles in the storm surge peak amplitude (Morton, 2002).

Figure 6: Boulder ridge at the crest of Green Cay along the northern portion of the washover zone. Note the imbrication of the boulders and the fresh unweathered appearance of some of the boulders. Measuring stick for scale with 2 cm increments. View toward the northeast.

During tropical storm surge inundation, the surge has the potential to carry a large amount of sediment, oceanic salts, and large debris inland. Material entrained in the floating mass is stranded

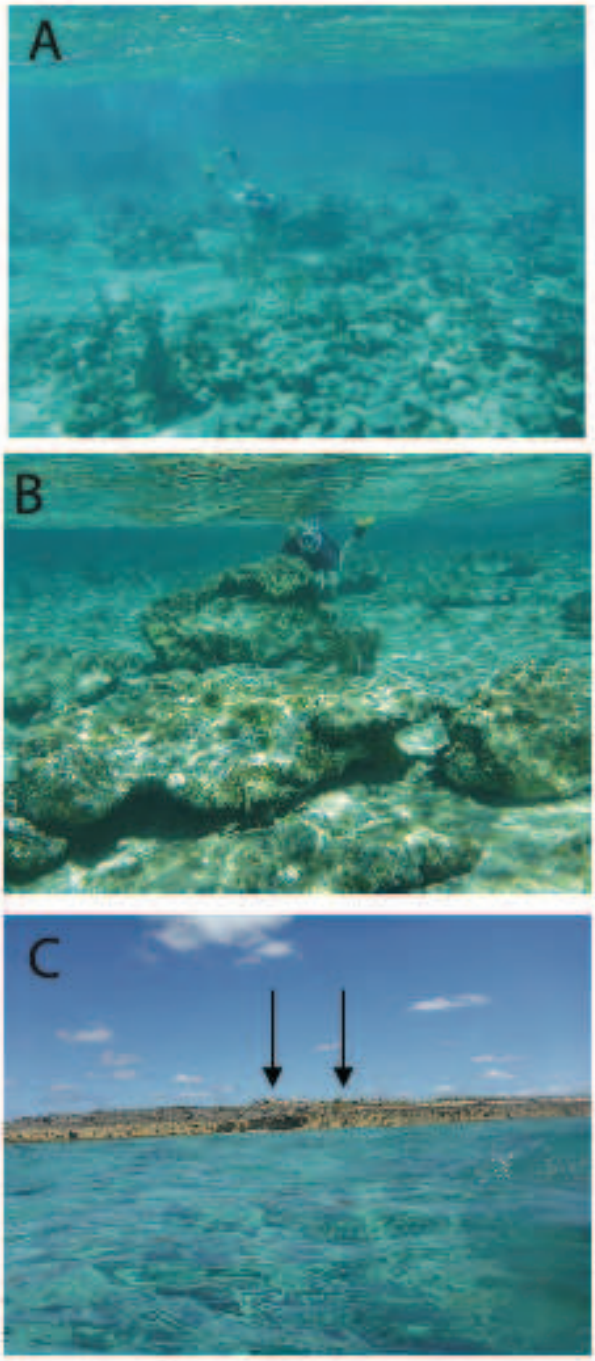

Figure 7: A) Underwater boulder field located south and southeast of Green Cay in ca. 3m of water. The clast size in this location is cobbles to small boulders. B) In very shallow water, a boulder field with boulders >1m in the long dimension was found. C) View from the offshore boulder field toward the northwest to Green Cay. Black arrows point to very large boulders on Green Cay.

as a wrack line. The wrack line, or wet line, is used as a marker to the line of inundation as the deposition tends to be at or very near the maximum water level before the time of retreat (Morton, 2002). The wrack line debris includes a substantial amount of human plastics and other materials as well as natural floating vegetation and debris. Only when the debris encounters a riparian vegetation zone does the wrack line lose accuracy (Bush et al., 1996).

Boulders as large as 2.7 m^3 have been determined to have been transported by means of storm surge inundation (Nott, 2003). These hydrodynamic formulas have been derived and used to provide a theoretical wave height needed for boulder transport. Based on the mass of the boulder in question, these formulas offer a numerical estimate for required wave amplitude of a storm surge. Researchers continue to debate over the true power of storm surge (Nott, 2003; Imamura et al., 2008; Spiske et al., 2008). However, one thing is certain, storm surge is very dangerous.

Previous study of boulder movement on Green Cay showed that a large boulder (8.5 m^3) that weighs approximately 16 metric tons was transported from a lower cove position up to the ridge by the storm surge in the Category 4 Hurricane Frances in 2004 (Niemi, 2017). These data suggest that the wave equations of Nott (2003) somehow underestimate the energy of storm surge transport. The eyewall of Hurricane Frances made direct landfall on San Salvador which led to very large storm surge heights (Parnell et al., 2004; Niemi et al., 2008). However, since Hurricane Matthew was only a Category 3 storm and passed southwest of the San Salvador, the storm surge height and duration were smaller that in Hurricane Frances. Thus, only small boulders moved with the Matthew storm surge on Green Cay.

ACKNOWLEDGMENTS

This research was conducted under a Bahamas Environment, Science & Technology (BEST) Commission permit to investigate hurricane storm surge. We thank Troy Dexter, Executive Director and Research Coordinator, and all the staff at the

Gerace Research Centre for assistance and logistical help while at the field station on San Salvador. Invaluable field assistance was provided by UMKC students John Rucker and Tori Rose, and University of Exeter Professor Jamie Stevens. A special thanks to Anniya Murray (Preisberga) and Genaro Martinez-Gutierrez for guidance with software applications and Linda Moore Rucker for proof-reading the final manuscript.

REFERENCES

Bush, D.M., Young, R.S., Webb, C.A., and Thieler, E.R. 1996. Soundside impacts of a northward tracking tropical cyclone: Hurricane Emily (31AUG93), Cape Hatteras area, North Carolina. *Journal of Coastal Research* 12: 229–239.

Carew, J.L., and Mylroie, J.E. 1995. A stratigraphic and depositional model for the Bahama Islands. Pp 5-31. In H.A. Curran, (Ed.). *Terrestrial and Shallow Marine Geology of the Bahamas and Bermuda*. Geological Society of America Special Paper 300, Boulder, CO.

Carew, J.L., and Mylroie, J.E. 1985. Pleistocene and Holocene stratigraphy of San Salvador Island, Bahamas, with reference to marine and terrestrial lithofacies at French Bay. Pp. 11-61. In H.A. Curran (Ed.). Guidebook for Geological Society of America, Orlando Annual Meeting Field Trip #2, Fort Lauderdale, Florida.

Curran, H.A., Delano, P., White, B., and Barrett, M. 2001. Coastal effects of Hurricane Floyd on San Salvador Island, Bahamas. Pp. 1-12. In *Proceedings of the 10th Symposium on the Geology of the Bahamas and Other Carbonate Regions.* Gerace Research Center, San Salvador, The Bahamas.

Hearty, P.J., and Kindler, P. 1993. New Perspectives on Bahamian Geology - San-Salvador Island, Bahamas. J*ournal of Coastal Research* 9: 577–594.

Imamura, F., Goto, K., and Ohkubo, S. 2008. A numerical model for the transport of a boulder by tsunami. *Journal of Geophysical Research* 113: 1–12, doi:10.1029/2007JC004170.

Irish, J.L., Resio, D.T., and Ratcliff, J.J. 2008. The influence of storm size on hurricane surge. *Journal of Physical Oceanography* 38: 2003–2013, doi:10.1175/2008JPO3727.1.

Morton, R.A. 2002. Factors controlling storm impacts on coastal barriers and beaches-A preliminary basis for near real-time forecasting. *Journal of Coastal Research* 18(3): 486–501.

Muhs, D.R., Budahn, J.R., Prospero, J.M., and Carey, S.N. 2007. Geochemical evidence for African dust inputs to soils of western Atlantic islands: Barbados, The Bahamas, and Florida. *Journal of Geophysical Research* 112: F02009, doi:10.1029/2005JF000445.

Mylroie, J.E., and Carew, J.L., 2008. *Field Guide to the Geology and Karst Geomorphology of San Salvador island.* Gerace Reserach Center, San Salvador, The Bahamas, 88 p.

Niemi, T.M. 2017. Large boulders on Green Cay, San Salvador Island, The Bahamas. Pp. 121-129. In C.L. Landry, L.J. Florea, and D.S. Kjar (Eds.). *Proceedings of the 1st Joint Symposium on the Natural History and Geology of The Bahamas*. Gerace Research Center, San Salvador, The Bahamas.

Niemi, T.M., Thomason, J.C., McCabe, J.M., and Daehne, A. 2008. Impact of the September 2, 2004 Hurricane Frances on the coastal environment of San Salvador island, The Bahamas. Pp. 43-63. In L.E. Park and D. Freile (Eds.). *Proceedings of the 13th Symposium on the Geology of the Bahamas and Other Carbonate Regions*. Gerace Research Center, San Salvador, The Bahamas.

Nott, J. 2003. Tsunami or storm waves? Determining the origin of a spectacular field of wave emplaced boulders using numerical storm surge and wave models and hydrodynamic transport equations. *Journal of Coastal Research* 19: 348–356.

Parnell, D.B., Brommer, D., Dixon, P.G., Brown, M.E., and Gamble, D.W. 2004. Hurricane Frances damage on San Salvador. *Bahamas Journal of Science* 12: 2–6.

Preisberga, A., Niemi, T.M., Nolan, J., Grady, J., Rucker, J.D., and Lamprise, S. 2016. High-Resolution UAV imaging and mapping of coastal erosion and boulder movement produced by the 2015 Hurricane Joaquin on San Salvador, The Bahamas. *Geological Society of America Abstracts with Programs* 48:7 doi:10.1130/abs/2016AM-287520.

Rego, J.L., and Li, C. 2009. On the importance of the forward speed of hurricanes in storm surge forecasting: A numerical study. *Geophysical Research Letters* 36: 1–5, doi: 10.1029/2008GL036953.

Rodgers, J.C., Murrah, A.W., and Cooke, W.H. 2009. The impact of Hurricane Katrina on the coastal vegetation of the Weeks Bay Reserve, Alabama from NDVI data. *Estuaries and Coasts* 2: 496–507, doi:10.1007/s12237-009-9138-z.

Sealey, N. 2006. *Bahamian Landscape: Introduction to the Geology and Physical Geography of the Bahamas.* Macmillan, Oxford, 174 p.

Shaklee, R.V. 1996. *Weather and climate, San Salvador Island, Bahamas.* Bahamian Field Station, San Salvador, The Bahamas.

Spiske, M., Böröcz, Z., and Bahlburg, H. 2008. The role of porosity in discriminating between tsunami and hurricane emplacement of boulders - A case study from the Lesser Antilles, southern Caribbean. *Earth and Planetary Science Letters* 268: 384–396, doi:10.1016/j.epsl.2008.01.030.

Stewart. S.R. 2017. Hurricane Matthew (ALI42016): National Hurricane Center Tropical Cyclone Report. NOAA, 96 p.

Teeter, J.W. 1995. Holocene saline lake history, San Salvador Island, Bahamas. Pp. 117-124. In H.A. Curran (Ed.). *Terrestrial and Shallow Marine Geology of the Bahamas and Bermuda*. Geological Society of America Special Papers 300, Boulder, CO.

Walker, S.E., Holland, S.M., and Gardiner, L. 2001. Cockburn Town fossil reef: A summary of effects from Hurricane Floyd. Pp. 13-19. In B.J. Greenstein and C.K. Carney (Eds.). *Proceedings of the 10th Symposium on the Geology of the Bahamas and Other Carbonate Regions*. Gerace Research Center, San Salvador, The Bahamas.

Weisberg, R., and Zheng, L. 2006. Hurricane Storm Surge Simulations for Tampa Bay: *Estuaries and Coasts.* 29: 899–913, doi:10.1007/BF02798649.

MOBILIZING CITIZEN SCIENTISTS IN HURRICANE DISASTER ASSESSMENTS

Nikita Shiel-Rolle[1] and Kathleen Sullivan Sealey[2]

[1] Young Marine Explorers, Orange Creek, Cat Island, The Bahamas

[2] University of Miami Coastal Ecology Lab, Coral Gables, Florida USA

ABSTRACT

Hurricane Matthew hit The Bahamas in October 2016 as a Category 3 and 4 hurricane causing an environmental disaster. The Bahamas and other Small Island Developing States in the Caribbean may be facing an increasingly large number of severe storm events in the future as hurricanes and tropical storms are strengthened by unusually warm ocean waters. There needs to be a proactive response to hurricane preparation and mitigation. The Hurricane Matthew Project jointly conducted by Young Marine Explorers, a Bahamian marine conservation organization, and the University of Miami Coastal Ecology Lab studied the impacts of Hurricane Matthew on New Providence. Part of the study looked at the role that citizens can play at proactively preparing for these hurricanes in advance through community mitigation and restoration projects that work in partnership with the government. This study looks at the experience of the citizen scientists who participated in the Hurricane Matthew Project and the potential for mobilize large numbers of people to collect valuable information that can assess hurricane damage and support policy making, while simultaneously developing marine citizenship.

INTRODUCTION

The Bahamas is a low-lying country and extremely susceptible to the effects of climate change. With sea level rise and global warming trends, The Bahamas may be facing an increasingly large number of severe storm events in the future as hurricanes and tropical storms are strengthened by unusually warm ocean waters (e.g. Sullivan Sealey, 2017). Caribbean nations are exposed to extreme weather events because of their geographical location with disasterous consequences due to their socio-economic state (Cashman and Nagdee, 2017). Over the past three years, the Atlantic basin has experienced devastating hurricanes that have long-lasting impacts on the economy and the well-being of the island residents. The Atlantic basin is infamous for tropical storm activity, having on average 11.7 named storms forming each year between the years of 1900-2016 (Landsea, 2017). Hurricane Matthew, a Category 3 and 4 hurricane on the Saffir-Simpson scale hit The Bahamas on the 5th and 6th of October 2016. The Hurricane came up from the southeast and passed through the entire country. With maximum wind speeds of 225 kilometers per hour, and a maximum rainfall estimated at over 20 cm (Sullivan Sealey, 2017). This hurricane had unprecedented impacts on the people and communities of The Bahamas. Young Marine Explorers (YME), a Bahamian marine conservation organization worked with the Coastal Ecology Lab at the University of Miami (UM-CEL) to document the impacts of Hurricane Matthew on coastal and marine resources. The study, titled the Hurricane Mathew Project, included a rapid impact assessment to document damage caused by the hurricane to the coastal zone, and looked specifically at developed and protected coastal environments along the southern and western coasts of New Providence Island. The project produced maps that illustrated the extent and severity of damage caused by Hurricane Matthew. The results showed that

irresponsible coastal development and the poor environmental decisions that have been made over the past decades in The Bahamas turned a bad hurricane into an environmental disaster by accelerating the rate of coastal erosion, dumping trash including plastic into the ocean, and increasing the pollution loading to nearshore marine habitats (Sullivan Sealey, 2017).

Historically, in The Bahamas, active hurricane preparation begins between a week, to a few days before landfall of the hurricane, and primarily consists of gathering necessary items and securing property. Post storm there is significant dependence on the government to restore private and public infrastructure. Such exclusive dependence on government agencies and the lack of long-term preparation and mitigation of potential storm damage is not sustainable. Citizens of these island nations need to be prepared to not only respond to natural disasters, but also proactively prepare for these hurricanes in advance through community mitigation and restoration projects that work in partnership with the government.

Young Marine Explorers is a non-profit organization with the mission to empower and inspire youth to restore and protect our marine ecosystems through education, leadership, stewardship, and citizen science, ultimately fostering positive behavioral change that drives conservation. Over the past ten years, YME has worked within the public-school system in New Providence offering marine science and youth development programs for senior high school students, working with over 1200 students. YME's role in the Hurricane Matthew Project was to engage citizen scientist. Recent high school graduates and high school students worked with the UM-CEL to collect data. The intent of this partnership was to look at how citizens and community members can become actively engaged in disaster response assessments, and to encourage citizens to take greater personal responsibility for hurricane preparation and mitigation. This project has laid the foundation for the expansion of the role of citizen science projects in the Young Marine Explorers programs. Additionally, it has increased our interest in conducting citizen science projects with the ability to inform data-driven decisions at the policy and management level.

STUDY SITE AND CITIZEN SCIENTISTS

The Hurricane Matthew Project focused on New Providence Island, the most populated island in The Bahamian Archipelago which spans 1,200-km in the Tropical Western Atlantic Ocean. The study focused on Southern New Providence and the citizen scientists participating in this study lived within the study region. Citizen science is the practice of using members of the general public to collect quantitative information in collaboration with scientists. Two groups of citizen scientists were used in this study. The first were high school students between the ages of 14 and 17. These high school students were enrolled in a Young Marine Explorers after school program and had between one to two years' experience in marine education and stewardship activities. The second and more engaged group in this study was the YME interns who had completed three years of the YME stewardship program and were participating in a two-year internship that exposed student to marine conservation projects in The Bahamas. Interns were recent high school graduates with no formal scientific training or college experience and received a small stipend for their commitment to the internship. All citizen scientists participating in this study were from low income and under-served communities.

METHODS

Before participating in the data collection processes of the Hurricane Matthew Project, the citizen scientists needed to be trained to ensure that the data collected was reliable. To facilitate this training the University of Miami's Coastal Ecology Lab created training videos and a Field Methods Manual. The Field Methods Manual has nine sections: 1) An introduction to the Hurricane Matthew Project and Citizen Science, 2) Building Damage Ranking Protocol, 3) Vegetation Damage Ranking

Protocol, 4) Flood Severity Ranking Protocol, 5) Solid Waste Assessment Underwater and Coastal Protocol 6) Coastal Assessment Protocol, 7) Sediment Sampling Protocol, 8) Waster Quality and Biodiversity Assessment Protocol, and 9) Quality Assurance Protocol. The five interns watched the different training videos and participated in an hour-long question and answer period following each video. The field manual was carried into the field and referenced continually. A scientist accompanied the five interns in the field. The scientist served as a reference and was able to answer questions and provide guidance when needed. At times the intern and scientist team worked as a unit conducting assessments around New Providence. Some data collections trips included high school students where each intern led a group of ten high school students in the data collection protocols. Interns were engaged in four components of the Hurricane Matthew Project. First, YME worked with students to document hurricane impacts in their neighborhoods and encourage students to share their hurricane experiences. Second, students worked with mentors from University of Miami to carry out coastal assessments in key locations around New Providence documenting coastal erosion, loss of vegetation, flooding and destruction of homes and buildings. Third, students participated in water quality sampling and learned about water quality and land-based sources of pollution to coastal water and what that means for the health of coral reefs and the impact that it can have on our economy. And fourth, students learned about mapping hurricane impacts along the coast and in the water. Data from the field were entered into Excel spreadsheets. Before sending the data to UM-CEL, the data were quality controlled by a scientist by reviewing the data to make sure that rankings were correctly assigned. The data was quality controlled an additional time by the UM-CEL lab. A digital survey tool was created to assess the interns experience during the Hurricane Matthew Project and to inform the development of future citizen science projects. The assessment tool looked at four different components of the Hurricane Matthew Project citizen science experience: 1) problems encountered during the project, 2) participants understanding of the project, 3) the training experience, and 4) attitudes about hurricane preparation and personal responsibility. Interns completed the survey upon completion of the Hurricane Matthew Project.

RESULTS

Problems

Before the Hurricane Matthew Project was completed, one of the five interns left because her stipend was not sufficient. Although some participants were satisfied with the pay, fifty percent said that they did not receive enough money. The problems that the interns highlighted were about the logistics of the data collection. The participants suggested that starting the project a few days or a week after the hurricane as opposed to waiting a few months would improve the data collection processes, especially when interviews were conducted. Participants were not extremely interested in the data entry component of the project and required direction and encouragement to enter the data. When the data were entered into the Excel spreadsheet, there were a number of errors. The errors were caught by the reviewing scientists and corrected before the data were submitted to the UM-CEL.

Perception

Participants said that their perspective on hurricane response had changed since their participation in the Hurricane Matthew Project. All participants said that they would be likely to participate in another citizen science project and were in agreement that Bahamians should be very involved in hurricane disaster assessments. Additionally, they were in agreement that there should absolutely be a similar project to the Hurricane Matthew Project after the next hurricane. Furthermore, when asked if mangroves and beach dunes can protect people's home and property from hurricanes, scores were '4' and '5', where '5' represented that

mangroves and dunes protected property and homes, and '1' represented that mangroves and dunes provided no protection.

About the project

When asked to describe the objectives of the Hurricane Matthew Project, all participants were able to articulate that the project was intended to assess the damage that Hurricane Matthew caused to New Providence Island and to identify the most negatively impacted areas. Additionally, interns mentioned that the study looked at the role that coastal development played on exacerbating the storm impact. All participants believed that the data collected were to be used to inform the government and to identify ways to prevent the scale of damage from occurring again. All participants agreed that the Hurricane Matthew Project was important and that they learned a lot through their participation in the project.

Training

Participants felt that the training was good. However, there was a difference in opinions about how helpful the training videos were at preparing interns to collect that data. Fifty percent of participants stated that the videos were not very helpful while the other fifty percent said that they were helpful. One of the participants stated that "a more hands-on training would have been preferred as the videos provided weren't beneficial and I couldn't remember most of the things [from the video]." When asked to provide other comments about the Hurricane Matthew Project, two participant responses were received. The first stated that, "The Hurricane Matthew Project was a great learning experience. A goal should be to get more young persons to participate in it as they will learn [more] about hurricanes [while participating] in the project than they will sitting down in a classroom reading books or watching videos." The second comment suggested that, "We should get the youth more involved in projects like these. Maybe communicate with schools to set up a school field trip whereas the students go out and conduct the study. Or maybe the University of The Bahamas students can take part in the study for extra credit."

DISCUSSION

The Hurricane Mathew project demonstrated how citizens and specifically youth can become actively engaged in disaster response and storm mitigation while developing critical life skills. There is a need for community stewardship programs that engage citizens in long-term biodiversity monitoring and ecosystem restoration. The methodology used in these monitoring programs should be adaptable to allow for post disaster assessments that serve as resources for planification and policy making. By engaging citizens in the Hurricane Matthew Project, we were expanding the role of hurricane response and mitigation to Bahamian citizens. One of the main objectives of the Hurricane Matthew Project was to use citizen scientists to collect information capable of informing data-driven policies.

Validating the data

A critical component of this citizen science project was the partnership with The University of Miami Coastal Ecology Lab. This allowed for the development of the training materials and protocol that the citizen scientists used. Although there is room to refine the citizen science training tools and data collection process, working directly with UM-CEL was a critical step to ensure quality of data. It was important to have the citizen scientist work closely with a scientist in the field. Additionally, the data entry quality control protocols were critical in addressing any human errors.

Socioeconomics of Citizen Science

The citizen scientists engaged in the Hurricane Matthew Project came from underserved and lower income communities. Unlike some citizen science projects such as EarthWatch, where

citizens pay an average of three thousand dollars to participate in a project (EarthWatch, 2017), the students participants in the Hurricane Matthew Project were participating in YME as an academic enrichment and extracurricular activity. The interns, participating in an internship received a small stipend. Unfortunately, the stipend offered by the Hurricane Mathew Project was not high enough to keep all the interns happy and one intern quit the project to take a job. The notion of an unpaid internship or stipend internship is not a sustainable model for long-term citizen science projects intended to inform policy, especially if the citizen scientists are from low income or underserved communities. There is, however, great potential to use citizen science projects as part of a structured youth development program for high school students while providing skills to youth from underserved communities. This can be mutually beneficially where the data they collect supports biodiversity monitoring and disaster response, and in exchange students are engaged in inspiring and fun activities.

Marine Citizenship

There is a need to develop the individual responsibility for disaster response management. Citizen science projects can play a role in this but must be coupled with a marine citizenship program that focuses on developing sustainable behavior. Marine citizenship is "the act of citizens taking greater personal responsibility for the oceans, as a policy channel to support the delivery of a healthy marine environment and to enhance marine governance" (McKinley and Fletcher, 2012). This builds on the existing model of citizenship, the central component of which is the relationship between an individual member of society and the state to which it belongs (McKinley and Fletcher, 2012, Purcell, 2003, Chamberlin, 1997). The conversation of marine citizenship expands the role of conservation and includes topics such as governance, democracy, accountability, social justice, personal responsibility, and the capacity to act (McKinley and Fletcher, 2012, Matti, 2006, Cruz, 2008, Donert, 2003). Marine citizenship transforms the role of conservation into an individual matter, because this is what needs to be done with disaster response management. A marine citizenship curriculum should be part of all disaster response citizen science projects.

Restructuring Young Marine Explorers

Over the past ten years, Young Marine Explorers has been addressing: 1) the lack of marine citizenship, 2) the poor educational output of youth in Bahamian Public Schools, and 3) the lack of professional and personal skills in Bahamian youth. These issues have been addressed by offering a three-year program for senior high school students that uses a marine citizenship curriculum that reinforces the Bahamian Ministry of Education learning objectives for math, biology, language arts, and geography, thus further preparing youth for their national exams. The marine citizenship curriculum fosters leadership and personal development and equips youth with the skills required to enter the workforce. As a result of the Hurricane Matthew Project, YME has added two additional issues to our agenda to address. The first is the lack of data for data-driven environmental decisions to be made. The second is the lack of capacity to gather large datasets about biodiversity and environmental disasters. To address these issues, we have redesigned our three-year curriculum so that it includes the aforementioned marine citizenship curriculum in addition to conducting citizen science projects that are designed to monitor biodiversity and conduct post-disaster assessments over long periods of time. The new YME program: 1) supports the personal development of young professionals and reinforces the importance that the ocean has in supporting Bahamian health and well-being; 2) develops environmental leaders who understand the function of Bahamian ecosystems and value the role of ecosystem services in supporting the Bahamian population; and 3) cultivates active citizens who understand the importance of and contribute to creating a sustainable Bahamas through their participation in citizen science projects.

The future for Young Marine Explores

The future plan for YME is to increase youth participation in long-term citizen science projects within The Bahamas. Citizen science programs have the capacity to drive conservation action through monitoring biodiversity, restoring ecosystems, assessing disasters, and contributing towards natural resource management. Young Marine Explorers has relocated our operations from New Providence to Cat Island, a remote Bahamian family island with a population of 1500. This move is reflective of our shift to focus on community-driven conservation and align our programs in support of achieving the United Nations's Sustainable Development Goals. We have identified eight UN Sustainable Development Goals that through our work, we are directly supporting. To truly achieve our environmental conservation objectives, we need to fully engage the local communities. Working within a smaller community like Cat Island will allow for us to better apply our methodology, engage all stake holders, and demonstrate the success of our model. YME will spend the next five years working in Cat Island implementing the YME marine citizenship curriculum within the two high schools on the island and implementing a long-term biodiversity monitoring citizen science project. The protocols adapted from the Hurricane Mathew Project will enable citizen scientists to be prepared to assess damages after the next hurricane. The five-year time frame will allow us to monitor trends in biodiversity, community engagement, and marine citizenship development.

CONCLUSIONS

The Bahamas and other Small Island Developing States (SIDS) do not have the luxury to only think about hurricanes during the hurricane season. Neglect and lack of preparation will cost money and resources needed to move SIDS foreward towards improving the lives of residents, measuring nation building against the UN 2030 agenda, and meeting the multilateral agreements that we are party to. Hurricanes and natural disasters could be the single largest threat to national development in the region. Partnerships are critical to collecting information and developing data-driven policies for coastal protection and management. Civic organisations like Young Marine Explorers have the capacity to mobilize large numbers of people to collect valuable information that can support plannification and policy making, while simultaneously developing marine citizenship. There is a need to replicate programs like Young Marine Explorers throughout the region in a proactive effort to prepare for hurricanes in advance through community mitigation and restoration projects that work in partnership with the government.

ACKNOWLEDGMENTS

The authors would like to thank the staff of the University of Miami Coastal Ecology Lab for their hard work and dedication to the Hurricane Matthew Project. Additionally, we would like to thank the Young Marine Explorers Citizen Scientists for their commitment to the project. Further thanks goes to the Government of The Bahamas for providing research permits and the Bahamas National Trust for providing permits for time spent in the National Park.

REFERENCES

Cashman, A., and Nagdee, M.R. 2017. Impacts of Climate Change on Settlements and Infrastructure in the Coastal and Marine Environments of Caribbean Small Island Developing States (SIDS). *Caribbean Marine Climate Change Report Card: Science Review 2017***:** 155-173.

Chamberlin, C. 1997. The practice of citizenship as support for deep ecology. *Canadian Social Studies* 31**:** 142-144.

Cruz, J. 2008. Dynamics of supply chain networks with corporate social responsibility through integrated environmental decision making.

European Jouranl of Operational Research 184**:** 1005-1031.

Donert, K. 2003. Aspects of European citizenship and environmental education through information and communications technology. First international conference on environemtnal reserach and assesment, 2003 Bucharest, Romania.

EARTHWATCH. 2017. Available: http://earthwatch.org/Expeditions/Expedition-Search [Accessed].

Landsea, C. 2017. *Atlantic Oceanogrphic and Meteorological Laboratory: Hurricane Research Division* [Online]. Available: http://www.aoml.noaa.gov/hrd/tcfaq/E11.html [Accessed December 8th 2017].

Matti, S. 2006. *The imagined environmnetal citizen: exploring the state- individual relationship in Swedish environmental policy.* Lulea University of Technology.

McKinley, E. and Fletcher, S. 2012. Improving marine environmental health through marine citizenship: A call for debate. *Marine Policy* 36**:** 839-843.

Purcell, M. 2003. Citizneship and the right to the global city; reimagining the capitalist world order. *International Journalof Urban and Regional Research* 27: 546-590.

Sullivan Sealey, K.L. 2017. Hurricane Matthew Project Final Report. Coastal Ecology Laboratory: unpublished, University of Miami Florida, USA.

NATURAL HISTORY CHARACTERISTICS OF *SYNAPTULA HYDRIFORMIS,* AN APODID SEA CUCUMBER FROM OYSTER POND, SAN SALVADOR ISLAND, THE BAHAMAS

Eric S. Cole, Leigh Anne Hahn, Jessica Choquette, and Miranda Thacker
Biology Department, St. Olaf College
Northfield, MN 55057

ABSTRACT

Synaptula hydriformis (Echinodermata, Holothuroidea, Apodida, Synaptidae: Lesueur, 1824) is a small, hermaphroditic sea cucumber commonly found creeping over the benthic pearl oyster communities in Oyster Pond, San Salvador Island, The Bahamas. Unusual features include possession of an ovo-testis; internal self-fertilization; embryonic brooding accompanied by matrophagy (juveniles feed on their mother's coleomic cells and tissues); and viviparous, live-birth of juveniles with adult characteristics. Through live-culture and paraffin histology, life history stages were characterized. The ovo-testis was found to contain both sperm and eggs supporting its characterization as a simultaneous hermaphrodite. Three unique color morphs were described: solid brown, brown striped, and translucent. In living transparent specimens, we are able to observe juveniles ambulating and feeding within the mother's body cavity. Autogamy (self-fertilization) and vivipary (live-birth) mark the synaptid family as unusual among sea cucumbers. Other families of sea cucumber tend to release gametes into the water column where they undergo external fertilization and develop into free-swimming planktonic larvae. We developed a method for inducing both synchronous spawning and birthing. Subsequently, a successful technique for culturing juvenile sea cucumbers was established. Developmental stages were characterized for the larvae. We found evidence for direct development, bypassing both auricularia and doliolarian stages and skipping the metamorphosis typical of other holothuroideans. We discuss *Synaptula* in the context of other hermaphroditic organisms that seem well-adapted for colonizing the island's inland, anchialine pond communities.

INTRODUCTION

While investigating invertebrate communities in the anchialine ponds of San Salvador Island in The Bahamas, we frequently encountered a small, "naked sea cucumber" identified as *Synaptula hydriformis* living in Oyster Pond. These soft-bodied echinoderms bear little resemblance to other, hard-bodied members of the phylum, (sea stars, brittle stars, and urchins) and have adapted a life style that seems to have converged with that of small benthic worms. At first viewed as a nuisance (they clung to wetsuits and booties with minute, hook-like ossicles embedded in their gelatinous skins), we soon became fascinated by their natural history and set out to investigate (and manipulate) their reproductive life cycle.

Synaptula hydriformis was first described by the accomplished French naturalist Charles-Alexandre Lesueur in 1824 during his association with William Maclure and Robert Owen, the remarkable founders of an intellectual commune established in New Harmony, Indiana. Lesueur first encountered *Synaptula hydriformis* on an expedition he made with William Maclure in the winter of 1815-1816 to the West Indies, in a rich mangrove community on the north side of the island of Guadeloupe. The species has been referred to by many different names, including *Holuthuria hydriformis, Holuthuria viridis, Synaptula vivipara, Synapta viridis, Synapta pourtalesii, Leptosynapta hydriformis, Leptosynapta pourtalesii, Heterosynapta viridis, Synapta vivipara, Synapta picta,* and *Chondrocloea vivipara* (Heding, 1928).

The second significant mention of *Synaptula hydriformis* involves a specimen collected by the U.S. Fish Commission on an expedition to The Bahamas in 1886 from the very first ship ever designed specifically for marine research, the *USS Albatross*. While exploring San Salvador Island (formerly Watling's Island), the *Albatross* obtained a second specimen of this sea cucumber. This was stored in the Smithsonian Museum, and later identified as *Synaptula hydriformis* (Lesueur 1824) when Hubert Clark uncovered it in the 1900s. Clark performed extensive (beautifully illustrated) research on this self-fertilizing, internally brooding species and wrote prolifically of its physiology, taxonomy, and embryology (Clark, 1897, 1907).
The Smithsonian obtained a more recent sample from The Bahamas in 1996, collected by Charlene D. Long (American Natural History Museum). The most-studied specimens were collected from Bermuda, Panama, Jamaica, and the Florida Keys. Since Clark's impressive monograph, there are only modest references to the species until Jennifer Frick (Smithsonian Marine Station, Fort Piece, FL) took up the study of their ovo-testis and matrophagy (or matrotrophy: feeding on, or deriving nourishment from ones' mother) in the late 1990s for her Ph.D. Frick collected specimens from Indian River Lagoon and Lake Surprise on Key Largo (Frick et al., 1996; Frick, 1998).

Synaptids are interesting from a variety of perspectives. Unlike most other sea cucumbers, the apodid species lack tube feet for motility. They adhere to the substrate through surprisingly clingy dermal hooks called ossicles and ambulate using their feeding tentacles to pull themselves along, while feeding on the substrate. As self-fertilizing hermaphrodites, they are well-adapted for colonizing novel habitats. A single specimen could theoretically establish an entire population without a mating partner. This has implications for genetic diversity. It is possible that the entire population within our field site is comprised of only a few genetic "clones". The life-style of embryonic brooding and matrophagy is also interesting. If laboratory cultures of the transparent adults can be established, and experimental triggers for fertilization and parturition developed, this organism offers promise as a novel model organism for the study of invertebrate (echinoderm) embryology. Their ability to undergo live-birth also provides an intriguing novelty rarely seen outside of the chordate phylum: a mechanism by which juveniles living within the mesoderm-lined coelomic space of their mothers are shunted to the animal's posterior, expressed into the outside world within a mesoderm/ectoderm "birthing sac", and released through a developmentally programmed (reversible?) rupture of that sac during birth. It seems likely that juveniles from multiple, asynchronous reproductive cohorts are delivered (exhibiting "superfetation") as evidenced by varying sizes and states of development of the progeny expressed at the time of birth from a single individual. It would be interesting to learn whether or not larval forms can be sorted and retained when older juveniles are birthed, or if they too are discharged without regard to their developmental maturity.

METHODS

Collection and laboratory culture of *Synaptula hydriformis*

Specimens were collected by hand while snorkeling over beds of scaly pearl oysters in Oyster Pond, San Salvador Island, The Bahamas. It is perhaps worth noting, that synaptids insinuate themselves deeply into the internal spaces of calcareous-algal aggregates that form biotic outcrops which also house a variety of bivalves and living sponge. It is often, unfortunately necessary to open such outcrops in order to extract living specimens. We would endorse an attitude of respectful prudence when it is necessary or desirable to collect living specimens. Individual specimens were isolated and maintained in finger bowls with seawater, and fed small droppers-full of sedimentary floc collected from Oyster Pond (a loose bottom sediment rich in microbial material that the *Synaptula* appear to feed on). Floc was maintained under full-spectrum lights to promote algal growth.

Induction of birthing and spawning

Adult *Synaptula* were placed in 90 mm petri dishes half-filled with seawater and floated on an ice-water bath for ten minutes. These gave birth within 6-18 hours (exhibiting a lot of individual variation). Juveniles of numerous developmental stages from a single adult were observed, confirming "superfetation" (multiple broods maintained within the same adult). We also used this cold-shock treatment to induce ovulation and internal spawning, which we confirmed by subsequently decapitating and expressing the coelomic contents onto a microscope slide. By doing this at various times after the cold shock, successive developmental of stages were recovered. It is not clear that this was a highly efficient method for obtaining larval stages, and we recently learned that Frick employed a light/dark transition to induce spawning. She held them in continuous illumination and then exposed them to darkness for approximately one hour. She then returned them to light, and egg release began within 5 minutes (Fricke et al., 1996).

Photography

Live images were taken with hand-held iPhones, focused through the microscope ocular lens, or deployed as makeshift macro-lens cameras. In one case the live image was taken with an Olympus BH40 microscope using bright field optics and a DP-71 digital camera. Fixed histological specimens were examined using the Olympus BH40 microscope.

Paraffin Histology

Sea cucumbers were collected in January 2017. Specimens were fixed in Bouin's fixative, dehydrated, and embedded in paraffin as described by Humason (1979). Eight to nine micron-thick sections were made and slices were stained in Gomori's trichrome stain (Fisher Scientific Inc.). Slides were examined using an Olympus BH40 microscope using brightfield optics. Images were taken with a DP-71 digital camera.

RESULTS

Synaptula hydriformis color morphs

Three distinct color morphs were identified from Oyster Pond on San Salvador Island in The Bahamas: a solid brown, a "tiger-striped" form, and a pale white or translucent (colorless) variety (Figure 1). The relative abundances of the various color morphs from a sample of 329 specimens were 108 brown, 118 striped, and 103 translucent.

Figure 1: Three color morphs of Synpatula hydriformis: brown (left), striped (center), and translucent (right). Note, individuals are typically ~5 cm long.

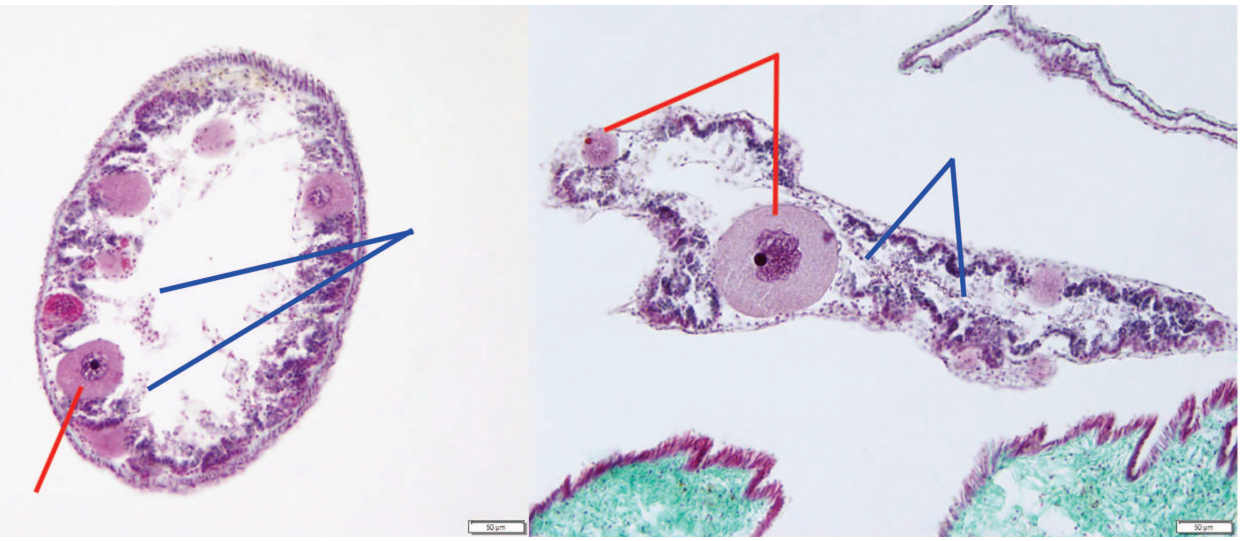

Figure 2: Paraffin histology, and Gomori's triple-stain sections of Synaptula ovo-testis. Red lines point to developing oocytes. Blue lines point to bundles of developing sperm cells. Scale bars = 50 um.

Histological observations of the gonad

Synaptula specimens were fixed, embedded in wax, sectioned, and stained using Gomori's tri-chrome. Examples appear in Figure 2. We could readily discern both developing sperm bundles and maturing oocytes within the same gonad, confirming this organ as an "ovo-testis".

Live observations of vivipary and matrotrophy

Translucent specimens allowed us to observe live juveniles ambulating and feeding within the parent's body cavity (Figure 3). Juveniles were fully formed and exhibited the classic holothurian "feed-walking" behavior in which they use their sticky, para-oral tentacles to both pull themselves along the substrate (in this case, their parent's body cavity) and feed. After drawing themselves forward, each tentacle is inserted into the oral cavity, and adherent food/substrate is "wiped off" by action of an oral sphincter as the tentacle is retrieved for its next step. Given the variety of sizes of juveniles, from 200 microns up to nearly 1 cm, it was clear that the juveniles were indeed growing within the parent's body cavity, deriving nourishment from their parental host (coelomocytes and possibly undeveloped eggs, Frick, 1998).

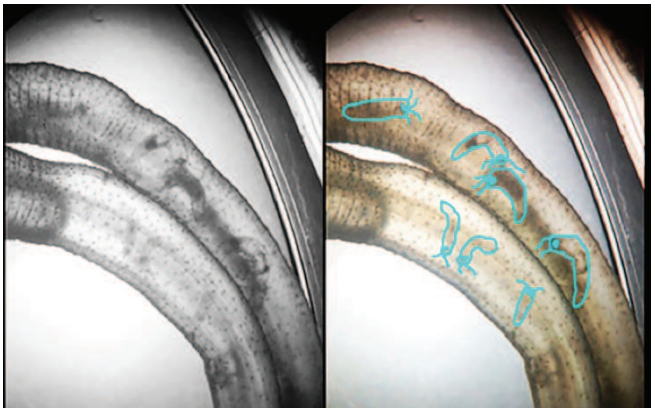

Figure 3: Translucent bodies of Synaptula hydriformis under low magnification microscopy. The left image is un-retouched. The right image highlights the outlines of juveniles in blue.

Parturition

Adult specimens were isolated into 90 mm petri dishes half-full of seawater. Individual dishes were floated on an ice-slurry for ten minutes and restored to room temperature (76° F). Within 6-18 hours, multiple juveniles were expressed from the

posterior cloaca of the adults. The process of birthing (at least by this artificial induction) appears to involve eversion of a membrane sack from the cloaca (Figure 4) that gradually fills with juveniles.

Figure 4: Five juveniles have been expressed into the birthing sac. Arrow indicates cloaca.

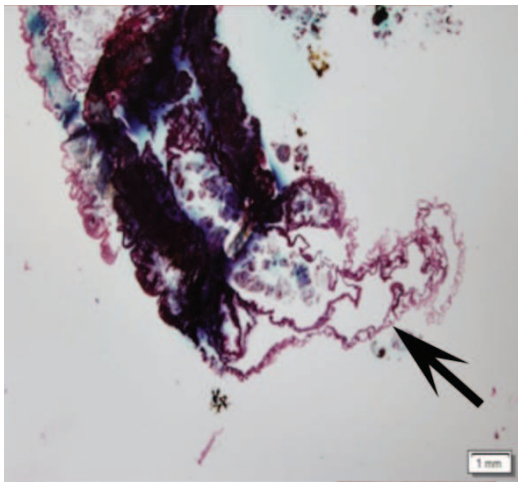

Figure 5: Complex double-membrane of birthing sac emerging from adult's cloaca (paraffin histology).

The membrane sack appears to be comprised of two membranes (Figure 5). We suspect that these twin membranes represent mesoderm and endoderm, respectively, as juveniles that are living inside a mesodermally-lined coleomic space are separated from the outside world by both the coelomic lining and either ectoderm or endoderm near the cloacal opening. Eversion of this dual-membrane "birthing sac" is an extraordinary event. At some point, an oval aperture appeared in the sac, through which juveniles were expressed into the seawater medium. Juveniles expressed in this manner have been kept alive on Oyster Pond floc culture for up to 52 days (Figure 6). It should be noted that cold-shock induced birthing (especially appearance of the "birthing sac") may differ from birth that occurs in nature. A "natural birth" video by Alvaro Migotto (2017) from the University of Sao Paulo shows juveniles (and embryos) being expelled from the cloaca directly.

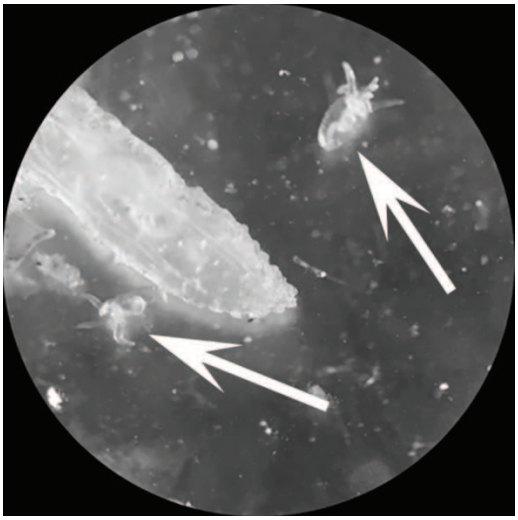

Figure 6: Two juveniles freshly born by cold-shock induced parturition. Image shows posterior of intact adult and two minute, live juveniles approximately 1-2 mm in length (arrows).

Superfetation

Cross-section histology revealed embryos and juveniles of conspicuously different reproductive cohorts within a common coelom. This suggests that multiple rounds of ovulation and self-fertilization can occur on a rolling schedule without intervening births—a process known as superfetation (Figures 7 and 8).

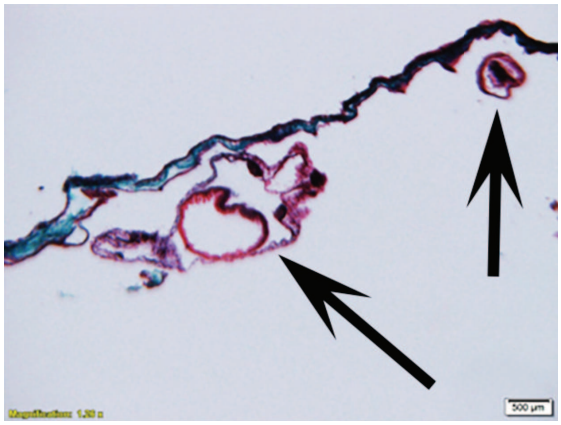

Figure 7: An embryo (upper right) and a much larger juvenile (middle) within a single coelomic space.

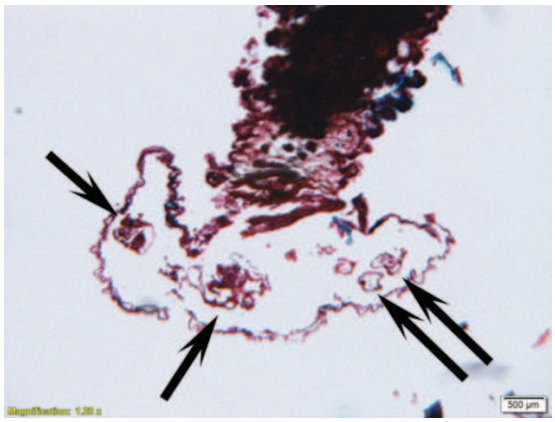

Figure 8. Four (or more) embryos and juveniles of different sizes (ages?) being expressed during parturition (arrows).

Induction of ovulation, self-fertilization, and embryogenesis

To avoid multiple environmental shocks accompanying collection and transport before lab work, and the consequent confusion of timing, we treated isolated adult *Synaptula* to an ice-shock in the field at the time of capture. Back in the lab, at various times after this initial shock, *Synaptula* adults were decapitated and coelomic fluids expressed by squeezing. In this way, juveniles (variable ages) and embryos from a variety of stages more tightly correlated with time of induction were obtained and photographed, resulting in a near complete gallery of developmental stages (Figure 9). In one specimen, 75 juveniles were found inside the adult body cavity. Although this technique of inducing gamete release and fertilization appeared to work, the frequency of early (presumably "induced") embryos produced seemed low. Since then, we have learned that Fricke deployed a light/dark entrainment to induce ovulation, triggered by a "lights-on" signal (Fricke et al., 1996).

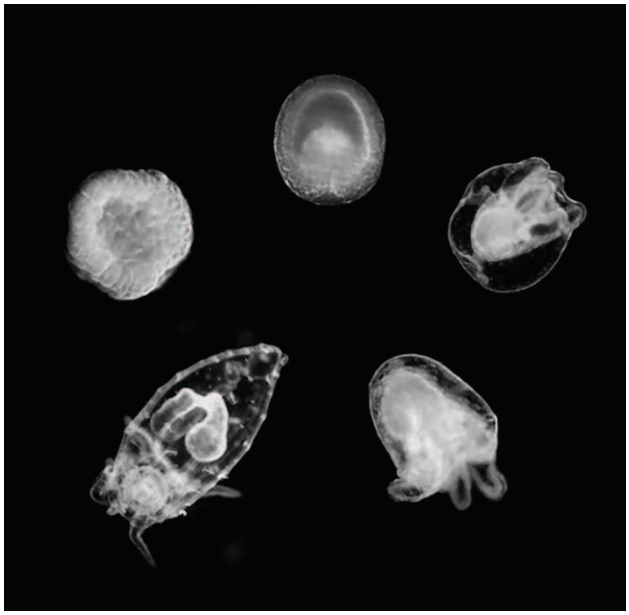

Figure 9: Embryos at various stages of development surgically expressed from shocked adults. Stages represent (beginning at center-left and traveling clockwise): (1) blastula, (2) gastrula, (3) complete juvenile with 5 tentacle buds, (4) tentacle elongation, and (5) appearance of ossicles (tiny endoskeletal hooks in the outer skin). Timing for stages: blastula: 3 hrs; gastrula: 6.5 hrs; tentacle buds: 12 hrs; ossicles: 24 hrs, post-fertilization.

DISCUSSION AND CONCLUSIONS

Synaptula hydriformis exhibit a broad repertoire of fascinating reproductive habits including simultaneous hermaphroditism, internal self-fertilization (they exhibit almost a clonal

form of propagation), direct development from gastrula to the adult body form without the intervening metamorphosis seen in most echinoderm larvae, matrotrophy (feeding on maternal cells or products), superfetation (brooding multiple cohorts of young from independent spawning events), and live birth. If nothing else, this study promises to expand our vocabularies. Our findings largely confirm earlier discoveries from the elegant works of both Clark (1897, 1907, 1933), Frick (1998) and Frick et al. (1992, 1996). Regarding matrophagy (or matrotrophy), a recent review by Ostrovsky et al. (2016) suggests that matrophagy has actually arisen five times independently within the holothuroidea, including the clade that encompasses both *Synaptula* and *Chiridota* (a second, less common apodid cucumber also found in Oyster Pond).

Since little other work exists on the species, it is nice to refresh these observations for a new generation of naturalists. The things that we may have contributed uniquely to this body of work on *Synaptula hydriformis* include the development of an ice-shock technique for inducing parturition, a photo-microscopic gallery of embryonic stages, and images of the remarkable "birthing sac" observed in our laboratory-induced cultures.

The discovery of a translucent morph of *Synaptulid* sea cucumbers, along with their direct pattern of development, raises the possibility of recruiting this species as a new model organism for the study of invertebrate embryology. Its pattern of self-fertilization also raises interesting questions about the genetic diversity of our population and highlights its ability to colonize. This is interesting in that several organisms from the inland ponds appear to exhibit hermaphroditic (or even parthenogenetic) life history patterns pre-adapting them for colonization. These include the scaly pearl oyster (*Pinctada longisquamosa*: a sequential hermaphrodite), most of the gastropods, and the mangrove killifish, *Rivulus marmoratus* (a self-fertilizing hermaphrodite we found in Mermaid Pond and another of the interior ponds). It would be interesting to explore whether these isolated anchialine pond environments are unusually rich in self-fertilizing species, reflecting their potentially rare episodes of colonization.

ACKNOWLEDGEMENTS

This work was conducted in The Bahamas under a permit granted by The Bahamas Environment, Science, and Technology (BEST) Commission. We would like to thank Dr. Troy Dexter, Executive Director of the Gerace Research Centre, San Salvador, The Bahamas for his unfailing technical support and encouragement. St. Olaf College provided travel support, and we are grateful for field assistance from a number of St. Olaf undergraduates including: Mark Li, Anthony Riesen, Tiffany Wong, Xiaoping Zhang, and Adrian Ripecky

LITERATURE CITED

Clark, H.L. 1897. *Synapta vivipara*: A contribution to the morphology of echinoderms. Memoirs of the Boston Society of Natural History V(2): 53-93.

Clark, H.L. 1907. The *Apodus holothurians*: A monograph of the Synaptidae and Molpadiidae. Smithsonian Contributions to Knowledge 35: 42-131.

Clark, H.L. 1933. Scientific survey of Porto Rico and the Virgin Islands. New York Academy of Sciences XVI.

Frick, J.E. 1998. Evidence of matrophagy in the Viviparous Holothuroid echinoderm *Synaptula hydriformis*. *Invertebrate Biology* 117(2): 169-179.

Frick, J.E., Ruppert, E.E., and Wourms, J.P. 1996. Morphology of the ovotestis of *Synaptula hydriformis* (Holothuroidea, Apoda): An evolutionary model of oogenesis and the origin of egg polarity in echinoderms. *Invertebrate Biology* 115(1): 46-66.

Frick, J., Ruppert, E.E., and Wourms, J.P. 1992. Nutrition of brooded young in a sea cucumber (*Synaptula hydriformis*). *American Zoologist* 32:113A.

Heding, S.G. 1928. Papers from Dr. Th. Mortensen's Pacific Expedition (1914-16). Smithsonian Libraries. 154-203.

Humason, G.L. 1979. *Animal Tissue Techniques.* W.H. Freeman and Company, San Francisco.

Migotti, A. 2017. A pregnant sea cucumber giving birth. YouTube video. https://www.youtube.com/watch?v=Pz_O1rT1QVE.

Ostrovsky, A.N., Lidgard, S., Gordon, D.P., Schwaha, T., Genikhovich, G., and Ereskovsky, A.V. 2016. Matrotrophy and placentation in invertebrates: a new paradigm. *Biological Reviews* 91: 673–711. doi:10.1111/brv.12189

SPELEOTHEM DEPOSITION IN EOGENETIC CARBONATES: THE CONSEQUENCES FOR STRONTIUM

Nicole Ridlen[1], John E. Mylroie[1], Jason Polk[2], and Joan R. Mylroie[1]

[1]Department of Geosciences, Mississippi State University,
Mississippi State, MS 39762

[2]Department of Geography and Geology, Western Kentucky University,
Bowling Green, KY 42101

ABSTRACT

Eogenetic carbonate rocks develop from allochems precipitated primarily as aragonite (e.g. green algae, mollusks, corals) and high-Mg calcite. (e.g. echinoderms, red algae). Relative to calcite, strontium (Sr) preferentially enters the orthorhombic aragonite crystal lattice, giving eogenetic carbonate rocks a higher Sr background than older teleogenetic rocks, in which the aragonite has inverted to calcite. Vadose speleothems (stalagmites) forming in caves in eogenetic carbonate rock should show a high Sr content. The Sr levels in the speleothems should decrease with rock age as the aragonite inverts and the Sr is lost. Climate can also affect aragonite inversion, with wetter climates leading to more rapid inversion. Strontium levels in speleothems have been used as a paleoclimate indicator, but the influence of eogenetic Sr has been under appreciated. This issue has become more important as oceanic island caves and speleothems hosted in eogenetic carbonates have recently been utilized as mid-ocean paleoclimate indicators.

Curacao, in the southern Caribbean, contains a series of tectonically uplifted reef terraces of eogenetic carbonate rock. These carbonate rocks contain flank margin caves in which speleothem growth is active. Surface samples and speleothems from each terrace show a progressive loss of Sr in each higher, and therefore older, terrace. The "Higher Terrace," older mid-Pleistocene age surface rock, is calcitic, less than 5% aragonite, with 0.44 ppm Sr; one speleothem from a cave in this rock contained 0.25 ppm Sr. The "Middle Terrace," younger mid-Pleistocene surface rock, is also calcitic, less than 5% aragonite, with 1.43 ppm Sr; two cave speleothems had Sr values of 0.30 and 0.31 ppm. The "Lower Terrace" surface rock, late Pleistocene in age, was 40% aragonite and 60% calcite, with a Sr value of 6.89 ppm; two cave speleothems had Sr values of 8.68 and 8.28 ppm. Utilizing caves from a single location removes any climatic differences in calcite inversion and speleothem deposition, leaving rock age as the major factor in the Sr variation in these speleothems. In The Bahamas, collection was done along a climatic gradient of decreasing rainfall, NW to SE, but the inability to accurately determine host rock age made the results here equivocal.

INTRODUCTION

The presence of strontium (Sr) in carbonate rocks has long been documented (Kulp et al., 1962) and has been recognized as a contributor to the trace element content of speleothems used for paleoclimate reconstruction (e.g. Goede et al., 1998). Strontium in speleothems can originate from multiple sources although for the majority of current research, the Sr is assumed to be infiltrated from a surface source (e.g. Roberts et al., 1998; Finch et al., 2003; White, 2004; van Beynen et al., 2008; Sinclair et al., 2012). In younger, eogenetic carbonates, the mineralogy is aragonite and the aragonite crystal structure accommodates Sr in replacement of Ca (White, 2004; Hill and Forti,

1997). Over time, aragonitic carbonate rocks will invert to the more stable polymorph mineral of calcite (Hill and Forti, 1997). This inversion releases Sr to the vadose zone, as the Sr cannot be accommodated in the calcite crystal lattice of the host rock.

The carbonate host rocks that are mineralogically aragonite will naturally have a greater Sr content than those rocks that are calcite. The older eogenetic rock units of the Caribbean typically have a higher calcite to aragonite ratio than those that are younger (Gaffey et al., 1995). It can then be surmised that younger carbonates in the Caribbean should have a greater amount of Sr contribution from the host rock into those speleothems than speleothems that form in older carbonates that are inverted to calcite. While Sr does not fit easily into the calcite crystal lattice, it can be incorporated into the growth bands on the growing stalagmite to leave a record of the dripwater geochemistry.

Uplifted island carbonates, such as the carbonate units in the study area of Curaçao in the Netherlands Antilles (Figure 1A and 1B), are often terraced; where the oldest unit is at higher elevations and the youngest at lower elevations (Schellmann et al., 2004). These units are composed of coral reef carbonates that were originally composed of aragonite (Schellmann et al., 2004). The inversion of aragonite to calcite is not only time dependent, but is also dependent on the flux of meteoric water through the limestone and thus a climatic signature. Abaco Island in The Bahamas is the wettest island in the Bahamian archipelago (Figure 1C); Long Island and San Salvador, The Bahamas are two of the drier islands in the archipelago, having negative water budgets (Sealey, 1990). However, the islands are assumed to have carbonates of the same approximate age, so any difference in aragonite inversion degree should be a climatic signal as opposed to an age signal as for the island of Curaçao. This interpretation also assumes past climates are similar to those seen today.

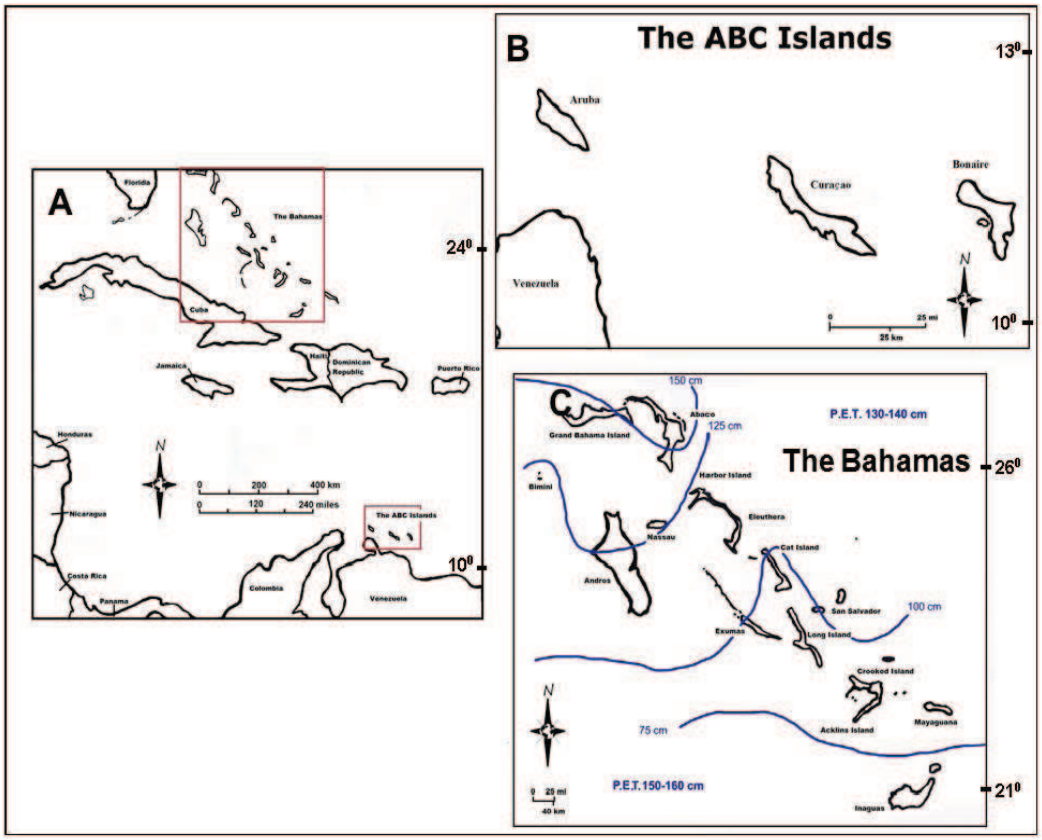

Figure 1: A. Caribbean and North Atlantic locations of the study sites. B. Curaçao is the middle of the three ABC Islands. C. Abaco, San Salvador, and Long Island trend across a climatic gradient (modified from Whitaker and Smart, 1997).

Speleothem research has become an integral part of paleoclimate reconstruction because cave deposits preserve the conditions that were present at the time of speleothem deposition. As cited earlier, most speleothem research seeks to interpret the local Earth surface conditions at the time of deposition, such as temperature, rainfall, vegetation. However, the state of the host rock itself can also be preserved in the speleothem record.

The research presented here sought to answer three questions: 1) does the Sr content of Caribbean speleothems have a direct relationship with the age of the host rock at the time of current speleothem precipitation? 2) do speleothems from older host rock contain less Sr than speleothems from younger host rock in the same climatic setting? and, 3) will speleothems record the change in Sr concentration of eogenetic carbonates as a faster depletion in climates of higher precipitation as opposed to drier climates?

Traditional work on speleothems has been concentrated on those located in much older geologic settings where the limestones are all calcite and Sr is more likely to be an infiltrate from an external source. The work on speleothems in younger, Sr-enriched host rocks will need to consider the possibly significant amount of host-rock sourced Sr within the speleothem record. This could affect the interpretations of paleoclimatic data from the use of speleothems in young carbonates. By determining the correlation of host-rock age with strontium concentration in the speleothem in contrast with the variation of strontium in differing climatic settings, a calibration could be developed to better interpret earlier paleoclimatic studies in young carbonates.

Recently, speleothem research has been shifting to oceanic islands to obtain speleothem climate records in mid-ocean areas not available on continents (e.g. Sinclair et al., 2012). The rocks hosting the speleothem-containing caves are commonly young and aragonitic, so the research for this project is timely and important. The work described here is preliminary. Other elements, such as Mg, were measured, but that work is still in progress. No age dating of sampled stalagmites is yet available, so time constraints remain unknown. Future work plans to complete a more robust data set and provide better interpretations using additional trace elements and age constraints.

METHODS

Fieldwork on the island of Curaçao took place in December, 2012, while the fieldwork on the islands of Abaco, Long Island, and San Salvador took place in June, 2013. Prior fieldwork on Curaçao conducted by Kambesis et al. (2015) and Sumrall et al. (2016) provided information on caves in these field areas that allowed for planning of sample collection. Due to the delicate nature of collecting and exporting cave samples, permission for six stalagmites (two each from three caves in each of the terrace levels) was obtained from the Carmabi Foundation for Curaçao which is equivalent to their national park service. In addition, permission for collecting multiple stalagmites from caves on Abaco Island, San Salvador Island, and Long Island was obtained from the Bahamas Environment, Science and Technology (BEST) Commission.

The Curaçao caves identified for collection were Lardem Cave in the Upper Pleistocene (MIS 5e) lower terrace; Raton Cave in the middle terrace of mid-Pleistocene age; and Hato Cave within the older and uppermost high terrace, also of mid-Pleistocene age. These caves are all flank margin caves that developed in the freshwater lens (Mylroie and Mylroie, 2007; Kambesis et al., 2015). For each terrace, the time window of speleogenesis was restricted to when the terrace was elevated and exposed to allow meteoric catchment to create a freshwater lens, but before the terrace was further uplifted and the freshwater lens was left behind. The stalagmites were carefully selected as the most optimum specimens within the caves (Figure 2A) and with growing apical tips (Frappier, 2008). They were collected from deep within the caves identified as primary candidates for this study to ensure humidity was high and airflow was

minimal. Rock samples were collected from within the caves close to the speleothem sample sites. For comparison purposes, rock samples were also taken from exposed rock surfaces above each cave. All speleothem and rock samples from within the caves were collected from hidden locations to preserve the caves' internal appearance and aesthetics.

The Bahamian Archipelago is dominated by eolian calcarenites with subtidal deposits from the last interglacial (MIS 5e, ~120 ka) exposed occasionally at elevations below 6 m (Carew and Mylroie, 1995). The specimens from The Bahamas were collected from three islands that are located in areas that have differing water budgets measured by the balance between precipitation and evaporation (Figure 1C). Abaco, the northernmost island in the study area, has a positive water budget with the highest annual precipitation rate of the three islands. Long Island has a negative water budget with the least amount of annual precipitation. San Salvador has a negative water budget and annual precipitation that falls between values at Ababo and Long Island. The two caves that were identified as prime candidates for collection on Long Island are Salt Pond Cave and Hamilton Cave. Hole in the Wall Cave and Roadside Cave from the southern end of Abaco were sampled. And Lighthouse Cave was the San Salvador Island sample site.

All rock samples were carefully cut into blanks for the creation of thin sections (Figure 2B and 2C). The rock blanks were each cut with a wet saw with a diamond tipped blade manufactured for the purpose of cutting tile and stone. They were cut to specifications set by Spectrum Petrographics—the company chosen to create the thin sections. Each blank was notched with the wet saw to preserve the upright direction previously marked on the samples in the field. Rock samples from Curaçao were analyzed for composition using laser ablation and ICP-Mass Spectometry at the Rensselaer Polytechnic Institute. The Bahamas rock samples, as well as additional samples of the Curaçao rocks, were prepared in powder form and analyzed using the ICP-Optical Emission Spectrometer at Western Kentucky University. The preparation of the stalagmites was conducted at Western Kentucky University. Stalagmites were cut in half parallel to the growth axis, perpendicular to the growth layers. They were then evaluated for feasibility of study. Analyses, interpretation, and data appendices of all samples for this study can be found in Ridlen (2014).

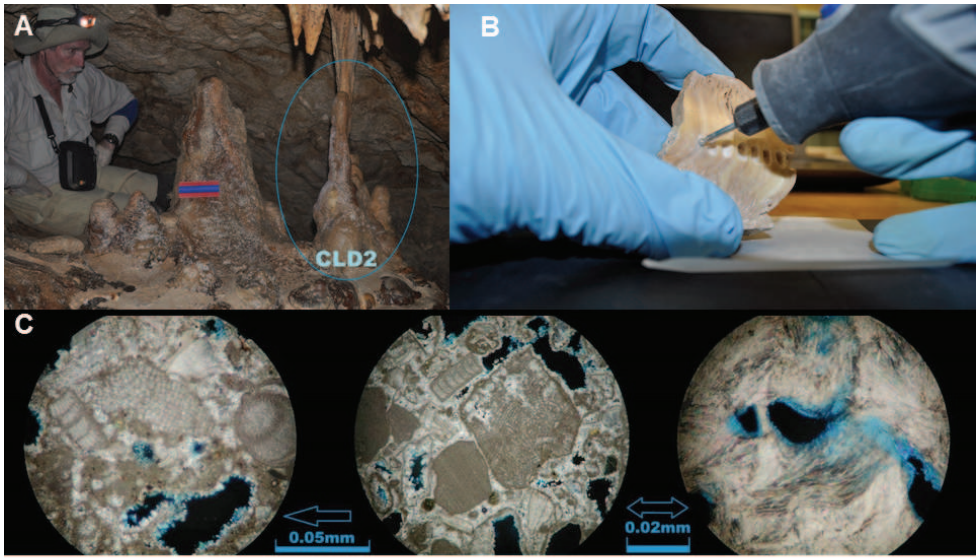

Figure 2: A. Collection site for sample CLD2 in Lardem Cave, Curaçao. Each sample site has a before and after image taken. B. Collection of powder sample every 0.5 cm from a stalagmite for analysis. C. Lardem thin sections. From left to right: cave wall rock, cave ceiling rock, and surface rock. Note the two thin sections on the right have a different scale from the thin section on the left.

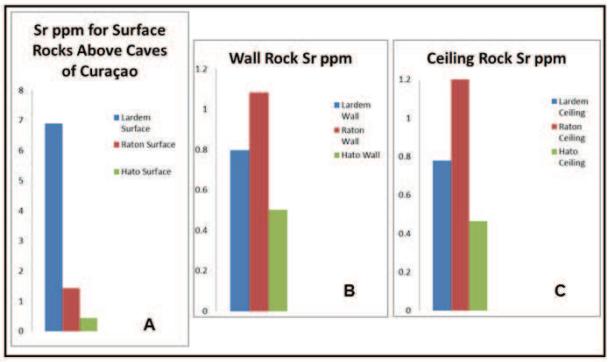

Figure 3. Results of strontium concentrations from rocks on Curaçao. A) Surface rocks, showing loss of Sr with increasing rock age, from youngest (Lardem) to oldest (Hato). B) Rock samples from cave wall rock, and C) Rock samples from ceiling rock within the caves, proximal to stalagmite collection sites. Lardem and Hato Cave follow the expected Sr trend, but Raton Cave is high, perhaps as a result of secondary speleothem aragonite which may have enriched Sr.

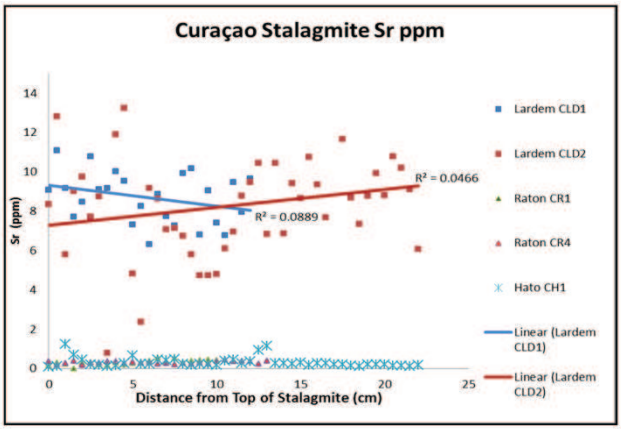

Figure 4. Stalagmite strontium concentrations, showing high levels in Lardem Cave but low levels in both Raton and Hato Caves on Curaçao.

RESULTS

Curaçao

Rock samples from within the lower terrace of Curaçao contained well-preserved fossils from inside the Lardem Cave (Figure 2C), whereas the rock specimen collected from the surface was highly altered by surficial weathering processes. In both cases, crystals growing into the pores of the rock from all directions indicated vadose conditions during subsequent post-deposition emergent crystallization. The caves in the higher terraces (middle and upper terraces) had progressively less well preserved fossils and altered pore spaces. The rock samples from within Raton Cave in the middle terrace revealed predominantly broken fossil pieces. The surface rocks showed lower Sr concentrations in the high terrace compared to the lower terrace; however, rock samples from within the cave tell a different geochemical story (Figure 3). Hato rocks seem overall depleted of Sr in comparison to the younger Raton and Lardem rocks. The Lardem cave rock samples, both wall and ceiling, seem to be overall lower in Sr concentrations than Raton.

The levels of Sr in the stalagmites from the Lardem Cave, located in the youngest eogenetic carbonate of this study, were notably higher than the Sr of Raton or Hato caves (Figure 4). The stalagmites in Raton and Hato caves were close to the same with very low Sr values (Figure 4). These data disagree with the high host rock values of Sr for Raton Cave, which suggests that the stalagmite-producing drip water comes from a surface rock source, and if secondary speleothem aragonite is present, it is not contributing to the drip water.

The majority of the stalagmites from Curaçao show a variation of Sr and Mg concentrations (Figure 5) progressing down the axis (from young apical to older basal material). The co-varying Sr and Mg concentrations are a topic of current research. The overall time span of stalagmite growth is not constrained, the degree of internal variation of Sr and Mg cannot be assumed to be a long-term trend. The data summary for Curaçao is shown in Figure 6.

The Bahamas

The increased meteoric water flux (Figure 1C) of the farthest north study area on Abaco island should deplete the speleothem Sr levels faster than

Long Island located in the southernmost part of the Bahamian study area. The concern for this part of the study was an accurate age for the host rock.

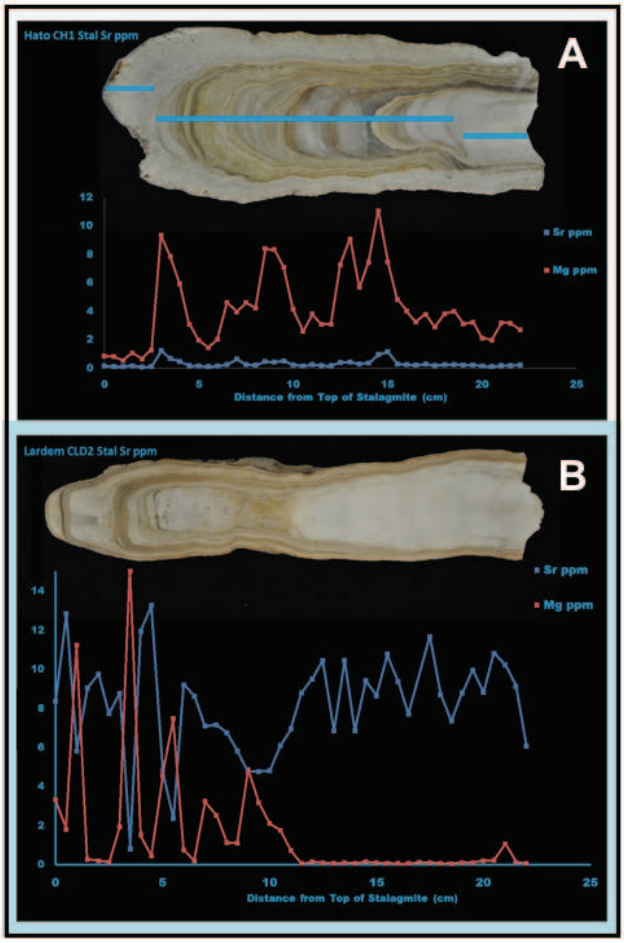

Figure 5. The Mg and Sr concentration from the stalagmites of Curaçao. A) Stalagmite (CH1) from Hato Cave in the oldest, highest terrace; Mg and Sr appear correlated. B) Stalagmite (CLD2) from Lardem Cave in the youngest, lowest terrace; Mg and Sr appear anti-correlated. Without age constraints, short-term variation in Sr and Mg cannot be separated from long-term trends.

The Bahamian Sr data for the stalagmites are variable (Figure 7). The stalagmite from Lighhouse Cave on San Salvador (SL4) had very high Sr concentrations in comparison to the stalagmites from Abaco from Hole in the Wall Cave (AH1) and Roadside Cave (AR1). The samples closest to the top of the SL4 stalagmite were likely to be contaminated by the tidal influx of modern seawater in Lighthouse Cave. The Sr content of the stalagmite from Hamilton Cave on Long Island (LH1) had the lowest Sr content of all the Bahamian stalagmites.

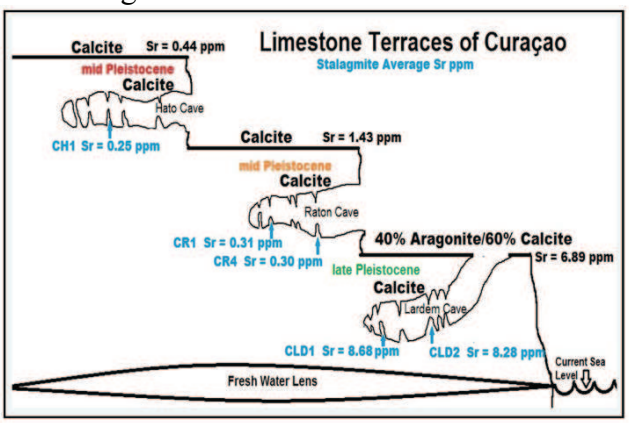

Figure 6. Summary data for Curaçao showing the decrease in Sr values with higher terrace levels and older surface rocks (which are the Ca and Sr source for current stalagmite growth in the caves). The stalagmites show a similar Sr decrease with higher elevations and thus increase in age of the host rock. Also shown are the locations of current sea level and the modern fresh water lens.

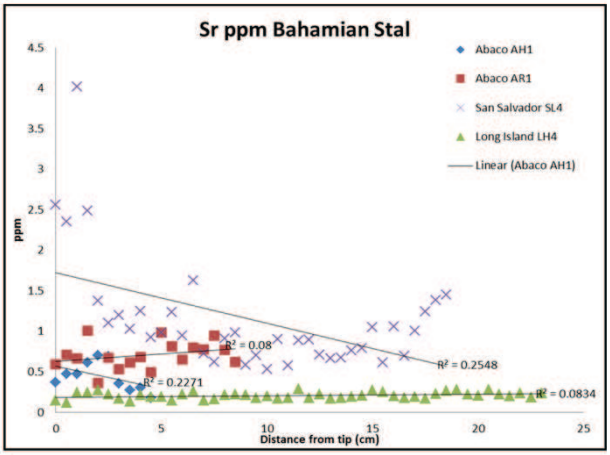

Figure 7. Results of strontium concentrations from stalagmites in The Bahamas. Abaco and San Salvador show expected Sr results, but the extremely low Sr concentrations for Long Island were not expected, perhaps as a result of age uncertainties for the host rock.

The rocks of the Bahamian study areas are equally as chaotic as the stalagmite data (Figure 8). As with Curaçao, the surface rocks followed the expected pattern, with Sr concentrations lowest in the wet northern Bahamas, and the highest Sr values for the dry southern Bahamas (Figure 8A). In contrast, the rocks from within Hamilton Cave on Long Island were relatively low in Sr concentration (Figure 8B and 8C). Sr concentrations of speleothems from caves on Abaco and San Salvador were as expected relative to one another. Abaco has a lower Sr concentration in the cave rocks than San Salvador, hypothetically due to the higher annual precipitation and larger water flux on Abaco. The data for the cave rocks of Long Island show depleted Sr.

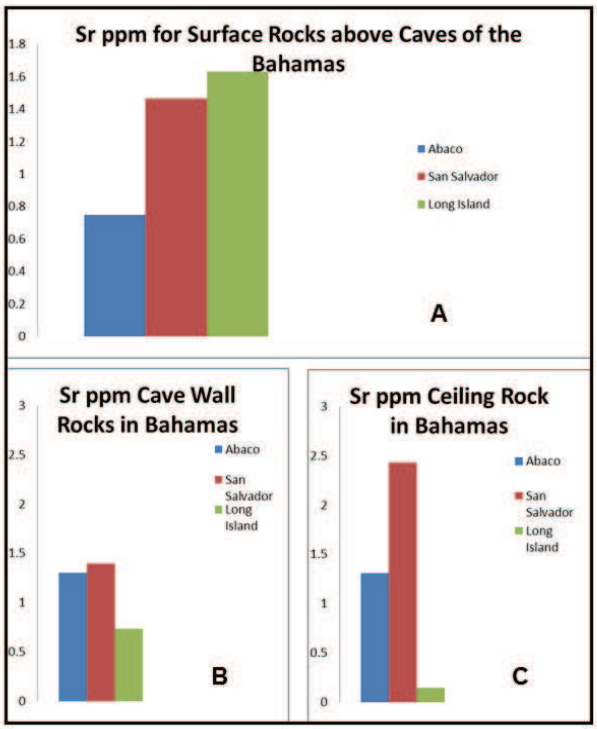

Figure 8. Results of strontium concentrations from Bahamian rocks. A) Surface rocks showing retention of Sr in the drier localities of San Salvador and Long Island. B and C) Wall and ceiling rocks show the expected increase in Sr for dry San Salvador versus wet Abaco. However, the Long Island data show unexpected loss of Sr; rock age is uncertain but the high Sr values for surface rocks makes these results confusing.

DISCUSSION

This study sought to find evidence of the Sr concentrations in speleothems deposited in eogenetic carbonate caves in relation to the relatively young mineralogy of the rocks. Three hypotheses with regards to Sr concentrations in speleothems of these settings were posed and described below.

Hypothesis 1. The Sr content of southern Caribbean speleothems has a direct relationship with the age of the host rock at the time of speleothem precipitation.

The stalagmites collected from within the youngest cave rock unit on Curaçao had a significantly higher concentration of Sr than currently growing stalagmites collected from the older carbonate terraces. The growing stalagmites in the caves of older rock units had lower Sr values indicating that the Sr had already leached out of the bedrock as a result of aragonite to calcite inversion.

The host rock Sr data is a bit confusing. For Curacao, the surface samples have Sr levels that decrease with increasing age of the rock, as expected. However, the cave wall and ceiling rock samples show Sr levels higher in the Raton Cave terrace rocks than in either the older Hato Cave terrace rocks or the younger Lardem Cave terrace rocks. Speculating, this might be the consequence of speleothem aragonite formation (Onac et al., 2001) in rock pores in the Raton Cave terrace rocks as a result of elevated Mg/Ca ratios in vadose water, with the Mg sourced from sea spray. This secondary speleothem aragonite could have trapped Sr that otherwise would have left the host rock. This speculation does not address the Sr depletion in the Hato Cave terrace rocks; it appears that the secondary aragonite precipitated in the host rock must later mobilize and be removed with the Sr. The same pattern holds for The Bahamas, but the age constraints there are weak so no conclusions can be drawn nor viable speculations made. The fact that the stalagmites show a Sr concentration pattern consistent with the host rock surface samples is an

indication that the drip water is sourced from the surface and near-surface epikarst.

Hypothesis 2. Growing speleothems in older rock contain less Sr than speleothems in younger rock in the same climatic setting.

The stalagmites collected from Curaçao were all obviously from within the same climate with no variation in precipitation or temperature. The only difference in these stalagmites are the times at which they were deposited and the age of the rocks that hosted the cave they were deposited in. The Lardem stalagmite could not be older than 115 ka at the end of the MIS 5e interglacial (Thompson, et al., 2011) and the last time the freshwater lens was at an elevation to permit speleogenesis of the cave. Dating would be needed to ascertain if the age of the Hato and Raton stalagmites are younger than those in the Lardem Cave, but they did have the opportunity to begin depositing long before Lardem Cave even existed. Their currently growing apical tips should record the same time record conditions as Lardem Cave's currently growing apical tips. In any case, the host rock is older. The Lardem stalagmite clearly has more Sr than the Raton and Hato stalagmites, but further investigation is necessary to determine the relative basal age of the two stalagmites from Raton Cave and the stalagmite from Hato Cave.

Hypothesis 3. Eogenetic carbonates within climates of higher precipitation will lose Sr content faster than those in climates of lower precipitation and the speleothems deposited in the caves within these rocks will record this trend.

The stalagmites from caves on the island of Abaco clearly show a lower Sr content than the stalagmite collected from the island of San Salvador. However, Long Island shows extremely low Sr concentrations in stalagmites, contrary to expectations (Figure 7). The cave rock (Figure 8) and stalagmite from Long Island seemed to be leached of Sr despite its dry climatic setting. Given that the surface rocks on Long Island have high Sr values, these results are unexpected. Unlike Curaçao, the high Sr values in surface rocks on Long Island do not appear to contribute Sr to the stalagmites in Hamilton Cave. These Long Island Sr values could be speculatively explained by either an unknown difference in age of the rock or the thickness of the rock unit where the cave is located, or perhaps a shift in glacial to interglacial climate. Carbonate rocks from the last interglacial (MIS 5e) deposited as the Grotto Beach Formation are easily identified based on their relationship with datable subtidal facies in The Bahamas (Carew and Mylroie, 1995). The eolianites of the Owls Hole Formation date from MIS 7, 9, 11 and possibly older, and are very hard to date, especially in the field (Carew and Mylroie, 1995). As the flank margin caves in The Bahamas are formed in these Owls Hole Formation eolianites, the host rock age cannot be constrained (Mylroie and Mylroie, 2013). Therefore, the climate-induced differences in aragonite (and hence Sr preservation) cannot be separated from a possible age-induced aragonite differences. The third hypothesis remains unproven.

SUMMARY

The study indicates that stalagmites growing in eogenetic rocks on Curaçao contain a Sr record that reflects the age of the host rocks at the land surface. Older, eogenetic rocks that have inverted mostly to calcite, create stalagmites with less included Sr compared to stalagmites in caves in the youngest rock. As the caves are all in the same climatic setting, the stalagmite Sr values reflect the age of the eogenetic host rock. These data have implications for studies using speleothem Sr values for paleoclimate reconstructions in young oceanic carbonate islands. Analysis of host rock Sr values within the caves indicates some storage mechanism, perhaps re-precipitated speleothem aragonite at the Raton Cave site. The Bahamian data, while similar to the Curaçao data, are not properly constrained as to host rock age, and therefore, the age versus climatic control of Sr flux cannot be established.

ACKNOWLEDGMENTS

None of this research would have been possible without the generous funding received from the William L Wilson scholarship awarded by the Karst Waters Institute, the grant received from the Cave Research Foundation, the Erwin Russell fund, and ExxonMobil. Dr. Rinat Gabitov of Mississippi State University arranged and conducted the laser ablation analysis at Rensselaer Polytechnic Institute. The Carmabi Institute on Curaçao, Netherlands Antilles, The BEST Commission, and the Gerace Research Centre on San Salvador Island, The Bahamas (permit number 180), are thanked for permission to do research, and to collect and export specimens.

REFERENCES CITED

Carew, J.L., and Mylroie, J.E. 1995. A stratigraphic and depositional model for the Bahama Islands. Pp. 5-31. In H.A. Curran and B. White (Eds.). *Terrestrial and Shallow Marine Geology of the Bahamas and Bermuda*. Geological Society of America Special Paper 300.

Finch, A.A., Shaw, P.A., Homgran, K., and Lee-Thorp, J. 2003. Corroborated Rainfall Records from aragonitic stalagmites. *Earth and Planetary Science Letters* 215: 265-273.

Frappier, A. 2008. A stepwise screening system to select storm-sensitive stalagmites: Taking a targeted approach to speleothem sampling methodology. *Quaternary International* 187: 25-39.

Gaffey, S.J., Zabielski, V.P., Bronnimann, C., 1995. Roles of organics and water in preneomorphic and early neomorphic alteration of coralline aragonites from San Salvador Island, Bahamas. Pp. 233-250. In H.A. Curran and B. White (Eds.). *Terrestrial and Shallow Marine Geology of the Bahamas and Bermuda*. Geological Society of America Special Paper 300.

Goede, A., McCulloch, M., McDermott, F., and Hawkesworth, C. 1998. Aeolian contribution to strontium and strontium isotope variations in a Tasmanian speleothem. *Chemical Geology* 149: 37-50.

Hill, C., and Forti, P. 1997. *Cave Minerals of the World.* National Speleological Society, Huntsville, AL, 463 p.

Kambesis, P.N., Mylroie, J.R., Mylroie, J.E., Larson, E. B., Owen-Nagel, A.M., and Sumrall, J.B. 2015. Influence of karst denudation on the northwest coast of Curaçao. Pp. 200-212. In B. Glumac and M. Savarese (Eds.). *Proceedings of the 16th Symposium on the Geology of the Bahamas and other Carbonate Regions*. Gerace Research Centre, San Savador, The Bahamas.

Kulp, J.L, Turekia, K., and Boyd, D.W. 1962. Strontium content of limestones and fossils. *Geological Society of America Bulletin* 63: 701-716.

Mylroie, J.E., and Mylroie J.R. 2007. Development of the Carbonate Island Karst Model. *Journal of Cave and Karst Studies* 69: 59-75.

Mylroie, J.E., and Mylroie, J.R. 2013. Caves and karst of the Bahama Islands. Pp. 147-176. In M.J. Lace and J.E. Mylroie (Eds.). *Coastal Karst Landforms*. Coastal Research Library 5, Springer, Dordrecht.

Onac, B.P., Mylroie, J.E., and White, W.B. 2001. Mineralogy of cave deposits on San Salvador Island, Bahamas. *Carbonates and Evaporites* 16: 8-16.

Ridlen, N.M. 2014. Speleothem strontium concentrations in eogenetic carbonates. MSc. Thesis. Mississippi State University, Mississippi State, MS, USA. 267 p. http://sun.library.msstate.edu/ETD-db/theses/available/etd-04032014-121434/

Roberts, M.S., Smart, P.L., and Baker, A. 1998. Annual trace element variations in a Holocene speleothem. *Earth and Planetary Science Letters*. 154: 237-246.

Schellmann, G., Radtke, U., Scheffers, A., Whelan, F., and Kelletat, D. 2004. ESR dating of coral reef terraces on Curacao (Netherlands Antilles) with estimates of younger Pleistocene sea level elevations. *Journal of Coastal Research* 20: 947-957.

Sealey, N.E. 1990. *The Bahamas Today.* MacMillan Education Ltd., London, 120 p.

Sinclair, D.J., Banner, J.L., Taylor, F.W., Partin, J., Jenson, J., Mylroie, J. Goddard, E., Quinn, T., Jocson, J., and Miklavič, B. 2012. Magnesium and strontium systematics in tropical speleothems from the western Pacific. *Chemical Geology* 294/295: 1-17.

Sumrall, J.B., Larson, E.B., and Mylroie, J.E. 2016. Caves within dolomitized sections of the Seroe Domi Formation on Curaçao, Netherlands Antilles. *Acta Carsologica* 45: 19-32.

Thompson, W.G., Curran, H.A., Wilson, M.A., and White, B. 2011. Sea-level oscillations during the last interglacial highstand recorded by Bahamian corals. *Nature Geoscience* 4: 684–687.

van Beynen, P.E., Soto, L., and Polk, J. 2008. Variable calcite deposition rates as proxy for paleoprecipitation determination as derived from speleothems in central Florida, U.S.A. *Journal of Cave and Karst Studies* 70: 25-34.

Whitaker, F.F., and Smart, P.L. 1997. Hydrogeology of the Bahamian Archipelago. Pp. 183-216. In H.L. Vacher and T. Quinn (Eds.). *Geology and Hydrogeology of Carbonate Islands*, Developments in Sedimentology 54, Elsevier, Amsterdam.

White, W.B. 2004. Paleoclimate records from speleothems in limestone caves. Pp. 135-175. In I.S. Sasowsky and J.E. Mylroie. (Eds.). *Studies of Cave Sediments: Physical and Chemical Records of Paleoclimate*. Kluwer Academic/Plenum Publishers, New York.

VEGEMORPHS AS A MEANS TO DIFFERENTIATE TRANSGRESSIVE-PHASE FROM REGRESSIVE-PHASE QUATERNARY EOLIAN CALCARENITES, SAN SALVADOR ISLAND, THE BAHAMAS

John E. Mylroie, Andrew N. Birmingham, and Joan R. Mylroie

Department of Geosciences, Mississippi State University,
Mississippi State, MS 39762

ABSTRACT

During the start of Quaternary interglacial conditions, rising sea level flooded the top of the steep-sided carbonate platforms of The Bahamas, and carbonate sediment production was significant. This carbonate sediment was rapidly produced in large volumes within relatively small lagoons, and eolian calcarenites immediately developed on the remaining dry ground adjacent to their source beaches. As these dunes form as sea level is rising, they are referred to as transgressive-phase eolianites. Continued reef growth to wave base as the highstand stabilizes diminishes lagoon wave energy, and further dune production is modest until the end of the interglacial, when sea level begins to fall and surf zone processes pass through the platform lagoons, where stored carbonate sediments are remobilized into beaches and a second episode of dune production occurs. The resulting dunes are regressive-phase eolianites.

These two eolianite packages bracket the leading and trailing portions of individual sea-level highstands. Various criteria have been developed to identify transgressive-phase and regressive-phase eolianites; however, the one with the most potential is based on plant trace fossils, variously called rhizomorphs, rhizoliths, or vegemorphs. Vegemorphs is used herein as it refers to any plant structures, not just roots. Extensive field work has demonstrated quantitatively that vegemorphs are found preferentially in regressive-phase eolianites, and that the presence of vegemorphs disrupts the fine-scale eolian bedding. Transgressive-phase eolianites have notably fewer vegemorphs, and as a consequence, exhibit undisturbed fine-scale laminations. An average vegemorph spacing distance of 15 cm separates transgressive-phase eolianites (>15 cm) from regressive-phase eolianites (<15 cm). Vegemorph low abundance or high abundance is readily observable in outcrop, and so paleodunes exposed at sea cliffs, in quarries and road cuts, or in caves can be categorized as transgressive-phase or regressive-phase deposits, respectively.

INTRODUCTION

The Bahamian archipelago is a carbonate province where the subaerially exposed rocks and sediments have been produced by Quaternary glacioeustasy, with sea-level highstands creating lagoonal and eolian deposition, and sea-level lowstands dominated by surficial weathering and terra rossa paleosol production and almost no carbonate deposition (Carew and Mylroie, 1995a; 1997). The sole exception is Mayaguana Island, where minor tectonic activity has allowed lagoonal deposits dating back to the Late Miocene to be present at the surface (Kindler et al., 2010). Sea-level highstands in the Quaternary have a duration of ~10 ka, and the intervening lowstands have a duration of ~100 ka, within each glacial-interglacial cycle (Carew and Mylroie, 1995b). All subaerial carbonate deposits seen in The Bahamas today had to form within a geologically short time window when the steep-sided Bahamian platforms were flooded and the carbonate sediment "factory" (Carew and Mylroie, 1995a; 1997) was turned on and operating. In The Bahamas, almost all sediments above 7 m elevation are eolianites. From sea level up to 7 m, eolianites exist, but subtidal facies representing lagoons and former coral reefs are also present. The subtidal

facies are almost exclusively from the last interglacial, or Marine Isotope Substage 5e (MIS 5e); tectonic subsidence and denudation have removed evidence of earlier highstand events (Carew and Mylroie, 1995b; Mylroie and Mylroie, 2017). Eolian deposits exist from the mid-Pleistocene, and represent at least three sea-level highstands prior to MIS 5e (Kindler et al., 2010) as they are high enough and massive enough to withstand both platform subsidence and denudation effects (Mylroie and Mylroie, 2017).

The eolianites of The Bahamas are difficult to place within a stratigraphy, as they contain almost no datable fossil material, and their patchy distribution means they are commonly not stacked one upon the other. In some locations, such as the Glass Window area of Eleuthera, the eolianites can be found stacked one upon the other to give an uncontestable field example showing eolianite production going back to the mid-Pleistocene (Kindler et al., 2010). The use of U/Th dating for eolianites is not possible as no coral fossils are present. Dating by amino acid racemization (AAR) has had some success in placing eolianites within a given interglacial episode, although the method has been controversial (Carew and Mylroie, 1995a; 1997; Kindler et al., 2010). Paleomagnetic studies have been successful using the paleomagnetic secular variation of terra rossa paleosols that separate the eolian units (Panuska et al., 1999), but these tests do not date the eolianite, they merely give the overlying terra rossa paleosol a unique magnetic fingerprint. This technique allows correlation in the field, but not an absolute age. Use of ^{14}C dating has been very successful in differentiating Holocene eolianites, but cannot be used on eolianites from MIS 5e or earlier. Electron Spin Resonance (ESR) analysis has been attempted, but with mixed success (Dealy et al., 2011). The problem using dating techniques to determine the stratigraphic position of a given eolianite is that the answer cannot be determined in real time in the field. The investigator must wait until the analyses have been completed in a laboratory somewhere other than in The Bahamas, often a year or more after sample collection. The techniques listed above also (with the exception of ^{14}C for Holocene rocks) cannot differentiate events within the eolianite deposits of a given interglacial highstand.

The simplified Bahamian stratigraphic model is shown in Figure 1 (Carew and Mylroie, 1995a; 1997) as it is most suitable for field investigations; for a more detailed stratigraphic column, see Kindler et al. (2010). The model postulates that when sea level is rising at the end of a glacial cycle, sediment production begins as soon as the sea water overtops the platform edge and begins to create lagoons on the platform top. Field evidence shows that even a small lagoon near the platform edge can produce sufficient carbonate allochems to allow almost immediate production of beaches on the remaining high ground of the platform, resulting in the deposition of eolianites sourced from those beaches. These eolianites are called *transgressive-phase eolianites* as they result from the initial transgression of the platform (Carew and Mylroie 1995a; 1997). Through time, sea-level rise will slow and stabilize. When this event occurs, reefs will grow up to wave base, and lagoons become quiescent compared to the early transgression. Eolian production continues, but produces dunes smaller than on the transgression as wave dynamics are less and sediment supply to the beach diminishes. At the end of the interglacial cycle, sea level regresses off the platform. In so doing, wave base passes through the accumulated lagoonal sediments, and another episode of eolianite production ensues, called *regressive-phase eolianites* (Carew and Mylroie 1995a; 1997). The transgressive-phase and regressive-phase eolianites therefore mark the beginning and end of each interglacial sea-level highstand, respectively.

It is important to bring up a cautionary note regarding regressive-phase eolianites. During the sea-level stillstand portion of a glacioeustatic sea-level highstand, strandplains can prograde into shallow lagoons, and eolianites can form on these strandplains. These are not true regressive-phase features, as sea level has not fallen. They are progradational. It can be difficult in the field to separate progradational eolianites from those formed by a true regression. In the first case, such eolianites

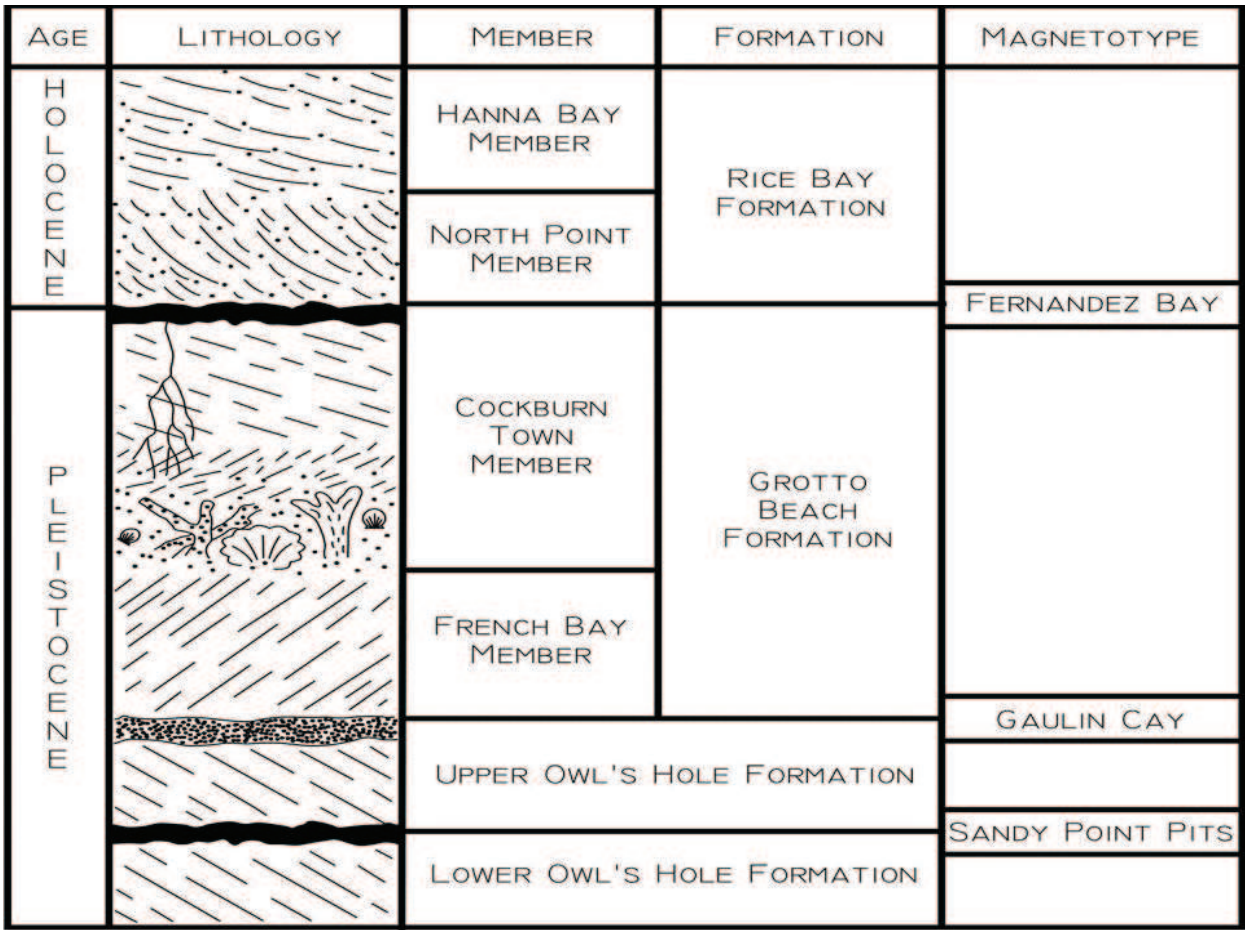

Figure 1: Simplified stratigraphic column for San Salvador, after Mylroie and Carew (2014). For a more detailed column, see Kindler et al. (2010).

will be found to overly beach sediments, which in turn overlie subtidal deposits, including coral reefs, with no evidence of a subaerial interval on top of the subtidal deposits. Such a progradational sequence can be seen at the Cockburn Town fossil reef on San Salvador Island. True regression would require evidence of a subaerial exposure between the subtidal facies and the entombing eolianite. Such evidence of regression can be seen at The Gulf on San Salvador Island. For these reasons, Carew and Mylroie (1995a; 1997) did not make a separate regressive-phase member within the Grotto Beach Formation, but included both progradational (sea-level stillstand) eolianites and regressive-phase eolianites (sea level falling) in the Cockburn Town Member, as only special field relationships can differentiate between the two. Such field relationships are rare, and the Carew and Mylroie (1995a; 1997) stratigraphy is designed to work in real time in the field.

Carew and Mylroie (1995a; 1997) developed a set of observational tools to determine if an eolianite was transgressive phase or regressive phase (Table 1). The top two of the criteria shown in Table 1 (inner dashed-line box in the table) are the degree of bedding disruption, and the abundance of vegemorphs. The term vegemorph is used here to indicate plant trace fossils such as root and stem casts. The terms rhizomorph and rhizolith are commonly used to identify these plant structures, but the term "rhizo" assumes a root origin, when stems and sometimes leaves are also preserved as trace fossils. The term vegemorph is inclusive and is used here, even though it is recognized that the

TABLE 1. PHASES OF DEPOSITION AND DIAGNOSTIC CHARACTERS

Transgressive Phase	Still-stand Phase	Regressive Phase
Fine-scale eolian bedding	Disrupted eolian bedding	Disrupted eolian bedding
Few vegemorphs	Abundant vegemorphs	Extensive vegemorphs
Penecontemporary cliffing and boulder paleotalus	Penecontemporary notching of beach and intertidal facies, and beach-face breccia facies	Lack of penecontemporary wave erosion
Penecontemporary sea caves	Rare sea caves	Lack of sea caves
Corals on wave-eroded benches	No corals on eroded benches	No penecontemporary benches
Lack of protosols	Protosols common	Protosols common
On lapped still-stand or regressive-phase deposits	Marine facies abundant	Commonly peleoidal/bioclastic
Predominantly eolianites, marine deposits rare	Ebb-tidal delta, lacustrine, and strand plain deposits	Eolianites overstepping marine deposits

most commonly observed plant trace fossil is from root structures, as would be expected from a preservational bias viewpoint. Carew and Mylroie (1995a; 1997) viewed the bedding disruption and vegemorph pattern as linked (Figure 2). If vegemorphs were abundant, then bioturbation of the eolian bedding by the root structures would occur high in the section, the trace fossils would form an ichnofabric (e.g. Drowser and Bottjer, 1989). The Carew and Mylroie (1995a; 1995b) model hypothesized that when the transgressive-phase eolianites formed, beaches had not yet had time to develop a full plant climax community (there had been no beaches on the platform for ~100 ka), and the dunes were only sparsely colonized by plants. When the regressive-phase eolianites formed, beaches had been present for ~10 ka, and the beach plant community was fully established. That plant community quickly colonized the regressive-phase eolianites, disrupting the upper section bedding and setting the stage for abundant preserved vegemorphs.

The Carew and Mylroie (1995a; 1997) list of criteria was solely observational and thereby somewhat subjective. No quantitative means for establishing an eolianite as transgressive phase or regressive phase had been established. The research presented here represents an attempt to create quantitative criteria to classify eolianites as transgressive phase or regressive phase based on the measurement of the actual vegemorph trace fossils present. The data presented here were developed as part of an unfinished master's thesis at Mississippi State University; the authors who all worked on the initial thesis project are using this venue as a means of placing the research into the Bahamian geologic community.

METHODS

Field work was conducted on San Salvador Island, The Bahamas in June and July 2008, and again during December 2008, and January 2009. During June and July 2008, numerous locations of outcrops throughout the island were investigated for the potential of measuring populations of plant trace fossils. After reconnaissance was complete, the plant trace fossils were measured at numerous locations throughout the island. These locations included both Pleistocene transgressive-phase and regressive-phase eolianites and Holocene transgressive-phase eolianites (there are as yet no regressive-phase Holocene eolianites in The Bahamas). All of the locations were examined thoroughly for the presence of plant traces prior to the determination of the best sites to retrieve data within a location. The fewest number of sites found to measure at a location was four at North Point. No less than four sites were measured at each location. The total number of measurements varied depending on the extent of the outcrop at a location and the presence of representative vegemorph populations. Further measurements were taken during December 2008, and January 2009. These measurements were primarily taken in order to fill any gaps in the data that were noticed during the preliminary analyses of the measurements from June and July 2008.

Two different types of plant traces were measured; casts and molds (Figure 3). The most abundant measurements were taken from the mold populations. These are 3-dimensional, bedding-

plane penetrative traces that appear to most likely be root systems. They have been observed qualitatively to be most abundant in regressive-phase eolianite suites (Carew and Mylroie, 1995a; 1997). Casts (impressions in the bedrock) were also observed and measured at almost all of the studied locations. These are solely bedding-plane parallel and were observed to be relatively similar in abundance regardless of the depositional phase. It is most likely that these traces formed from the railroad vine, *Ipomoea pes-caprae,* or some similar species (Curran and White, 1987).

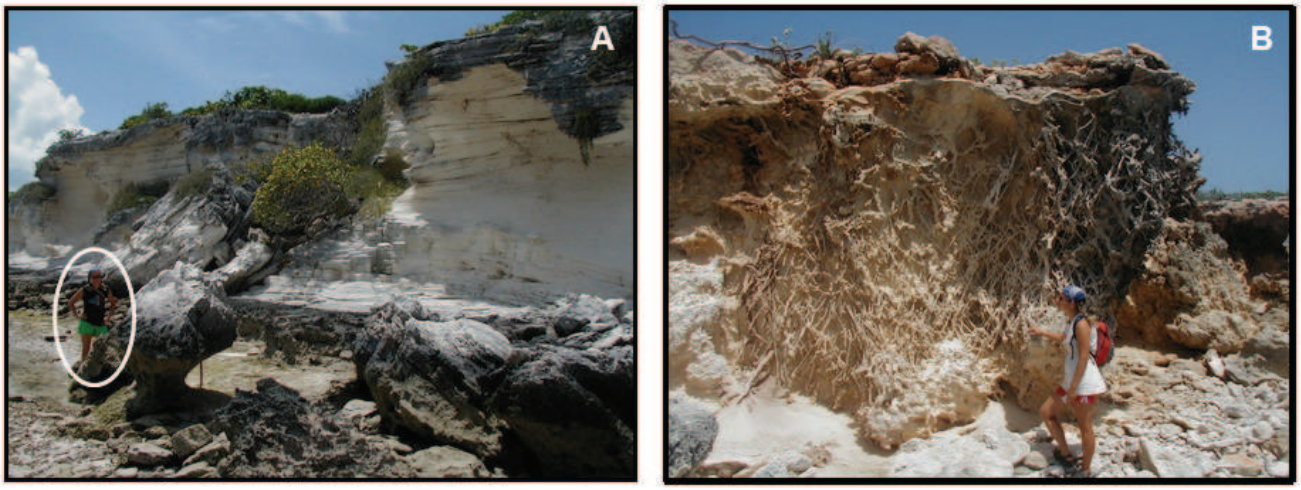

Figure 2: Comparison of transgressive-phase eolianites with regressive-phase eolianites, San Salvador Island, Bahamas. A) Holocene North Point Member of the Rice Bay Formation, Cut Cay. Fine-scale bedding can be followed from the water line up to the dune top, and vegemorphs are rare. These observations indicate a transgressive-phase eolianite (person on left in white oval for scale). B) Late Pleistocene Cockburn Town Member of the Grotto Beach Formation, Crab Cay. No bedding is visible, and vegemorphs are present though-out the entire outcrop exposure to create an ichnofabric. These observations indicate a regressive-phase eolianite (same person as in A for scale).

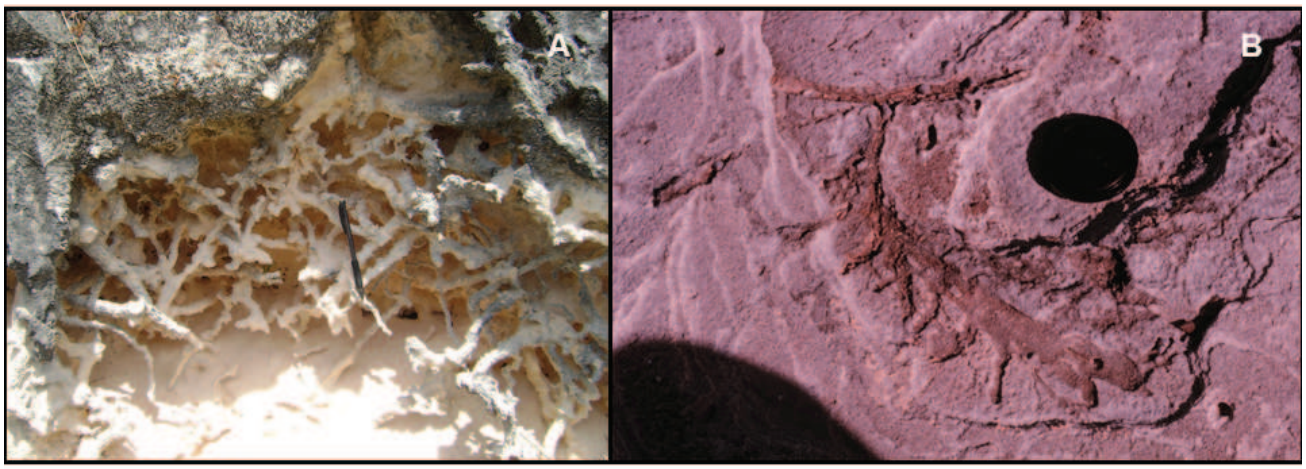

Figure 3: Vegemorph trace fossils, San Salvador Island, Bahamas. A) Molds of plant roots penetrating through bioturbated beds. Pencil, 13 cm long, for scale. B) Casts of plant stems, likely the railroad track vine, Ipomoea pes-caprae (Curran and White, 1987), along a bedding plane. Lens cap, 6 cm across, for scale.

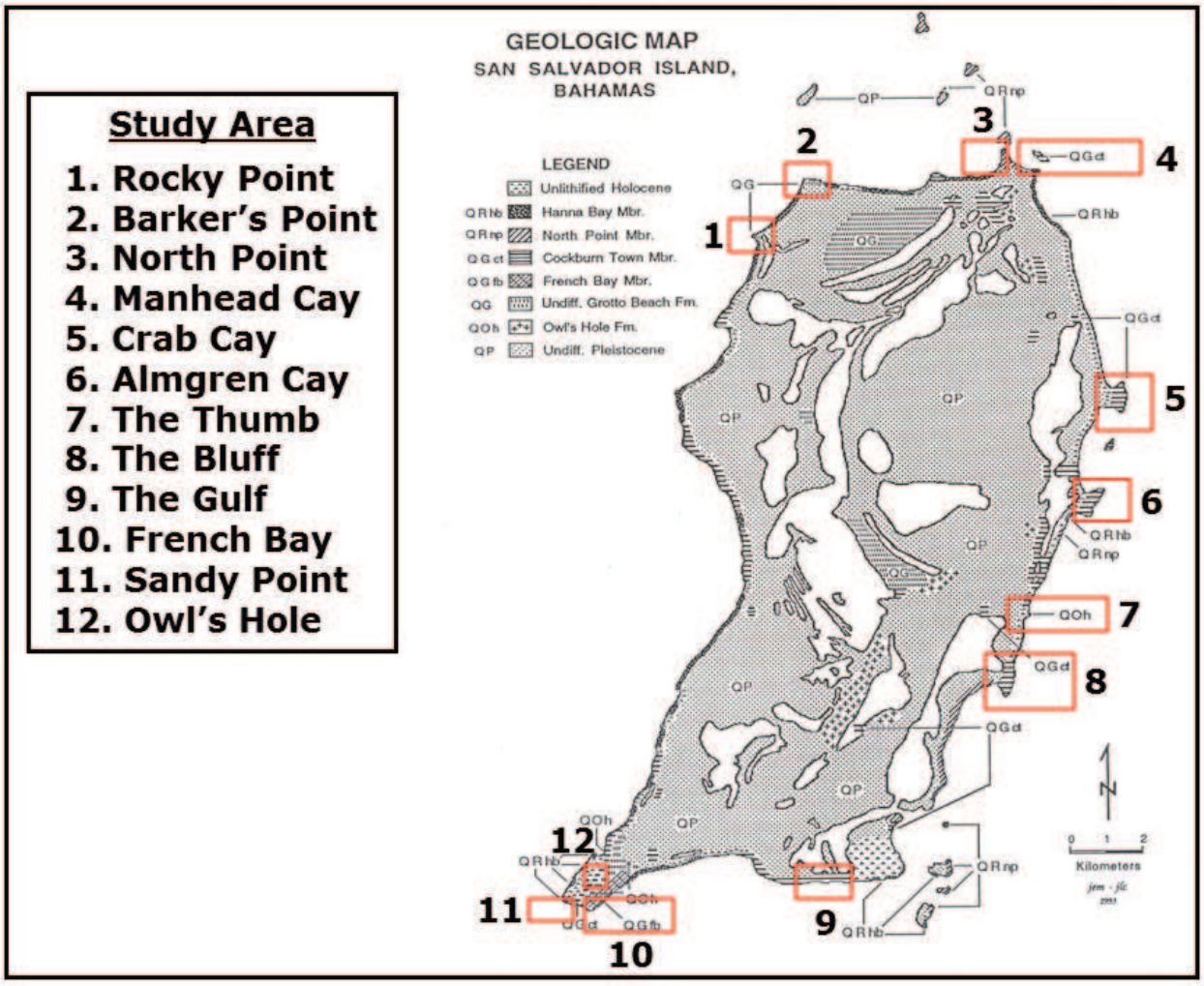

Figure 4: Map of San Salvador Island showing field locations for this study. Geology is based on Carew and Mylroie (1995a; 1997).

Study area

Data were collected from 12 locations on San Salvador (Figure 4). The locations were chosen according to whether or not they were accessible and whether or not the outcrops hosted populations of plant trace fossils. Representative samples were collected from the Pleistocene Owl's Hole Formation and Grotto Beach Formation, and the North Point Member of the Holocene Rice Bay Formation. No data were collected from the Hanna Bay Member of the Rice Bay Formation simply because no vegemorph root traces were found during reconnaissance.

Locations 7 (The Thumb) and 12 (Owl's Hole) are mapped as the Pleistocene Owl's Hole Formation. As stated earlier, there have been numerous attempts at dividing the Owl's Hole Formation into separate members or formations. The stratigraphic column (Figure 1) used for this study shows an Upper and Lower Owl's Hole Formation based on Panuska and coworkers' (1998) Sandy Point Pits Magnetotype; the more complete stratigraphic column of Kindler et al. (2010) depends on AAR data to assist eolian classification. There are few reliable ways to differentiate the Owl's Hole Formation in real time and no conclusive field indicators besides fortuitous areas where three or

more separate paleosols can be seen, as at the previously mentioned Glass Window on Eleuthera. Data collected from the two Owl's Hole locations may provide further insight to separating at least areas of transgressive-phase versus regressive-phase deposits within that unit.

Locations 1 and 2 on the map are Rocky Point and Barker's Point. These two areas are both mapped as undifferentiated Pleistocene Grotto Beach Formation (Carew and Mylroie, 1995; 1997). Location 10 is the type section for the French Bay Member of the Upper Pleistocene Grotto Beach Formation. This is a transgressive-phase eolianite dune suite. Plant trace populations are visually less dense than that of most known Cockburn Town Member eolianites. Locations 4, 5, 6, 8, 9 and 11 are mapped as Cockburn Town Member of the Grotto Beach Formation. These outcrops represent regressive-phase eolianite dune suites. The eolianite dunes overlie fossil reef and underlie a terra rossa paleosol in many places, indicating that they are indeed part of the Cockburn Town Member.

Location 3 represents the type section of the North Point Member of the Rice Bay Formation. The North Point Member is differentiated from the overlying Hanna Bay Member in that its foreset beds dip below modern sea level. Both units are recognizable in the field as Holocene in age as they lack a terra rossa paleosol, indicating too little time to collect the aerosol dust from the Sahara that contains the iron oxides that give those paleosols their red color (Foos, 1987). The ^{14}C data confirm the age of the North Point Member rocks to be mid-Holocene in age (Carew and Mylroie, 1995a; 1997). The North Point Member is obviously a transgressive-phase eolianite sequence due to the fact that there has not yet been a regression during the Holocene, and that the stillstand did not occur until ~3 ka, two thousand years after the North Point Member was deposited at ~5 ka (Carew and Mylroie, 1995a; 1997).

Data collection

Each of the 12 locations was investigated prior to any measurements or data collection. Sites for data collection were determined at each location based on the presence or absence of plant trace fossils, the level of preservation or lack thereof, and accessibility. Crab Cay and French Bay were the most extensively measured outcrops with 10 measurements each of 3-dimensional (3-D) trace populations. As the French Bay Member has been mapped as MIS 5e transgressive-phase, and Crab Cay of the Cockburn Town Member as MIS 5e regressive phase (Carew and Mylroie, 1995a, 1997), the expanded collection regime offered a good comparison suite of last interglacial sample data. Data taken were the compass orientation of the quadrat, strike and dip of local eolian bedding, and thorough descriptions of the local bedding features, fossil characteristics, and other geologic features at each site. Also measured at each location were the aforementioned bedding parallel trace fossils that seemed to be similar regardless of depositional history (Figure 3B). These measurements were treated as a separate data set for later analysis, which is not reported here.

North Point and Sandy Point were the least measured with 4 sites. North Point had fewer measurements due to the lack of plant trace populations (not unexpected given its transgressive nature and its young age). There were also fewer measurements at Sandy Point because it is a very small area of outcrop. Most of the other locations consisted of approximately 5 to 6 sample sites each.

The goal was to establish a simple, field-based methodology that would allow assessment of the vegemorph abundance while field operations were on-going, and from that assessment, determine if the eolianite unit was transgressive or regressive phase as defined by Carew and Mylroie (1995a; 1997). A variety of measurements were considered. Vegemorph diameter and vegemorph length were investigated, but determined to be in part controlled by later diagenesis and preservational bias, and so were not utilized. The number and spacing of vegemorphs was interpreted to be a measure of vegemorph abundance, and a technique to do such a data collection regime was designed

Data collection was conducted at each site using a 50 cm x 50 cm quadrat and a tape measure

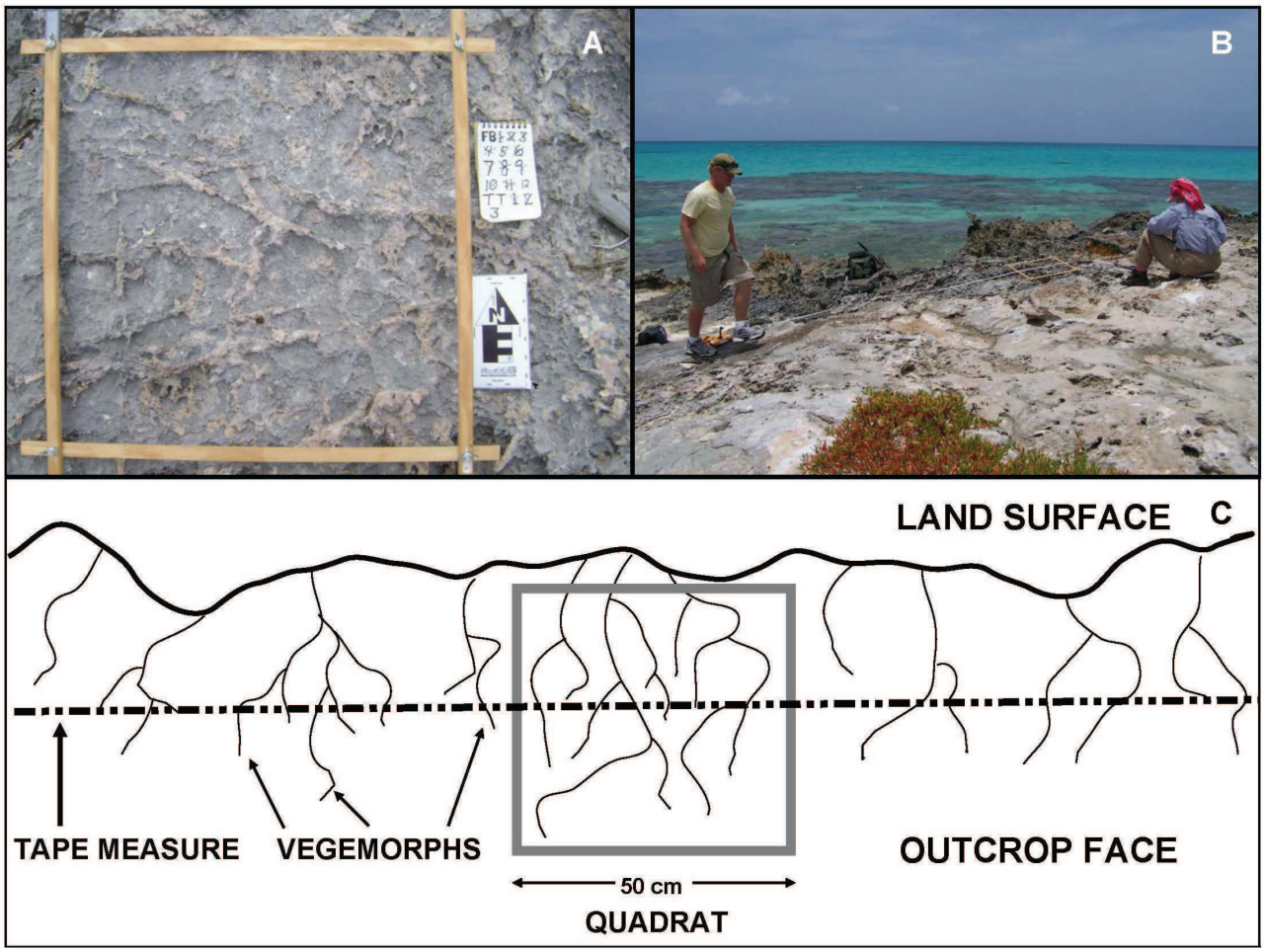

Figure 5: Vegemorph data collection. A) 50 cm x 50 cm quadrat placed over vegemorphs at their locally most visually dense concentration. Notebook was used to show site identity, scale bar is 6 cm long on its long axis. B) View showing a tape measure stretched out along the outcrop, centered on the quadrat to determine how vegemorph spacing changes with distance from the area of highest vegemorph concentration. C) Cartoon to show how the quadrat was placed at the densest vegemorph location, and how the tape measure was extended through the quadrat center to 20 m out on each side, or the edge of the outcrop, which ever came first. Each vegemorph intersection was recorded as a distance from the quadrat center.

(Figure 5). The quadrat was placed at each site where traces were visually most abundant or densest. This was typically at the top of the outcrop, as the vegemorph traces resemble a fibrous root system that is most dense toward the soil surface (in this case, a red-colored terra rossa paleosol or a white protosol). A picture was taken of the quadrat at each site with the location name, site number, and scale in the photograph (Figure 5A). A tape measure was then used to mark each occurrence of a plant trace fossil (Figure 5B), beginning in the center of the quadrat and continuing through the quadrat to the edge of the outcrop, or 20 m, which ever came first. The tape measure was consistently oriented so that it ran through the middle of the quadrat and along the section provided by the outcrop. Each occurrence of a vegemorph was recorded as a distance from the quadrat center moving along the tape measure (Figure 5C), using the center of the vegemorph as the measurement point.

The tape entrance and exit points on the quadrat were also recorded for later statistical use. This technique created both a total number of intersections of the tape with the vegemorphs, and the spacing, or interval, between them. This interval value could be averaged for the width of the outcrop, important as many outcrops had a width less than the 20 m measurement distance from each side of the quadrat.

Statistical analyses

Field data were entered into spreadsheets in two separate ways. The interval or spacing between each successive vegemorph trace was entered along with the distance from center for each vegemorph site at each location. The intervals for each site at each location were then averaged. The data were also entered into two other, separate spreadsheets as number of counts per 10 cm and number of counts per 25 cm. These data simply represent the number of observances within a fixed distance from start to finish.

In order to test the hypothesis that the populations of plant traces measured in transgressive-phase and regressive-phase deposits are in fact different, one-way analysis of variance (ANOVA) of the interval spacing data was conducted. The assumptions for all ANOVA tests are that observations are independent both within and between samples, variance is homogeneous in all samples, data are normally distributed, and observations are assigned to groups using one or more factors.

First, the Kolnogorov-Smirnov Test for goodness of fit for continuous data was used to test whether the data sets from each location in the study area were normally distributed. Next, the homogeneity of variance among all samples was determined using Levene's test for equal variance. The homogeneity of variance among the samples determined which post-hoc analyses would be used to compare the means from the different locations. In cases where variance was determined to be homogeneous, the Bonferroni Test was used. In cases where variance was not homogeneous, the Tamhane's T2 test was used. The Tamhane's T2 test is a more conservative ANOVA test that is appropriate when variances are unequal or when variances and group sizes are unequal.

After the assumptions for performing a comparison of means using ANOVA were met, several hypotheses were tested:

1. Populations from regressive eolianites are the same.
2. Populations from transgressive eolianites are the same.
3. Populations from transgressive and regressive eolianites are different.

The data were also used to attempt to answer other questions:

1. Is there a difference among populations from Pleistocene and Holocene deposits?
2. Can the data be used to determine where Rocky Point and Barker's Point fit within the Grotto Beach Formation or Owl's Hole Formation?
3. Can the data be used to differentiate the Owl's Hole Formation into separate, transgressive and regressive phases?

The ANOVA tests were performed for both the overall interval spacing length averages among locations as well as the averages that were obtained from measurements solely within the quadrat. This was done in part to see whether the populations were the same or different when measured at their most dense areas. The results of these tests were also used to help set a specific distance to which one should measure in order to get a representative sample that can accurately distinguish dune suites based on the population of plant trace fossils.

Interval spacing was then plotted against distance from the starting point of measurement for each site at each location. Linear Regression was performed for each location and trendlines were added to each plot showing the formula ($y=mx+b$), R^2-values, and p-values. This was done to try and show any disparity among the trendlines between the transgressive-phase locations and regressive-phase locations. In the field, it was observed and noted that regressive-phase populations such as at Crab Cay and The Gulf tended to maintain

uniformity in interval spacing of successive fossils even when measured far from the starting point. Populations observed in transgressive-phase deposits such as at French Bay seemed to become much more spread out the farther the measurements strayed from the starting point. The difference in the curves also aided in the determination of a proper distance of measurement needed to get a representative sample.

Graphs plotting distance versus the total number of counts were created for the 10 cm count data. These graphs were planned to reveal a trend among transgressive-phase and regressive-phase plant trace populations. In transgressive-phase eolianites, where plant traces are sparse, the total count of observations should not go up much as distance is increased. In regressive-phase eolianites, where populations are dense and extensive, the total count of observations should trend toward a more dramatic increase as distance increases.

The quadrat photographs from each site were used to apply the Droser and Bottjer (1986) Ichnofabric Index to determine which indices fit for each site. The results were then analyzed to determine which index or range of indices fit best for each location. The final step in this process was to assign indices to both transgressive-phase and regressive-phase dune suites as a whole. That work was never completed.

RESULTS

The extent of plant trace fossils, or vegemorphs, in The Bahamas has been documented observationally on San Salvador and other Bahamian Islands: New Providence Island (Carew et al., 1996; Mylroie et al., 2012), South Andros Island (Carew et al., 1998), Eleuthera Island (Panuska et al., 2002; Kindler et al., 2010), Long Island (Curran et al., 2004), Cat Island (Mylroie et al., 2006) and Rum Cay (Mylroie et al., 2008). The model has also been used successfully on Abaco Island (Walker et al., 2008). Qualitatively, it seems that vegemorphs are more abundant in regressive-phase eolianite dune suites than in transgressive-phase eolian dune suites (Carew and Mylroie 1995; 1997). However, in some locations there are quantities that are not of this observational norm and confusion can occur. The results of this study should not only prove that there is a difference between the populations observed within transgressive and regressive eolianites, but also establish a method of determining this difference in the field. Because the MSc thesis was never finished, not all the data applications mentioned in the methods section were completed. Presented below is what can be confirmed from the work.

Statistical analyses

Interval spacing

Interval spacing data were derived from the original measurements in the field that noted each occurrence along a measuring tape at a given site. Each site yielded total measurements, and measurements taken within the 50 cm quadrat. The intervals were averaged for each site at each location for both the total average and the 50-cm-quadrat average interval spacing. The averages from each site were then averaged for a total average from each location. Figure 6 shows the total averages and the 50-cm-quadrat averages for each location.

Figure 6 shows that many of the known regressive-phase eolianite locations such as Crab Cay and The Gulf have average intervals that persist throughout the entire length of measure. That is, the 50-cm-quadrat interval average is approximately the same as the total length average. Some of the total lengths measured are up to 40 m. On the other hand, transgressive-phase deposits such as North Point and French Bay have average intervals that are much less at the 50-cm-quadrat length than the total length interval average. Figure 6 shows this result as a percentage. This approach is important because it determines that one must measure the full length of a population in order to be able to clearly distinguish between transgressive-phase and regressive-phase plant trace fossil populations. For instance, if only a 50-cm-quadrat length is measured for a transgressive-phase population, an accurate representation of the data

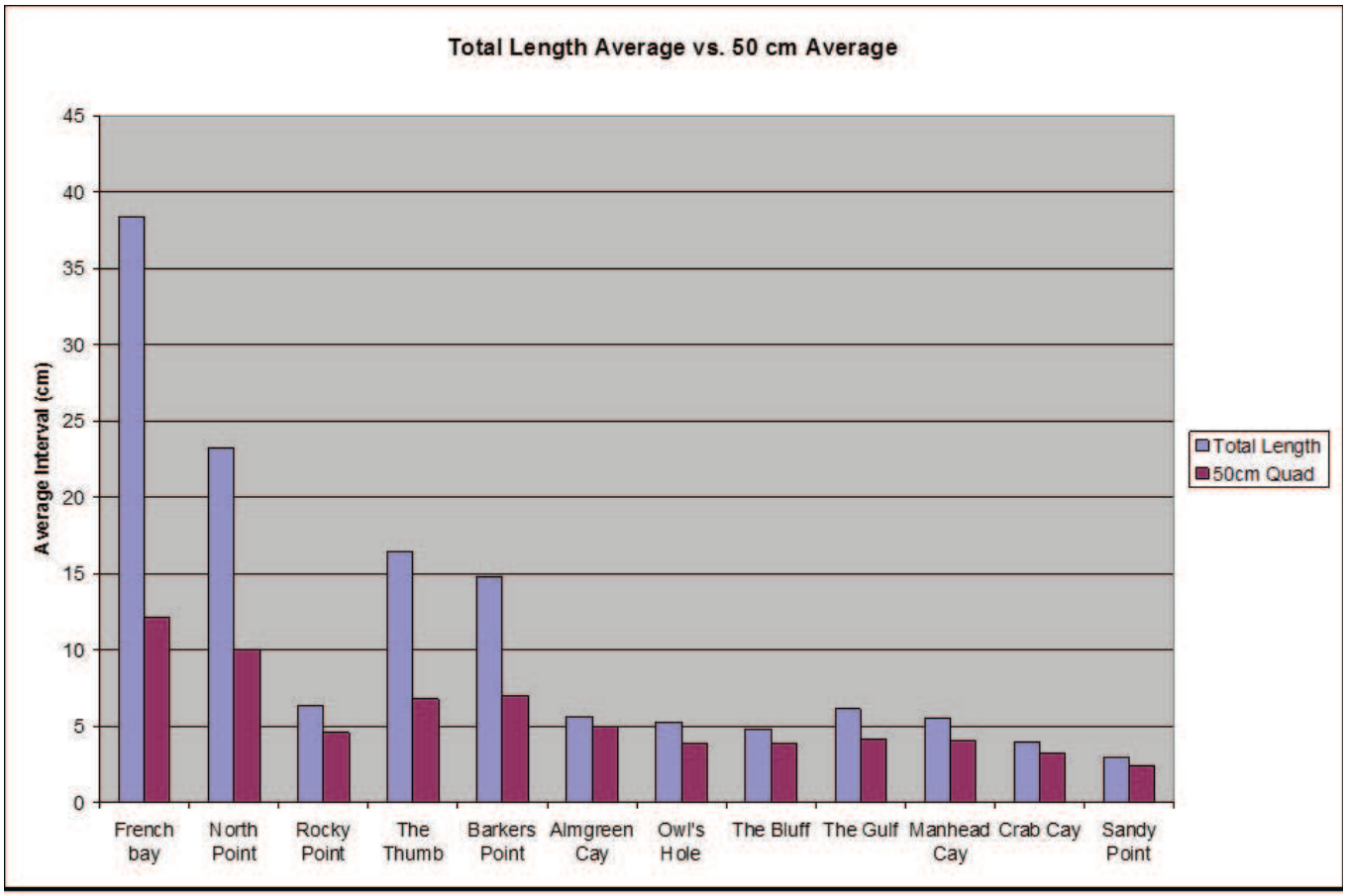

Figure 6. Bar graph plot of total length average and 50-cm-qudrat length average for all 12 sites. The vertical axis is percentage, to normalize different total lengths of measurement within each site. Known transgressive-phase eolianites, French Bay and North Point, show a large disparity between the two length averages, indicating vegemorph abundance decreases away from the center of highest concentration. The Bluff, The Gulf, Manhead Cay, Crab Cay and Sandy Point, all known regressive-phase eolianites, show equivalency between the two length averages, indicating a constant vegemorph density across the transect. Barkers Point and Rocky Point, unclassified at the time of the study, seem to fall into the transgressive-phase and regressive-phase categories, respectively.

would not be retrieved and the dune suite may not be correctly classified as a transgressive-phase versus a regressive-phase deposit.

One-way ANOVA tests were then performed for both the total average intervals and the 50-cm-quadrat average intervals. As previously stated, the conditions for the use of an ANOVA test are that the data are normally distributed and homogeneous in variance. To test whether or not the data was normally distributed, the Kolmogorov-Smirnov Test (K-S test) was used. The K-S test gives 2 tailed p-values that indicate whether or not the data are normally distributed. The null hypothesis was that the distribution of data is not significantly (p value < 0.05) different from normal. The results show that the null hypothesis that the data are not significantly different from normal can be accepted for each location.

In order to meet the condition of homogeneity in variance, the Levene test for variance was used. The null hypothesis is that the population variances are not significantly different and will be rejected if the p value is less than 0.05. The results show that for both the total interval average and the

50-cm-quadrat interval average data the variances are in fact heterogeneous as p-values are less than 0.05 and the null hypothesis that the population variances are equal can be rejected.

The two conditions for ANOVA were tested for. The condition that the data are normally distributed checked out. However, the variance between populations was proven to be heterogeneous. Because the variance between populations was heterogeneous a more conservative ANOVA test known as the Tamhane's T2 test was used. This test is often used when populations are either heterogeneous with respect to variance or when population group sizes (number of sites in this case) are unequal. The null hypothesis was that the means from all of the locations are the same. This would only be rejected for p values less than 0.05 at the 95% confidence interval. This analysis was used to compare both the means among locations from the total interval counts and the 50-cm-quadrat interval counts. The comparison of the means obtained from averaging the interval spacing from observation to observation has shown that there is significant difference among some of the populations. The most important difference that the results show is that the transgressive-phase eolianite location of French Bay is in fact significantly different than all other locations except for North Point which is also a transgressive-phase deposit. However, the results of the test are quite conservative because the variance among populations was different and the conservative Tamhane's T2 test had to be used.

Next, the interval data from each station at each location were plotted against distance from the measurement starting point. The data from all stations at each location were then combined and scatter plots were created for each location to show any trends in variability in interval spacing as distance increases (Figures 7). A trendline representing the average interval spacing for each location was also added to each chart to show how far individual measurements strayed from this average. Because populations of plant traces are more dense in regressive-phase deposits than in transgressive-phase deposits, scatter plots from locations measured in regressive-phase eolianites should not stray as far from the average interval as locations from transgressive-phase eolianites. Figure 7 shows data from transgressive-phase deposits at North Point and from regressive-phase deposits at Almgreen Cay. Figure 8 shows data from undifferentiated Pleistocene deposits at Barkers Point and Rocky Point, indicating that they are transgressive-phase and regressive-phase, respectively. The data are less compelling than for Figure 7, and reflect the reason for their initial classification as undifferentiated by Carew and Mylroie (1995a; 1997). Simple visual assessment of these outcrops was insufficient at the time of the original field work, but measurements demonstrate an actual difference that can be compared to known examples, as displayed by Figure 7.

The interval versus distance scatter plots show that the interval spacing between successive plant traces varies with distance as measurements are taken further from the starting point. It seems that in regressive-phase eolianites, the change in interval spacing with distance is less pronounced than in transgressive-phase eolianites (Figure 7). In this case, the starting point is at, or close to, the top of the population as viewed in outcrop. This was done because one would expect a root population to thin out deeper underground. In most cases, observances were very dense up-section and less dense down-section and sometimes draped by a terra rossa paleosol.

10 cm counts

The 10-cm-count data are simply the amount of plant traces that were observed every 10 cm until the end of the measurement. These counts were then averaged for each station at each location and then the total average for each location was calculated in order to perform an ANOVA test to compare the means among the locations. The 10 cm counts were used as another measure for determining any significant difference among populations of plant traces between the different locations. The Figure 9 shows the total average counts from each location.

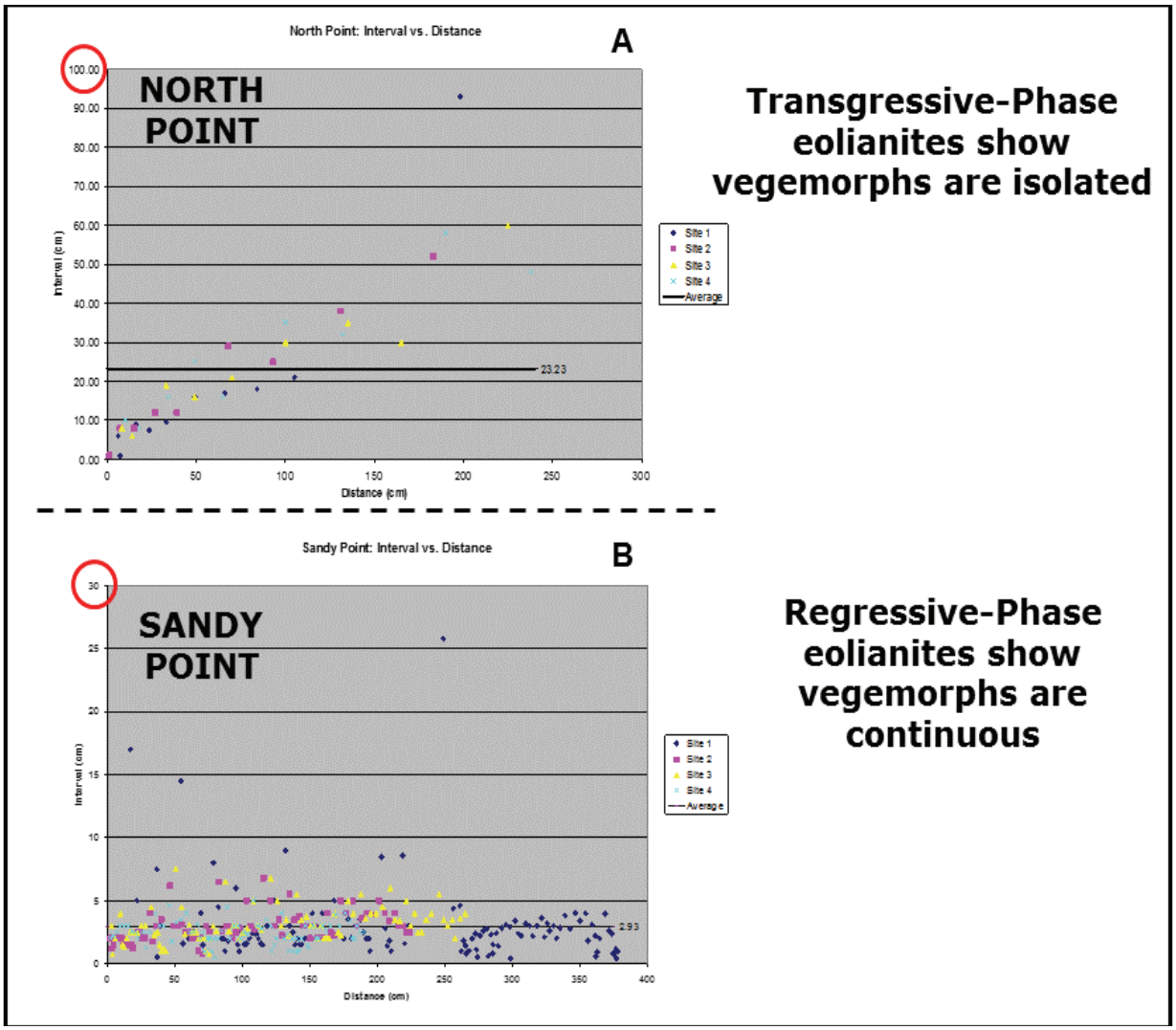

Figure 7: Plot of interval distance (vertical axis) between individual vegemorphs versus distance from the quadrat (horizontal axis). A) Plot for North Point, showing a continuing increase in separation interval or spacing of vegemorphs as distance from the quadrat increases, a key identifier of transgressive-phase eolianites. Average separation distance is 23.23 cm (horizontal black line). B) Plot for Sandy Point, showing compact and low separation interval or spacing of vegemorphs as distance from the quadrat increases, a key identifier of regressive-phase eolianites. Average separation distance is 2.93 cm (horizontal black line). Red circles show that the vertical scale on each plot is different (100 cm for A and 30 cm for B, respectively).

Again, for the ANOVA to be conducted the data must be normally distributed and variances between the data sets must be homogeneous. The Kolmogorov-Smirnov (K-S) test for goodness of fit for continuous data was again used to verify a normal distribution. The K-S test gives 2 tailed p-values that indicate whether or not the data is normally distributed. The null hypothesis was that the distribution of data is not significantly (p value < 0.05) different from normal. That is, if p-values are less than 0.05, the null hypothesis is rejected and the data are not normally distributed. The results

show that the null hypothesis that the data are not significantly different from normal can be accepted for each location. The Levene Test for equality among variances was then used again to test for homogeneity. The null hypothesis was that the populations variances are not significantly different ($p < 0.05$). Resulting p-values that are less than 0.05 indicated that the null hypothesis is rejected and the data do not share homogeneous variances.

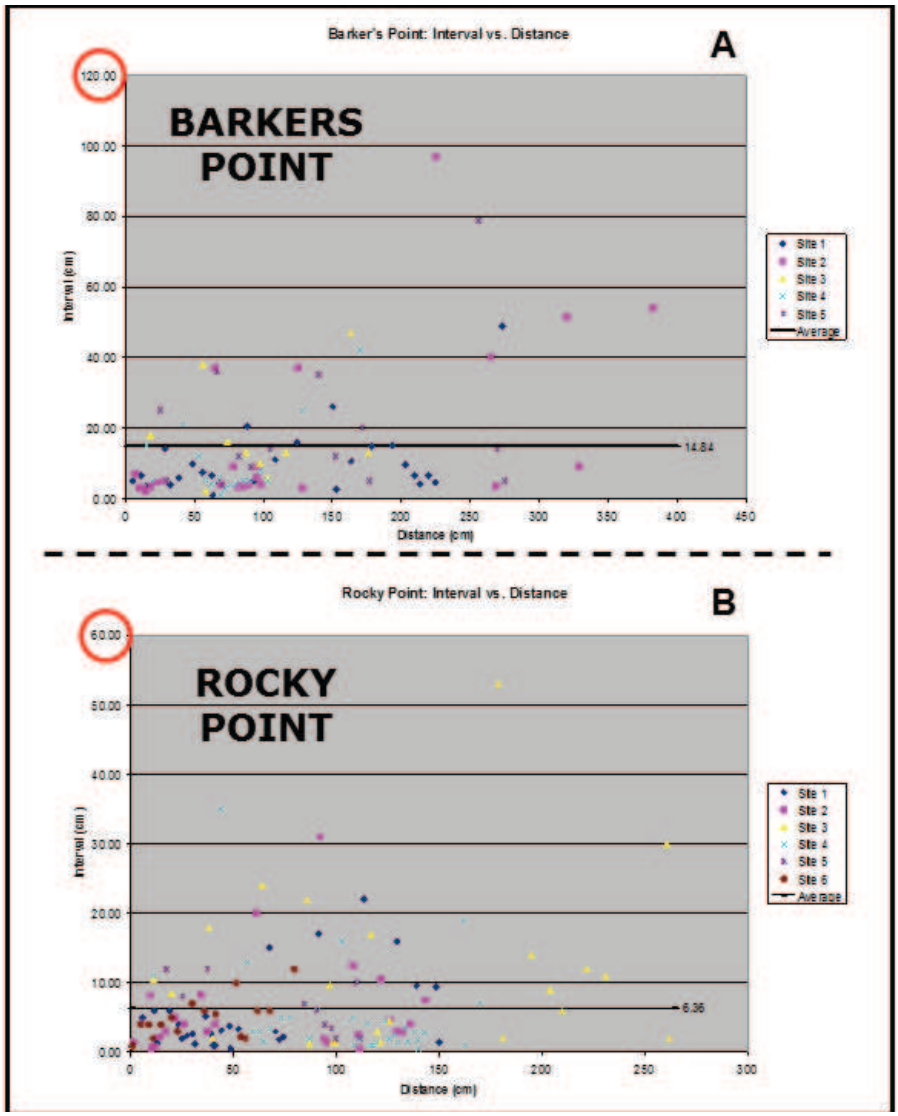

Figure 8: Plot of interval between individual vegemorphs versus distance from the quadrat; axes as in Figure 7. A) Plot for Barkers Point, showing an apparent continuing increase in separation interval or spacing of vegemorphs as distance from the quadrat increases. Average separation distance is 14.84 cm (horizontal black line). B) Plot for Rocky Point showing a smaller increase in separation interval or spacing of vegemorphs as distance from the quadrat increases. Average separation distance is 6.36 cm (horizontal black line). Red circles show that the vertical scale on each plot is different (120 cm for A and 60 cm for B, respectively). The data suggest that Barkers Point is transgressive-phase, and that Rocky Point is regressive-phase, but the data are less compelling than that shown in Figure 7, and reflects why these outcrops were left undifferentiated during the Carew and Mylroie (1995;1997) field work.

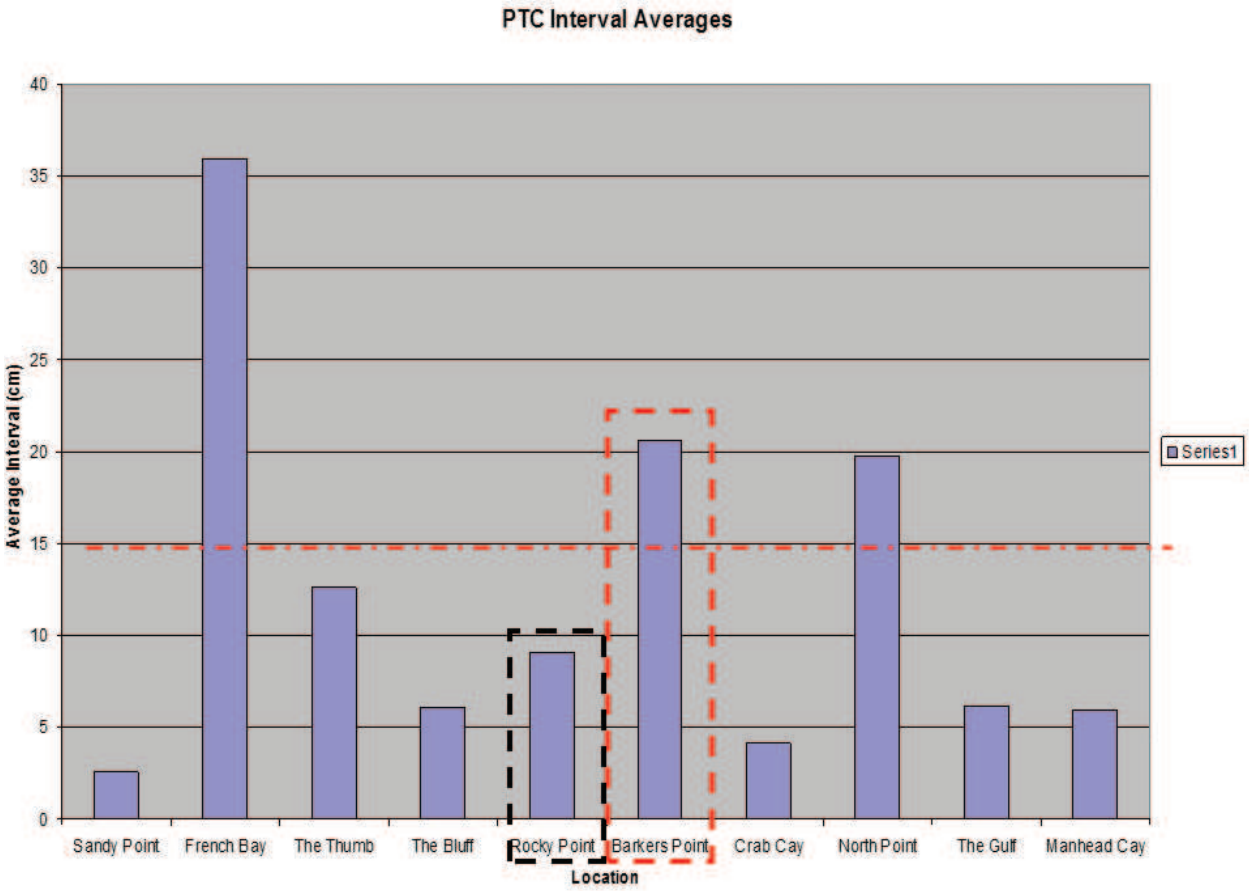

Figure 9: Bar graph of 10 of the 12 locations (Owl's Hole not studied, Almgren Cay not shown due to similarity with other regressive-phase sites, see Figure 6). Picking a 15-cm-average spacing interval for vegemorphs (dashed-dotted horizontal line), the eolian outcrops fall into two classifications: above 15 cm, trangressive phase; below 15 cm, regressive phase. Dashed boxes indicate undifferentiated eolianites from Barkers Point and Rocky Point, classified for the first time into transgressive phase and regressive phase, respectively. The Thumb, based on other criteria (Mylroie and Carew 2014) has been classified as regressive phase; however, it is close to the 15 cm cutoff (for example, the cutoff could be set at 12 cm and The Thumb would be included but not any of the regressive phase examples).

Just as was the case with the interval spacing data, the 10 cm data are normally distributed but are not homogeneous with respect to variance. Thus, the more conservative Tamhanes T2 ANOVA test must be used to compare the means from the data set. The null hypothesis was that the means from all of the locations are the same. This would only be rejected for p-values less than 0.05 at the 95% confidence interval. This analysis was used to compare both the means among locations from the total interval counts and the 50-cm-quadrat interval counts. The 10 cm ANOVA test results show more significant difference among the locations than the interval spacing results showed. Most importantly it shows that the known regressive deposit locations of Crab Cay, Almgreen Cay, and Sandy Point are all significantly different from the two known transgressive deposit locations of North Point and French Bay (Figure 9).

DISCUSSION

The data show that measurements of vegemorph abundance and spacing in Bahamian eolianite outcrops can be used as a quantitative tool to differentiate transgressive-phase eolianites from regressive-phase eolianites. Outcrops previously mapped by Carew and Mylroie (1995a; 1997) as transgressive or regressive phase using a variety of criteria (Table 1) were shown to be identifiable using solely vegemorph data. These results have bearing on a question in Bahamian stratigraphy involving an interpretation that some of the deposits mapped by Carew and Mylroie (1995a; 1997) as regressive phase eolianites of the Cockburn Town Member of the Grotto Beach Formation. Based on AAR results, Hearty and Kindler (1993) mapped the units at Crab Cay, Almgren Cay, and The Bluff as MIS 5a, approximately 85 ka in age. The issue is fully discussed in Chapter 3 of Vacher and Quinn (1997), with presentations by workers on both sides of the issue. Regardless of the actual stratigraphic position, the vegemorph data indicate that these units are clearly different from transgressive-phase units, be they either Pleistocene in age (French Bay Member of the Grotto Beach Formation) or Holocene in age (North Point Member of the Rice Bay Formation). As noted earlier, the outcrop at The Gulf also falls in the regressive-phase position. That outcrop shows the eolianites have been deposited on top of a MIS 5e reef of the Cockburn Town Member (Mylroie and Carew, 2014). Between the two units is a calcarenite protosol, indicative of a short time of subaerial exposure (<2 ka), as opposed to the terra rossa paleosol that forms from long exposure (>10 ka). The vegemorph data indicates that The Gulf is regressive phase; given that it overlies a MIS 5e fossil reef without a long-term time of subaerial exposure before being buried by the eolianite eliminates MIS 5a as a stratigraphic option. By extension, Crab Cay, Almgren Cay, and The Bluff are also MIS 5e regressive-phase deposits; i.e. Cockburn Town Member of the Grotto Beach Formation. There remains the chance that Crab Cay, Almgren Cay, and The Bluff are MIS 5a regressive phase, but if so, no MIS 5a transgressive-phase eolianites have yet been identified.

The vegemorph data also allow two undifferentiated outcrops to be classified. Barkers Point fits the criteria for transgressive-phase eolianites, and Rocky Point fits the criteria for regressive-phase eolianites. Both of these outcrops are important, as they sit on the northwest side of San Salvador (Figure 4). This part of San Salvador displays a pattern of wind from the northwest in the interior dune structure (Figure 4), whereas the dunes on the east and central part of San Salvador show wind direction from the east (trade winds or easterlies). The northwest wind pattern associated with the Barkers Point and Rocky Point outcrops is thought to be the result of winter storms that come off the North American continent (Carew and Mylroie, 1995a; 1997). It is important that these two sites show the transgressive-phase and regressive-phase couplet of eolianite generation seen elsewhere on the island, independent of wind direction. On the east coast, the outcrop at The Thumb displays the highest vegemorph spacing interval of any regressive-phase eolianite. It is the only Owl's Hole unit in the data base (Owl's Hole itself was not used as the limited space within that pit cave did not allow for a long enough outcrop width for proper analysis), so it is not known if this spacing value is diagnostic of the Owl's Hole regressive-phase eolianites.

The data of Figure 9 suggest that a vegemorph spacing interval average of 15 cm separates transgressive-phase eolianites (>15 cm) from regressive-phase eolianites (<15 cm). If this relationship is truly valid, it means that workers in the field, after a few minutes of taking measurements and creating an average, can properly classify eolianites in terms of formation on the transgression or the regression. These results are preliminary, being restricted to the study of a few outcrops on a single island. San Salvador was an excellent choice for such a preliminary study, as the large amount of geologic data collected there over the years by many workers allowed a better characterization of the eolianites prior to the study. These factors give the authors' confidence that the tool is

valid and useable. Given that outcrops similar to those found on San Salvador are common over the entire Bahamian archipelago, it may prove a useful tool for bracketing transgressive-phase and regressive-phase eolianite depositional events during the interglacial cycles of the Quaternary.

CONCLUSIONS

A study of vegemorph abundance and spacing in Quaternary eolianites of The Bahamas allows differentiation of trangressive-phase eolianites from regressive-phase eolianites while in the field. In particular, an average vegemorph spacing distance of 15 cm separates transgressive-phase eolianites (>15 cm) from regressive-phase eolianites (<15 cm). Two outcrops of previously unknown classification, Barkers Point and Rocky Point on San Salvador Island, are now shown to be transgressive phase and regressive phase, respectively. Their location on a portion of the island displaying influence by northwesterly winds demonstrates that the transgressive-phase to regressive-phase couplet pattern holds true independent of wind direction. Using vegemorphs may assist in determining when eolianites on other Bahamian islands formed during each interglacial sea-level highstand. The work may also be applicable to other Quaternary eolianite locations, such as Bermuda in the North Atlantic, or Rottnest and Kangeroo Islands off the Australian coast.

ACKNOWLEDGEMENTS

The authors thank the Gerace Research Centre for logistical and technical assistance, and for the research permit, G-102, under which the work was done. Permission to visit private lands on San Salvador is greatly appreciated. The authors also thank the many geologists who have worked on San Salvador to provide the geological background that made this work possible. Thanks go in particular to Jim Carew and Al Curran.

REFERENCES CITED

Carew, J.L., and Mylroie, J.E. 1995a. A stratigraphic and depositional model for the Bahama Islands. Pp. 5-31. In H.A. Curran and B. White (Eds.). *Terrestrial and Shallow Marine Geology of the Bahamas and Bermuda.* Geological Society of America Special Paper 300.

Carew, J.L., and Mylroie, J.E. 1995b. Quaternary tectonic Stability of the Bahamian Archipelago: Evidence from fossil coral reefs and flank margin caves. *Quaternary Science Reviews* 14: 144-153.

Carew, J.L., Curran, H.A., Mylroie, J.E., Sealey, N.E., and White, B. 1996. *Field Guide to Sites of Geological Interest, Western New Providence Island, Bahamas*. Bahamian Field Station, San Salvador Island, Bahamas, 36 p.

Carew, J.L. and Mylroie, J.E. 1997. Geology of the Bahamas. Pp. 91-139. In H.L. Vacher and T.M. Quinn (Eds.). *Geology and Hydrogeology of Carbonate Islands.* Elsevier Science Publishers.

Curran, H.A. and White, B. 1987. Trace fossils in carbonate upper beach rocks and eolianites: Recognition of the backshore to dune transition. Pp. 242-254. In H.A. Curran and B. White (Eds.). *Proceedings of the 3rd Symposium on the Geology of the Bahamas.* CCFL Bahamian Field Station, Ft Lauderdale, FL.

Curran, H.A., Mylroie, J.E., Gamble, D.W., Wilson, M.A., Davis, R.L., Sealey, N.E., and Voegeli, V.J. 2004. *Geology of Long Island Bahamas: A Field Trip Guide.* Gerace Research Centre, San Salvador Island, The Bahamas, 24 p.

Droser, M.L. and Bottjer, D.J. 1986. A semiquantitative field classification of ichnofabric. J*ournal of Sedimentary Petrology* 56: 558-569

Foos, A. 1987. Paleoclimatic interpretation of paleosols on San Salvador Island, Bahamas. Pp. 67-72.

In H.A. Curran and B. White (Eds.). *Proceedings of the 3rd Symposium on the Geology of the Bahamas.* CCFL Bahamian Field Station, Ft Lauderdale, FL.

Hearty, P.J. and Kindler, P. 1993. New perspectives on Bahamian geology: San Salvador Island, Bahamas. *Journal of Coastal Research* 9: 577-594.

Kindler, P., Mylroie J.E., Curran , H.A., Carew, J.L., Gamble, D.W., Rothfus, T.A., Savarese, M., and Sealey, N.E. 2010. *Geology of Central Eleuthera, Bahamas: A Field Trip Guide.* Gerace Research Centre, San Salvador Bahamas, 74 p.

Mylroie, J.E., Carew, J.L., Curran, H.A., Freile, D., Sealey, N.E., and Voegeli, V.J. 2006. *Geology of Cat Island, Bahamas: A Field Trip Guide.* Gerace Research Centre, San Salvador Island, The Bahamas, 43 p.

Mylroie, J.E., Carew, J.L., Curran, H.A., Martin, J.B., Rothfus, T.A., Sealey, N.E., and Siewers, F.D. 2008. *Geology of Rum Cay, Bahamas: A Field Trip Guide.* Gerace Research Centre, San Salvador Island, The Bahamas, 59 p.

Mylroie J.E., Carew, J.L., Curran , H.A., Godefroid, F.M., Kindler, P., and Sealey, N.E. 2012. *Geology of New Providence Island, Bahamas: A Field Trip Guide.* Gerace Research Centre, San Salvador, The Bahamas, 57 p.

Mylroie J.E. and Carew J.C. 2014. *Field Guide to the Geology and Karst Geomorphology of San Salvador Island.* Gerace Research Centre, San Salvador Island, 90 p.

Mylroie, J.E. and Mylroie, J.R. 2017. The role of karst denudation on accurate assessment of glacio-eustasy and tectonic uplift on carbonate coasts, In M. Parise, F. Gabrovsek, G. Kaufmann, and N. Ravbar. (Eds). *Advances in Karst Research: Theory, Fieldwork, and Applications*, Geological Society, London, Special Publication 466, https://doi.org/10.1144/SP466.2

Panuska, B.C., Mylroie, J.E., and Carew, J.L. 1999. Paleomagnetic evidence for three Pleistocene paleosols on San Salvador Island. Pp. 93-100. In H.A. Curran and J.E. Mylroie (Eds.). *Proceedings of the Ninth Symposium on the Geology of the Bahamas and Other Carbonate Regions,* Bahamian Field Station, San Salvador Island, Bahamas.

Panuska, B.C., Boardman, M.R., Carew, J.L., Mylroie, J.E., Sealey, N.E., and Voegeli, V. 2002. Eleuthera Island Field Trip Guide, *Eleven Symposium on the Geology of the Bahamas and Other Carbonate Regions.* Gerace Research Center, San Salvador Island, The Bahamas, 20 p.

Vacher, H.L, and Quinn, T., 1997, *Geology and Hydrogeology of Carbonate Islands,* Elsevier Science Publishers.

Walker, L.N., Mylroie, J.E., Walker, A.D., and Mylroie, J.R. 2008. The Caves of Abaco Island, Bahamas: Keys to Geologic Timelines. *Journal of Cave and Karst Studies* 70: 108-119.

THE 2ND JOINT SYMPOSIUM ON THE NATURAL HISTORY AND GEOLOGY OF THE BAHAMAS

June 8th to June 12th, 2017

GERACE RESEARCH CENTRE
UNIVERSITY OF THE BAHAMAS
SAN SALVADOR, THE BAHAMAS

PROGRAM CO-CHAIRPERSONS:

Tina M. Niemi

Department of Geosciences
University of Missouri-Kansas City
Kansas City, MO

Kathleen Sullivan Sealey

Department of Biology
University of Miami
Coral Gables, FL

KEYNOTE SPEAKER:

Kam-biu Liu

Department of Oceanography and Coastal Sciences
Louisiana State University
Baton Rouge, LA

ORGANIZER:

Troy A. Dexter

Executive Director
Gerace Research Centre
University of The Bahamas
San Salvador, The Bahamas

DYNAMICS OF PHYSICAL DEPOSITION AND BIOTURBATION OF PLEISTOCENE CARBONATE SUBTIDAL SEDIMENTS, HARRY CAY SITE, LITTLE EXUMA, BAHAMAS

Beckham, Abigail, Smith College, Northampton, MA; **Graveline, Alyssa,** Smith College, Northampton, MA; **Reyna Alvarez, Nathaly,** Smith College, Northampton, MA; **Glumac, Bosiljka ,** Smith College, Northampton, MA; **Curran, H. Allen,** Smith College, Northampton, MA.
Presenter: Bosiljka Glumac, Poster 15

Pleistocene subtidal carbonate deposits of the Cockburn Town Member, Grotto Beach Formation at Harry Cay on Little Exuma Island contain a diverse assemblage of trace fossils, which can be used to assess the impact of burrowing organisms within these sediments. We conducted fieldwork, collected hand samples, and did petrographic analysis of thin sections of individual trace fossils and host rock samples in order to determine how the trace fossils differ from and have modified the host rocks. The stratigraphic section exposed in a large boulder present at Harry Cay Marina exhibited three distinct units and contained individual well-developed *Ophiomorpha*, *Conichnus*, and *Planolites* trace fossils (*Skolithos* also was present, but could not be sampled owing to its small diameter). Unit 1 is 30-50 cm thick and composed of ooid-peloidal grainstone, with some horizontal laminations and an ichnofabric index of 3. Unit 2 is 25-30cm thick and has the same composition as Unit 1, but is extensively bioturbated with a ichnofabric index of 5 (maximum). Unit 3 is 45 cm thick and composed of ooid-skeletal grainstone with well-developed cross bedding and an ichnofabric index of 1. A thick caliche crust tops the unit. Individual trace fossil samples were collected *in situ* from Unit 1 and as loose specimens weathered out from Unit 3 and its equivalents. All units were initially lithified in the marine realm but subsequently were subjected to meteoric diagenesis.

Ophiomorpha burrows, formed by callianassid shrimp, are common at Harry Cay. There are significant compositional differences between the micrite-rich walls of *Ophiomorpha* and the ooid-peloidal grainstone host rock. Like the mature *Ophiomorpha*, the samples of the juvenile *Ophiomorpha puerilis* have much more micrite in the pellets forming the burrow walls relative to the host rocks. This suggests the shrimp are concentrating micrite during their pellet-making and burrow-construction activities, while selectively eliminating coarser sediment grains. A comparative analysis of a subtidal exposure (equivalent to Harry Cay Unit 3) on nearby Great Exuma Island also revealed greater concentration of micrite in *Ophiomorpha* burrow walls relative to their ooid-skeletal packstone/grainstone host rock.

The interiors of *Planolites*, which are burrows filled with sediment that has passed through the gut of ballanoglossid worms, are finer grained than the host rock suggesting that the worms sorted the sediment while ingesting it, with larger grains pushed aside.

The trace fossil *Conichnus conicus*, thought to have formed by the upward movement of burrowing sea anemones, shows a difference in sediment fabric: sand grains appear more closely packed in the host rock compared to *Conichnus* trace fossil, which also seems better lithified relative to the surrounding sediment. This could be explained by the burrowing of the anemone creating a more open, porous fabric that allows for greater concentration of diagenetic fluids and more cement precipitation.

Our results demonstrate that burrowing organisms can modify the composition, texture, and fabric of subtidal carbonate sand-rich sediment through processes of micrite concentration and compaction (*Ophiomorpha*), sand sorting (*Planolites*) and repacking (*Conichnus*), respectively. In conjunction with ichnogenic megaporosity formation associated with open-burrow networks and differential lithification of sediment, these processes can increase heterogeneity of porosity and permeability distribution in carbonate rocks, impacting their aquifer properties.

IMPACT OF OCTOBER 2016 HURRICANE MATTHEW ON SEDIMENT-STARVED SOUTHERN COAST OF LITTLE EXUMA ISLAND, BAHAMAS

Chang , Jessica , Smith College, Northampton, MA; **Eastman, Elsie,** Smith College, Northampton, MA; **Howard, Susannah,** Smith College, Northampton, MA; **Glumac, Bosiljka ,** Smith College, Northampton, MA; **Curran, H. Allen,** Smith College, Northampton, MA; **Savarese, Michael,**
Florida Gulf Coast University, Fort Myers, FL.
Presenter: Bosiljka Glumac, Poster 16

Conch House Beach is a leeward, sediment-starved setting on the south coast of Little Exuma Island, Bahamas that was recently impacted by Hurricane Matthew, a major category 3 hurricane whose eye passed just offshore to the southwest of the study site on October 6, 2016. The goal of our research was to better understand the storm's impact and general depositional patterns along this reach of coast through field and petrographic observations and analysis of historical aerial imagery.

Petrographic analyses of beach sand indicate that it is predominantly composed of heaviliy micritized ooids and lithoclasts derived from weathering of the bedrock (mainly Holocene beachrock and eolian ooid grainstones), with subordinate amounts of skeletal fragments. The unusual brown color of beach sand at this site indicates subaerial weathering in the presence of iron oxides and supports low rates of sediment transport to and deposition in this setting. Historical Google Earth images from 2013 and 2016 also indicate a consistently sand-starved beach environment, with large quantities of dark, weathered bedrock exposed.

The presence of abundant ooids in beach sand and bedrock here supports the interpretation that leeward settings of Bahamian islands are conducive to ooid formation. Our observations suggest that ooids are likely forming in wave-agitated shallow offshore waters <2 m deep. In deeper waters farther offshore, sediment is being stabilized by an organic microbial film. In conjunction with relatively low fair-weather wave energy, this prevents large quantities of sand from being easily transported and deposited on the beach, leading to the general sediment-starved conditions observed here.

Erosion by hurricanes is also a major factor that impacts this coastal setting. Evidence of erosion by Hurricane Matthew, observed in January 2017, included the abundance of freshly exposed, light color bedrock with erosional scars reaching as high as 3.5 m above mean sea level along these steep coastal cliffs. The striking color contrast with dark, weathered bedrock can also be used to examine the formation of new bedrock-derived boulders and their movement and deposition by storm waves. Imbrication direction of recently moved tabular boulders as large as 90 cm in diameter is consistent with their landward transport by storm waves. Boulders encrusted with fresh bivalves were found on the beach more than 10 m from the water's edge, indicating substantial transport by recent storm waves from the shallow offshore subtidal environment. Another major evidence of beach and dune sand erosion and landward transport by Hurricane Matthew was the deposition of a 1 m-thick washover fan into the adjacent mangrove swamp. These observations indicate that storms have a major impact on the style and rate of sedimentation and erosion in this otherwise relatively low-energy coastal setting. This should be taken into account, together with the documented low rates of sediment deposition and high rates of erosion, in any future plans for development along this reach of coast.

CONFIRMATION OF THE OCCURRENCE OF *SYNAPTULA HYDRIFORMIS*, THE "NAKED SEA CUCUMBER", IN OYSTER POND, SAN SALVADOR ISLAND, AND DEMONSTRATION OF INDUCIBLE "LIVE BIRTH" AND SELF-FERTILIZATION

Cole, Eric, S, St. Olaf College, Northfield, MN; **Hahn, Leigh Anne,** St. Olaf College, Northfield, MN; **Thacker, Miranda, C,** St. Olaf College, Northfield, MN; **Choquette, Jessica, M,** St. Olaf College, Northfield, MN.
Presenter: Eric S. Cole, Friday 8:30 AM

We confirm the wide-spread occurrence of the Apodid sea cucumber *Synaptula hydriformis*, in Oyster Pond on San Salvador Island, Bahamas. Three color morphs are described including one that is nearly transparent. Visible inside the colorless morphs, we detect growing juveniles exhibiting "matrophagy" (deriving nourishment from their

mother's tissues). We describe a technique for inducing live birth, and stimulating self-fertilization. Histology reveals an "ovo-testis" capable of simultaneously expressing eggs and sperm. All these observations confirm that this species is capable of simultaneous hermaphroditism, and internal self-fertilization (consistent with its identification). Developmental analysis reveals direct development without a plantkonic larvae, and completion of the adult body form within 24 hours of fertilization. All these traits recommend this holothurian as a "model organism" for the study of invertebrate embryology. The life-history of this organism suggests that it can propagate clonally, making it an ideal colonist of the inland anchialine pond habitats.

EFFECTS OF HURRICANE JOAQUIN ON SILVER THATCH PALMS ON SAN SALVADOR: WIND AND OVERWASH

Cross, Randall, E, Florida Gulf Coast University, Fort Myers, Florida; **Goebel, Anna, M,** Florida Gulf Coast University, Fort Myers, Florida.

Presenter: Randall Cross, Poster 7

Hurricane Joaquin's impact on San Salvador in October of 2015 had dramatically different effects on three populations of silver thatch palm (Coccothrinax argentata). Two populations (Rocky Point and Grotto Beach were part of a long-term study of population structure and dynamics initiated more than a year before the hurricane. Data was collected for the first time at Sandy Hook, on the southern part of the island, in 2016, 8 months after the hurricane. We expected to find extensive mortality of palms across the island. We were surprised to observe very little mortality that could be attributed to the storm in our study populations at Rocky Point and Grotto Beach. However, we found significant mortality at Sandy Hook, but the heavy mortality was confined to a relatively small area. Because the heavily impacted area had a significant overwash event from the storm, we set up study plots in the overwash area and an adjacent unaffected area to quantify the level of mortality of juvenile and adult trees in this area. The level of mortality in the overwash area was > 76% while the level of mortality in the nearby unaffected area was < 0.1%. Since dead adult trees were still standing the likely cause of mortality seemed to be not from direct wind damage or direct wave impact from the storm. We hypothesized that the main cause of mortality in the affected overwash area was indirectly due to storm surge through the inundation of sediments with salt water. We collected soil samples from both of the areas and found that the soil salinity was significantly greater ($p < 0.05$) in the over wash area (872.8 uS/cm versus 207.7 uS/cm). These data demonstrate a significant difference in soil salinity at this site and support the hypothesis that the likely cause of mortality was due to the higher soil salinity levels and mortality from wind and waves was minimal. This study also demonstrated that elevated soil salinity levels can persist for almost 9 months following overwash events.

LATE HOLOCENE HISTORICAL ECOLOGY: THE TIMING OF VERTEBRATE EXTIRPATION ON CROOKED ISLAND, COMMONWEALTH OF THE BAHAMAS

Delancy, Kelly, M, National Museum of The Bahamas, Marsh Harbour, Abaco; **Albury, Nancy, A,** National Museum of The Bahamas, Marsh Harbour, Abaco; **Steadman, David, W,** Florida Museum of Natural History, Gainesville, Florida;
Singleton, Hayley, M, Florida Museum of Natural History, Gainesville, Florida; **Soto-Centeno, J. Angel,** American Museum of Natural History, New York, New York.

Presenter: Kelly Delancy, Friday 9:00 AM

We report eight new accelerator-mass spectrometer (AMS) radiocarbon (14C) dates done directly on individual bones of extirpated species from Crooked Island, The Bahamas. Three dates from the hutia (Geocapromys ingrahami), recovered from a culturally derived bone assemblage in McKay's Bluff Cave (site CR-5), all broadly overlap from AD 1450 to 1620, which encompasses the time of first European contact with the Lucayan on Crooked Island (AD 1492). Marine fish and hutia dominate the bone assemblage at McKay's Bluff Cave, shedding light on vertebrate consumption by the Lucayans just before their demise. A fourth AMS 14C date on a hutia bone, from a non-cultural

surface context in Crossbed Cave (site CR-25), is similar (AD 1465 to 1645) to those from McKay's Bluff Cave. From Pittstown Landing (site CR-14), an open coastal archaeological site, a femur of the Cuban crocodile (*Crocodylus rhombifer*) yielded an AMS 14C date of AD ~1050-1250, which is early in the Lucayan cultural sequence. From a humerus in a non-cultural surface context in 1702 Cave (site CR-26), we document survival of the Cuban crocodile on Crooked Island until AD ~1300-1400, which is several hundred years later than the well documented extinction of Cuban crocodiles on Abaco in the northern Bahamas. We lack a clear explanation of why Cuban crocodiles likely survived longer on Crooked Island than on a larger Bahamian island such as Abaco. One AMS 14C date on Crooked Island's extinct, undescribed species of tortoise (*Chelonoidis sp.*) from 1702 Cave is BC 790 to 540 (2740 to 2490 cal BP), which is ~1500-1700 years prior to human arrival. A second AMS 14C date, on a fibula of this tortoise from McKay's Bluff Cave, is AD 1025 to 1165, thereby demonstrating survival of this extinct species into the period of human occupation.

LIFE AMONG THE WASPS: A REVIEW OF STUDIES ON *CERCERIS WATLINGENSIS* ELLIOTT & SALBERT (HYMENOPTERA: SPHECIDAE) IN THE BAHAMAS

Elliott, Nancy, B, Siena College, Loudenville, NY; **Landry, Carol, L,** The Ohio State University, Mansfield, OH.
Presenter: Nancy Elliott, Friday 9:30 AM

In November 1975, the first Hartwick College class on Bahamian arthropods was conducted on San Salvador. Experts at the U.S. National Museum determined that one of the collected wasps was a new species, which Elliott later described. The wasp was named *Cerceris watlingensis*; the species has since been collected on other southern islands of the Bahamas archipelago. Over the years, we conducted a number of field studies on the behavior of *C. watlingensis* on San Salvador, including several aspects of nesting behavior. Females preyed on weevils, primarily an *Artipus* species that was carried to the nest in flight but was not paralyzed. In contrast, most sphecids paralyze prey before carrying them to the nest. Nest excavations showed numerous nest cell chambers below the end of a main entrance channel; the oldest cells were as deep as 60 cm below the soil surface. Since females spent little time within the nest between foraging flights, we assumed that prey were initially deposited in the main channel and later moved to cells deeper in the nest. At first, most nests appeared to contain a solitary female, but we found one nest that contained at least two. In subsequent studies, wasps were labeled with unique patterns of paint that allowed us to identify each individual. These studies demonstrated that nest sharing was more common than previously thought, and is the result of two different aspects of behavior: young females remained within the parental nest for several days after emergence, or switched into a pre-existing nest some distance from the natal nest. In either case, nest sharing did not result in obvious aggressive behavior. We also observed individually-marked males on *Croton linearis* at a nesting site near the north end of San Salvador. There was a significant linear relationship between male visits to the plants and the number of days that nearby nests were active. This behavior might increase the probability that males find and mate with virgin females as they emerge from their nests. Since that time, we have observed wasps making floral visits to at least seven additional plant species.

HURRICANE JOAQUIN IMPACTS ON OYSTER POND, SAN SALAVADOR, BAHAMAS

Ford, Dawn, M, The University of Tennessee at Chattanooga, Chattanooga, TN; **Abernathy, Jalana,** The University of Tennessee at Chattanooga, Chattanooga, TN; **Mitchell, Ashton,** The University of Tennessee at Chattanooga, Chattanooga, TN;
Black, Luke, The University of Tennessee at Chattanooga, Chattanooga, TN; **Schwartz, Alex,** The University of Tennessee at Chattanooga, Chattanooga, TN; **Novak, Sabrina ,** University of Tennessee at Chattanooga, Chattanooga, TN.
Presenter: Dawn Ford, Friday 7:30 PM

Over the past 4 years, studies of interior pond biota have been conducted by UTC on San

Salvador, Bahamas. In 2015, Hurricane Joaquin directly impacted the island and disturbed the mangrove vegetation, pond biota, and sediment of many of the interior ponds, including Oyster Pond. Oyster Pond is a fully marine pond lined by red mangroves (*Rhizophora mangle*) and has a number of conduits connecting the pond to the ocean and perhaps other ponds. The post-hurricane recovery of pond biota, specifically those living on biotic outcroppings and mangrove prop roots, is currently being investigated with a focus on macroalgae and invertebrates. Comparisons with pre-hurricane data reveal that in general green macroalgal species have recovered, while several red and brown macroalgal species have not successfully reestablished. In comparing the western side of the pond to the less impacted eastern side of the pond, the data suggest that the more impacted mangroves can support fewer algal and invertebrate species and in less abundances than healthy mangroves. This finding might be explained by the detrital nature of mangrove systems.

THE LONG-TERM IMPACTS OF A BAHAMAS FIELD EXPERIENCE ON STUDENT PARTICIPANTS

Ford, Dawn, M, The University of Tennessee at Chattanooga, Chattanooga, TN; **Eshbaugh, Hardy,** Miami University, Oxford, OH; **Branson, R. Christopher,** Jane and Terry Semel Research Institute for Neuroscience and Human Behavior at UCLA, Los Angeles, CA.
Presenter: Dawn Ford, Poster 9

For many years, Bahamian field courses have been taught by faculty at Miami University and the University of Tennessee at Chattanooga (UTC). While it is assumed that these experiences are very impactful on students, little is documented about the long-term effects of such experiences on students' personal and professional development. The purpose of this study was to assess the perceived impacts of these courses on former students' development using a 25-question instrument. In November 2015-January 2016, the online survey was administered to former students of Bahamas field courses offered by these institutions between 1977 and 2014. Of the 450 former students contacted, 156 responded to the survey. Survey results showed that a high proportion of respondents "agreed" that the experience had a high impact on their personal development, professional development, and international perspective. Additional analyses indicated no statistically significant differences between groups or within groups, suggesting that perceived impacts are the same for both institutions, males and females, and all age groups. The top benefits of Bahamian field courses reported by the respondents included exposure to Bahamian culture, establishing relationships with faculty and peers, and participating in hands-on experiences. There were overwhelmingly positive comments made by respondents and many cited the course as life-changing. These findings support the continued offering of such experiences.

STORM-DEPOSITED BOULDER RIDGES ALONG ROCKY SHORELINES OF SAN SALVADOR ISLAND, BAHAMAS: LONG-TERM MONITORING AND SIGNIFICANCE

Glumac, Bosiljka , Smith College, Northampton, MA; **Curran, H. Allen,** Smith College, Northampton, MA.
Presenter: Bosiljka Glumac, Friday 8:00 PM

Monitoring changes in morphology and distribution of coastal boulder ridges and the direction and amount of movement of individual large boulders can provide useful information about the intensity and effects of storms that impact Bahamian island coasts. We have ongoing monitoring projects for two boulder ridges on San Salvador: one along the reef- and lagoon-protected northern coast around Singer Bar Point (SBP, length ~790 m) and the other on the high-energy southern coast west of The Gulf (TG, length ~460 m).

Our initial work in January 2012 described the SBP ridge as wide (up to 14 m) and with a low crest (~1.5 m above mean sea level), whereas the TG ridge was generally narrower, with a sharp crest located on a cliff-bench 3-5 m above mean sea level. The largest boulders from each site were photographed, located with GPS coordinates, measured (length, width, thickness), and characterized by composition (subtidal calcarenite, coral

rubblestone, eolianite, lithified paleosol), shape (tabular or irregular), and degree of roundness.

Largest boulders at SBP are generally smaller (15 total; ~150-4000 kg; with most <1500 kg) and more rounded than those at TG (12 total; ~700-4500 kg; with all but one >1000 kg). Boulders are eroded from the seaward rocky coast, transported and deposited by high-energy storm waves. Smaller size and better rounding of clasts are more common at SBP than TG, indicating multiple events of milling in the surf prior to deposition along this low-profile coast as compared to the high cliff-profile TG coast. The presence of larger boulders and fossil coral rubblestone boulders at TG indicates that stronger storm waves were required to erode and transport them.

Our monitoring from January 2013, 2016, and 2017, after Hurricanes Sandy (October 2012), Joaquin (October 2015), and Matthew (October 2016), respectively, resulted in only modest modifications to the SBP ridge along the protected northern shore. In contrast, the TG area along the high-energy southern shore was drastically modified: we were not able to relocate 2 boulders post-Sandy, and only 5 of the remaining boulders were relocated with certainty after Joaquin. Two of those, weighing ~2 tons each, were transported as much as 20 m and 26 m inland to the NNW. The southern edge of the boulder ridge moved landward by 4-5 m exposing an underlying Pleistocene/Holocene boundary *terra rossa* paleosol, which stands out in aerial images and can be used to map the extent of storm erosion. Joaquin modified the formerly sharp-crested, narrow boulder ridge into a larger, broad boulder field stripped of vegetation. Boulders of various sizes covered sections of the island's main coastal road (cleared and back in service as of spring 2017). Post-Hurricane Matthew, which passed too far from the coast of San Salvador to have any major impact, 10 new boulders and high-resolution drone aerial imagery were added to our monitoring program at TG. Information on the distribution and morphology of boulder ridges and the dynamics of their modification are long-term indicators of storm patterns and activity and should be used to inform coastal development on San Salvador and elsewhere in the Bahamas.

PLANT-SEDIMENT INTERACTIONS IN TERRESTRIAL AND SHALLOW MARINE ENVIRONMENTS OF THE BAHAMAS: EXAMPLES AND IMPLICATIONS

Glumac, Bosiljka , Smith College, Northampton, MA; **Curran, H. Allen,** Smith College, Northampton, MA.
Presenter: Bosiljka Glumac, Poster 14

Quaternary deposits in the Bahamas reveal multiple examples of substrate modification by terrestrial and marine plants that constitute important evidence of past vegetation and can be used as paleoclimate indicators of temperature and precipitation regimes. Modification of sediment by plants can also produce significant amounts of post-lithification porosity and permeability, which can increase reservoir quality of the host rocks. Various modes of plant root preservation in the form of rhizoliths are the most common evidence of such plant-sediment interactions in the Bahamas. Another well-known example includes the role of red mangrove (*Rhizophora mangle*) root systems in trapping sediment and preventing coastal erosion. Here we discuss other less well documented examples of plant interactions with carbonate sediment from Bahamian coastal and shallow subtidal settings to demonstrate their highly variable nature and products. These examples include: 1) eolian deposits with impressions of silver thatch palm fronds (*Coccothrinax argentata*); 2) impressions of terrestrial plant roots (sea grape = *Coccoloba uvifera*), prostrate stems (bay geranium = *Ambrosia hispida*), runners (railroad vine = *Ipomoea pes-caprae*), and blades (sea oats = *Uniola paniculata*) in eolian and back-beach deposits; 3) large vertical pipes present in Holocene eolianite and possibly representing buried palm tree trunks and/or roots, which may also exploit pre-existing paths created by dissolution or other mechanisms; 4) highly porous "spongiform" texture of Holocene eolianite, which likely forms by sand trapping and lithification around dense roots, stems and organic litter of grass and shrub vegetation, including various microbial, fungal and insect communities, as well as

accumulation and burial of marine algae (e.g., *Sargassum*) and seagrasses in beach sediment; and 5) extensive modern seagrass (*Thalassia testudinum*) root systems that trap sediment in shallow marine subtidal settings and have potential to leave traces in the geological record, but have not commonly been documented from ancient strata. Similarly, large and extensive palm tree roots do not seem to be easily preserved and recognized in carbonate grainstones, but they may be partially responsible for producing the commonly observed spongiform texture of Holocene non-marine deposits in the Bahamas.

DISTRIBUTION AND NATURE OF MICROBIALITES IN THE COCKBURN TOWN FOSSIL REEF (PLEISTOCENE, GROTTO BEACH FORMATION), SAN SALVADOR ISLAND, BAHAMAS: PRELIMINARY RESULTS

Griffing, David, H., Hartwick College, Oneonta, NY; **Kortright, Skylar,** Hartwick College, Oneonta, NY; **Glumac, Bosiljka,** Smith College, Northampton, MA; **Curran, H. Allen,** Smith College, Northampton, MA.
Presenter: David Griffing, Poster 17

The Sangamonian (MIS 5e) Cockburn Town reef (Grotto Beach Fm.) on San Salvador Island, Bahamas, is an important source of data for the debate regarding rapid sea-level changes during the last interglacial highstand. Although Cockburn Town reef microbialites have been previously identified, details of their distribution remained unexplored. Preliminary re-examination of these deposits reveals a complex distribution of microbialites in relation to major and minor discontinuities within the reef deposit. A widespread erosional hardground surface separates Reef I and II developmental phases. Exposures of coral floatstone and framestone well below this hardground surface exhibit pristine coral material as well as fragments with 1-5 mm-thick skeletal encrustations typical of normal post-mortem colonization in modern Bahamian reefs. Higher Reef I strata exhibit branching corals and fragments with discrete upward-thickening coatings of laminated micrite-skeletal silt that cover early skeletal crusts. SEM examination of broken laminar surfaces reveals small tubular casts resembling microbial filaments, supporting a microbial origin for these coatings. Microbial coatings increase in abundance and in thickness upward, from a few thin coatings that comprise 2-5% of the rock, to 30-80mm thick coatings on most branches. Immediately below the Reef I-II boundary hardground, both laminated and clotted microbialite forms microbial-skeletal boundstone that coalesces between coral branches to comprise 40-50% of the rock (and locally > 80%). In one area, thin drapes of skeletal-ooidal grainstone form shingled partitions within the dense microbial-skeletal boundstone and indicate episodes of lateral accretion. In contrast to Reef I deposits, most of the corals and coral fragments in overlying (Reef II) deposits examined lack microbialite coatings, and display little or no skeletal encrustation, abrasion or corrosion. Still, Reef II strata are truncated by two hardgrounds (one mid unit and one capping the reef deposit that is part of the major regression leading into the last glacial). Assuming the reef coral to microbialite transition developed in response to environmental changes associated with sea-level drop, then the Cockburn Town reef microbialites and hardgrounds support previous interpretations that at least one (and perhaps more) short-term sea-level fluctuation occurred during the last interglacial highstand.

LIFE HISTORY AND SEXUAL HISTOLOGY OF *SYNAPTULA HYDRIFORMIS*

Hahn, Leigh, A, St. Olaf College, Northfield, MN; **Cole, Eric, S,** St. Olaf College, Northfield, MN.
Presenter: Leigh Anne Hahn, Poster 6

Synaptula hydriformis (Lesueur, 1824) is a hermaphroditic self-fertilizing sea cucumber. A unique feature of this species is their ovo-testis and viviparous abilities. Through histology done in January 2016, this organ was found to contain both sperm and eggs. The ovo-testis's existence has been verified by past researchers who studied the species, although there was debate over whether or not an individual could self-fertilize. Its viviparity is fairly unique among other synapula who tend to release gametes into the water instead. *S.*

hyrdriformis was first found in the Bahamas in 1886, but little research has been done on specimens from the area. The species has been found everywhere from Bermuda to Brazil, but the coloration of local species appears to be different than most places. Specimens are mostly commonly observed as either red or green, but individuals from Oyster Pond come in clear, brown, and striped varieties.

TROPICAL ANCIENT DNA REVEALS RELATIONSHIPS OF THE EXTINCT BAHAMIAN GIANT TORTOISE *CHELONOIDIS ALBURYORUM*

Kehlmaier, Christian, Museum of Zoology, Senckenberg Dresden, Germany; **Albury, Nancy, A,** National Museum of The Bahamas, Abaco, The Bahamas; **Barlow, Axel,** University of Potsdam, Potsdam, Germany; **Hastings, Alexander, K,** Virginia Museum of Natural History, Martinsville, Virginia; **Steadman, David, W,** Florida Museum of Natural History, Gainesville, Florida.
Presenter: Nancy Albury, Poster 1

Ancient DNA of extinct species from the Pleistocene and Holocene has provided valuable evolutionary insights. However, these are largely restricted to mammals and high latitudes because DNA preservation in warm climates is typically poor. In the tropics and subtropics, non-avian reptiles constitute a significant part of the fauna and little is known about the genetics of the many extinct reptiles from tropical islands. We have reconstructed the near-complete mitochondrial genome of an extinct giant tortoise from the Bahamas (*Chelonoidis alburyorum*) using an approximately 1000-year-old humerus from a water-filled sinkhole (blue hole) on Great Abaco Island. Phylogenetic and molecular clock analyses place this extinct species as closely related to Galapagos (*C. niger* complex) and Chaco tortoises (*C. chilensis*), and provide evidence for repeated overseas dispersal in this tortoise group. The ancestors of extant *Chelonoidis* species arrived in South America from Africa only after the opening of the Atlantic Ocean and dispersed from there to the Caribbean and the Galapagos Islands. Our results also suggest that the anoxic, thermally buffered environment of blue holes may enhance DNA preservation, and thus are opening a window for better understanding evolution and population history of extinct tropical species, which would likely still exist without human impact.

TEMPORAL STABILITY OF *ORBICELLA ANNULARIS* SYMBIOSES: A BAHAMIAN CASE STUDY

Kennedy, Emma, V, University of Exeter, Exeter, UK; **Stevens, Jamie, R,** University of Exeter, Exeter, UK.
Presenter: Jamie Stevens, Friday 10:30 AM

Orbicella annularis is unusual among Caribbean corals in being flexible in terms of the symbiont taxa it can associate with. Recent papers have explored the extent of this flexibility across a large spatial scale (almost the entire species range), describing symbioses with 22 endosymbiont clades and exploring a variety of environmental gradients, geographic distance and host genetic diversity. However, the *Symbiodinium* communities of *O. annularis* have also been shown to fluctuate on a temporal scale, both in terms of density (e.g., seasonal fluctuations in abundance), and in response to environmental stressors (sporadic changes in abundance and in community composition). Some corals, such as *Acropora millepora*, demonstrate very variable symbiont communities from year to year. In order to explore the robustness of observed spatial patterns, it is necessary to investigate the temporal stability of symbiont communities. In this paper we describe a small-scale study in which we used denaturing gel gradient electrophoresis (DGGE) and ITS2 ribosomal DNA sequence profiles to assess the stability of symbiont communities in *O. annularis* at four sites in the Bahamas, across a period of six years.

THE IMPACT OF HABITAT TYPE ON COMPETITIVE INTERACTIONS BETWEEN ALIEN FIRE ANTS AND ANT SPECIES ASSEMBLAGES ON SAN SALVADOR ISLAND, THE BAHAMAS

Kjar, Daniel, Elmira College, Elmira, NY; **Park, Zachory,** Georgetown University, Washington, DC.
Presenter: Daniel Kjar, Poster 2

On San Salvador Island, The Bahamas, Solenopsis invicta (Red Imported Fire Ant) is an invasive species that was believed to be introduced into the Caribbean around 1890. The purpose of this study was to determine if habitat type affects the competitive interactions between the alien fire ant, S. invicta, and native ant species assemblages on the island. Extensive ant sampling and observation were conducted in three distinct habitat types on San Salvador Island; palmetto, blackland (coppice), and plantations during 2014 and 2015. Here we create an index (PK index) which ranks ant species based on their effectiveness as competitors across all habitats based on how often they come to baits in a particular habitat, how quickly they arrive, and how quickly they recruit to the bait compared to the average of other ants in the study. Our data show that interactions and foraging behavior among ant species change substantially among habitats. Solenopsis invicta and other invasive species appear to have a competitive advantage in terms of arrival and recruitment to baits in the once heavily disturbed plantation habitat and the continuously disturbed palmetto habitat. However, S. invicta had the highest PK index in only the plantation habitat. This suggests that some set of factors present in the plantation habitat are contributing to the success of the species in that habitat and are not present in the other habitats in this study.

GENETIC DIVERSITY AT 6 MICROSATELLITE MARKERS IN THE LONG HORNED CRAZY ANT OF SAN SALVADOR ISLAND, THE BAHAMAS, AND ITS ASSOCIATION WITH HABITAT DOMINANCE.

Kjar, Daniel, Elmira College, Elmira, NY; **Yaw, Bridget,** Elmira College, Elmira, NY; **Miller, Ashley,** Elmira College, Elmira, NY.
Presenter: Ashley Miller, Poster 3

During the field summers of 2014 and 2015 field observations of ant interactions at baits on San Salvador Island, The Bahamas, showed that *Paratrechina longicornis*, an introduced invasive ant species, appeared to have two distinct behaviors. In some locations *P. longicornis* rapidly recruited massive numbers of foragers to baits and in other locations had very poor competitive abilities with other species (regardless of apparent nest density or local abundance). In order to further examine these outcomes we collected *Paratrechina* from as many locations as possible, along with behavioral data, and we will look at the genetic diversity among these populations using 6 microsatellite markers. Due to the nature of species introductions (often a single queen or nest), populations of introduced ant species often have little genetic variability leading to increased cooperation among nests and release from conspecific competition. We believe that there may be two distinct genotypes on the island and areas where competitive abilities are low may be a different population from those where *Paratrechina longicornis* has dominated the local ant community.

DORYMYRMEX ANTILLANA, RED IMPORTED FIRE ANTS, AND THE LONG HORNED CRAZY ANT: A LOOK AT WHAT I HAVE LEARNED ABOUT THE ANT COMMUNITY ON SAN SALVADOR

Kjar, Daniel, Elmira College, Elmira, NY.
Presenter: Daniel Kjar, Friday 11:00 AM

On San Salvador Island, The Bahamas, ants are a dominant member of the animal community. No matter where you go, and sit, you will encounter ants and often more than just one. Over the last 9 years I have been examining several aspects of this community. Habitat plays a very important role in determining the ant community and the competitive interactions among species. Along with habitat, genetics may play a role in these interactions and I will discuss the genetics and habitat of one of the world's most invasive species, the Long Horned Crazy Ant, present all over the island but not always in dense populations. Lastly, I will describe our recent work on an interesting ant species, *Dorymyrmex antillana*. A common native species on San Salvador and throughout the Bahamas, but one that has a only recently been recognized as its own species.

SPATIAL VARIATION IN MOLLUSK COMMUNITIES AROUND SAN SALVADOR ISLAND, BAHAMAS

Kowalewski, Michal, Florida Museum of Natural History, University of Florida, Gainesville, FL; **Casebolt, Sahale,** Florida Museum of Natural History, University of Florida, Gainesville, FL.
Presenter: Michal Kowalewski, Friday 11:30 AM

Surficial accumulations of mollusk shells may provide minimally invasive, quantitative data potentially suitable for assessing spatial organization of local benthic ecosystems. We collected 61 bulk samples along 12 transects to evaluate distribution and ecological characteristics of mollusk-dominated benthic communities around San Salvador Island, Bahamas. The samples yielded a total of 20,608 specimens, which represented a minimum of 181 mollusk species. Indirect multivariate ordinations (NMDS) separated samples by locality (even in the case of transects sampling different parts of the same bay) indicating that shell assemblages faithfully archive local differences in mollusk communities. At the regional scale, a clear faunal separation is observed between windward and leeward sides of the island, suggesting that water energy represents an overriding regional driver controlling local community composition. Within each energy regime, the faunal composition of mollusk assemblages is primarily controlled by seagrass vegetation. The results indicate that San Salvador benthic communities are characterized by a predictable spatial organization controlled primarily by physical and, secondarily, biological (seagrass vegetation) processes. That these patterns can be discerned so clearly by sampling shell assemblages suggests that studies centered on dead mollusks provide a viable and largely non-invasive strategy for examining processes that drive spatial structuring of marine communities locally and regionally.

TRENDS IN FLOWERING PHENOLOGY AND FLOWERING INTENSITY FOLLOWING THREE HURRICANES

Landry, Carol, L, The Ohio State University, Mansfield OH; **Elliott, Nancy, B,** Siena College, Greenlawn NY.
Presenter: Carol Landry, Friday 7:00 PM

The purpose of this study was three-fold: to describe trends in the flowering phenology and flowering intensity of plants in coastal communities following hurricanes, to compare these characteristics in years with and without hurricanes, and to determine if plants that produced flowers received visits from insect pollinators at the same rate in years with and without hurricanes. The study is part of a larger research program investigating the role of plant-insect interactions in the maintenance of biodiversity in Bahamian coastal plant communities, which experience frequent, sometimes catastrophic, hurricanes. Data were collected on San Salvador Island, The Bahamas, during the first half of December in years 2010-2016, and in October 2011. Three hurricanes impacted San Salvador during this timeframe: Irene (Category 3, August 2011), Sandy (Category 2, October 2012), and Joaquin (Category 4, October 2015). Data were collected over 6-12 days at the same site locations on the island. In years following hurricanes, we recorded vegetative damage within 200 m of the coast; in all years, we recorded the floral condition of all coastal plant species, estimated flowering intensity, and recorded floral visitors observed incidently or during 10-15 minute watch intervals. Depending on the year, we spent 40-90 person hours recording observations of floral visitors between 0900 hours and 1630 hours. Damage to plants increased with storm intensity and duration, distance from the coast, and local topography. The type of damage sustained by the plants ranged from stripped leaves, flowers and fruits, to broken branches, to broken trunks and/or uprooted plants. Preliminary analysis demonstrates that plant species varied in their response to hurricanes in terms of phenology, and that pollinator visitation rates to most plant species were lower in years with hurricanes versus years without hurricanes. Pollinator diversity also declined with hurricane strength, but this does not appear to be correlated with the phenology of specific plant species.

FLANK MARGIN CAVE COLLAPSE IN THE BAHAMAS: PREDICTIVE METHODS

Lawrence, Orry, P, Mississippi State University, Mississippi State, MS; **Mylroie, John, E,** Mississippi State University, Mississippi State, MS.
Presenter: John Mylroie, Poster 18

The risk of sinkhole collapse in The Bahamas is almost entirely caused by failure of cave roofs; cover-collapse sinkholes, common elsewhere and caused by catastrophic sediment flow into underground voids, is almost non-existent because soil cover is thin. On the large banks of The Bahamas, conduit flow at depth leads to large collapse features that under current sea-level conditions become blue holes. Predicting this collapse is difficult. On large and small banks, flank margin caves, formed in the distal margin of the fresh-water lens at a past sea-level highstand, are common, as is a subset of that cave type, the banana hole. Flank margin caves have three entrance types: dissolution pit, side breach, or ceiling collapse. The latter two are the result of mass erosional forces; pits form by focused vadose dissolution. Banana holes typically result in roof collapse due to their location in Pleistocene strand plains which cause them to form with thin roofs predisposed to failure. It was suggested that slope could be used as a proxy for controlling factors in Bahamian flank margin cave collapse. This study demonstrated that 7.5 minute topographic maps cannot resolve slopes in enough detail to predict potential collapse locations. Field surveys with 1 m contours allowed for a more concise slope range in which each entrance type preferentially occurred; collapse breaches and pits were common on gentle slopes and side breaches on steep slopes. Flank margin caves and banana holes are easy to localize in a general sense, but the specific position of these voids within those localities eludes easy analysis. Further investigation into the location of subsurface voids and the collapse risk associated with such voids can be performed using various geophysical methods including GPR and gravity surveys, although these methods are labor intensive and time consuming.

THE EFFECTS OF HURRICANE JOAQUIN ON THE ONSHORE-OFFSHORE ZONATION OF ENCRUSTING FORAMINIFERA AT SAN SALVADOR, BAHAMAS

Lewis, Ronald , Auburn University, Auburn, Alabama; **Asher, Sarah,** Auburn University, Auburn, Alabama; **Speetjens, Sara,** Auburn University, Auburn, Alabama; **Sundbeck, Sally,** Auburn University, Auburn, Alabama.
Presenter: Ronald Lewis, Poster 8

Benthic foraminifera that are firmly attached to hard substrates (encrusting foraminifera) have been studied as part of the reef ecosystem and in actualistic studies to aid in paleoenvironmental reconstructions of shallow-water carbonates. A common research technique is to investigate their distribution by collecting cobble-sized pieces of reef rubble and other clasts from a range of environments. One benefit of focusing on encrusting foraminifera is that they are less likely to be transported out of their habitats than are free foraminifera. However, even large clasts can be transported great distances during high-energy storm events, an issue that has caused some concern for researchers. The small Bahamian island of San Salvador provides a good test case as its encrusting foraminifera are well known, and the island was impacted directly by a major hurricane. Hurricane Joaquin, a category 4 hurricane with sustained winds of 130 mph, which moved very slowly (5-6 mph), impacted San Salvador in early October 2015. We visited the island March 13-18, 2016 (5.5 months after the event). Cobbles were examined in situ, and five or more clasts were collected from the following, previously studied sites: Telephone Pole Reef, Dump Reef, and Salt Pond 1 (near-shore); Snapshot Reef and Salt Pond 2 (patch reefs); Gaulin's Reef (bank barrier reef); and Vicki's Reef (platform margin). Previous studies on San Salvador have shown that near-shore assemblages are dominated by well-preserved *Homotrema rubrum*; lagoonal patch reefs are varied but typically have prominent *Planorbulina* spp.; bank barrier reefs are dominated by *Homotrema rubrum* but with some *Gypsina plana*; and shelf-margin assemblages are dominated by large *Gypsina plana.*

None of the reefs examined in this study showed effects of recent storm damage, and only one cobble was clearly upside down. The high proportion of *Planorbulina* on cobbles found at Dump Reef may indicate transport shoreward from the lagoon. This was also found on the south end of the island, however even cobbles with encrusting foraminifera found on land at The Gulf did not seem to have been moved large distances based on the foraminiferal assemblages. Overall, the pattern of distribution observed previously was still intact.

STATISTICAL EVALUATION OF FORAMINIFERAL DEATH ASSEMBLAGES IN BEACH SANDS OF SAN SALVADOR ISLAND, BAHAMAS

Mattheus, Christopher, R, Lake Superior State University, Michigan; **Diggins, Thomas, P,** Youngstown State University, Ohio; **Stockmaster, Brittany, A,** Coastal Carolina University, South Carolina; **Klein, Veronica, J,** Lake Superior State University, Michigan.
Presenter: Thomas Diggins, Poster 11

Coastal paleoenvironmental investigations benefit from microfossil analyses of sedimentary deposits, particularly when aiming to distinguish washover from ambient sedimentation in lagoonal settings or evaluating strandplain deposits from a provenance perspective. Coastal reconstructive work subsequently benefits from an inventory of species assemblages along the shore, the proximal source of overwash and aeolian materials. Sediment grab samples were collected, as part of a class project, from thirteen separate beaches along the isolated Bahamian platform of San Salvador Island in an effort to inventory and evaluate potential influences of varying coastal geologic framework, offshore reef occurrence, sedimentology, and inferred nearshore hydrodynamics on foraminiferal death assemblages along the shoreline. Analogous foreshore, backshore, and dune sedimentary subenvironments were sampled and a sediment splitter was used to generate unbiased sub-samples for particle-size analysis and micropaleontological assessment, respectively. The foraminifera identified from these samples encompass shallow-water benthic varieties of the calcareous Miliolina and Rotaliina as well as the agglutinated Textulariina suborders. Their relative abundances vary from beach to beach and among individual beach subenvironments. The Miliolina dominate the overall fossil assemblage, comprising over 75% of all specimens sampled. However, this percentage ranges spatially from 29% to 100%. The Rotaliina are the second-most abundant suborder in the overall assemblage while only one Textulariina specimen was sampled. Differences in assemblage composition are suggested to relate, in part, to varying dispersal patterns along the coast of San Salvador Island and the differential weathering and erosion of tests. The latter is showcased by comparing highest-energy to lowest-energy beach samples. Sandy Point, the beach with the coarsest shoreline materials, is dominated exclusively by specimens of *Archaias angulatus*. Prior studies show this species of the Miliolina suborder to represent the most erosion-resistant of sampled species. More heavily sheltered/lower-energy beaches, characterized by smaller grain sizes, are subsequently associated with higher relative abundances of the less robust Rotaliina species. Accordingly, PCA analyses integrating grain-size and foraminiferal species data resolve a distinction between low- and high-energy beach settings. Additional work may provide insights into the effects of patchy habitat distribution, irregular coastal geologic framework, and complex nearshore hydrodynamics on coastal foraminiferal dispersal patterns.

GEOMORPHOLOGY OF THE LATE HOLOCENE SANDY HOOK STRANDPLAIN, SAN SALVADOR ISLAND, BAHAMAS

Mattheus, Christopher, R, Lake Superior State University, Sault Sainte Marie, MI; **Farhan, Salam, A,** Youngstown State University, Youngstown, OH; **Fowler, Joshua, K,** Youngstown State University, Youngstown, OH.
Presenter: Christopher R. Mattheus, Poster 12

The landform succession and stratigraphic architecture of Sandy Hook, a late Holocene strandplain on the isolated Bahamian carbonate platform of San Salvador Island, are evaluated from ground-penetrating radar data, sedimentary analyses, and a GIS-based assessment of beach-

ridge orientation and spacing. The integrative dataset establishes a conceptual evolutionary model for Sandy Hook, which covers around 1.75 kmý of the island's southeastern coast. Late Holocene sea-level rise, storm climate, and sediment supply are investigated as potential geomorphic forcing mechanisms. Four distinct en-echelon beach-ridge sets, each characterized by distinct ridge orientations and spacing, are delineated across Sandy Hook from aerial photographs. The most shore-distal ridges are spaced an average 50 m apart while the youngest and most shore-proximal set is characterized by an average spacing of around 30 m. Beach-ridge sets are bound by topographically prominent ridges that truncate paleoshorelines, are demarked by changes in vegetation type and/or density, and mark a transition to new ridge spacings. Subsurface geophysical data, collected perpendicular to coastal strike using a 200 MHz GPR setup, resolve shoreward-prograding clinoform geometries at 1-4 m in depth. Shoreward-inclined radar surfaces, characterized by slopes around 0.2, represent paleo-foreshore environments and document the progradational history of the strand. The internal architecture of Sandy Hook is generally defined by conformable sedimentary successions, recognized as parallel-inclined stratal surfaces of uniform geometry bound by unconformities. These bounding surfaces truncate underlying, older stratal units and are characterized by onlap of overlying, younger ones. This subsurface framework is suggestive of a pattern of strandplain growth that is punctuated by episodic ravinement. The general compartmentalization of the Sandy Hook strand implies changing environmental conditions. Studies of similar strandplain environments have related such landform juxtapositions to variances in storm climate and/or sediment supply. The continued reduction in shallow shelf area fronting the prograding beach system at Sandy Hook likely affected strand evolution by progressively altering nearshore hydrology and sediment supply. The intrinsic influence of accommodation-space loss across the shallow shelf is reflected in seaward-decreasing ooid contents across beach-ridge sets and strongly implied by the accompanied reduction in ridge spacing.

SUPERSTORMS: THE BAHAMIAN EVIDENCE FOR THE LAST INTERGLACIAL (MIS 5E)

Mylroie, John, E, Mississippi State University, Mississippi State, MS.

Presenter: John Mylroie, Sunday 7:30 PM

Sea level during the last interglacial (MIS 5e) was ~6m above present, and has been interpreted to represent a warmer climate than today's current interglacial. It has been speculated that such warmer temperatures could have increased storm intensity and storm frequency. Recently, two hypotheses have been advanced that purport to demonstrate an increase in storm intensity during MIS 5e. The first hypothesis considers fenestrae at elevations up to 43 m in The Bahamas to be evidence of superstorm washover. Additional observations include rip-up clasts and loss of bedforms and root structures as a result of wave scour. Such an event should produce a tempstite with a wide-ranging footprint, but none exists. The fenestrea can be explained as rainfall slurries, the rip-up clasts are weathering products of calcarenite protocol development, and the bedforms and root structure absence or presence is a difference in transgressive versus regressive eolian formation, respectively. Eleuthera Island contains chevron ridges proposed to be large washover structures, and boulders assumed to have beenflung up onto the land by superstorm waves. The chevron contain climbing wind ripples and are eolian; tempestites are not present. The boulders are karrentisch and rest on pedestals,. To emplace them would require extreme energies, but other interpretations such a fossil tower karst and boulders rolling down slope remain viable. The boulder area has an extremely small footprint, extending a few kilometers on the northeast shore of Eleuthera, and such a small footprint is more than an order of magnitude smaller than that for Sandy or Katrina, recent large storms. Hurricane Joaquin, the largest category 4 hurricane in the Bahamas since 1866, produced no boulder or chevron structures of the magnitude described for MIS 5e superstorms.

VEGEMORPHS AS A MEANS TO DIFFERENTIATE TRANSGRESSIVE-PHASE FROM REGRESSIVE-PHASE QUATERNARY EOLIAN CALCARENITES, SAN SALVADOR ISLAND, BAHAMAS

Mylroie, John, E, Mississippi State University, Mississippi State, MS; **Birmingham, Andrew, N,** Mississippi State University, Mississippi State, MS; **Mylroie, Joan, R,** Mississippi State University, Mississippi State, MS.
Presenter: John Mylroie, Sunday 8:30 AM

During the start of Quaternary interglacial conditions, sea-level rise floods the top of the steep-sided carbonate platforms of The Bahamas, and carbonate sediment production is significant. This carbonate sediment is rapidly produced in large volumes within relatively small lagoons, and eolian calcarenites immediately develop on the remaining dry ground adjacent to their source beaches. As these dunes form as sea level is rising, they are referred to as transgressive-phase eolianites. Continued reef growth to wave base as the highstand stabilizes diminishes lagoon wave energy, and further dune production is modest until the end of the interglacial, when sea level begins to fall and surf zone processes pass through the platform lagoons, where stored carbonate sediments are remobilized into beaches and a second episode of dune production occurs. The resulting dunes are regressive-phase eolianites. These two eolianite packages bracket the leading and trailing portions of individual sea-level highstands. Various criteria have been developed to identify transgressive-phase and regressive-phase eolianites; however, the one with the most potential is based on plant trace fossils, variously called rhizomorphs, rhizocretions, or vegemorphs (vegemorphs is used herein as it refers to any plant structures, not just roots). Extensive field work has demonstrated quantitatively that vegemorphs are found preferentially in regressive-phase eolianites, and that the presence of vegemorphs disrupts the fine-scale eolian bedding. Transgressive-phase eolianites have notably fewer vegemorphs, and as a consequence, exhibit undisturbed fine-scale laminations. Vegemorph absence or presence is readily observable on vertical faces, and so paleodunes exposed at sea cliffs, in quarries or road cuts, or in caves can be easily categorized as transgressive-phase or regressive-phase deposits, respectively.

KARST DENUDATION IMPACT ON QUATERNARY GLACIOEUSTASY DETERMINATIONS

Mylroie, John, E, Mississippi State University, Mississippi State, MS; **Mylroie, Joan, R,** Mississippi State University, Mississippi State, MS.
Presenter: Joan Mylroie, Sunday 11:00 AM

Fossil coral reefs and related subtidal deposits have been used as indicators of Quaternary glacioeustasy, traditionally by examination of fossil coral reef terraces on carbonate islands and coasts that have been tectonically uplifted. These studies do not account for dissolutional denudation, which lowers the terrace surface; the terrace surface has been assumed to be the depositional surface. Denudation is cumulative over time, making higher and therefore older terrace placement far below their actual depositional elevation. Examination of karst pedestals (karrentische) on Guam reveals the denudation to be ~50 mm/ka); this value correlates with theoretical denudation models corrected for eogenetic carbonates in tropical settings. Flank margin caves, which form in the distal margin of the fresh-water lens within a carbonate island, are excellent sea-level indicators. Analysis of flank margin cave elevations throughout the Bahamian Archipelago indicates that the archipelago has had past sea-level highstands greater than 6 m, perhaps up to 15 m or more, for which no fossil coral data exists. Denudational removal of these older corals has biased the record to younger events. Older fossil corals may exist in settings in which they were entombed by eolian calcarenites and protected from denudation. Only flank margin caves commonly remain as viable terrestrial signatures of these older sea-level highstands.

HIGH-RESOLUTION UAV MAPPING OF COASTAL EROSION AND BOULDER MOVEMENT PRODUCED BY THE 2015 HURRICANE JOAQUIN ON SAN SALVADOR, THE BAHAMAS

Niemi, Tina, M, UMKC, Kansas City MO; **Preisberga, Anniya,** UMKC, Kansas City MO; **Rucker, John, D,** UMKC, Kansas City MO; **Nolan, Joseph, A ,** UMKC, Kansas City MO; **Rose, Tori, L,** UMKC, Kansas City MO.
Presenter: Tina M. Niemi, Sunday 8:00 PM

The Bahamian island of San Salvador was directly affected by Hurricane Joaquin over a two-day period in Oct. 2015 when the storm travelled SW from Bermuda, passed SE of the island then turned, intensified to a Category 4 hurricane, and then passed across the island from the S-SW. To map the hurricane related changes in the coastal environment, we utilized a DJI Quadcopter 3 mounted with 12 Megapixel, 4K video camera to collect aerial data at four locations. We preprogrammed flight paths designed to acquire 70% image overlap using a smartphone app designed by Pix4D. The data were processed using Agisoft PhotoScan to render both a high-resolution digital orthomosaic, as well as a georeferenced digital elevation model (DEM). These datasets were then compared to our pre-hurricane aerial photography collected with a kite in March and June 2014 and to satellite imagery from Google Earth. These before and after images allow us to determine how the coastline changed. Our field research in March (2015, 2016, 2017) and June (2015, 2016) provide ground-based photographic and orientation data on boulder location, imbrication, and beach conditions. The high-resolution, low-altitude imagery allowed us to map the boulder field, measure the evidence of storm surge height by flotsam lines surrounding the boulder field, and calculate boulder movement by matching erosion scars to boulder position, and boulder size to position. We also noted where road construction debris provided boulders that had moved. It is clear that boulders that are exposed along the wave-cut platform at low tide of the Pleistocene Cockburn Town Reef have been transported up the cliff and inland in this storm event based on boulder identification. We have previously noted that coastal reentrants are the location of coves where wave action is focused and thus increase lift. Coastline retreat where cliffs collapse downward are located along these coves and provide large boulders which are available for transport upward. These coves become the staging ground for boulders to be elevated in extreme storm events. Our data show that the coves are locations of wave focusing and greater storm surge and landward transport of boulders. Our aerial UAV imagery from Green Cay along Grahams Harbour on the northwest side of the island show that large boulders previously noted there did not move in this hurricane.

WHAT MAKES THE HOLE? TOOL AND ORNAMENT CONSTRUCTION OF *CODAKIA ORBICULARIS* AND ITS ROLE IN RECYCLING OF THE ARCHAEOLOGICAL RECORD BY THE BLUE CRAB *CARDISOMA GUANHUMI*, SAN SALVADOR ISLAND, BAHAMAS

Park Boush, Lisa, E, University of Connecticut , Storrs, CT; **Buynevich, Ilya, V,** Temple University, Philadelphia, PA; **Curran, H, A,** Smith College, Northampton, MA; **Gnivecki, Perry, L,** Miami University, Oxford, OH; **Berman, Mary Jane,** Miami University, Oxford, OH; **Kopcznski, Karen,** Temple University, Philadelphia, PA; **Shkembi, Bruno,** University of Connecticut, Storrs, CT .
Presenter: Lisa Park Boush, Poster 13

The bivalve *Codakia orbicularis* (Linnaeus, 1758), Family Lucinidae and common name tiger lucine, is found throughout the Caribbean and Florida. *C. orbicularis* shells are found typically in Lucayan middens, with Lucayans being the indigenous inhabitants of the Caribbean. Of significance is the fact that the blue land crab, *Cardisoma guanhumi*, commonly recycles shells in the process of burrowing, thereby exporting *C. orbicularis* to the surface. Some of these shells are abraded in various areas, including the ventral, anterior and posterior margins, as well as in the umbo region. We measured 174 *C. orbicularis* shells from surface collections (N=29), the 18 cm depth interval (N=17) from Pigeon Creek Dune 1 site, the 30-40 cm interval (N=14) at SSP82-16 and the 0-20 cm depth interval (N=126) at SSP82-5, San Salvador, Bahamas, examining the amount of abrasion in these four regions of the valve. Of the surface-collected materials that were recycled by *C. guanhumi*, 7% were abraded on the anterior margin, 17% on the

posterior, 24% along the ventral margin and 10% within the umbo region. Ventral margin abrasion was most likely caused by Lucayans using shells as scrapers. Umbo abrasion was likely due to working the shell for bead or adornment purposes, or to use the shells as fishing net weights. In our sample, only 33% of the shells that were abraded in this way culminated in a complete hole. Of the other two, one was a failed attempt and broken and the other did not penetrate the valve. There was no correlation between valve size and abrasion area or frequency. Similarly, there was no difference in abrasion in shells of variable sizes collected from the surface and those found within the archaeological record. The fact that abraded shells occurred on the surface in areas adjacent to *C. guanhumi* burrows indicates significant recycling of shell material to the surface by these powerful burrowers. Thus, "crabturbation" has had a significant role in preservation of these archaeological sites, and other sites presently within the habitat of blue land crabs are vulnerable to similar disruption.

A 6000 YEAR MULTI-PROXY PALEOCLIMATE RECORD FROM TWO LAKES ON ELEUTHERA, BAHAMAS

Park Boush, Lisa, E, University of Connecticut, Storrs, CT; **Myrbo, Amy,** University of Minnesota, Twin Cities, MN; **Yakabowskas, Dana,** University of Connecticut, Storrs, CT; **Berman, Mary Jane,** Miami University, Oxford, OH; **Gnivecki, Perry, L,** Miami University, Oxford, OH; **Brown, Erik, T,** University of Minnesota, Duluth, MN.
Presenter: Lisa Park Boush, Sunday 9:30 AM

High resolution paleoclimate records for the past 6,000 years have been recovered from two lakes of differing types-a coastal lagoon and a blue hole-on the island of Eleuthera, Bahamas. Multi-proxy records were analyzed on sediment cores from three sites (254, 114 and 104 cm in length) taken along shore-normal transects in Shad Pond (SHAD), a hypersaline coastal lagoon, and three sites (170, 155 and 151 cm in length) from Duck Pond Blue Hole (DPBH). Sediment composition and granulometry, loss on ignition (LOI), X-ray fluorescence (XRF) measurements, as well as oxygen isotope and trace element measurements on ostracods provide the basis for our reconstruction of the paleoclimate history from these two basins. High resolution XRF scans of Ca, Br, Fe and Sr as well as loss on ignition show a marked change around 3700 cal BP that correlates with the top of a peat layer in Shad Pond and potential rapid sea level rise. This is followed by a period of high variability from 3700 cal BP until approximately 2000 cal BP possibly representing wet/dry cycles, corroborated by the .18O record recovered from ostracod shells as well as their trace element Mg:Ca and Sr:Ca ratios. The .18O records show an overall depletion from +1.47 ppm to -2.04 ppm (VPDB) throughout the 6000-year record, with highest variability between the 4000-3000 cal BP period. Trace element analyses reveal a Mg:Ca and Sr:Ca record that positively co-varies and trends with the .18O record. Evidence for a meteoric lens collapse at 1.6-1.8 ka as sea-level rise breached a local sill and altered coastal circulation in Shad Pond is also apparent. Despite the differences in lake type (i.e. coastal lagoon vs. blue hole), the records from these two lakes record climate-driven changes in the Late Holocene. These multi-proxy records correspond to other patterns seen regionally in the Caribbean, as well as globally.

SPELEOTHEM DEPOSITION IN EOGENETIC CARBONATES: THE CONSEQUENCES FOR STRONTIUM

Ridlen, Nicole, M, Mississippi State University, Mississippi State, MS; **Mylroie, John, E,** Mississippi State University, Mississippi State, MS; **Polk, Jason, S,** Western Kentucky University, Bowling Green, KY; **Mylroie, Joan, R,** Mississippi State University, Mississippi State, MS.
Presenter: John Mylroie, Poster 19

Eogenetic carbonate rocks develop from allochems precipitated primarily as aragonite (e.g. green algae, mollusks, corals) and high-Mg calcite. (e.g. echinoderms, red algae). Relative to calcite, Strontium (Sr) preferentially enters the orthorhombic aragonite crystal lattice, giving eogenetic carbonate rocks a higher Sr background than older teleogenetic rocks, in which the aragonite has inverted to calcite. Vadose speleothems (stalagmites) forming in caves in eogenetic carbonate rock

should show a high Sr content. The Sr levels in the speleothems should decrease with rock age as the aragonite inverts and the Sr is lost. Strontium levels in speleothems have been used as a paleoclimate indicator, but the influence of eogenetic Sr has been under appreciated. This issue has become more important as oceanic island caves and speleothems hosted in eogenetic carbonates have recently been utilized as mid-ocean paleoclimate indicators. Curacao, in the southern Caribbean, contains a series of tectonically uplifted terraces of eogenetic carbonate rock. These carbonate rocks contain flank margin caves in which speleothem growth is active. Samples from caves in each terrace show a progressive loss of Sr in each higher, and therefore older, terrace. The ?Higher Terrace?, older mid-Pleistocene age host rock, was calcitic with 0.44 ppm Sr; one speleothem from a cave in this rock contained 0.25 ppm Sr. The "Middle Terrace", younger mid-Pleistocene host rock, was also calcitic, with 1.43 ppm Sr; two cave speleothems had Sr values of 0.30 and 0.31 ppm. The "Lower Terrace", late Pleistocene in age, was 40% aragonite and 60% calcite, with a Sr value of 6.89 ppm; two cave speleothems had Sr values of 8.68 and 8.28 ppm. Utilizing caves from a single location removes any climatic differences in calcite inversion and speleothem deposition, leaving rock age as the major factor in the Sr variation in these speleothems.

DAMAGE FROM HURRICANE MATTHEW TO THE CLIFTON HERITAGE PARK ON NEW PROVIDENCE ISLAND IN THE BAHAMAS

Rucker, John, D, UMKC, Kansas City MO; **Niemi, Tina, M,** UMKC, Kansas City MO; **Nolan, Joseph, A,** UMKC, Kansas City MO; **Rose, Tori , L ,** UMKC, Kansas City MO.

Presenter: John Rucker, Sunday 10:30 AM

Hurricane Matthew passed from SE to NW over New Providence Island on October 6, 2016 as a category 4 Hurricane on the Saffir-Simpson scale. Clifton Heritage Park, located on the western coast of the island, and containing the ruins of the Loyalist period Clifton plantation, was severely impacted by Hurricane Matthew. In addition to damage to park facilities, the shoreline was heavily affected by the scouring of soil, movement of large boulders, and movement and deposition of large flotsam and jetsam. We mapped and documented the hurricane-related changes at two locations using a DJI Quadcopter 3 mounted with a 12 Megapixel, 4K video camera to collect aerial data. The data were processed using Agisoft PhotoScan to render both a high-resolution digital orthomosaic, and a georeferenced digital elevation model (DEM). We also documented these areas with ground based photography as well as measurement of size and orientation of boulders. At Flipper Beach, there is a distinct line of boulders near the shoreline, and another distinct line of more buoyant flotsam along the line of a Loyalist period field wall approximately 80 m from the shoreline. Between these two locations, the soil has been scoured away in some areas down to bedrock. It is likely that this location was particularly affected due to the focusing effect of the cove in which Flipper Beach lies, as well as the previous anthropogenic clearing of vegetation in the area. Farther south, at the historic period "Pirate Stairs", the large stone that originally covered the archway over the stairs has been moved roughly 2 m to the north. At this location, approximately 6 m above sea level, there is clear evidence of overwash, including the movement of large boulders, scouring of soil, and deposition of fan corals and marine plant fragments. Taken together, this evidence allows a reconstruction of the energy of the hurricane, as well as the height of its storm surge - which was significant.

A VULNERABILITY ANALYSIS OF HURRICANE JOAQUIN'S EFFECTS ALONG THE PERIMETER OF SAN SALVADOR ISLAND, BAHAMAS

Savarese, Michael, Florida Gulf Coast University, Ft. Myers, FL; **Buynevich, Ilya,** Temple University, Philadelphia, PA; **Glumac, Bosiljka,** Smith College, Northampton, MA; **Curran, H. Allen,** Smith College, Northampton, MA; **Park Boush, Lisa, E,** University of Connecticut, Storrs, CT; **Caris, Jon,** Smith College, Northampton, MA; **Kopcznski, Karen,** Temple University, Philadelphia,

PA.
Presenter: Lisa Park Boush, Sunday 7:00 PM

Effects of Hurricane Joaquin (Sept/Oct 2015) were highly variable on the perimeter of the small, exposed Bahamian island of San Salvador. Following the USGS storm impact scale method, the geological effects of Joaquin were assessed relative to foredune elevation and swash height. Damage was categorized, in order of increasing severity, as: swash, collision, overwash, and inundation damage. Assessment of 9 representative regions was undertaken in Jan 2016 using orthophotos and digital elevation models generated from drone flights, georadar, and ground surveys. Storm surge was not a critical factor for most of the island, and persistent flooding and breaching of coastal barriers was not common. Consequently, minimal overwash and inundation damage occurred. The south shore was an exception, where wave action was extreme. Here, 5-m-high cliffs were overtopped, causing erosion at the leading edge and extensive landward movement of boulders within a 6.3 ha area. New boulders, as large as 3 m in diameter, were generated, and older blocks from prior storms, estimated to weigh 1-3 tons, moved up to 26 m inland. The principal road was damaged and inundated by debris. Along the east (windward) and west coasts, hurricane impact caused substantial dune scarping and some overwash, though no dune systems were breached. Overtopping into the backdune occurred at numerous locations along both coasts, onto the circum-island Queen's Highway, and into several swale lakes. Scarped dunes lost as much as half their volume with retreat as far as the dune crest. Some dune scarps at the time of assessment had already shown signs of eolian repair. These scarps will remain as recognizable subsurface features in future geophysical images. A rejuvenated tidal channel was scoured along the southeastern coast, establishing an ephemeral connection to Pigeon Creek, and a massive overwash fan of approximately 1 ha now blocks the mouth of this channel. Overall, no significant, irreparable coastal change occurred as a consequence of Joaquin. Although the storm imposed economic hardship, much of its geomorphologic legacy has already being modified by fair-weather processes. Because of the potential consequence of future storm activity, we recommend that a comprehensive assessment of storm vulnerability be undertaken throughout the archipelago.

HURRICANE MATTHEW PROJECT: DOCUMENTING THE COASTAL ECOSYSTEM COSTS OF HURRICANES ON NEW PROVIDENCE, BAHAMAS WITH COMMUNITY PARTNERS

Sullivan Sealey, Kathleen, University of Miami, Coral Gables, FL; **Shiel-Rolle, Nikita,** Young Marine Explorers, Nassau, Bahamas.
Presenter: Kathleen Sullivan Sealey, Thursday 8:00 PM

The Hurricane Matthew Project (HMP) was initiated to document the damage to coastal resources from the historical Category 4 hurricane that impacted four major islands in The Bahamas. A team of scientists and students started with an assessment of the damage done by Hurricane Matthew on the most populous island of New Providence. Coastal neighborhoods and citizen scientists participated to develop a rapid impact assessment protocol to document damage to the coastal environment, looking specifically at developed and protected coastal environments (including two national parks). The assessment evaluated building damage, vegetation damage, flooding, solid waste as well as coastal erosion to produce GIS maps to visualize the severity of damage. The HMP has evaluated the cost of coastal erosion as well as degradation of coastal water quality and decline of biological diversity to identify high priority areas for coastal restoration. The role of coastal protected areas in preventing and minimizing damage to nearby human communities was considered. The final outcome was a community-based rapid ecological assessment protocol. The severity of this hurricane damage is unprecedented and offers an opportunity to re-develop to mitigate damage from future storms.

PALEOSOL AND CAVE MINERALOGY FROM ELEUTHERA, THE BAHAMAS

Sumrall, Jonathan, B, Fort Hays State University, Hays, KS; **Sumrall, Jeanne, L,** Fort Hays State University, Hays, KS; **Gauvey, Kaitlyn, L,** Fort Hays State University, Hays, KS; **Sides, Kristin, E,** Sam Houston State University, Huntsville, TX; **Larson, Erik, B,** Shawnee State University, Portsmouth, OH.
Presenter: Jeanne Sumrall, Poster 20

Paleosols on Eleuthera, The Bahamas were sampled to determine the clay mineralogy from outcrops and from within Hatchet Bay Cave. In addition, cave mineral samples were collected from additional flank margin and littoral sea caves. Paleosol samples were processed to remove carbonates and organics before fractionating by size. Treatments (K-saturation, Mg-Saturation, Heating, and Gylcolnation) were used to determine the specific clay mineralogy of each sample. Petrographic thin sections were also prepared to determine characteristics of each type of paleosol (porosity, cementation, allochems, iron oxide content). Cave mineral samples were powdered and analyzed using powdered X-ray Diffraction (XRD). The dominant clay mineral present in the paleosols on Eleuthera was Fe-rich chlorite ((Fe+2,Mg,Al,Fe+3)6(Si,Al)4O10(OH,O) 8) and Illite (K0.6(H3O)0.4Al1.3Mg0.3Fe+20.1Si 3.5O10(OH)2ú(H2O)) based on 14 and 10 peaks. The larger [002] 7 peak compared to the [001] 14 peak indicates a Fe-rich chlorite. In addition, a small peak shift from 14 to 6.1 in several samples may suggest the presence of Boehmite (AlO(OH)). Non-clay materials include low-Mg calcite and quartz. Cave minerals included carbonates (calcite and aragonite), sulfates (gypsum), phosphates (hydroxyapatite, fluorapatite, chlorapatite, and woodhouseite), and Mn-oxides. All minerals except woodhouseite have previously been reported from Bahamian caves. Woodhouseite (CaAl3(SO4)(PO4)(OH)6) is part of the Alunite supergroup and has been previously reported as the product of bat guano in cave environments. Woodhouseite samples came from Hatchet Bay Cave, specifically from small crusts found on the exposed paleosol within the cave. The presence of woodhouseite was confirmed in three samples from various locations within the cave. Woodhouseite presence in this instance likely represents phosphate-rich leachate derived from the combination of seawater and guano interacting with the various aluminum-rich phases found within the clay fraction of the paleosol. Previous Bahamian cave mineral studies did not have access to exposed paleosols within caves, making this an interesting addition to the diverse cave mineral inventory of The Bahamas.

DENUDATION ANALYSIS OF CEMENTED CARBONATE DUNE COMPLEXES ON ELEUTHERA, THE BAHAMAS

Sumrall, Jeanne, L, Fort Hays State University, Hays, KS; **Jordan, Miranda, M,** Sam Houston State University, Huntsville, TX; **Larson, Erik, B,** Shawnee State University, Portsmouth, OH.
Presenter: Jeanne Sumrall, Sunday 9:00 AM

The denudation rates of three cemented eolian carbonate dunes on Eleuthera, The Bahamas, one at the North Twin Coves (NTC) complex, and two at South Point (SP1 and SP2), were calculated using geometric field analysis, carbon dating, and laboratory analysis. Five samples were collected from the truncated dunes. Carbon dating of whole rock samples confirmed that the upper and lower dunes are Holocene. Radiocarbon dates from the dunes suggests an 88-59 year (+/- 30yrs) difference in ages from the lower truncated surface to the upper truncated surfaces for NTC and SP1 dune complexes. An approximate denudation of 2 meters from apex of the dune to truncation surface was established for SP2 using the geometry of the dune bedding planes and estimated initial dune height. A sample was collected from the lateral bedding planes used to establish initial dune height on the lower outer edge of the dune. The analysis of this sample provided a maximum dune age of 6,602 cal yrs BP (+/- 30yrs). If the mechanical and chemical denudation is the approximated 2 meters for the SP2 dune, it is possible that the dune was exposed and denuded at a relatively constant minimum rate of 30.3cm/1000yrs. This rate is well below the maximum denudation rate of 107.1cm/1000yrs,

based off of maximum theoretical dissolution calculations. Carbon dates of TC and SP1 suggest either an unrealistic total denudation between 0.88-3.6cm or an unrealistic denudation rate. It is possible that the carbon dates do not show the correct gap in time between the upper and lower dune surfaces because they likely came from the same offshore source material that blew onshore over time. Similar allochems found in all of the dunes, and porosity differences associated with higher cementation rates in the lower dunes when compared to the upper dunes provide evidence for this idea. However, if the carbon dates are accurate, it is possible that a catastrophic event, such as a storm, mechanically weathered and truncated the poorly cemented lower dune. More substantial sampling and analysis of dune complexes needs to take place to better determine the actual rate of denudation.

LABORATORY CULTURE AND LIFE HISTORY CHARACTERSTICS OF THE APODID SEA CUCUMBER, SYNAPTULA HYDRIFORMIS FOUND ON SAN SALVADOR ISLAND, BAHAMAS.

Thacker, Miranda, St. Olaf College, Northfield, MN; **Cole, Eric, S.,** St. Olaf College, Northfield, MN.
Presenter: Miranda Thacker, Poster 5

We investigated natural history characteristics of an abundant Apodid sea cucumber collected from Oyster Pond on San Salvador Island in the Bahamas. Three color morphs were identified for Synaptula hydriformis, (brown, striped and pale green), as well as another genus and species, possibly Chiridota rotifera. We developed a method for inducing both spawning and birthing. This is achieved through a cold-shock treatment administered to the adult sea cucumbers. Larvae are born within 24 hrs of a 10-minute cold shock. This same treatment may also induce internal spawning. We confirm details of a simultaneous hermaphroditic lifestyle, self-fertilization, internal brooding of the larvae, and a pattern of direct embryonic development that bypasses the planktonic auricularia larval form. A successful technique for culturing juvenile sea cucumbers was established. This initially involved culturing the floc found at the bottom of their home habitat and eventually progressed to feeding them on cultured dinoflagellates. The transparent adult body, and the ease with which embryonic development can be induced and observed recommend Synaptula as an alternative model organism for exploring problems of echinoderm embryology. It is also intriguing to speculate on their ability to establish genetic clones during colonization of new habitat.

HIDDEN HISTORY ON SAN SALVADOR ISLAND

Winter, John, Molloy College, Rockville Centre, New York.
Presenter: John Winter, Sunday 11:30 AM

After Hurricane Joaquin passed over San Salvador Island in October 2015, Google Earth provided satellite images of the island for October 10, 12, and 16, 2015. These images revealed the extensive coastal damage that was done to the island. In addition, these images revealed the ruins of buildings that had been hidden under the vegetation over the years. One set of buildings was located 1900 feet west from the Queens Highway by the old Fortune Hill settlement, which lies north of the Kerr Mount ruins. These eight buildings lie at the base of the western slope of the second lithified dune ridge from the Queens Highway. The buildings are arranged in a row style. Each of the buildings has a built in fireplace, which has two wooden beams over the opening. The chimneys collapsed over the years. These buildings had two facing doors on the east and west sides, but lacked windows. The style of these buildings is similar to slave homes from the plantation era. These buildings might be related to the early days of the Kerr Mount plantation or a larger building up the hill to the east. More modern buildings were observed in the area from the 1900's with a diversity of architectural design.

IF A TREE FALLS IN THE FOREST . . .

Winter, John, Molloy College, Rockville Centre, New York.
Presenter: John Winter, Poster 10

When high speed winds hit San Salvador Island, many people are interested in searching for coastal impacts. Yet there is evidence of high speed winds affecting the island's interior. Fallen and uprooted trees that survive these winds can be observed within the island's interior. Some of these uprooted trees die, while others develop new vertical growth. No specific time frame has been assigned to these disasters.